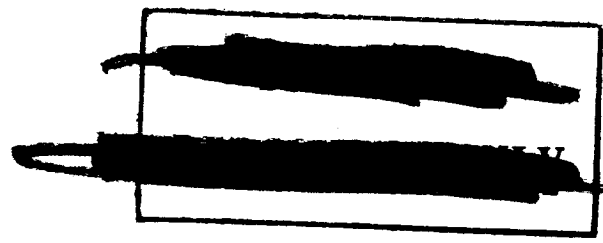# NATIONAL AERONAUTICS AND SPACE ADMINISTRATION

NASA-MSC-G-R-65-5
Supplemental Report 1

GEMINI AGENA TARGET VEHICLE 5002 SYSTEMS TEST EVALUATION (45 DAY REPORT)

CONTRACT AF 04(695)-545

Issued as: Supplement 1
to: Gemini Program Mission Report
Gemini VI, MSC-G-R-65-5
by: Gemini Mission Evaluation Team
National Aeronautics and Space Administration
Manned Spacecraft Center
Houston, Texas

SSD-545-65-18 • 9 DEC 1965   **LMSC-A774454 • 9 DEC 1965**

X67-14132
(ACCESSION NUMBER)
215 (PAGES)
NASA-CR-83307
(NASA CR OR TMX OR AD NUMBER)
(THRU)
(CODE)
(CATEGORY)
FACILITY FORM 602

UNCLASSIFIED

MANNED SPACECRAFT CENTER
HOUSTON, TEXAS

U. S. Government Agencies Only

(NASA-CR-83307) GEMINI/AGENA TARGET VEHICLE
5002 SYSTEMS TEST EVALUATION (45 DAY REPORT)
(Lockheed Missiles and Space Co.)   215 p

N75-75317

Unclas

LMSC-A774454 ● 9 DEC 1965

SSD-545-65-18 ● 9 DEC 1965

GEMINI AGENA TARGET VEHICLE 5002
SYSTEMS TEST EVALUATION
(45 DAY REPORT) (U)

CONTRACT AF 04(695)-545

Issued as: Supplement 1
to: Gemini Program Mission Report
Gemini VI, MSC-G-R-65-5
by: Gemini Mission Evaluation Team
National Aeronautics and Space Administration
Manned Spacecraft Center
Houston, Texas

APPROVED:

A. J. STEELE
MANAGER
NASA PROGRAMS ENGINEERING

APPROVED:

J. L. SHOENHAIR,
ASSISTANT GENERAL MANAGER
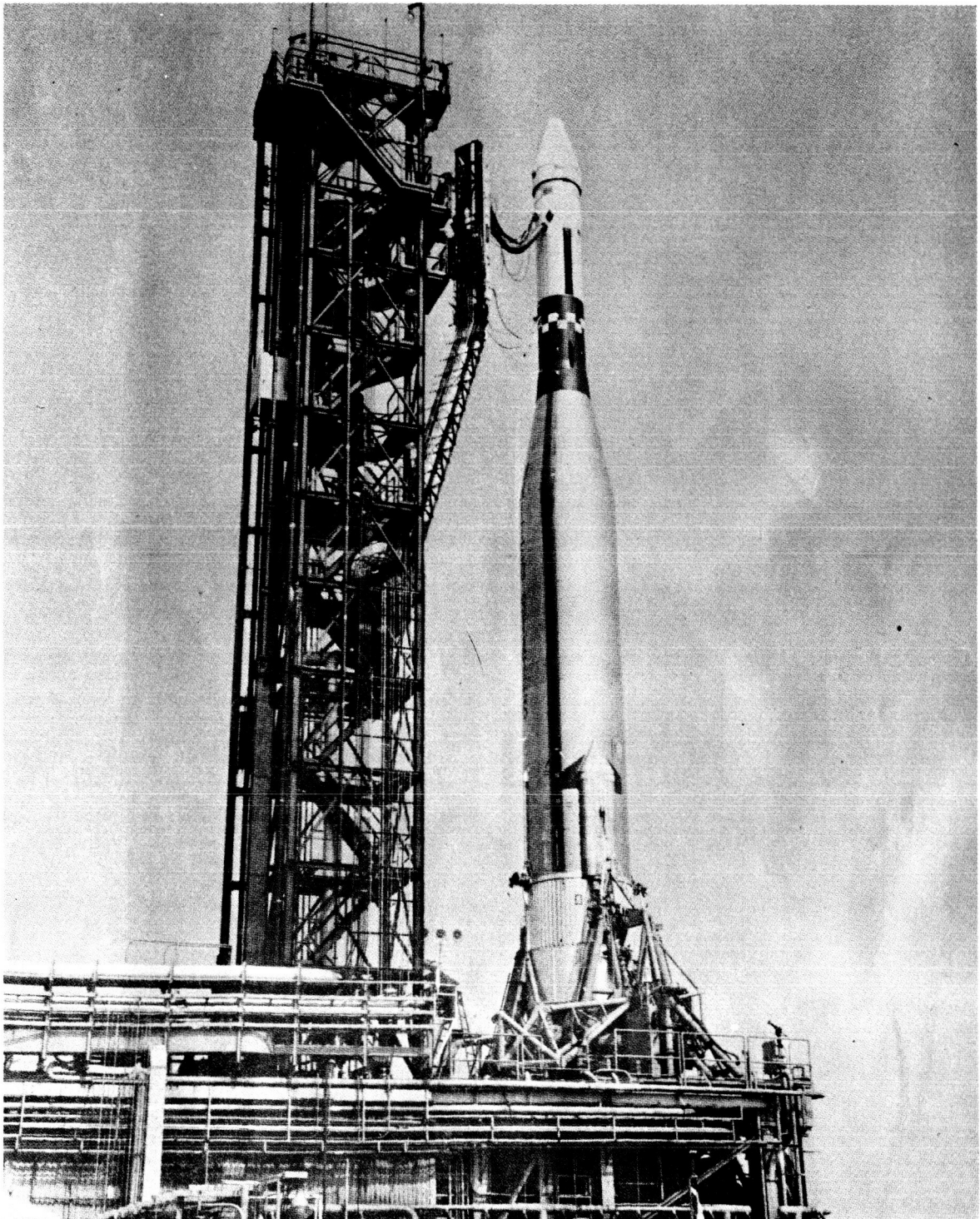NASA AGENA PROGRAMS

L. A. SMITH
MANAGER
GEMINI PROGRAMS

U. S. Government Agencies Only

LOCKHEED MISSILES & SPACE COMPANY

Gemini Atlas Agena Target Vehicle in Launch Configuration
on Cape Kennedy Complex 14

LOCKHEED MISSILES & SPACE COMPANY

FOREWORD

This report, prepared by Lockheed Missiles & Space Company
in compliance with Contract AF 04(695)-545, documents the
flight performance evaluation and failure diagnostic analysis of
Gemini Agena Target Vehicle 5002 launched from the Air Force
Eastern Test Range on 25 October 1965.

Pertinent evaluations for the performance of Atlas Vehicle 5301
and of the target docking adapter are based on information trans-
mitted to Lockheed by General Dynamics Convair (GD/C) and by
McDonnell Aircraft Corporation (MAC), respectively.

LMSC-A774454
Revised Page
6 Jan 1966

SUMMARY

After approximately 18 sec of secondary propulsion system operation, the signal was given to start the engine. At 368.404 sec, a major vehicle disturbance occurred.

Lockheed has investigated all failure modes that have been suggested as possible causes for the subsequent flight events. The failure mode described herein appears most likely to represent the cause of the flight failure of GATV 5002. During the limited duration of the flight, it appears that all subsystems of the GATV, except the PPS, performed within design parameters. At the start of the anomaly, the turbopump had provided sufficient pressure to have opened the main propellant valves. Based upon supplemental analysis, it appears that approximately 1.9 lb of fuel had preceded the oxidizer into the thrust chamber. At this time, a high-pressure pulse occurred in the primary propulsion system as evidenced by several transducers malfunctioning in a mode indicating mechanical deformation of the sensing mechanisms. This pressure pulse may have occurred as a result of combustion instability or decomposition of the fuel into a monopropellant; or critical mixture ratios of propellants were ignited in the combustion chamber.

Drastically lowering temperatures monitored on the shear panels, aft bulkhead, and start tanks then indicated that propellants were being sprayed throughout the engine compartment, probably resulting from a ruptured element in the feed system. At 368.404 sec after liftoff, the electrical circuitry that provides power to the engine failed, either in the turbine overspeed shutdown gate or in the cabling nearby. When power was removed from the engine, the engine shut down. Lacking the normal propellant flows from the main tanks, ullage volume remained very small, and the actuated helium blowdown pressurization system continued to pressurize the tanks until rupture occurred. Finally (375.4 sec), telemetry signals were lost.

LOCKHEED MISSILES & SPACE COMPANY

Since Lockheed believes the failure centered on a hard engine start, recommendations have been made to return to an engine oxidizer lead ignition, to adjust the sampling rates on many of the data channels, to shock-mount all pyrotechnic shock-sensitive assemblies, and to provide a modified electrical control system to the engine.

LMSC presented to AFSSD and NASA/MSC a series of recommended modifications entitled Project Sure Fire that were approved and are now being implemented for the remaining flight vehicles. These are modifications to the PPS, which is being subjected to an extensive program. The modifications will eliminate possible sources of engine anomaly.

CONTENTS

LOCKHEED MISSILES & SPACE COMPANY

LOCKHEED MISSILES & SPACE COMPANY

ILLUSTRATIONS

LOCKHEED MISSILES & SPACE COMPANY

xv

LOCKHEED MISSILES & SPACE COMPANY

TABLES

LOCKHEED MISSILES & SPACE COMPANY

ABBREVIATIONS

ACS	Altitude Control System
AEDC	Arnold Engineering Development Center
AFETR	Air Force Eastern Test Range
AGE	Aerospace Ground Equipment
BAC	Bell Aerosystems Company
BECO	Booster Engine Cutoff
DRAPE	Data Reduction and Processing Equipment
EST	Eastern Standard Time
F/C	Flight Control
FCLP	Flight Control Logic Package
GAT	Gemini Agena Target orbital stage
GATV	Gemini Agent Target Vehicle second stage, including adapter section, payload fairing, and other droppables
GD/C	General Dynamics/Convair
GE	General Electric Company
GG	Gas Generator
GGFSV	Gas Generator Fuel Solenoid Valve
GGOSV	Gas Generator Oxidizer Solenoid Valve
GLV	Gemini Launch Vehicle
GMT	Greenwich Mean Time
H_e	Helium
H/S	Horizon Sensor
IRFNA	Inhibited Red Fuming Nitric Acid
IRP	Inertial Reference Package
LMSC	Lockheed Missiles & Space Company
LOS	Loss of Signal
LOX	Liquid Oxygen
LSB	Least Significant Bit

MAP	Message Acceptance Pulse
MDF	Mild Detonating Fuse
MSB	Most Significant Bit
N_2	Nitrogen
ODPS	Oxidizer Discharge Pressure Switch
OMPS	Oxidizer Manifold Pressure Switch
PAFB	Patric Air Force Base
PCM	Pulse Code Modulation
PDT	Pacific Daylight Time
PFRT	Preliminary Flight Rating Tests
PHCV	Pyrotechnic Helium Control Valve
PIV	Propellant Isolation Valve
POSV	Pyro-Operated Solenoid Valve
PPS	Primary Propulsion System
PRF	Pulse Repetition Frequency
PTVA	Propulsion Test Vehicle Assembly
RTC	Real Time Command
SCCM	Standard Cubic Centimeters per Minute
SDP	Status Display Panel
SECO	Sustainer Engine Cutoff
SEP	Separation of the GAT from the Atlas Booster
SMRDD	Spin Motor Rotation Direction Detector
S/N	Serial Number
SPC	Stored Program Command
SPS	Secondary Propulsion System
TCA	Thrust Chamber Assembly
TCP	Thrust Chamber Pressure
TCPS	Thrust Chamber Pressure Switch
TDA	Target Docking Adapter
TOS	Turbine Overspeed Switch
UDMH	Unsymmetrical Dimethyl Hydrazine
VECO	Vernier Engine Cutoff
V/M	Velocity Meter

LOCKHEED MISSILES & SPACE COMPANY

LMSC-A774454
6 Jan 1966

Copy No.
Sheets

REPORT CHANGE RECORD
FOR

GEMINI AGENA TARGET VEHICLE 5002
SYSTEMS TEST EVALUATION (45 DAY REPORT) (U)

The following additions, revisions, or errata corrections, should be incorporated into the document identified above. This Report Change Record page should be inserted as the first page of the affected report preceding the title page. If a page in the original document is eliminated and/or replaced by the instructions which follow, the page must be destroyed according to the Air Force directive governing such destruction.

CONTRACT NUMBER AF 04(695)-545

ADDENDUM PAGE	REVISION		ERRATA		REVISION OR ERRATA CORRECTION (CORRECT IN INK)	CORRECTION MADE	
	REMOVE PAGE	INSERT PAGE	REMOVE PAGE	INSERT PAGE		INITIAL	DATE
	vii	vii					
	xiii	xiii					
	xix	xix			1-2 3rd par., line 2 - change to Figs. 1-1 and 1-2	*84+8*	
	1-5	1-5			1-4 In Fig. 1-2, change to 161 nm	*84+8*	
	1-7	1-7					
	1-9	1-9					
	1-11	1-11			2-2 1st par., line 9 - delete a ; next to last line - change for to from.	*84+8* *84+8*	
	2-3	2-3					
	2-7	2-7			2-9 1st par., line 3 - change 268 to 368.	*84+8*	
					3-4 Under listing item d., last line - change to 3.4.4.4.	*84+8*	
	3-5	3-5					
	3-7	3-7			3-13 3rd par., line 1 - delete s from systems.	*84+8*	
					3-26 Under listing item g., line 2 - change to 3-6.	*84+8*	
					3-30 In Fig. 3-7, change to START OF ANOMOLY.	*84+8*	
					3-31 In Fig. 3-10, clarify that A152 is near by triangular symbol.	*84+8*	
	3-33	3-33					
	3-35	3-35					
	3-39	3-39			3-42 1st bullet, line 2 - delete and were normal.	*84+8*	

Copy No.

Sheets

REPORT CHANGE RECORD
FOR

GEMINI AGENA TARGET VEHICLE 5002
SYSTEMS TEST EVALUATION (45 DAY REPORT) (U)

The following additions, revisions, or errata corrections, should be incorporated into the document identified above. This Report Change Record page should be inserted as the first page of the affected report preceding the title page. If a page in the original document is eliminated and/or replaced by the instructions which follow, the page must be destroyed according to the Air Force directive governing such destruction.

CONTRACT NUMBER   AF 04(695)-545

ADDENDUM PAGE	REVISION		ERRATA		REVISION OR ERRATA CORRECTION (CORRECT IN INK)	CORRECTION MADE	
	REMOVE PAGE	INSERT PAGE	REMOVE PAGE	INSERT PAGE		INITIAL	DATE
	3-43	3-43					
	3-47	3-47			3-56 3rd par., line 6 - correct spelling of environment.	8t/8	
					3-61 1st par., line 6 - correct spelling of concerning.	8t/8	
					3-62 3rd par., line 1 - change 3-21 to 3-27.	8t8	
	3-63	3-63			3-66 In Fig. 3-31, add arrow head at dotted line.	8t8	
	3-67	3-67			3-75 Last par., line 4 - delete immediately	8t8	
					3-81 1st par., last line - delete word exit.	8t8	
	3-85	3-85					
	3-87	3-87			3-89 Change 2nd par. heading to d.	8t8	
					3-99 1st par., line 3 - change first is to in.	8t8	
	3-101	3-101					
	3-103	3-103					
	4-1	4-1					
	4-3	4-3					
	4-5	4-5					
	A-3	A-3					
	A-5	A-5					
	A-7	A-7					
	A-9	-					
	C-3	C-3					
	C-5	C-5					
	C-9	C-9					

Sheet 2 of 3

Copy No.

Sheets

REPORT CHANGE RECORD
FOR
GEMINI AGENA TARGET VEHICLE 5002
SYSTEMS TEST EVALUATION (45 DAY REPORT) (U)

The following additions, revisions, or errata corrections, should be incorporated into the document identified above. This Report Change Record page should be inserted as the first page of the affected report preceding the title page. If a page in the original document is eliminated and/or replaced by the instructions which follow, the page must be destroyed according to the Air Force directive governing such destruction.

CONTRACT NUMBER   AF 04(695)-545

ADDENDUM PAGE	REVISION		ERRATA		REVISION OR ERRATA CORRECTION (CORRECT IN INK)	CORRECTION MADE	
	REMOVE PAGE	INSERT PAGE	REMOVE PAGE	INSERT PAGE		INITIAL	DATE
					C-13 In Table C-3, second item in 1st column – correct spelling to circuit.		
					C-19 1st par., line 1 – correct spelling to unbonded.		

Sheet 3 of 3

Section 1

INTRODUCTION

Section 1

INTRODUCTION

1.1 PURPOSE AND SCOPE

This report has been prepared to provide an evaluation of the flight performance of Gemini Agena Target Vehicle 5002, which was launched from Complex 14, Cape Kennedy, Florida, on 25 October 1965.

The report documents the test objectives and results, the flight performance, and the conclusions and recommendations. The flight performance and the degree of success are evaluated on the basis of preflight checkout and launch preparation records, visual observations of flight, and telemetry and tracking data. Conclusions and recommendations are based on interpretation of all available information. Atlas-derived data are discussed, where applicable, to the extent made known to Lockheed Missiles & Space Company (LMSC). The General Dynamics/Convair (GD/C) report of the Atlas performance should be consulted for detailed performance data.

In Section 2, flight performance is discussed in detail. Section 3 presents Agena Target Vehicle subsystem performance data, a description of the major anomaly that occurred, and an interpretation of the obtained data. Conclusions and recommendations are presented in Section 4.

A description of the Model 8247 engine is presented in Appendix A; the test history of the engine, in Appendix B; instrumentation characteristics, in Appendix C; and the instrumentation schedule for Agena Target Vehicle 5002, in Appendix D.

1.2 MISSION DESCRIPTION

The primary purpose of the Gemini Program is to demonstrate the feasibility of rendezvous and docking in earth orbit as an operational technique. The function of the

1-1

Agena Target Vehicle is to provide a target for the Gemini spacecraft, to participate in docking and undocking operations, and to maneuver in space in the docked and undocked configurations.

The rendezvous missions of the Gemini Program have been designed to develop the operating techniques for maneuvering, performing rendezvous procedures, and docking a manned Gemini spacecraft with an unmanned Gemini Agena Target Vehicle (GATV) in near-earth orbit. For each rendezvous mission, the GATV is launched from ETR Launch Complex 14 and the Gemini spacecraft, from ETR Complex 19. Orbital adjustments of both the spacecraft and the target vehicle (Figs. 1-1 through 1-3) are used to accomplish rendezvous and docking.

GATV 5002 was to be launched one orbit earlier than the Gemini spacecraft. The illustrated sequence of five orbit patterns (Figs. 1-2 and 1-3) demonstrates how the spacecraft would maneuver to catch up to the target vehicle. (1) The standard Atlas would boost GATV 5002 into a nearly circular orbit of 161-nm altitude. (2) After the target vehicle completed one orbit, the Titan booster would launch the spacecraft into an elliptical orbit with a 146-nm apogee and an 87-nm perigee. Because the smaller orbit has a shorter period, the Gemini spacecraft would catch up with the target vehicle in approximately four orbits. (3) If a plane difference existed between the two orbits, the astronauts would change the spacecraft's orbital plane so that it coincided with that of the target vehicle. (4) At apogee of the third orbit, the spacecraft would fire rockets to achieve a 146-nm circular orbit. (5) On the fourth orbit, when the spacecraft was slightly "behind" and 15 nm "below" the target vehicle, the spacecraft engines would be fired again to move it into an intercept trajectory. This final rendezvous maneuver would place the spacecraft on the same orbit and within docking distance of the target vehicle. The L-band radar system, capable of locating and tracking the target vehicle from a distance of 250 nm, would assist the astronauts during the maneuver. The L-band system would also allow the astronauts to signal the target vehicle, ensuring its readiness for the docking maneuver. At the rendezvous distance, the flashing beacons on the target vehicle would guide the astronauts to the

LOCKHEED MISSILES & SPACE COMPANY
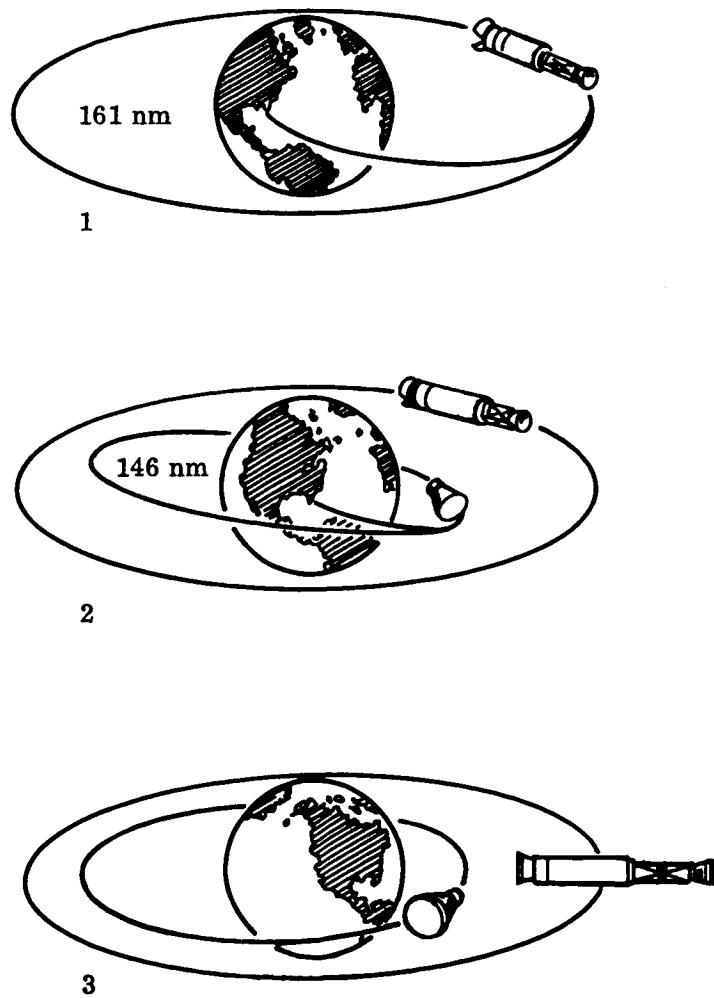
Fig. 1-1 Gemini Rendezvous Maneuver

LOCKHEED MISSILES & SPACE COMPANY
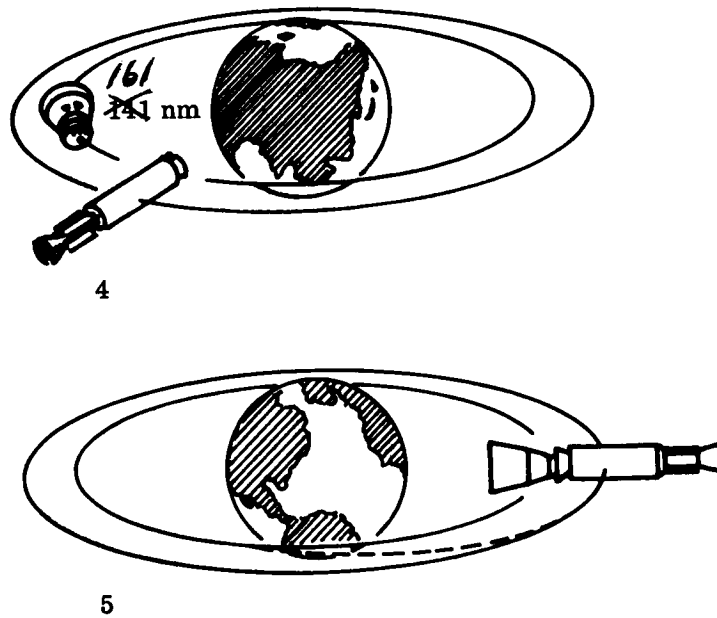
Fig. 1-2 Gemini Rendezvous and Docking

docking cone. A status display panel on the docking cone would be read by the astro-
nauts as the spacecraft approached the target vehicle. After the nose of the spacecraft
had been maneuvered into the target docking cone, the mechanical latches would fasten
the two vehicles together.

1-4
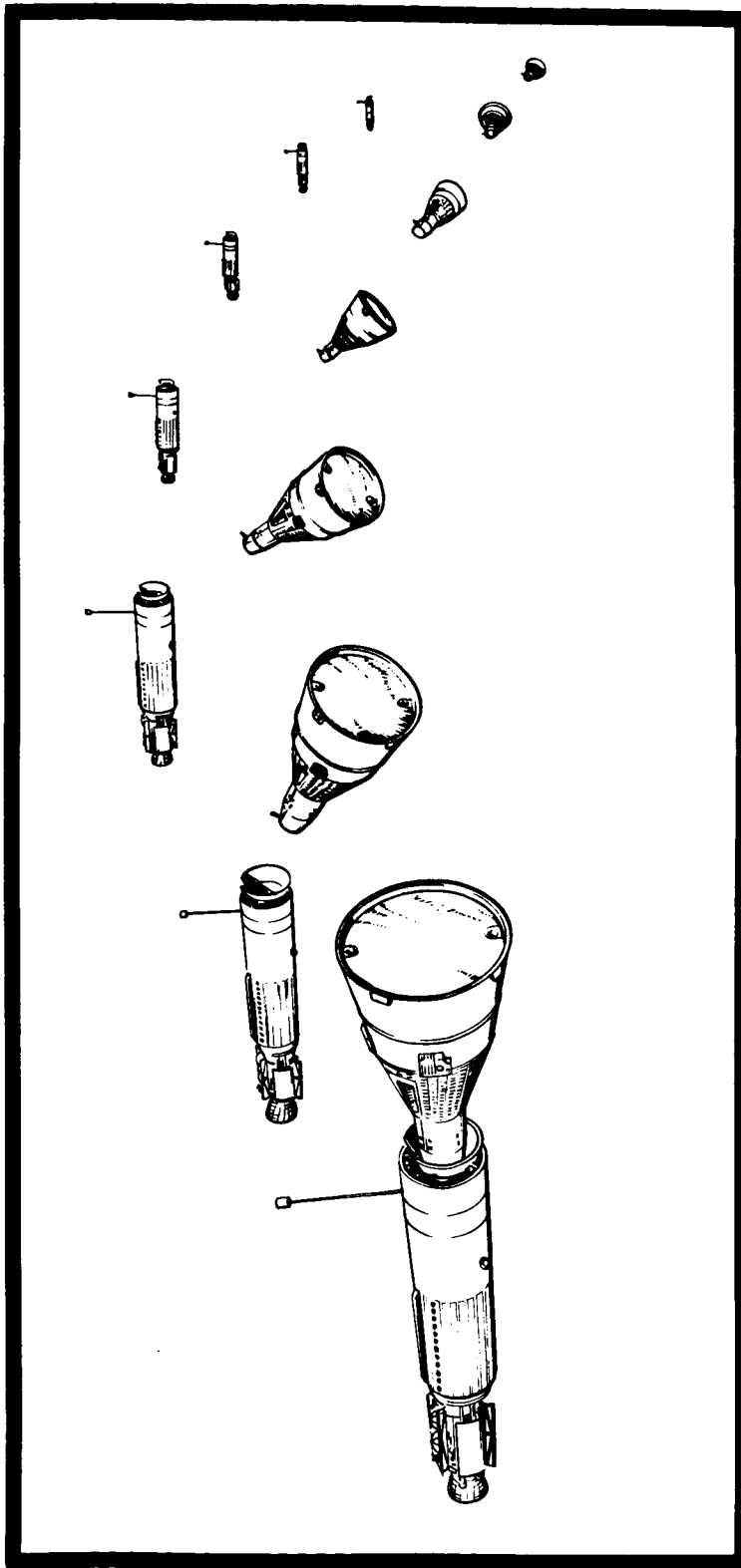
Fig. 1-3 Orbital Adjustments of Spacecraft and Target to Accomplish Rendezvous and Docking

1.3 GATV DESCRIPTION

1.3.1 General

The GATV is a program modification of the standard Agena second-stage vehicle.
The standard Agena incorporates equipment that is identified in three categories:
basic equipment, optional equipment, and program- or mission-peculiar equipment.

The Gemini mission capability is established by providing a group of optional flight
items and by installing a third group of items identified as program- or mission-
peculiar items. The GATV program-peculiar items include the two BAC Model 8250
modules for the secondary propulsion system, and a range-safety- command thrust
termination/inhibit system. The BAC Model 8247 multiple-start rocket engine is
optional equipment to the basic Agena D vehicle. For purposes of the following
discussion, the vehicle will be described by functional subsystems that represent
the GATV configuration (Fig. 1-4.)

1.3.2 Airframe

The Agena airframe, a cylindrical structure approximately 5 ft in diameter and 20.6 ft
long, consists of four major sections:

a. Forward Section. Carries the guidance, flight-control electronics,
telemetry, command, tracking, electrical power, and propellant-
pressurization equipment

b. Tank Section. Stores the fuel and oxidizer necessary for operation
of the main rocket engine; also provides the supporting surface
between the forward and aft vehicle sections

c. Aft Section. Provides for structural support and attachment of the
rocket engine assemblies, pneumatic attitude-control thrust valves,
and nitrogen storage spheres

d. Booster-adapter Section. Interconnects structures between the
GATV and the Atlas and houses the two retrorockets used for vehicle
separation and destruct charge

1-6
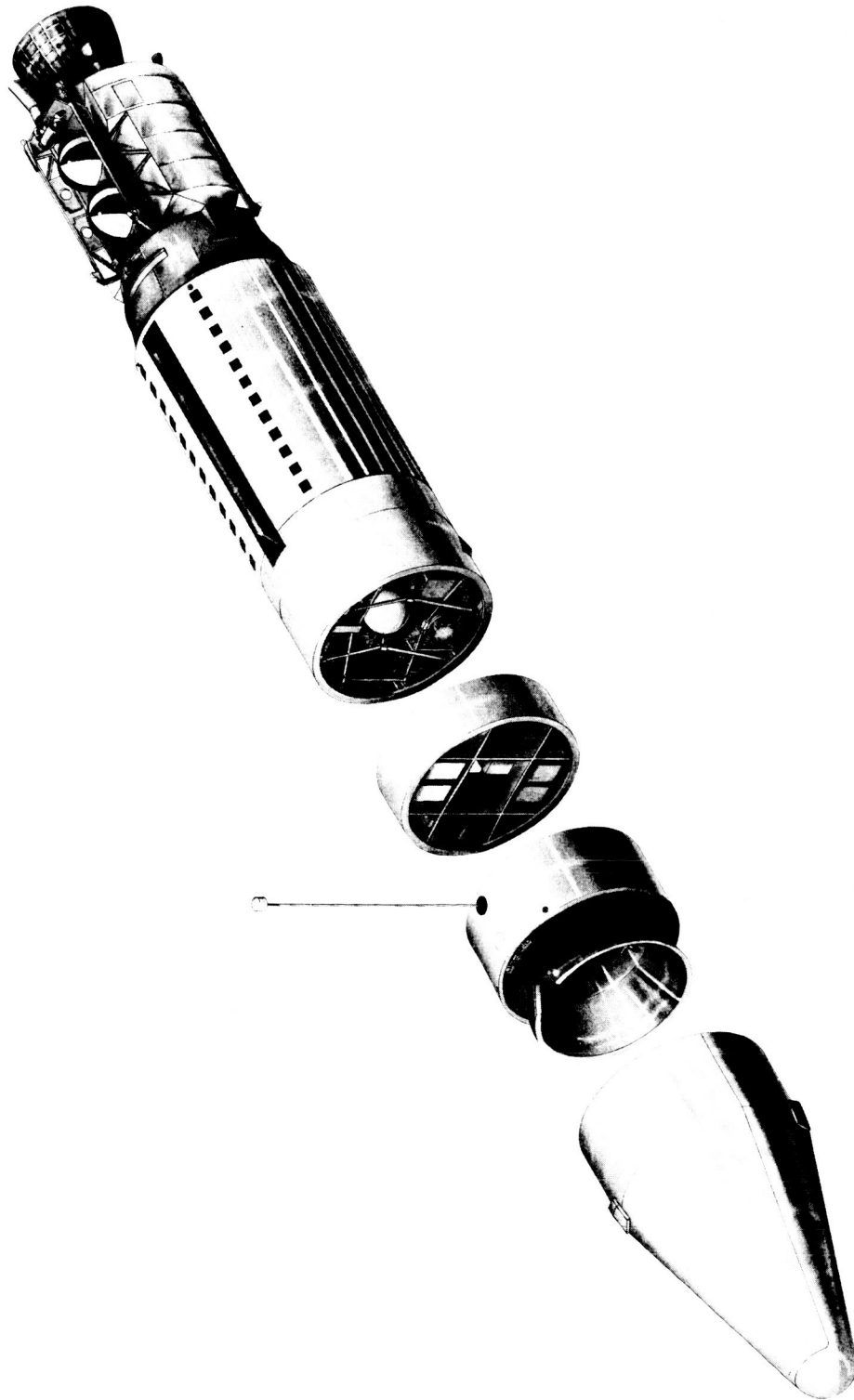
Fig. 1-4 Gemini Agena Target Vehicle Configuration

LOCKHEED MISSILES & SPACE COMPANY

1.3.3 GATV Propulsion System

Two separate propulsion systems are provided on the GATV, the primary propulsion system (PPS) and the secondary propulsion system (SPS). The PPS, which incorporates the Model 8247 rocket engine, provides the velocity gain to inject the vehicle into orbit and the thrust for larger maneuvers in orbit. The SPS includes two Model 8250 modules and provides propulsive force for small on-orbit corrections and ullage thrust for Agena PPS start.

1.3.3.1 Primary Propulsion Subsystem (PPS). The PPS (Appendix A, Fig. A-1) comprises a BAC Model 8247 engine with multiple-start capability and a propellant and pressurization system.

The engine is designed for a nominal thrust duration of 240 sec with an overall nominal thrust rating of 16,000 lb (vacuum); it uses unsymmetrical dimethylhydrazine (UDMH) as fuel and inhibited red fuming nitric acid (IRFNA) as oxidizer. Main propellant tanks are pressurized with helium to ensure proper engine turbo-pump operation.

The propellant and pressurization system maintains the desired pressures in the propellant tanks and at the engine turbopump inlet and provides for passage of propellants between these units. This system consists of a helium supply sphere, pyro operated helium control valve and gas and propellant couplings, propellant isolation valves, and associated propellant lines and bellows. (A typical start sequence is presented in Appendix A.)

1.3.3.2 Secondary Propulsion System (SPS). The SPS is installed in the GATV to provide small increments of thrust for making changes to the vehicle position and orbit. The SPS is used for orbit maneuver when the required velocity increment is less than the minimum impulse capability of the PPS. The SPS also provides ullage thrust for orientation of the propellants in the PPS main tanks for Agena engine start.

1-8

1.3.4 Electrical Subsystem

The electrical power system provides and distributes various forms of power to the GATV equipment. Internally mounted primary batteries begin to furnish power shortly before launch when the ground-supplied electrical power is disconnected and the primary battery circuit is energized. Unregulated 28v dc power is supplied for most of the using components. Electrical power system components also modify the battery-supplied power to provide regulated 28v dc and 115v ac power. Power is distributed through a network of harnesses and junction boxes, with power for pyrotechnic devices routed separately.

1.3.5 Guidance and Control Subsystem

The guidance and control system has the following primary functions:

a. To maintain the GAT* at the proper attitude at all times

b. To provide switch closures at the proper times to accomplish the desired ascent sequence-of-events

c. To provide the propulsion shutdown signal after the desired velocity-to-be-gained has been achieved

The major components of the system are the inertial reference package (IRP), horizon sensor, flight-control electronics unit, hydraulic attitude-control system, pneumatic attitude-control system, velocity meter, flight control logic package, and electro-mechanical timer. An inertial space reference is provided by the IRP, and an earth reference for the IRP is supplied by the horizon sensor.

The IRP controls the attitude of the GAT by applying attitude-error signals to the flight-control system, which in turn applies torques to the GAT. Attitude corrections are made by two hydraulic actuators that gimbal the engine, providing thrust vector control during engine operation, and six pneumatic thrust valves that emit gas jets, torquing the vehicle during the steady-state orbit condition. The velocity meter provides an

---

*GAT is an acronym used to designate the Gemini Agena Target orbital stage. It constitutes what remains of the GATV after the shroud, adapter, and other droppables are ejected.

engine-shutdown signal when the desired velocity-to-be-gained has been achieved, and the standard sequence timer provides the programming for the ascent sequence-of-events and engine start.

1.3.6 Communications and Command Subsystem

Functional and environmental conditions of the GATV are monitored and transmitted by the PCM communications system during the ascent phase and on orbit. The C&C system receives ground and Gemini spacecraft signals for command of the GAT on orbit. Tracking capability is also provided by pulse-coded beacons. Major components of this subsystem are two VHF 2-watt transmitters, a tape recorder, PCM telemeter, and instrumentation; a UHF command receiver, programmer, and controller; and S-band, C-band, and L-band beacons.

1.4 COUNTDOWN

The range countdown was initiated at 0040 Eastern Standard Time (EST) 25 October 1965. The countdown was exceptionally smooth with no technical holds called. All countdown tasks were started and finished on time.

The only anomaly observed concerned the temperature of the case of battery No. 2 (measurement C13). This temperature was reported to be 127°F during Task L-4 (Agena Power Preparations). A check was made to determine whether the transducer or the ground instrumentation was the source of the high reading. A pyrometer check of the battery case temperature was performed and reported as 58°F. NASA and Air Force personnel discussed the matter and decided not to take any further action. The access door to the battery compartment was reinstalled.

Liftoff occurred at 1500:04.490 GMT (1000:04.490 EST).

1.5 ASCENT

The ascent of Vehicle 5002 as compared to the typical GATV ascent is described as follows:

Actuation of General Electric (GE) relay K1 in the Atlas guidance system, which initiates the GATV sequence-of-events by starting the sequence timer, typically occurs at liftoff plus 274.2 sec (as compared to liftoff plus 273.61)* by discrete command from the GE Mod III ground guidance system. Other discretes issued by the GE system include booster engine cutoff (BECO),sustainer engine cutoff (SECO), vernier engine cutoff (VECO), and separation of the GAT from the Atlas booster (SEP) – all within 2 sec of the nominal time. (SECO also ejects the L-band transponder cover; VECO ejects the horizon-sensor doors, uncages the Agena gyros, and resets the turbine overspeed circuit; and SEP fires the circumferential mild detonating fuse and the two retrorockets on the Agena booster adapter. The Agena pneumatics are activated by a separation switch.)

At 335.2 sec (334.8 sec),* the sequence timer initiates the following two events: (1) opening of the SPS pressurization start valve, thereby preparing the SPS for 16-lb thrust operation prior to PPS first burn, and (2) application of a -90-deg-per-min pitchover command to the IRP pitch gyro, thereby causing the GAT to rotate about its pitch axis and the longitudinal axis to approach the desired flight path. At 348.2 sec (347.65),* the sequence timer disconnects the -90-deg-per-min pitch program, applies the -3.99 deg-per-min orbital geocentric rate to the pitch gyro, and connects the horizon-sensor pitch channel to the pitch gyro. The horizon sensor is maintained at a bias angle of 0 deg, 18.6 min, to ensure nose-up attitude of the GAT during PPS first burn. At 348.2 sec (347.65 sec),* the sequence timer enables the velocity meter, and its counter starts counting down any pulses generated by the velocity meter accelerometer.

---

*Actual flight times (seconds after liftoff) of Vehicle 5002 are presented in brackets.

The SPS 16-lb thrust chamber bipropellant valves are opened at 350.2 sec (349.71 sec)*
by the SPS 16-lb thrust initiate signal from the sequence timer. The SPS provides a
slight acceleration for PPS propellant orientation prior to PPS thrust initiate. At this
time, the sequence timer also removes the geocentric rate ON signal from the flight
command logic package and starts the SPS status display panel (SDP) clock.

The PPS thrust-initiate signal is generated by the sequence timer at 368.2 sec
(367.53 sec).* (Refer to Appendix A for the complete PPS start sequence.)

It was at this moment that the anomaly occurred (approximately 368.404 sec),* and
telemetry was lost (at 375.4 sec),* as verified by loss of signal strength.

Subsequent events for a nominal ascent are as follows: SPS "OFF," at 377.53 sec
(3 sec after the SPS SDP clock stops) a signal is generated that fires the nose shroud
squibs. Normal PPS first burn lasts for approximately 183.5 sec. During this period,
pitch and yaw gyros control the attitude of the GAT by gimbaling the PPS rocket
engine. The attitude of the GAT in roll is controlled by the IRP roll gyro, gyro error
compensation being provided by the signal from the horizon sensor roll channel. The
roll gyro controls the roll attitude of the GAT by pulsing the appropriate pneumatic gas
valves.

At 533.2 sec, the sequence timer arms the PPS thrust cutoff circuit, and approximately
10.5 sec later the velocity meter generates the PPS thrust cutoff signal (velocity
meter counter has been counted down to zero, indicating that the velocity-to-be-gained
has been achieved). This signal enables the attitude control system (ACS) pitch and
yaw pneumatic channels, opens the pilot-operated solenoid valve (thereby allowing
actuation pressure to vent causing the fuel valve to close), and closes the two
gas-generator solenoid valves. At 555.7 sec, the sequence timer generates a PPS
thrust cutoff backup signal. Five seconds later, at 560.7 sec, the sequence timer
generates a signal that supplies closing power to the PPS propellant isolation valves
and the oxidizer lipseal pressure valve. At 566.7 sec, the sequence timer generates

---

*Actual flight time (seconds after liftoff) of Vehicle 5002 are presented in brackets.

a signal that removes power from the PPS propellant isolation valves and the oxidizer lipseal valve and generates a signal that changes the ACS deadband to its wide setting (gas-saving mode). Thirty-five seconds later, the sequence timer disables the velocity meter; cycles the pitch, roll, and yaw horizon sensor gain circuits to their low mode (gas-saving mode); and turns on the gyrocompassing circuit. At 604.7 sec, the sequence timer switches the telemetry transmitters from the ascent antenna to the orbit antenna and also disables the flight termination receivers. At 695.7 sec, the sequence timer fires the squibs that position the horizon sensor to its zero position (orbit mode) and generates the shutdown sequence timer signal that causes the sequence timer to shut down. One-half second later, at 696.2 sec, the last action of the sequence timer is to remove the shutdown sequence timer signal. At this point, the GAT is injected into the desired orbit, the guidance and flight control systems are maintaining the target at the proper attitude, the C-band and S-band transponders are functioning (tracking), telemetry is functioning, and the sequence timer is permanently turned off. Any further control and maneuvering of the GAT is accomplished by real-time or stored-program commands from the UHF digital command system or by L-band or hardline commands from the spacecraft.

1.6 MISSION OBJECTIVES

The mission objectives for the Gemini VI mission were as follows:

- Achieve rendezvous and docking of the Gemini spacecraft with the Agena Target Vehicle, using both the spacecraft and Agena capabilities, as required
- Complete rendezvous using the radar-computed closed-loop orbital mechanics rendezvous mode
- Perform Agena vehicle checkout, determine its safety status, and test the Agena attitude maneuver capability while the vehicles are docked
- Evaluate the Agena maneuver capability after the vehicles are separated. Also evaluate the capability to command Agena maneuvers from the spacecraft and from the ground
- Perform experiments as assigned by NASA Office of Manned Spaceflight.

Objectives and general degree of achievement are listed in Table 1-1.

Table 1-1

ACHIEVEMENT OF OBJECTIVES

Test Objectives	Achievement		
	Yes	Partial	No
ATLAS PRIMARY OBJECTIVES			
1. Boost the GATV into the coast ellipse as defined by the ascent guidance program	X		
2. Initiate or relay the discrete startup command for the GATV ascent sequence time and the Atlas/GATV separation command	X		
ATLAS SECONDARY OBJECTIVE			
Determine Atlas systems performance utilizing telemetry data	X		
GATV PRIMARY OBJECTIVES			
1. Boost itself into a 161-nm circular orbit with an orbital inclination angle of 28.87 deg			X
2. Maintain itself in a stable attitude for a nominal 5-day active orbital life			X
3. Receive, store, and execute ground-initiated commands and receive and execute spacecraft-initiated commands for orbital control of guidance, propulsion, docking, and communications systems			X
4. In response to commands, maneuver into a new orbit			X
5. Provide a man-safe environment during the rendezvous phase of the 5-day mission and participate in docking and undocking operations with the Gemini spacecraft			X
6. Provide a man-safe environment in the docked configuration while operating the primary or secondary propulsion system*			
GATV SECONDARY OBJECTIVE			
Determine GATV systems performance utilizing telemetry data		X	

*Eliminated as objectives for Gemini Mission VI immediately before launch.

LOCKHEED MISSILES & SPACE COMPANY

Section 2

FLIGHT PERFORMANCE

Section 2

FLIGHT PERFORMANCE

Countdown for the Gemini VI launch began at 0040 EST on 25 October 1965 and proceeded smoothly without incident to liftoff. Liftoff occurred from AFETR Complex 14 at 1000:04:490 EST on 25 October (1500:04.490 GMT). Launch azimuth was 85.70 deg.

Evaluations of the coast ellipse of Vehicle 5002 were derived from the received sets of AFETR radar data, which were inconsistent; the following deviations are averages based on the two near-real-time Burroughs vectors:

    a.   Apogee Radius − 565 ft
    b.   Apogee Velocity − .27 fps
    c.   Inclination − .003 deg

The General Electric (GE) tracking radar data provided a value of approximately 3 fps for the retrovelocity applied to the booster at separation.

The 0.18 (PAFB) tracking data were selected for anlaysis of the flight subsequent to SPS ignition. The performance of the SPS was deduced to be close to nominal, and it was shown that the PPS delivered an impulse of approximately 3550 lb-sec and of approximately 0.5 sec duration. It was not practical to define the impulse shape more accurately from the radar data.

It was apparent from the data that a failure occurred at a time consistent with the loss of telemetry signals.

LOCKHEED MISSILES & SPACE COMPANY

2.1 SUMMARY

The estimates from the near-real-time Burroughs vectors indicated that system performance prior to SPS ignition was close to nominal, and that the 5002 vehicle was placed on an ellipse with close to the desired energy. Sequence-timer start was commanded to provide the SPS ignition signal at close to the desired time, and there was no evidence in the radar data of anomalous SPS performance. The PPS ignition signal also occurred at close to the desired time, but analysis of the radar data provided confirmation of a problem with 5002 performance after PPS ignition. It was deduced that the PPS had delivered an impulse of approximately 3550 lb-sec starting at 368.15 sec after liftoff that lasted for not more than 0.5 sec. The plot of the slant range residuals indicated that, at a time corresponding to that when loss of telemetry signals occurred, there was an aprupt loss of radar beacon lockon. The skin track data from the PAFB 0.18 radar for times past this event were extremely noisy because of the high slant range and the multiple targets that were observed. No performance analysis was practical from this skin track.

2.2 SEQUENCE OF EVENTS

Table 2-1 shows the sequence of significant flight events.

LOCKHEED MISSILES & SPACE COMPANY

Table 2-1

SEQUENCE OF FLIGHT EVENTS

Event	Flight Time (Sec)	
	Nominal	Actual
Liftoff (1500:04.490 GMT)	0	0
Booster engine cutoff (BECO)*	131.0	130.45
Start sequence timer	274.2	273.61
Sustainer engine cutoff (SECO)*	281.99	281.39
Vernier engine cutoff, (VECO)*	302.34	303.70
Gyros uncaged	302.34	303.72
Horizon-sensor doors jettisoned	302.34	303.72
Atlas/GATV separation — primacord and retros fired	304.5	305.96
Enable ACS (pneumatics)	307.0	308.42
Set pitch rate to -1.5°/sec	335.2	334.8
Open SPS press. start valve	335.2	334.8
Pitch program "Off"	348.2	347.65
Geocentric rate "On" (3.99°/min)	—	—
Enable velocity meter	—	—
Open SPS 16 lb bipropellant valves (SPS thrust initiate)	350.2	349.71
PPS thrust initiate	368.2	367.53
Disable pneumatics (P & Y)	368.2	367.53
SPS cutoff	370.2	369.51
Start of anomaly	—	368.404
Loss of telemetry signal	—	375.4

*Verified by GD/C telemetry measurements.

The GATV 5002 weight sequence is presented in Table 2-2. Table 2-3 is a summary of weight, center of gravity, and moment of inertia. These data reflect actual weight, propellant and control gas loadings, expenditures of control gas and propellants as determined from telemetered data, and Atlas booster data provided by GD/C.

Table 2-2

POSTFLIGHT WEIGHT DATA

Item	Weight (lb)
GATV Weight Empty	4,043
Total Propellants and Gases Loaded*	14,051
Gross Weight, Atlas Payload	18,094
Less: Booster Adapter and Extension	-384
Self-Destruct Items	-11
Separation Detonator and Charge	-1
Retrorockets	-10
Horizon Sensor Fairings	-7
Separation Weight	17,681
Less: Attitude Control Gas	-2
SPS Propellant	-2
Propellant Preflow	-6
Flight Termination	17,671

---

*Propellants and gases loaded included the following:

Helium (Propellant Tank Pressurization)	4
Attitude Control Gas	141
PPS Oxidizer Loaded (IRFNA)	9,732
PPS Fuel Loaded (UDMH)	3,825
SPS Oxidizer Loaded (MON)	179
SPS Fuel Loaded (UDMH)	157
SPS Nitrogen Pressurization Gas	9
PPS Start Tank Propellants	4

2-4

Table 2-3

WEIGHT, CENTER-OF-GRAVITY, AND MOMENT OF INERTIA SUMMARY

Condition	Weight (lb)	Center of Gravity (In.)			Moment of Inertia (Slug-Ft^2)		
		X	Y	Z	I_{xx}	I_{yy}	I_{zz}
Liftoff	278,500	843.2	-0.5	-0.4	10,440	2.67×10^6	2.67×10^6
Agena Gross Weight	18,094	339.8	0.5	0	538	13,808	13,825
Separation	17,681	337.1	0.5	0	454	12,359	12,377
Flight Termination	17,671	337.2	0.5	0	454	12,375	12,393

2.3 PERFORMANCE

2.3.1 System Performance Prior to SPS Ignition

The sources available for analysis of the coast ellipse prior to SPS ignition were the two Burroughs vectors, five AFETR radars (PAFB, Merritt Island, Grand Bahamas, Grand Turk, and Antigua) and the GE Mod III guidance radar. The Burroughs vectors were selected for times after VECO and prior to separation; therefore, the coast ellipse estimates are valid for the 5002 vehicle, assuming no disturbing influence from the separation events. The estimates from the five AFETR radars also are valid for the 5002. However the GE guidance radar tracked the Atlas 5301 booster, and the corresponding apogee conditions refer to the booster coast ellipse after separation.

Figure 2-1 presents a plot of the apogee radii and apogee velocities for the coast ellipses derived from the indicated sources, and Table 2-4 lists the relevant parameters. The estimates from the AFETR 0.18 and 19.18 radars, rather than the other radars, are used because they are in agreement with the two Burroughs estimates that provided the evaluation of the 5002 vehicle coast ellipse. Compared with the preflight

LOCKHEED MISSILES & SPACE COMPANY

CONFIDENTIAL
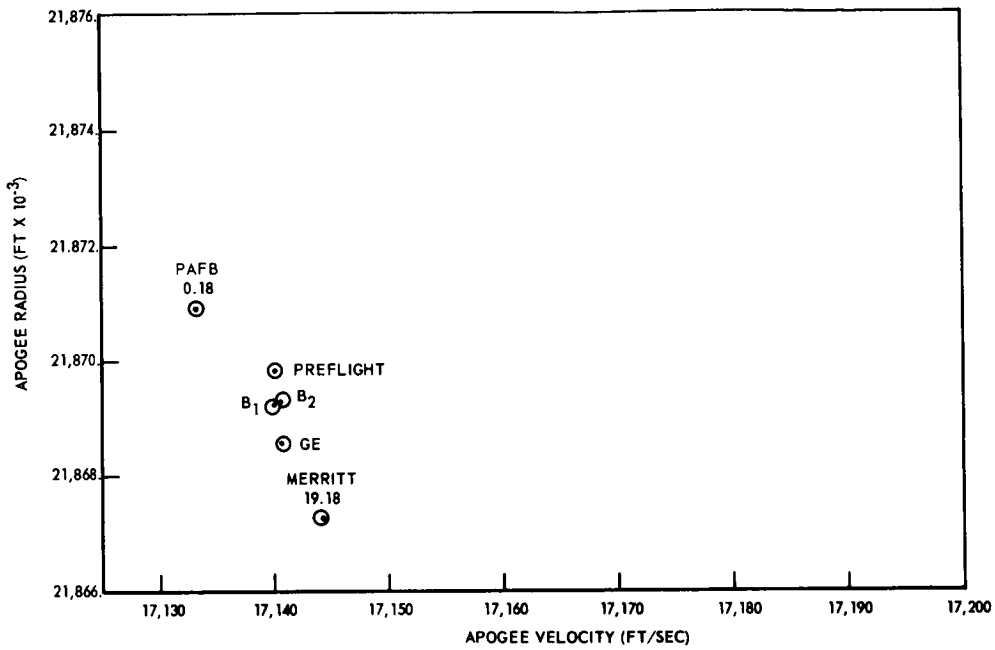
Fig. 2-1 Coast Ellipse Evaluation, Apogee Radius vs Apogee Velocity

Table 2-4

COAST ELLIPSE PARAMETERS

Item	Units	Preflight Nominal	Burroughs		PAFB 0.18	Merritt Island 19.18	General Electric
			Vector 1	Vector 2			
Time	sec	475.93	476.31	476.33	475.44	474.56	474.70
Apogee Radius	ft	21,869,850	21,869,270	21,869,300	21,870,590	21,867,300	21,868,590
Apogee Altitude	nm	158.09	157.99	158.00	158.26	157.67	157.88
Apogee Velocity	fps	17,140.12	17,140.20	17,140.58	17,138.45	17,144.25	17,140.70
Eccentricity		.54356	.54357	.54355	.54390	.54339	.54356
Inclination	deg	28.890	28.886	28.886	28.884	28.883	28.883
Vis Viva x 10^9	fps^2	-.99350	-.99354	-.99352	-.99352	-.99351	-.99356

CONFIDENTIAL

LOCKHEED MISSILES & SPACE COMPANY

nominal values, the actual apogee velocity was 0.27 fps high, the apogee radius 565 ft low, and the inclination angle 0.003 deg low. It may be concluded that the system performed satisfactorily and placed the 5002 vehicle on a coast ellipse with close to nominal parameters.

An estimate of the retrovelocity imparted to the Atlas at separation may be obtained from Fig. 2-2, which is a plot of the R component of the GE data. The difference in the position of the slope of the data before and after separation corresponds to a retrovelocity of approximately 3 fps applied to the booster.
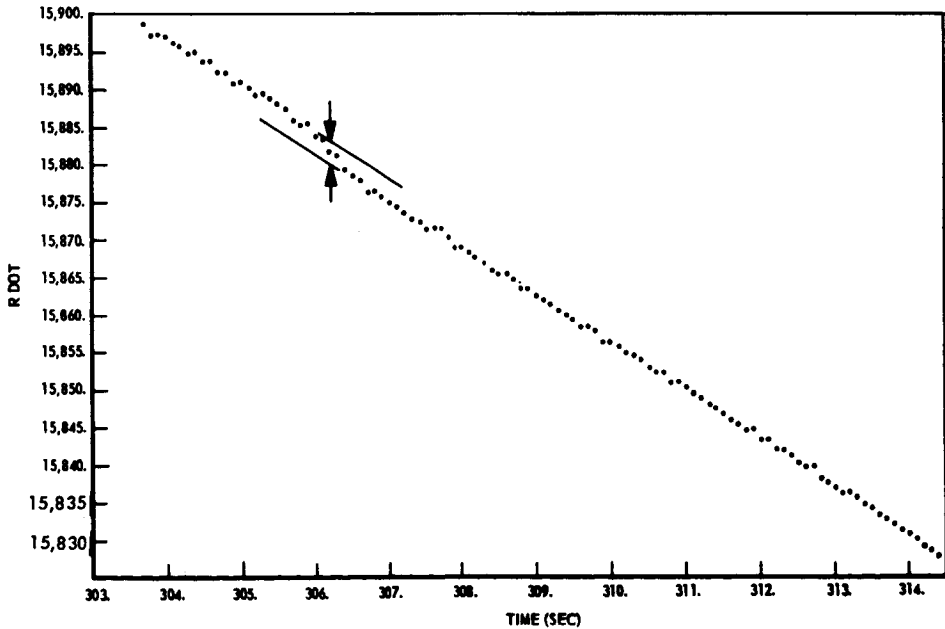
Fig. 2-2 R vs Time (303 Through 314 Sec)

CONFIDENTIAL

LOCKHEED MISSILES & SPACE COMPANY

An additional function of the system is to start the sequence timer to provide the SPS and PPS signals at the correct times. From the preflight nominal trajectory, the delay from sequence-timer start to SPS ignition was 76.00 sec and to PPS ignition was 94.00 sec. From the actual postflight sequence of events, the respective delays were 76.10 sec and 93.92 sec. It is not practical to resolve these small differences, and it is concluded that performance was nominal.

2.3.2 Vehicle 5002 Performance

Normal procedure when available radar coverage from several trackers overlaps would be to obtain a composite least-squares fit to all the data. This was not considered desirable in the present case because of the differences in the results from the AFETR data. The best approach was judged to be an analysis of the data from a single radar that provided continuous coverage through loss of signal. It was assumed that any bias in the data would be constant and would still yield valid performance data. The Patrick Air Force Base (PAFB) 0.18 radar was selected for the analysis.

Prior to the receipt of the radar data, it was known that the secondary propulsion system (SPS) had performed satisfactorily, but that the primary propulsion system (PPS) had delivered a very small impulse. The magnitude of the PPS impulse however was not known. The postflight fitting computer program was set up to simulate the nominal SPS, but no PPS, impulse. The starting point was the position and velocity vector obtained from the 0.18 (PAFB) tracking data during the coast ellipse analysis, and the postflight simulation was fitted to the 0.18 data over the time span of the SPS impulse. This step provided small corrections to compensate for unavoidable slight inaccuracies of the simulation. The adjusted simulation was then integrated through the radar data for the time period from SPS start to a point beyond loss of signal. Using an averaging technique to reduce the effects of noise, the residuals in slant range are plotted in Fig. 2-3.

LOCKHEED MISSILES & SPACE COMPANY
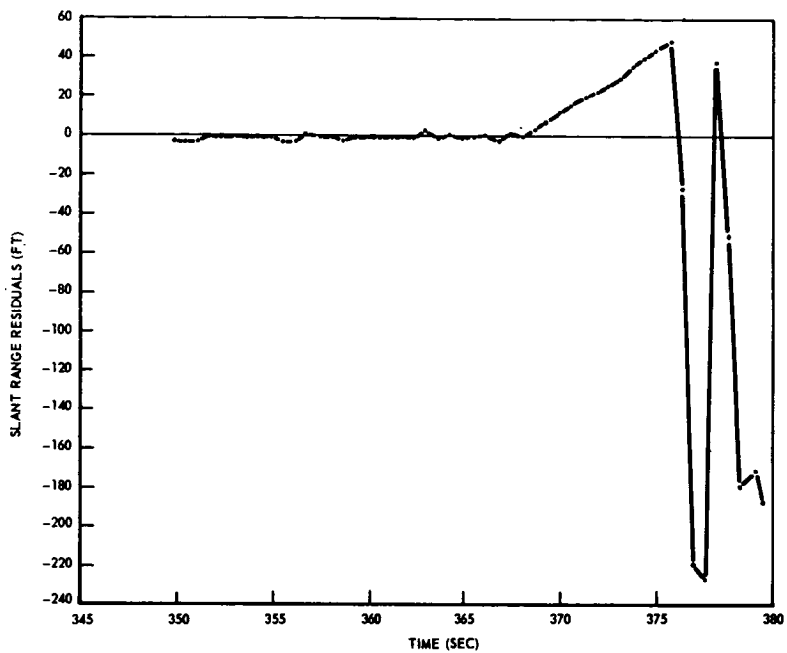
Fig. 2-3 Slant Range Residuals vs Time With No PPS Impulses (Average Between 345 and 380 Sec)

From this plot it was deduced that the adjusted postflight simulation provided an adequate representation of the system performance from the start of the SPS up to approximately 368 sec from liftoff, at which time a short duration impulse introduced a velocity not included in the simulation. This is consistent with an impulse from the PPS shortly after ignition was commanded. In addition it is apparent from Fig. 2-3 that an anomaly was introduced at a time consistent with the loss of signal experienced on telemetry channels.

The residuals for the individual data points for a 6-sec interval spanning the discontinuity at 368 sec are plotted on an expanded scale in Fig. 2-4. From the slopes of these residuals before and after the impulse, it was determined that the velocity deviation was 6.4 fps corresponding to an impulse from all sources of 3550 lb-sec. To determine the time of the start of the impulse and its duration, reference was made to the X-axis accelerometer trace, and the impulse was simulated by a square-wave function starting at 368.15 sec and lasting for 0.5 sec. The residuals obtained with the PPS simulation are plotted in Fig. 2-5 for comparison with Fig. 2-3.

2-9
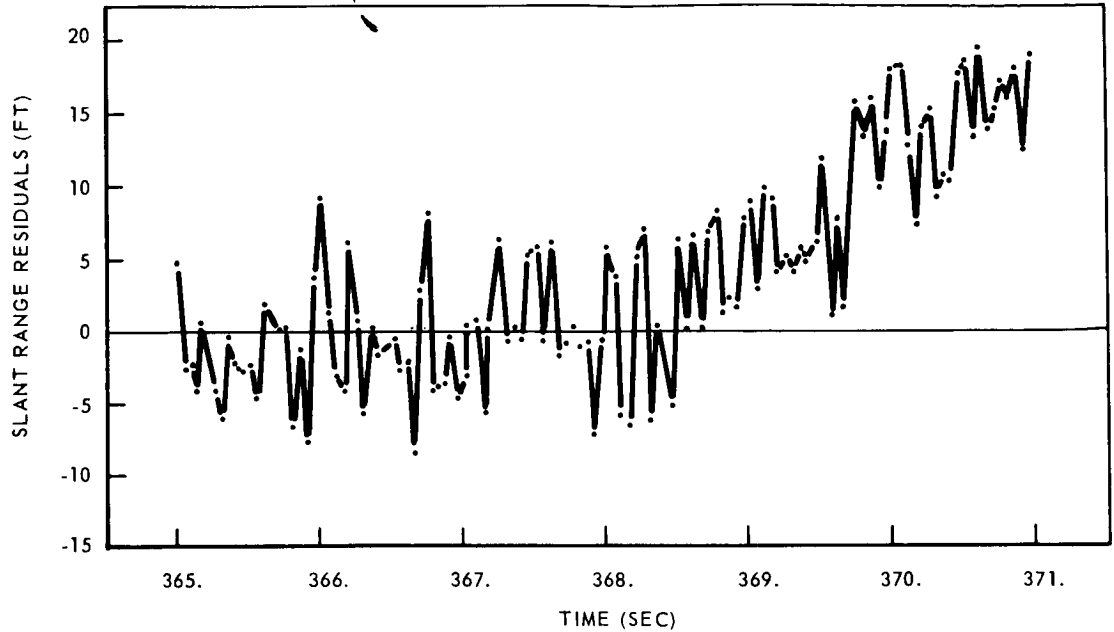
Fig. 2-4 Slant Range Residuals vs Time With No PPS Impulses (Detail Between 365 and 371 Sec)
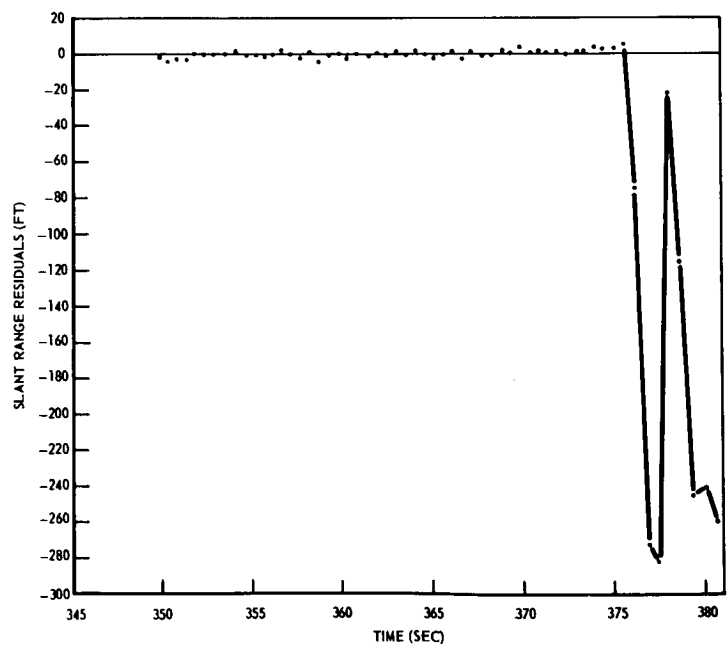
Fig. 2-5 Slant Range Residuals vs Time With PPS Impulses (Average Between 345 and 380 Sec)

2-10

The slant range residuals for the portion of Fig. 2-5 prior to the loss of signal anomaly are replotted in Fig. 2-6 on a larger scale. This plot shows the degree to which the post flight fitting program has succeeded in matching the 0.18 radar data. There are apparent errors in the initial position and velocity of approximately 2.5 ft and 0.17 fps, which are within the accuracy capabilities of the analytical techniques employed and were not artificially removed. Figure 2-6 also shows that the residual scatter is essentially random and that the simulation of the Vehicle 5002 PPS impulse by a rectangular function was adequate. Attempts to define more accurately the shape or time span of the 3550 lb-sec impulse would not provide meaningful conclusions.
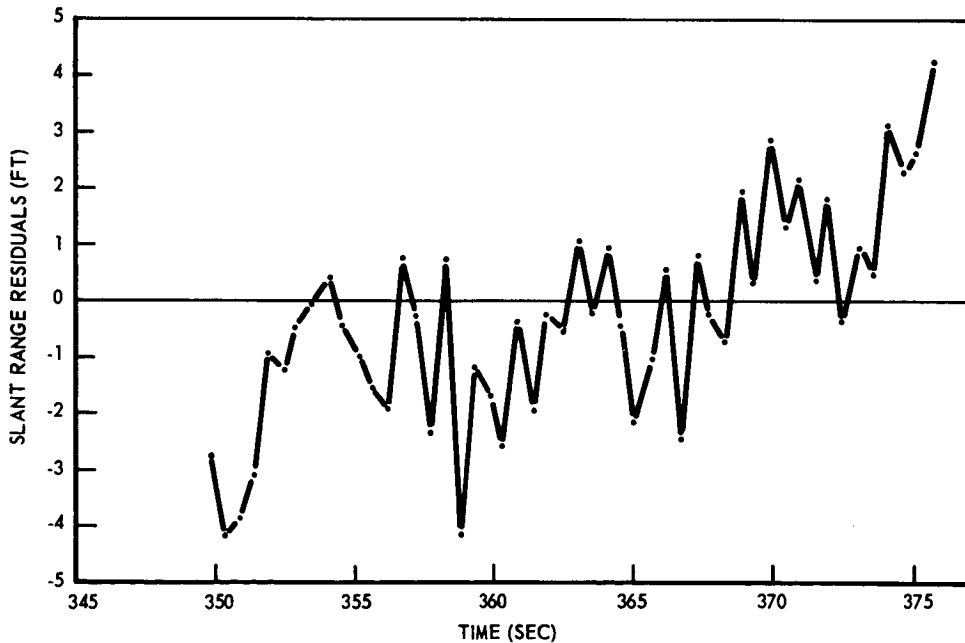
Fig. 2-6 Slant Range Residuals vs Time With PPS Impulses (Detail Between 349 and 375.7 Sec)

LOCKHEED MISSILES & SPACE COMPANY

The time span of the 0.18 radar data extended to 561 sec after launch. The slant range at beacon dropout was in excess of 3,500,000 ft and the 0.18 radar operator log reported two targets at this time. Consequently, the data for the skin lockon portion of the tracking were extremely noisy; they were useful only in confirming that some anomaly had occurred.

Of interest was the distance between the 5002 and booster vehicles at the time of loss of signal. With three assumptions: (a) the 3-fps velocity differences from the separation retromaneuver, (b) an additional 1-fps average from SPS ignition to the start of the PPS impulse, and (c) a 6-fps contribution from the PPS impulse, it was estimated that the 5002 vehicle was approximately 260 ft from the Atlas 5301 booster at loss of signal. The differences between the 0.18 and GE radar data made it impossible to obtain a verification of this estimate.

LOCKHEED MISSILES & SPACE COMPANY

Section 3

DATA ANALYSIS

Section 3

DATA ANALYSIS

3.1 GATV DATA TRANSMISSION SYSTEM

The pulse code modulation (PCM) telemetry formatting employed on the GATV provides status information on the GAT subsystems. The amount of data that must be transmitted by this system (231 measurement points), and the basic limitations of PCM data encoding and transmission, place severe restrictions on the interpretation of data in the event of an anomaly. The sampling rate of the points of interest ranged from one sample per second (temperatures) to 96 samples/sec (thrust chamber pressure). A brief description of the PCM encoding method is given in the following paragraphs.

3.1.1 PCM Telemeter Bit Stream

The PCM telemeter bit stream is the data structure of the main multiplexer that contains 128 channels and is commutated at a fixed rate of 16 frames/sec. The frame is composed of 128 channels, each of which contains pertinent data or binary words. Therefore, the transmission word rate is 2048 words/sec. Each word has 8 bits, therefore the bit rate is 16,384 bits/sec.

The telemeter bit stream is composed of "ones" and "zero's." Each of the 16,384 bits/sec will be either a "one" or a "zero." The sync word is assigned to the first three channels of the main frame.

3.1.2 Telemetry Sampling

To obtain the 8-bit digital structure of the data word, an analog-to-digital converter (encoder) is employed. Prior to this point, however, a sampling technique is required.

3-1

The electrical commutator (the multiplexer) provides for this sampling by switching internal data gates in such a manner as to present an output that is of the same d-c amplitude as the data input level presented to the data gate. The sampling and switching operation occurs during a 488 μ sec (1/2048 sec) interval. Within this time period, the encoder samples the amplitude and digitizes this level into a binary format. The sampling time is very rapid (56 μ sec) and is not initiated until one-fourth of the 488 μ sec sample period has passed to insure that switching currents do not affect the amplitude and cause erroneous encoding. An uncertainty period exists during the interval between successive data channel readouts. If a change in measurement occurs during this time interval, it can not be ascertained as to the exact instant the change did occur. For a 16 sample/sec measurement, then, this time uncertainty is 62.5 ms. (See Fig. 3-1.)
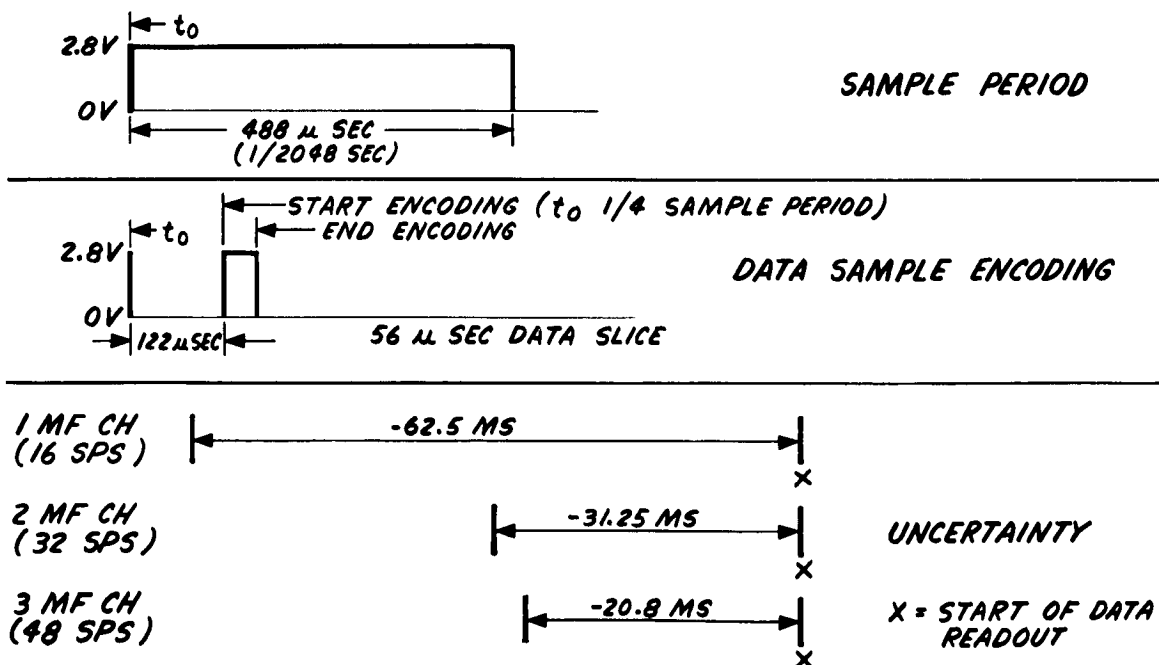
Fig. 3-1 Telemetry Sampling

3-2

3.2 COMMUNICATIONS AND COMMAND C&C SYSTEM

The C&C system consists of the following: (1) the PCM telemetry system that contains two 2-watt transmitters, a tape recorder, encoders, and instrumentation; (2) a command system that contains a UHF receiver, a programmer, and a controller; (3) a tracking system that employs L-band, S-band, and C-band beacons; and (4) a range safety system. Only the telemetry system, the C- and S-band beacons, and the range safety system are employed during ascent. This section will describe the operation of all C&C equipment during ascent.

3.2.1 Summary

The C&C subsystem performed within specification during the countdown and throughout the flight until loss of signal (LOS). There was no spurious commanding of the vehicle. Tracking and range safety systems functioned nominally.

The telemetry system operated satisfactorily throughout the flight. Out of a total of 231 discrete measurements, 223 were programmed without apparent fault.

3.2.2 PCM Telemetry System

Operation of the telemetry system was satisfactory throughout the flight. During the terminal count at T-7 min, a sync loss was noted at the ground station; it was caused by procedural requirements to start the vehicle clock and verify reset to zero. A sync loss during this operation is inherent in the design of the equipment.

The telemeter operation was normal until 3 sec after liftoff, at which time a sync loss was noted. This is an expected event that signifies phase lock with the programmer.

During the ascent phase, a momentary loss of data was experienced at 134 sec after liftoff. The data loss was due to the "staging" or booster stage passing between the telemeter antenna on the GATV and the ground station antenna and blocking the signal, which is normal occurence. At 378 sec, the transmitter carrier frequency was lost, and no additional data were received.

3-3

3.2.2.1 <u>Instrumentation Summary</u>. The instrumentation system was programmed to provide 231 discrete measurements. Each measurement was derived from a stimulus applied to a pressure transducer, a temperature sensor, or a voltage source within the indicated subsystem hardware.* Performance of the total instrumentation program during the flight was as follows:

- Programmed tabulated measurements totaled 231
- Ten measurements were lost, including three lost at anomaly
- One measurement, A523, was inadequate
- Two hundred twenty three of the measurements performed without apparent fault
- Satisfactory performance was indicated by 95.25% of the measurements

Eleven anomalies,*summarized as follows, occurred during the flight of Vehicle 5002:

a. <u>A522, "Acceleration Y Axis" Measurement.</u> The indication was normal until T + 306 sec, at which time the primacord for separating the Agena from the Atlas was programmed to fire. Then the signal went instantaneously to zero. This accelerometer is located approximately 14 in. radially in from the primacord installation, and failure is attributed to pyrotechnic shock to the amplifier at separation.

b. <u>A5, "Acceleration Z Axis Aft" Measurement.</u> Same as measurement A522, above.

c. <u>A523, "Acceleration Z Axis TDA" Measurement.</u> The output became intermittent during the following times: from T + 83 sec to T + 99.5 sec and from T + 261 sec to T ± 306 sec. Operations at other than the above periods appear satisfactory, based on previous flight data. This anomaly is attributed to a loose connection in the accelerometer or amplifier.

d. <u>B184, "Nozzle Extension Skin Temperature" Measurement.</u> Normal temperatures were measured until T ± 369.2 sec; then the output rose in 1 sec to full scale, where it remained thereafter. This anomaly could have been caused by a broken thermocouple wire, although it may also have been indicating properly as described in par. 3.4.4.4.

---

*Appendix C should be consulted for further information and detailed failure mode analysis.

e. <u>C13, "Battery Case Temperature No. 2" Measurement</u>. Excessive tempera- ▌
ture (119°F) was indicated during countdown. The battery was verified to
be within correct operating limits by hand-held instrumentation during the
countdown. This anomaly is attributed to a faulty sensor possibly damaged
during installation of the battery.

f. <u>A14, "Atlas-Agena Separation Monitor"</u>. The separation monitor indicated
an excessive voltage increase, 3.5v instead of 1.5v normally expected during
the first closure of the microswitch. During the second closure of the micro-
switch, the voltage increased beyond the 5v telemetry input limit, which pre-
vented the third step from being observed. The most probable cause for this
indication is a failure of a capacitor (C1) in the circuit. This type of failure
has not been previously observed.

g. <u>B201, "-Y Nitrogen Sphere Pressure (SPS)" Measurement</u>. The transducer
was found to be anomalous during F-2 day checks. The output remained at
zero when the sphere was pressurized to 4000 psi and verified by landline ▌
instrumentation. The anomaly is attributed to a broken input power or out-
put signal lead.

h. <u>B3, "Turbine Manifold Pressure No. 1" Measurement</u>. The measurement
indicated zero until T + 150 sec; it then drifted steadily upwards until it
reached 42 psig at 187 sec. At engine ignition, it jumped to 80 psig and
then dropped back to 42 psig.

The failure was most likely caused by a broken component or wire in the
transducer electronics package.

i. <u>B82, "Fuel Valve Actuation Pressure" Measurement</u>. The indication was
normal until T + 368.5 sec, then it rose sharply to full scale and remained
there until flight termination. The failure has not been determined; however,
the most probable cause is an abrupt mechanical shock that permanently
jammed or distorted the armature sufficiently to unbalance the reluctance
bridge or produce an off-scale zero shift.

j. <u>B6 Combustion Chamber Pressure No. 1</u>. The indication was normal until ▌
engine ignition, at which time an approximate 20-ms pressure rise
was recorded. The signal then dropped abruptly to zero. The ▌
transducer then became intermittent.

The failure may have occurred through an abnormally high-pressure surge that mechanically deformed the pressure element or damaged the electronic bridge circuitry of the transducer or through an abrupt mechanical shock.

k. B148, "Oxidizer Injector Pressure" Measurement. The output was normal during all phases of flight until after engine shutdown, when the transducer signal remained at a value of 100 psi, indicating that the transducer has sustained a zero shift. Zero shift can occur through mechanical deformation of the Bourdon tube that provides actuation of the sensing electronics.

3.2.2.2 Conclusions. After analysis of the preceding data and the additional data contained in Appendix C, the following significant conclusions on instrumentation can be drawn:

a. Pressure. The transducers measuring pressure in the thrust chamber failed in a mode indicating an abnormal pressure pulse (mechanical shock). Analysis of 168 Agena flights during the preceding 5 years shows a total of only 10 high-pressure failures. Three pressure transducers failed almost simultaneously during this flight because of the pressure pulse; this failure can be authenticated as a nonelectrical failure from the observed fact that other transducers excited through the same interface connectors did not fail.

b. Acceleration. Failure of the two accelerometer systems can be definitely attributed to pyro shock inasmuch as recent research at LMSC has shown that this shock can produce amplitudes in the vicinity of the engine ring as high as 1700g for 10 ms. Reference to the technical specifications for installed accelerometer systems (see Appendix C) shows that the output is essentially flat to 150 cps and is down 20 db at 1500 cps so that the TDA accelerometer measured only "real" rather than pyro-shock accelerations. In addition, the maximum system shock specified for these accelerometer systems is 200 g for 1 ms or 55 g for 9 ms.

c. Temperature. Temperature measuring systems are adequate as designed. A brief review of test procedures used at the launch base reveals some weaknesses in checks of functional performance of temperature measurements in the as-installed condition.

3-6

d. <u>Separation Monitor</u>. A failure occurred in the signal conditioning of this monitor. Checkout at the launch base of the functioning of the monitor may have revealed the discrepancy.

e. <u>Sampling Rates</u>. In some cases, residual sampling rates were inappropriate for good failure-diagnostic analyses. In particular, the unregulated +28v buss current monitor was sampled too infrequently, and the ampere-hour meters were sampled too much.

3.2.2 Command System

Prior to liftoff the command system is turned on. Two commands were stored in the memory prior to launch. None were transmitted from the ground during ascent. The command system performed nominally during the flight, the only exception being a spurious message acceptance pulse (MAP) generated shortly after the anomaly. The two commands stored prior to liftoff were RESET TIMER RESET and L-BAND TRANSPONDER OFF.

a. <u>H38, "Message Acceptance Pulse" (MAP) Measurement</u>. Sensor H38 is a pulse-type measurement with full scale (5.12v) indicating programmer acceptance of a command and zero level indicating no commands accepted. No commands were transmitted during the flight of GATV 5002, and therefore no MAP's should have been received. At T + 368.6 sec, a message acceptance pulse was generated by the command programmer, processed by the PCM telemetry, and recorded at the ground station. (See Fig. 3-2.) At 368.4 sec, 200 ms prior to the MAP pulse, the engine switch group voltage went to zero volts.

The most reasonable explanation of the spurious MAP pulse is that, during the severe mechanical shock, a short-duration short circuit occurred. This happened during the severing of the electrical harnessing, which in turn, caused a fast rise-time transient to be coupled from the adjacent wiring into the MAP pulse generation circuit.
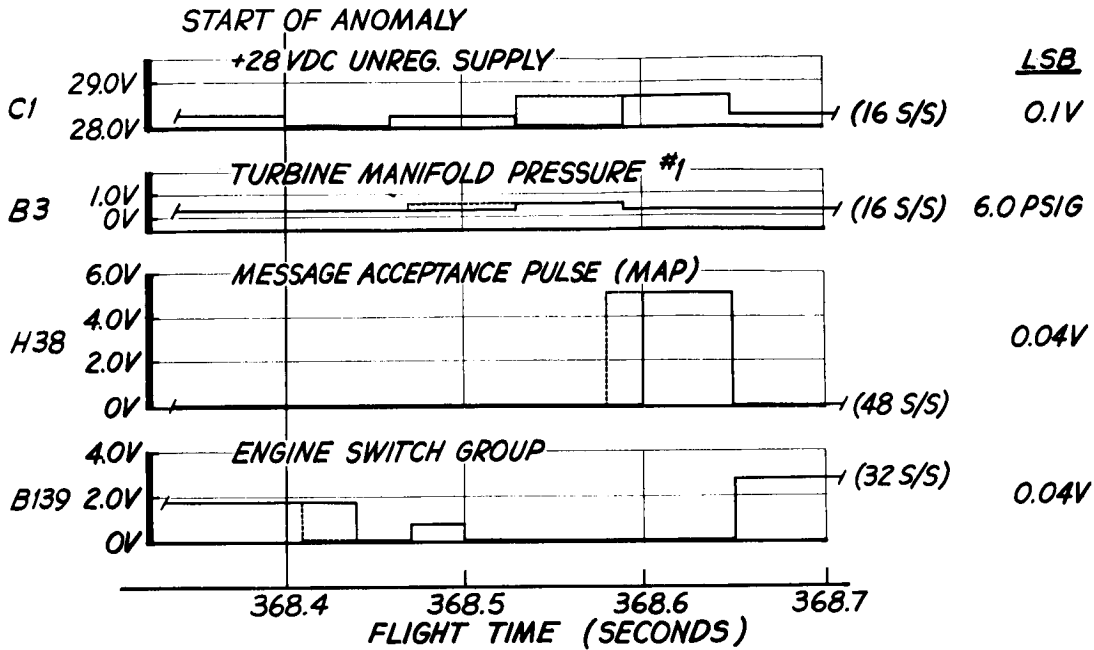
Fig. 3-2 Message Acceptance Pulse Anomaly

During the simultaneous launch demonstration (SLD) of Vehicle 5001 at AFETR, spurious MAP pulses were reported by the Hangar E ground station. This problem was evaluated, and it was found that the MAP-generating circuit in the command programmer was at threshold when its output was subjected to a 1-μsec rise-time, 0.8v amplitude transient. A modification to reduce the circuit sensitivity was therefore incorporated by grounding the negative MAP line at the programmer.

b. H165, "Vehicle Time Word" Measurement. The vehicle clock operated correctly and kept perfect time from its start at Atlas liftoff until LOS. The vehicle time word lagged flight time by 1 sec after liftoff, with a final vehicle time word reading of 374 sec at a flight time of 375 sec, which is within tolerance. An examination of the memory readout (H32) shows that the memory readout was correct at LOS (375.4 sec). In order for the memory readout to be correct, the clock must be functioning correctly. Therefore, the vehicle clock operated correctly until LOS.

c. <u>H32, "Memory Readout" Measurement</u>. The memory readout was correct at all times throughout the flight.

d. <u>Other Measurements</u>. All other command system measurements indicated normal operation throughout the flight. (See Table 3-1.)

3.2.4 Tracking System

The tracking system performed satisfactorily throughout the flight.

3.2.4.1 <u>C-Band Transponder</u>. The performance of the C-band transponder is indicated by measurement H174, "C-Band Transponder Output PRF Monitor." The variations in output PRF were due to the number of range tracking stations interrogating at that time. Each tracking station interrogates at 160 interrogations/sec except when one station adds an identifier; i.e., the PRF of that station is increased to 320 interrogations/sec. Table 3-2 presents the number of tracking stations that interrogated at various times during the flight. It should be noted that the PRF monitor was within the telemeter accuracies. The momentary decreases in PRF at about 161 sec and 230 sec was due to one of the tracking stations making adjustments for pulse spacing, etc.

3.2.4.2 <u>S-Band Transponder</u>. The performance of the S-band transponder is indicated by the H47 and H48 measurements, the S-band input PRF monitor, and the S-band output PRF monitor, respectively. The S-band input PRF monitor indicated rapid variations in interrogation rate. The S-band output monitor and the range tracking verify that the interrogation rates as shown in Table 3-2 over certain periods were not changing as rapidly as indicated by the input monitor. These variations could be due to some spurious signals in the S-band frequency range. The performance is determined from the comparison of tracking station interrogations with the replies as shown in Table 3-2.

LOCKHEED MISSILES & SPACE COMPANY

Table 3-1

C&C EQUIPMENT DATA

Measurement Number	Measurement	Specification Range	5002 Flight Result
H33	Programmer Power Supply Temperature	-30° F to 165° F	71° F to 67° F
H6	Programmer Clock Temperature[a]	170° F to 180° F	175° F to 180° F
H7	Programmer Memory Temperature	-30° F to +165° F	62° F to 57° F
H27	Programmer Voltage Regulator (+60v)	56v to 64v[b]	60.6v[c]
H28	Programmer Voltage Regulator (+40v)	37v to 43v[b]	40.3v[d]
H29	Programmer Voltage Regulator (+5.7v)	5.45v to 5.96v[b]	5.75v[e]
H30	Programmer Voltage Regulator (-5.7v)	-5.43v to 5.98v[b]	-5.90v[f]
H35	Controller Voltage Regulator (6v)	5.4v to 6.6v	6.00v
H57	UHF Receiver B+		28.3v
H59	UHF Receiver Temperature	-30° F to +165° F	71.5° F
H60	UHF Receiver Signal Level	-120.5 dbw to 37.5 dbw	Shows limiting[g]
H171	UHF Phase Lock	0.1v inhibit/3.5v lock	3.28v[h]

(a) Oven controlled temperature.
(b) The specified limits are correct when the vehicle clock is running. The vehicle clock was off for 7 min prior to liftoff and started at liftoff.
(c) Indicated 66.6v before liftoff.
(d) Indicated 42.1v before liftoff.
(e) Indicated 5.91v before liftoff.
(f) Indicated -5.80v before liftoff.
(g) Superior signal at all times.
(h) Phase lockon (nominal)

3-10

LOCKHEED MISSILES & SPACE COMPANY

Table 3-1 (Cont.)

Measurement Number	Measurement	Specification Range	5002 Flight Result
H52	Coder Lockon	3.25v ±0.5v for lock 0 to 1v no lock	1.16v[i]
H62	VHF Transmitter No. 1 Temperature	-30° F to +165° F	69° F to 81° F[j]
H63	VHF Transmitter No. 2 Temperature	-30° F to +165° F	57° F[k]
H180	PCM Tray Temperature	-30° F to +165° F	54° F to 57° F
H49	S-Band Beacon Temperature	-30° F to +165° F	74° F to 78° F
H172	C-Band Beacon Temperature	-30° F to +165° F	73° F to 80° F
H357	Range Safety Receiver No. 1 Temperature	-30° F to +165° F	57° F to 61° F
H367	Range Safety Receiver No. 2 Temperature	-30° F to +165° F	61° F to +65° F
H354	Range Safety Receiver No. 1 Signal Limits	5-8 μv	5.5 μv to 5.2 μv
H364	Range Safety Receiver No. 2 Signal Limits	5-8 μv	Shows limiting

(i) No coder lockon (Nominal). MAC responsibility.
(j) Transmitter ON
(k) Transmitter OFF

3-11

Table 3-2

TRACKING SYSTEM PERFORMANCE

Tracking System	Time (sec)	Number of Tracking Stations	Number of Interrogations Per Second	Number of Transmitted Replies Per Second	Comments
C-Band	0 to 60	2	320	315	
	60 to 75	3	480	475	
	75 to 84	4	640	635	
	84 to 153	4 + identifier	800	810	
	153 to 218	5 + identifier	960	965	Tracking station adjustments
	218 to 337	6 + identifier	1120	1170	Tracking station adjustments
	337 to 341	5 + identifier	960	965	
	341 to 375	6 + identifier	1120	1150	
S-Band	0 to 74	1	205	205	Gradually decreases to about 170 at 74 sec
	74 to 230	2	410	395−410	Gradually decreases to 410 about 172 sec
	230 to 298	3 (one station 410 prf)	820	780−820	Gradually increase, difficulty in acquiring
	298 to 375	2	615	Varied rapidly	Difficulty in acquiring

3.2.5 Range Safety System

The data show that the range safety signal from the AFETR range safety officer's control was being received with adequate signal strength by both receivers of Vehicle 5002 throughout the flight. (See Table 3-1.)

3.3 PROPULSION

The possible initiating causes of the flight failure have been narrowed down to the following propulsion system occurrences:

- Thrust chamber ignition/combustion produced shock(s) that caused damage to the engine and/or vehicle.
- Vehicle or engine electrical failure caused shutdown and subsequent anomalies.
- Pyrotechnic-separation shock caused damage to engine mechanical or electrical components that resulted in failure during engine start transient.
- Failure or leakage in the main-fuel-valve actuation line or its instrumentation caused valve closure and subsequent anomalies.
- Leakage from other propellant flow circuit lines or components (i.e., sump, bellows, etc) caused shutdown and subsequent anomalies by itself or by damaging other components.

3.3.1 Secondary Propulsion Systems

3.3.1.1 Summary. The operation of the Model 8250 secondary propulsion systems (SPS) on the flight of Vehicle 5002 appeared normal, except for a few minor, unexplainable data anomalies. SPS operation was limited by virtue of the flight anomaly to operation of the Unit I thrust chamber assemblies (TCA's) to provide propellant orientation for the main engine first burn. During launch, gas and liquid pressures and temperatures were as expected. The start-valve lead time was normal, and on fire command, thrust chamber pressure and temperature reacted as expected. Steady state values were within nominal operating bands, and thrust chamber shutdown was normal. No corrective action is recommended.

3-13

Data anomalies noted were as follows:

a. Neither system indicated a rise in propellant tank manifold pressure during the start valve lead period. For most cases, this would be expected during a regulator lockup condition.

b. The -Y system experienced a minor, unexpected, thrust-chamber-pressure overshoot on start, and the overshoot condition prevailed for the first 3 sec of operation.

c. The thrust-chamber-pressure data on both systems had unexpectedly high fluctuations.

Limited tests of the components involved should provide a better understanding of the anomalies.

3.3.1.2 Discussion. The operational characteristics of the important SPS parameters are presented in Fig. 3-3; operation of both SPS's was limited to one Unit I TCA operation each, for propellant orientation for the main engine. The prelaunch gas and liquid pressures were within nominal limits. During ascent, gage pressure readings, showed an increase with the corresponding drop in reference pressure on the gage transducers. During the boosted phase of ascent, the propellant feed pressures on both systems changed for vehicle acceleration, as expected, and the gas pressures held constant, also as expected. The start-valve lead period was normal,except propellant tank pressures did not increase as expected, but remained at a constant value. For regulator lockup conditions, propellant tank pressures should have been approximately 212.5 psia for both systems (see Table 3-3). Since propellant tank pressures were approximately 205 psia prior to start-valve actuation, and for a 16-sec lead it is expected that a regulator lockup will occur, the propellant tank pressures should have increased on both systems. (This anomaly is discussed below.)

On fire signal (bipropellant valve open), thrust-chamber pressure and temperature for the Unit I thrust chambers on both systems increased as expected. The +Y system thrust-chamber pressure peaked normally and decayed for the remainder of the run, reflecting the decay in propellant feed pressures. The -Y system thrust-chamber

LOCKHEED MISSILES & SPACE COMPANY
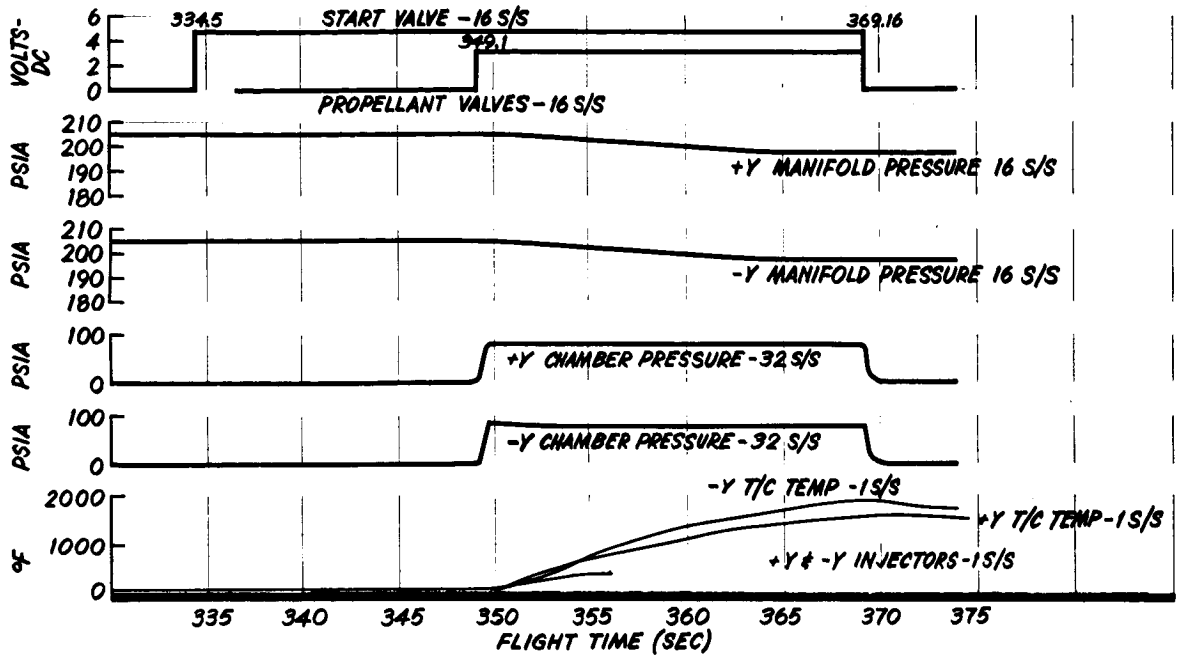
Fig. 3-3 Secondary Propulsion System Performance

Table 3-3

SECONDARY PROPULSION SYSTEM PREDICTED DATA VS FLIGHT DATA

Performance Item	SPS S/N 4 (+Y)		SPS S/N 5 (-Y)	
	Predicted	Flight	Predicted	Flight
Propellant-tank pressure at regulator lockup (psia)	212. 7	204. 4	212. 5	205. 0
Propellant-tank pressure during Unit I TCA flow (psia)	200. 4	197	199. 6	198
Thrust-chamber pressure for nominal regulator pressure (psia)	79. 5	–	78. 3	–
Thrust-chamber pressure based on indicated propellant tank pressure (psia)	82. 1– 79. 1	81. 0– 78. 5	80. 8– 77. 7	81. 0– 76. 0
Thrust-chamber peak-to-peak fluctuation (psia)	8	11	5	8
Thrust-chamber skin temperature at shutdown for a 20-sec firing (° F)	1900 ±100	1615	1800 ±150	1920

LOCKHEED MISSILES & SPACE COMPANY

pressure rose as expected but peaked at approximately 6 percent above steady-state value. (The normal maximum expected is about 3 percent.) After peaking, the thrust-chamber pressure decayed, but it was above the normally expected pressure for approximately 3 sec of operation. For the remainder of the run, thrust-chamber pressure was normal and decayed, reflecting the decay in propellant feed pressures. During steady-state operation, thrust-chamber pressures for both systems were approximately as expected for the propellant tank pressures observed. (See Table 3-3.)

During the entire 20-sec operating period for both systems, propellant tank and feed pressures decayed for approximately 16 sec and then leveled out for the remainder of the run. These data indicate that both systems experienced a blowdown condition for the first 16 sec of operation.* For the remainder of the thrust-chamber operating period, propellant-tank pressures stabilized at values of 197 psia and 198 psia for the +Y and -Y systems, respectively. As shown in Table 3-3, these pressures were below the predicted values for both systems, but the slight differences are within the expected run-to-run variation of the regulator and are therefore not considered abnormal. On main engine start, the fuel feed pressure on both systems fluctuated. The condition is not considered abnormal. On previous vehicle ground testing, all secondary propulsion systems liquid pressures experienced severe pressure disturbances due to the hydrostatic pressure change caused by shock acceleration.

After the bipropellant valve-open signal, the thrust chamber skin temperature for both systems began to increase, as expected. The thrust-chamber skin temperature observed for the -Y system reached a maximum of 1920° F and occurred at shutdown. The skin temperature was within the expected band for the entire 20 sec of thrust-chamber operation.

The thrust-chamber skin temperature (TCST) recorded for the +Y system was approximately 1615° F at shutdown. (See Fig. 3-3.) Since expected temperature at shutdown for a 20-sec firing would be in the 1800° F to 2000° F range, it is concluded

---

*This is the normally expected condition for a 20-sec Unit I thrust-chamber firing after a 16-sec start-valve lead, as regulator lockup would be expected. In fact, for a nominal regulator lockup condition (220 psia propellant-tank gas pressure) it would take 30 to 40 sec of Unit I TCA operation before propellant tank pressure would decay to a value where the regulator would flow.

LOCKHEED MISSILES & SPACE COMPANY

that the thermocouple was making only partial contact and was not indicating actual thrust-chamber skin temperature. The above conclusions are substantiated by the data, which shows the following: (1) a lower-than-expected temperature was recorded, (2) during the run, TCST decreased twice, then increased, whereas a continuously increasing then decreasing slope would be expected. Due to prelaunch damage, the thermocouple in question was rewelded, at AFETR, onto the second hottest spot, with the use of equipment that had a power rating less than recommended. It is concluded that the thermocouple in question was partially loose because of an inadequate weld and/or improper placement.

Shutdown characteristics were normal, with thrust chamber pressures and temperatures decaying as expected. (See Fig. 3-3.)

3.3.1.3 Discrepancies Noted

Lack of Propellant-Tank-Pressure Increase During Start-Valve Lead Period. During normal operation, it is expected that the propellant-tank pressure will increase during the start-valve lead period, since the regulator goes to lockup and regulator lockup pressure is higher than either propellant tank prepressurization or regulated flow pressures. While lack of propellant-tank-pressure increase during the start-valve lead period has been noted during system ground firing operations, such a condition normally occurs only if the propellant tank pressure is approximately the same or higher than the expected lockup pressure of the particular regulator.

During prelaunch servicing, both system were prepressurized to propellant tank pressures of 204.5 psia for the +Y system and 205 psia for the -Y system. These pressures held during launch and ascent; they remained at the above values through the start-valve lead period and began decaying after thrust-chamber operation began. An analysis of the prelaunch functional test data of all interrelated components results in predicted nominal values for propellant tank lockup pressures of approximately 212.5 psia for both systems. Therefore a nominal 7-psi increase would have been expected in the propellant-tank pressures on both systems shortly after start-valve actuation. While run-to-run variations are expected in regulator lockup and flow

LOCKHEED MISSILES & SPACE COMPANY

pressures, and could explain the lower than predicted values, the family of dash 9 regulators has not normally had lockup pressures in the 209 to 210 psia range (which would have been required for no-pressure-rise for propellant-tank pressures in the 204-205 psia range).

At this time, sufficient ground test data are not available that will explain the apparent low lockup of the regulators used on the systems on Vehicle 5002. While propellant-tank pressures did not increase during the start-valve lead periods, it is concluded that both regulators did, in fact, lock up. If start-valve operation did not occur, then thrust-chamber operation would not have occurred, as the bipropellant valve-actuation lines were not prepressurized prior to flight. Regulator lockup was evident since propellant tank pressures were adequately controlled by the regulators.

While check-valve leakage could have resulted in pressurization of the actuation lines, these lines, even at maximum leak rate, could not have been pressurized to a value high enough to open the bipropellant valves. In fact, the functional test results on both check valves indicate minimal leakage.

Since three pressure readings (oxidizer feed, fuel feed, and propellant tank) on each system exhibited the same no-pressure-rise profiles, it is concluded that the instrumentation system was not a factor in the results noted.

While the discrepancy cannot be explained, it is possible that lower-than-expected regulator lockups can occur at propellant-tank pressures approximately the same as expected lockup, and the gas-check-valve cracking pressure increased slightly because of the large differential across the valve during the long prepressurization period of 2 days. It is therefore recommended that limited testing be accomplished to ascertain whether the noted discrepancy could be due to the above possibilities.

Unusual Thrust-Chamber-Pressure Overshoot During Start of -Y System. During the start transient of the Unit I thrust chamber assembly, the thrust-chamber pressure (TCP) increased as expected but peaked at a value of 86 psia, which is approximately 3 psia higher than expected. Peaks greater than steady-state value are

expected during the start transient, but the peak experienced was about 6 percent above the steady-state value as compared with the nominal peak of about 3 percent over steady state. The normal peak endures for approximately 1 sec, whereas the discrepancy noted had a duration of approximately 3 sec. (See Fig. 3-3.) For the remainder of the thrust-chamber operation, TCP was normal and decayed as expected, reflecting the decay in feed pressures.

The abnormal peak in TCP is unexplainable but could be due to excess propellant flow, partial thrust-chamber-throat blockage, or a partially plugged thrust-chamber-pressure sensing port. If any of the above occurred, the condition would have become normal during the first 3 sec of operation as TCP for the remainder of the run was approximately as predicted for the feed pressures noted. On shutdown, the decay in TCP was normal, which indicates no blockage in the pressure sensing port. While there could have been excess propellant flow due to leakage around either the oxidizer or the fuel trim orifices, the normal operation after 3 sec contradicts this possibility. If a leaking trim orifice did cause the discrepancy, it is not considered a problem on future flights as all subsequently delivered systems will incorporate the redesigned trim orifice seat.

Abnormal Thrust-Chamber-Pressure Fluctuations. The peak-to-peak fluctuations noted in the recorded thrust-chamber pressures were approximately 11 psi and 8 psi for the +Y and -Y systems, respectively. These values are considered to be slightly abnormal, especially the 11-psi fluctuation. Pressure fluctuations approaching the magnitudes noted are not normally observed except on Unit I thrust chamber operations where the pressure transducer is close-coupled to the thrust chamber. While the flight-instrumentation installation is not close-coupled, line volumes are small for the Unit I thrust-chamber-pressure sensing system, and a close-coupled effect would be expected. The foregoing conclusion is substantiated by the rapid increase in recorded thrust-chamber pressure during the start transient. This results in pressure readings that approximate those recorded for the start-response tests conducted during the thrust-chamber level acceptance tests. (See Table 3-3.) Since the flight instrumentation system has shown close-coupled instrumentation characteristics for the Unit I TCP sensing system, it is expected that peak-to-peak

LOCKHEED MISSILES & SPACE COMPANY

pressure fluctuations of approximately 7 psi would be observed. While the pressure fluctuations recorded are considered to be slightly abnormal, a firm conclusion cannot be made as no past fire-test history of the pressure sensing system, with similar line volumes, is available.

Thrust-chamber-pressure fluctuation attenuation has been noted on system acceptance tests, where sensing system line volume is relatively large. Therefore, it is recommended that limited testing be conducted on the Unit I TCA, with a chamber-pressure sensing system similar to the one used on flight vehicles to ascertain the characteristics of the pressure measurements.

3.3.1.4 Conclusions. It is concluded that the operation of the secondary propulsion systems on the flight of Vehicle 5002 was normal except for the four apparent data anomalies noted. While anomalies did occur, no major corrective action is required, and basic operation of the systems was as expected.

3.3.2 Primary Propulsion System

3.3.2.1 Summary. Primary propulsion system (PPS) data for the Vehicle 5002 flight indicated normal operation from liftoff to the engine fire signal at 367.53 sec. The engine start sequence appeared normal until 368.40 sec. At that time, a series of events occurred that resulted in premature engine shutdown. The pyrotechnic helium control valve (PHCV) operated normally at 369.02 and allowed the main-propellant-tank pressurization to begin. Gross overpressurization of the main propellant tanks occurred when the engine did not continue to withdraw propellants from the tanks. Rupture of the main propellant tanks then occurred and resulted in vehicle breakup at 375.98 sec (loss of telemetry signals).

3.3.2.2 Discussion. This discussion includes consideration of the following items:

    a. PPS configuration

    b. Model 8247 (XLR81-BA-13)/Model 8096 (YLR81-BA-11) engine comparison

    c. PPS flight data analysis

    d. Evaluations conducted since flight

3.3.2 2.1 <u>PPS Configuration</u>. Vehicle 5002 was equipped with the standard Agena basic alternate primary propulsion system with the exception of a program-peculiar helium pressurization sphere. The PPS* consists of the following:

    a. , High-pressure helium storage sphere

    b. Pyrotechnic-operated helium control valve

    c. Main propellant tank assembly (including containment sumps)

    d. Propellant fill bellows

    e. Propellant isolation valves

    f. Propellant feed bellows

    g. Model 8247 rocket engine (multistart)

    h. Hydraulic power package UDMH supply circuit

    i. Associated lines and quick disconnects

3.3.2.2.2 <u>Model 8247/Model 8096 Engine Comparison</u>. The Model 8247 engine is a modified version of the flight-qualified 8096 engine. Major hardware and performance differences between the two engines are presented in Appendix A.

3 3 2.2.3 <u>PPS Flight Data Analysis</u>. The Vehicle 5002 PPS flight data were in the form of a series of individual data points. The time interval between adjacent data points for any given measurement was determined by the sampling rate for that particular measurement. Sampling rates varied from as low as one sample per second for most temperature measurements to as high as 96 samples per second for the wide range TCP measurement. This type of readout does not allow direct establishment of the exact time that a measurement began to change and also does not show a complete picture of fluctuations having durations approaching the time interval between adjacent data samples. The PPS data obtained from the flight of Vehicle 5002 are discussed below. Referenced times are associated with actual data points. Any indicated changes could have occurred at any time between the data point of indicated change and the previous data point.

---

*Vehicle electrical-control circuitry for the engine is not considered to be part of the PPS. However, the turbine overspeed electronic gate is a part of the Model 8247 rocket engine and therefore is a portion of the PPS.

LOCKHEED MISSILES & SPACE COMPANY

Prior to Fire Signal. A review of PPS data from liftoff to fire signal indicates that the PPS condition was normal during this time period.

Irregularities were observed in many propulsion system measurements during the time intervals of from 3 to 12 sec and 130 to 145 sec after liftoff. These irregularities have been attributed to transmission interference and are not considered to be reflecting actual measurement anomalies,

B3, the "Turbine Manifold Pressure No. 1" measurement was lost at some time prior to the PPS fire signal. This measurement showed a zero shift to approximately 45 psi during the time interval between 150 and 165 sec after liftoff. It remained at that level for the remainder of the flight except for a small spike to 85 psi which was followed by a decrease to 30 psi and a recovery to 45 psi at approximately the same time as the initiation of the thrust-chamber area measurement anomalies. The spike, decrease, and recovery occurred within an 18-ms time period and reflects only one data point at 85 psi and one at 30 psi. A comparison with measurement B132, "Turbine Manifold Pressure No. 2," and pressure measurements that reflect pump speed shows that neither the magnitude, time of initiation, nor duration can be correlated in any way with actual turbine manifold pressure. Loss of this measurement had a certain impact on the failure analysis since turbine manifold pressure provides a direct indication of power available to the turbine. It would have been useful for correlation with turbine speed and main-fuel-valve closure and would have given a direct indication of time of closure of at least one gas generator valve.

Fire Signal to Loss of Telemetry. The PPS fire signal occurred at 367.53 sec, and all telemetry signals were lost at 375.98 sec. A review of available data during this time span of 8.45 sec indicates that an engine start sequence was initiated by the fire signal and apparently progressed normally until 368.40 sec. At 368.40 sec, a series of events was initiated that resulted in engine shutdown prior to completion of the

---

*Thrust-chamber pressure, oxidizer injector pressure, and fuel-valve actuation pressure anomalies.

LOCKHEED MISSILES & SPACE COMPANY

start transient. Normal main-propellant-tank pressurization system operation, which began at 369.02 sec, eventually produced gross overpressurization of the tanks due to the fact that propellants were not being withdrawn. Rupture of the tanks and vehicle breakup caused loss of signal, which occurred at 375.98 sec.

Plots of significant PPS data and temperature measurements in the aft rack area during the time period between fire signal and loss of the telemetry are presented in the following pages. An expanded time scale plot of significant PPS data during the engine start/shutdown period is presented in Fig. 3-4. Individual measurements and the significant PPS data they provided are as follows:

a. P139, "Engine Switch Group" Measurement (Figs. 3-4 and 3-5). B139 rose normally from zero to 1.75v at fire signal and indicated that pilot-operated solenoid valve (POSV), the oxidizer gas generator valve (OGGV), and the fuel gas generator valve (FGGV) were drawing power. At 368.44 sec, B139 abnormally dropped to zero volts, indicating removal of power from the engine solenoid valves. B139 continued to present the abnormal indication of zero volts until 368.62 sec, except for a single 0.8v reading at 368.47 sec and another single 0.15v reading at 368.50 sec, then rose to 2.90v at 368.66 sec and remained at 2.90v until loss of telemetry. To date, no single electrical malfunction mode has been found that offers a satisfactory explanation for these data.

b. D60, "Hydraulic Oil Pressure" Measurement (Fig. 3-5). D60 showed normal buildup to approximately 2500 psi between 367.88 and 368.40 sec and showed fluctuations due to actuator demands and/or relief valve operation between 368.40 and 368.82 sec. Beginning at 368.82 sec, D60 decreased to zero psi in a manner similar to that observed during normal engine shutdown.

c. B9, "Fuel Tank Pressure" Measurement (Fig. 3-5). B9, at 54.4 psi, began to decrease at 368.12 sec. At 368.61 sec, it showed 50.4 psi, a loss of 4.0 psi due to fuel being withdrawn from the tank. B9 then remained constant until 369.01 sec, increased to 57.5 psi at 369.07 sec (pyrotechnic helium-control-valve operation) and finally increased to 60.4 psi (out of band) during the 0.30-sec time interval to 369.37 sec. The data after 368.61 sec indicate that fuel is not being withdrawn from the tank at a normal rate.

LOCKHEED MISSILES & SPACE COMPANY
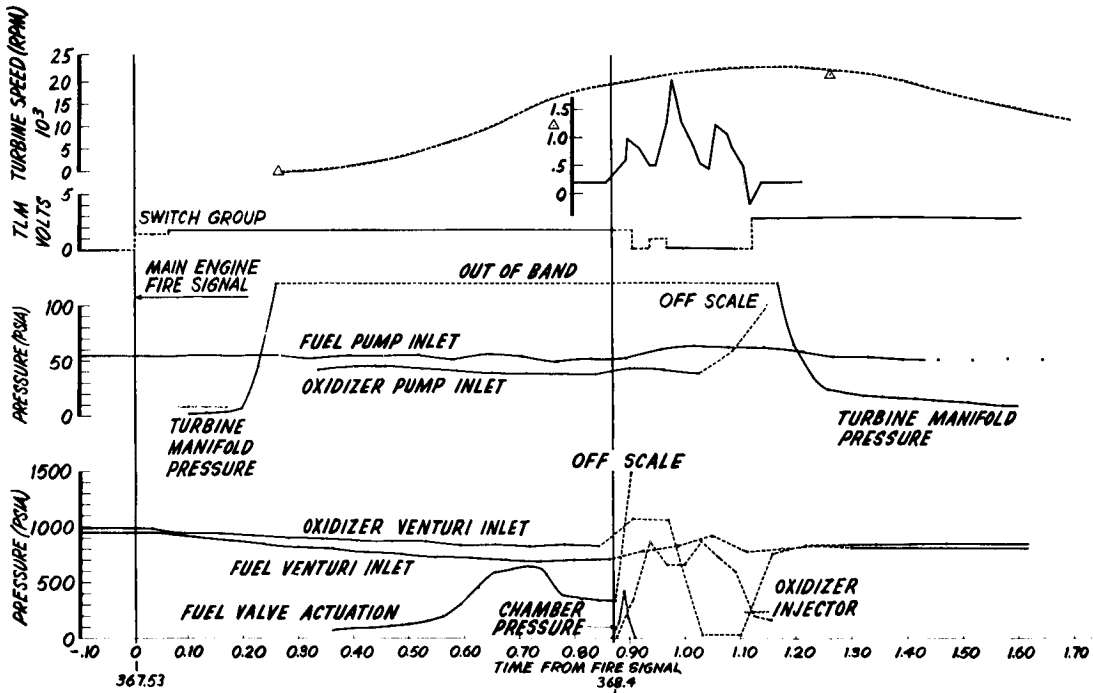
Fig. 3-4 Primary Propulsion System Start and Shutdown Data
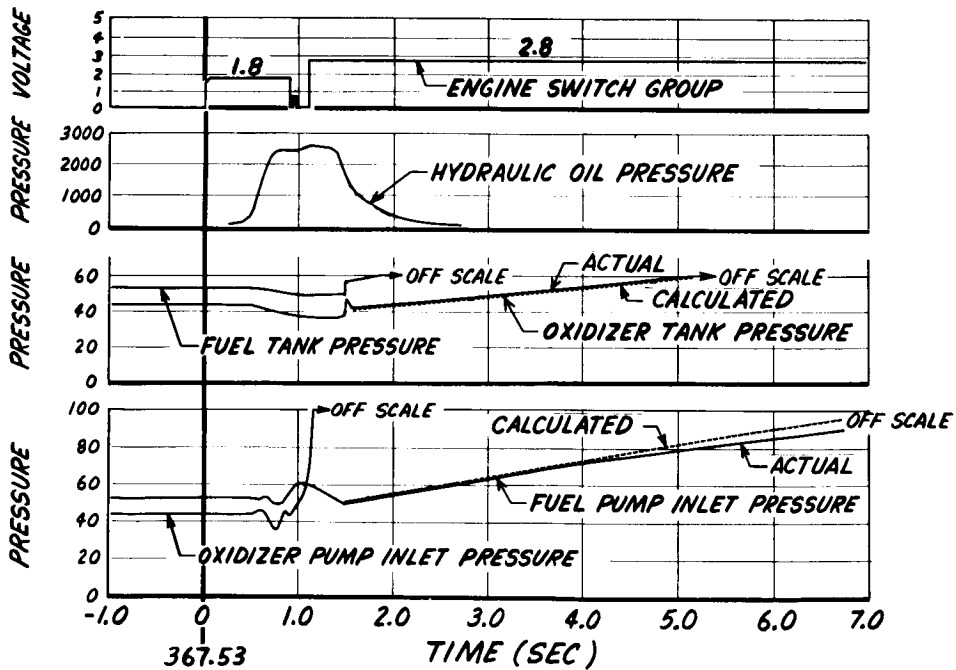
Fig. 3-5 Engine Switch Group and Hydraulic-Oil, Propellant-Tank, Pump-Inlet Pressures

LOCKHEED MISSILES & SPACE COMPANY

d. <u>B8, "Oxidizer Tank Pressure" Measurement (Fig. 3-5)</u>. B8 was initially at 47.5 psi and began to decrease at 368.06 sec. At 368.94 sec, it indicated 38.8 psi, a loss of 6.7 psi due to oxidizer withdrawal from the tank. B8 increased to 46.5 psi and decreased to 42.5 psi at 369.02 sec and 369.07, respectively (pyrotechnic helium-control-valve operation), remained constant until 369.19 sec, and then finally increased to 60.0 psi (out of band) during the time interval to 372.40 sec. The data after 369.19 sec indicate that oxidizer is not being withdrawn from the tank at a normal rate.

e. <u>B1, "Fuel Pump Inlet Pressure" Measurement (Figs. 3-4 and 3-5)</u>. B1 began to fluctuate normally at 367.80 sec, indicating fuel pump spin-up. It continued to fluctuate and also to decrease normally as fuel flow began to the hydraulic motor package, to the fuel gas generator system, and finally to the thrust chamber. It showed a rise from 52 psi to 63 psi during engine-start operation and then a decrease back to 52 psi. Finally, the measurement rose from 52 psi at 369.02 sec to 98.5 psi at telementry loss, which indicates that fuel was not being withdrawn from the system and that the measurement was tracking tank pressure.

f. <u>B2, "Oxidizer Pump Inlet Pressure" Measurement (Figs. 3-4 and 3-5)</u>. B2 began to fluctuate and increase normally at 367.80 sec, indicating oxidizer pump spin-up. It began to decrease normally at approximately 368.0 sec because of the opening of the main oxidizer valve and subsequent flow to the thrust chamber. A rise from 37.5 to 42.5 psi was indicated at the time of thrust-chamber ignition, which is due to the thrust-produced liquid head. Decreases to 38.5 psi occurred during the next 125 msec, which reflects continuing oxidizer flow to the thrust chamber. At 368.68 sec, the measurement increased to 59.0 psi and then went off scale and remained there until loss of telemetry. This indicates either a pressure surge in the oxidizer system and resultant transducer damage, or starting shock damage to the transducer.

LOCKHEED MISSILES & SPACE COMPANY

g. B35, "Turbine Speed" Measurement. The curve shown in Figs. 3-4 and 3-6 has been adjusted based on a comparison with fuel valve actuation and hydraulic oil pressures and represents a best estimate of what the turbine speed must have been. It should be noted that the nature of this measurement is such that total revolutions are recorded at half-second intervals, and therefore speeds are averages over half-second periods. The total counts indicate an apparently normal rise and then a decrease that is normally associated with engine shutdown.

h. B11, "Oxidizer Venturi Inlet Pressure" Measurement (Figs. 3-4 and 3-6). B11 began to blow down normally due to oxidizer flow into the gas generator following the engine start signal. It showed a sudden rise from 830 psi to 1080 psi at 368.44 sec, a drop to almost zero psi at 368.56 sec, a recovery to 760 psi at 368.69 sec, and a final rise to 840 psi at 368.75 sec. It remained at 840 psi until loss of telemetry, which indicates closure of the oxidizer gas generator valve. The pressure fluctuation began approximately at the same time as the beginning of thrust-chamber area measurement anomalies (thrust-chamber-pressure, oxidizer-injector-pressure, and fuel-valve-actuation-pressure anomalies). This measurement may actually be reflecting a pressure surge that had been distorted and elongated by the start tank acting as an accumulator. The relatively large mass of the start-tank bellows makes the bellows continue to move, once it has been set in motion by a pressure surge, because of inertia. Once the surge has passed, movement of the bellows away from the liquid for a finite period of time would account for the zero psi indications for the referenced period.

i. B12, "Fuel Venturi Inlet Pressure" Measurement (Fig. 3-4 and 3-6). B12 began to blow down normally due to fuel flow into the gas generator following the engine start signal. It showed a rise from 715 psi to 920 psi between 368.39 and 368.58 sec and a decrease to 780 psi at 368.64 sec, which is similar to what is normally observed on engine shutdown. A rise normally occurs between the time of main-fuel-valve closing and oxidizer-gas-generator-valve closing (fuel pump is unloaded). A decrease normally
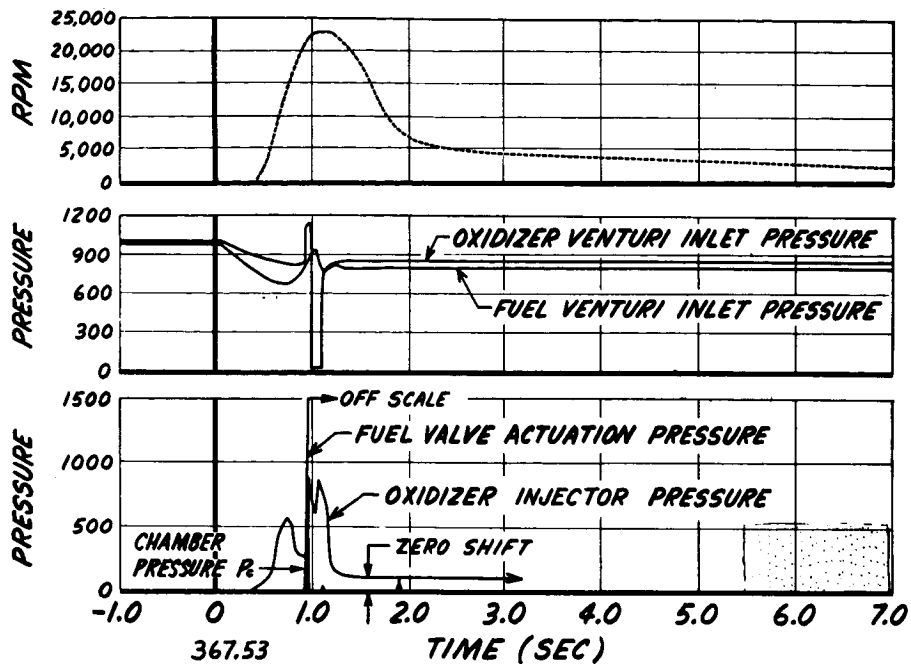
Fig. 3-6 Turbine RPM and Venturi-Inlet, Fuel-Valve Actuation, Oxidizer-Injector, and Thrust-Chamber Pressures

occurs between the time of oxidizer-gas-generator-valve closure and fuel-gas-generator-valve closure (power is removed from turbine, pump speeds decrease, and fuel flows into the gas generator from the fuel start system).

j. B82, "Fuel Valve Actuation Pressure" Measurement (Figs. 3-4 and 3-6). B82 showed a normal rise of fuel-pump-discharge pressure, a decrease in slope at 368.19 sec that is indicative of main-fuel-valve cracking, and a decrease to a lower level between 368.25 and 368.40 sec that is indicative of main-fuel-valve poppet movement. At the approximate time when poppet travel should have been completed (based on a comparison with ground firing data), and approximately at the time of thrust chamber ignition, B82 suddenly went off scale (1500 psi) and stayed there. Normal pressure during engine steady-state operation is approximately 1060 psi. This characteristic is indicative of a pressure surge and/or shock damage to the transducer or physical loss of the transducer (i.e., failure of the mounting hardware).

LOCKHEED MISSILES & SPACE COMPANY

k. **B148, "Oxidizer Injector Pressure" Measurement (Figs. 3-4 and 3-6).** The B148 pressure indication increased from zero at 368.40 sec to 870 psi at 368.47 sec, dropped to 660 psi at 368.50 sec, repeated the 660 psi reading at 368.53 sec, rose to 870 psi at 368.56 sec, and then decreased relatively slowly to 130 psi at 369.00 sec; it remained there until loss of telemetry. The sampling rate on this measurement was not high enough to show an accurate picture of the rapid fluctuations that existed in the oxidizer injector manifold. However, it is considered that B148 was providing a slow-response measurement of actual manifold pressure during the start/shutdown transient.

l. **B6 and B91, "Thrust Chamber Pressure" Measurement (Figs. 3-4 and 3-6).** B91 is a narrow range (475 to 550 psi) transducer that has relatively poor response, and B6 is a wide range (0 to 750 psi) transducer that has relatively good response. The narrow range measurement (B91) showed no change, which could either be due to poor response during the thrust-chamber-pressure rise and decay or due to thrust chamber pressure not having reached a value of 475 psi. The wide range measurement (B6) measured a pressure of approximately 425 psi followed by a decrease to zero psi during the time period between 368.41 and 368.43 sec. These data do not correlate with oxidizer injector pressure, and therefore there is reason to doubt that it reflects actual chamber pressure following the initial rise period.

m. **B3 and B132, "Turbine Manifold Pressure" Measurement (Fig. 3-4).** B132 is a low range (0 to 120 psi) transducer, and B3 is a wide range (0 to 750 psi) transducer. The wide range measurement became nonoperative either prior to, or during, ascent. It showed a zero shift to 45 psi between 150 and 165 sec after liftoff and did not respond to turbine manifold pressure during engine start. The low range measurement showed normal buildup during start until it reached full scale at 367.79 sec (normal); then it showed a decay beginning at 368.70 sec, which indicates gas generator shutdown.

n. <u>B184 and B185, "Nozzle Extension Temperature" Measurement (Fig. 3-7)</u>. These measurements are located on the exterior of, and approximately 2 in. from, the exit plane of the thrust-chamber-nozzle extension. B184 indicated a temperature approximately 50° F higher than B185 prior to engine start; its performance is considered normal because of its proximity to one of the operating SPS chambers. B184 abruptly went full scale and was lost at approximately 369.00 sec (coincident with SPS shutdown); during the engine start period, it showed a rise from 52° F to 70° F, followed by a decrease to 27° F, terminating with a rise to 340° F during the last 4 sec of data. This last rise raises the question of a possible fire in the area of the measurement.

o. <u>B31, "Fuel Pump Inlet Temperature" Measurement (Fig. 3-8)</u>. B31 showed a slight rise between fire signal and loss of telemetry, which is indicative of little or no fuel flow.

p. <u>B32, "Oxidizer Pump Inlet Temperature" Measurement (Fig. 3-8)</u>. B32 showed a slight decrease between fire signal and loss of telemetry, which is indicative of oxidizer flow during engine start and shutdown transient.

q. <u>Aft Rack Temperatures (Figs. 3-9 through 3-13)</u>. Temperature measurements in the aft rack that were not significantly shielded from the engine area showed a marked decrease during the time period from thrust chamber area measurement anomalies to loss of telemetry. These decreases could have been caused by propellant leakage, but it has not been possible to establish firmly whether the leak started before, coincident with, or after the thrust-chamber-area-measurement anomalies because of uncertainties in predicting time periods for transfer of liquid from leak point to measurement area, boiloff, and measurement response.

3.3.2.4 <u>Initial Flight-Data-Failure-Analysis Results</u>. The initial flight-data failure analysis was based on a comparison of PPS normal operating characteristics with the observed flight data to define all anomalies. These measurement anomalies were then analyzed to determine what physical occurrences they might represent.
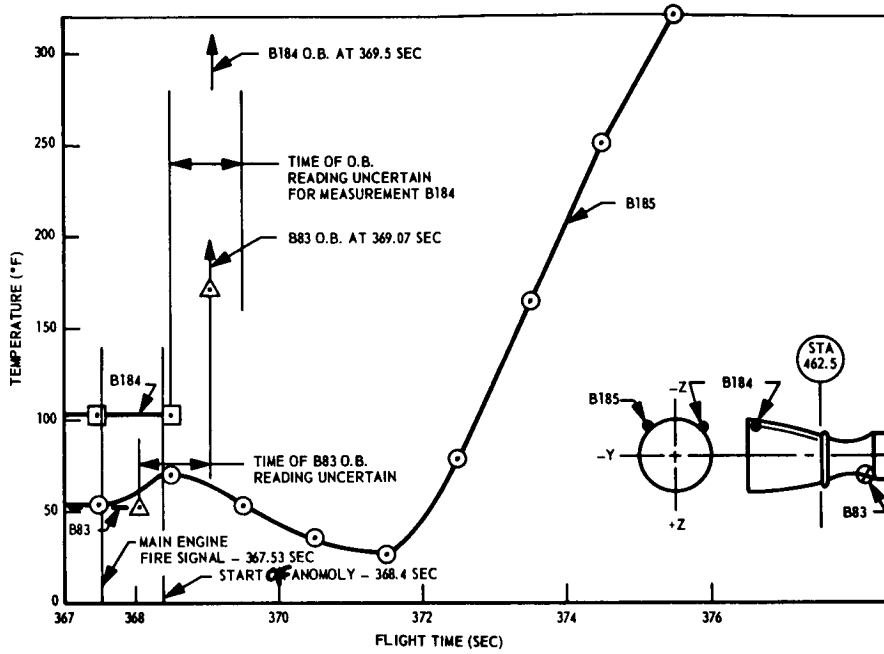
Fig. 3-7 Nozzle-Extension (B184 and B185) and Thrust-Chamber (B83) Surface Temperatures
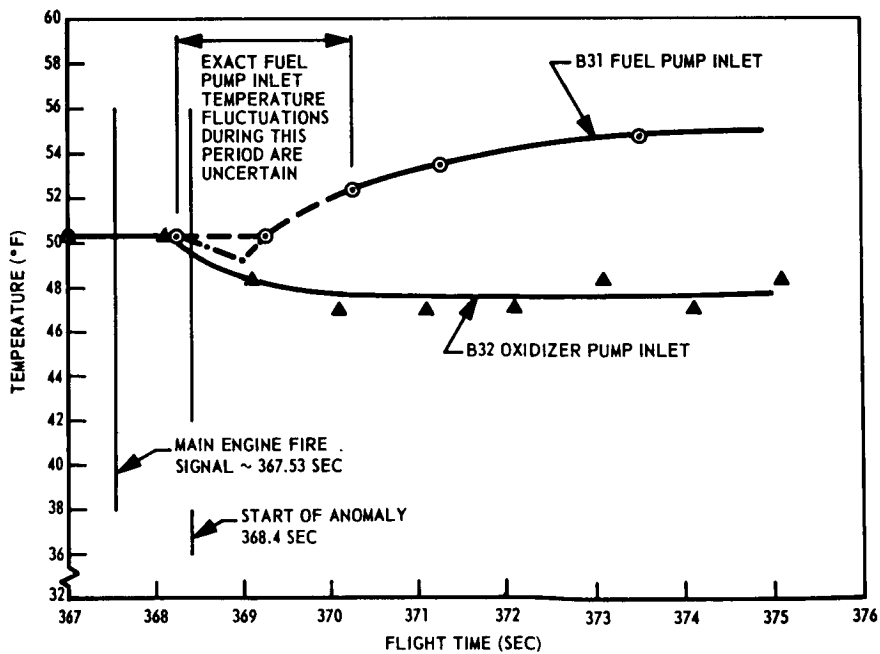
Fig. 3-8 Propellant-Pump-Inlet (B31 and B32) Temperatures
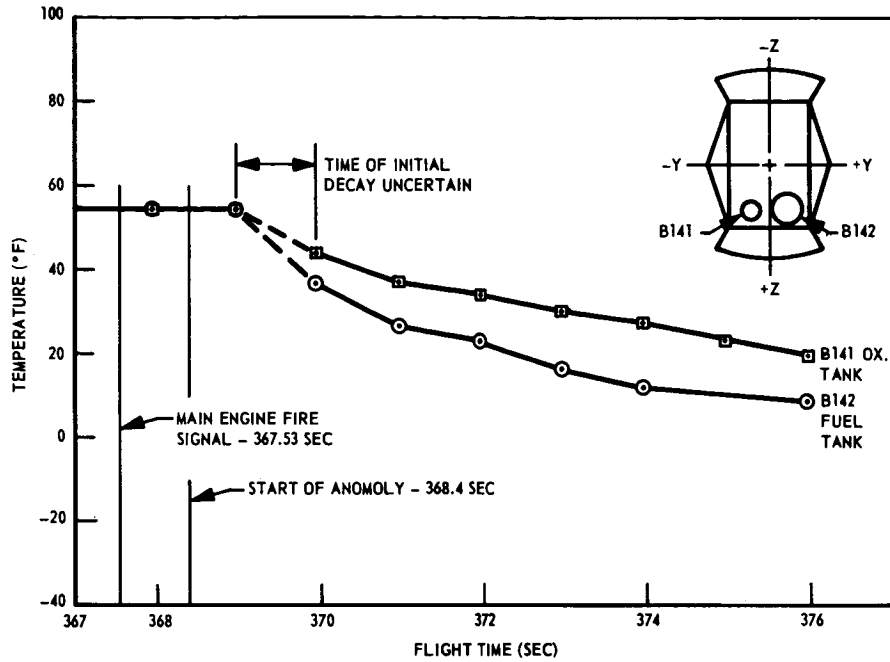
Fig. 3-9 Propellant Start Tank (B141 and B142) Temperatures
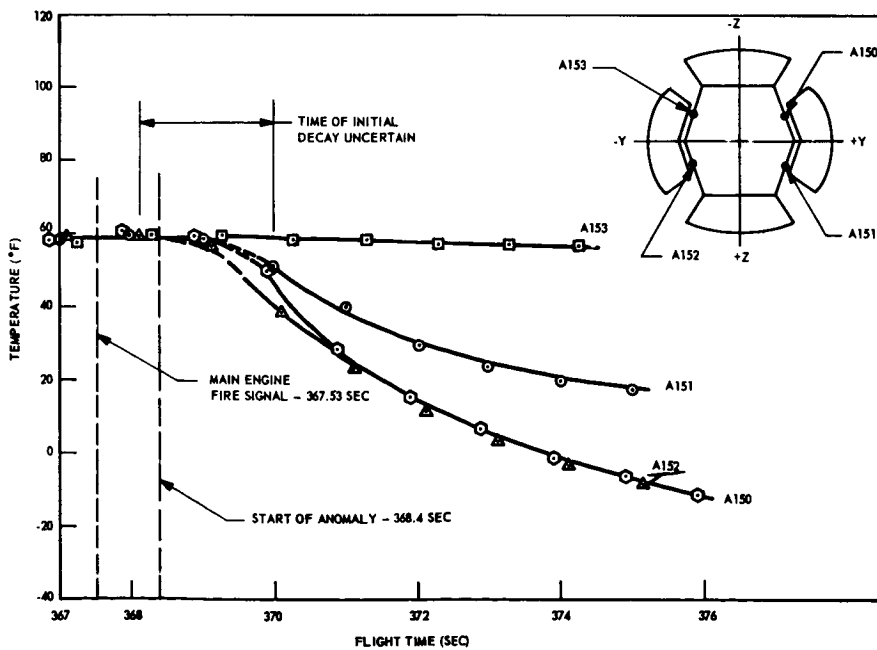
Fig. 3-10 Aft Rack Shear Panel (A150 Through A153) Temperatures

LOCKHEED MISSILES & SPACE COMPANY

A150

-Z

-Y

+Y

+Z
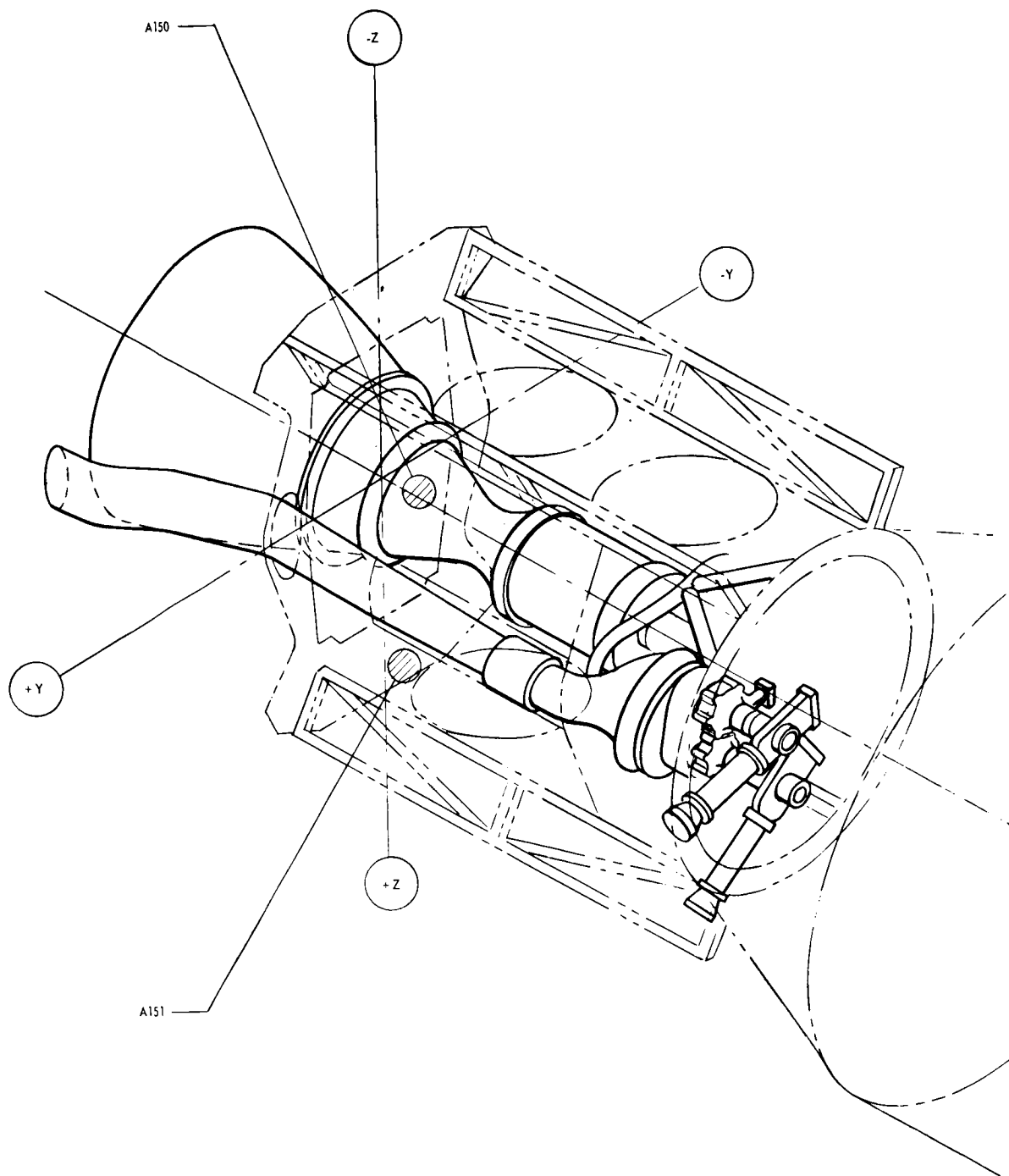
A151

Fig. 3-11 Location of Shear Panel Temperature Measurements A150 and A151

3-32

-Z

A153

+Y

-Y

+Z

A152

OXIDIZER TURBO-PUMP

OXIDIZER BELLOWS

FUEL BELLOWS

OXIDIZER FILLER
PIPE / COUPLING
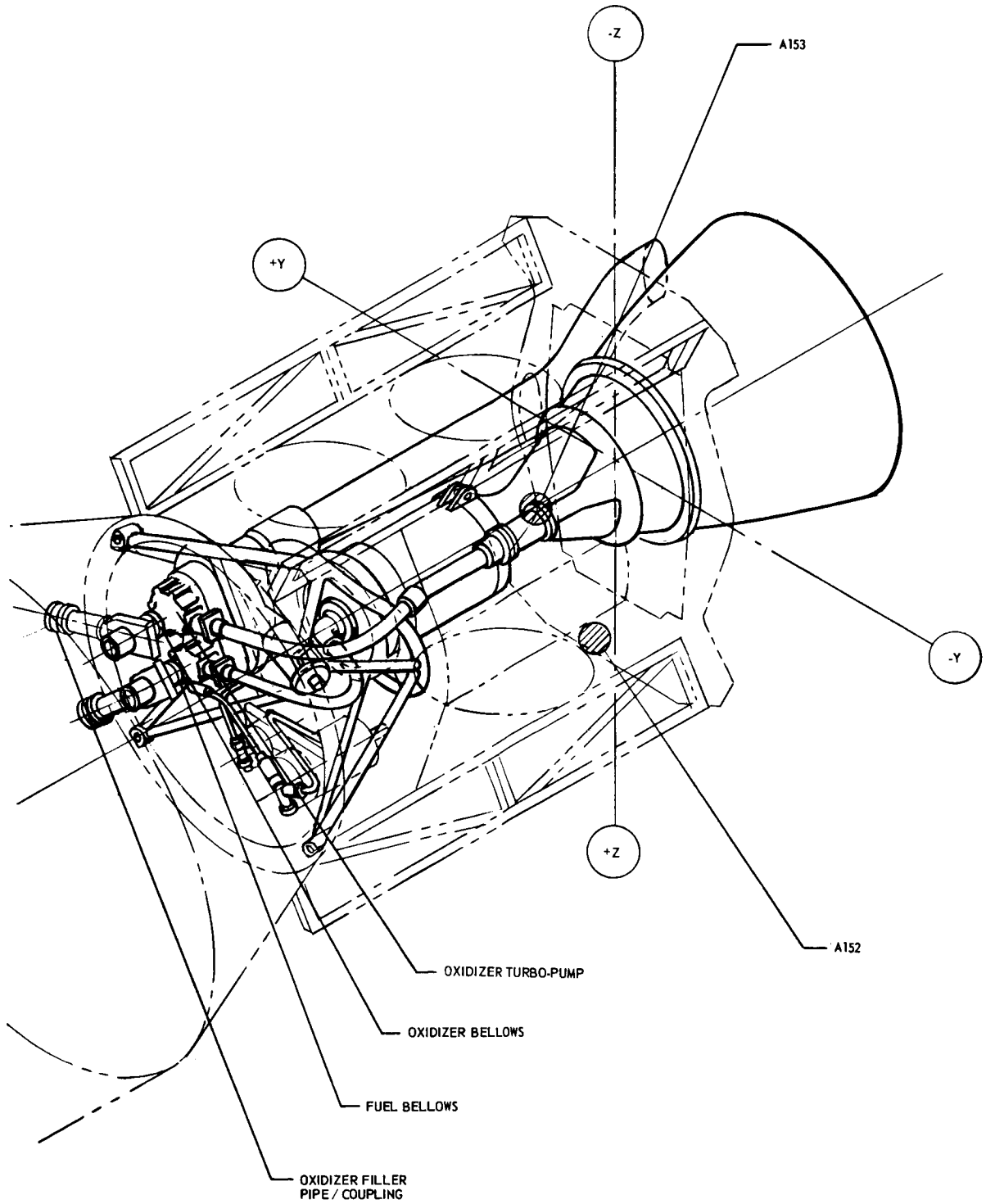
Fig. 3-12 Location of Shear Panel Temperature Measurements A152
and A153

3-33
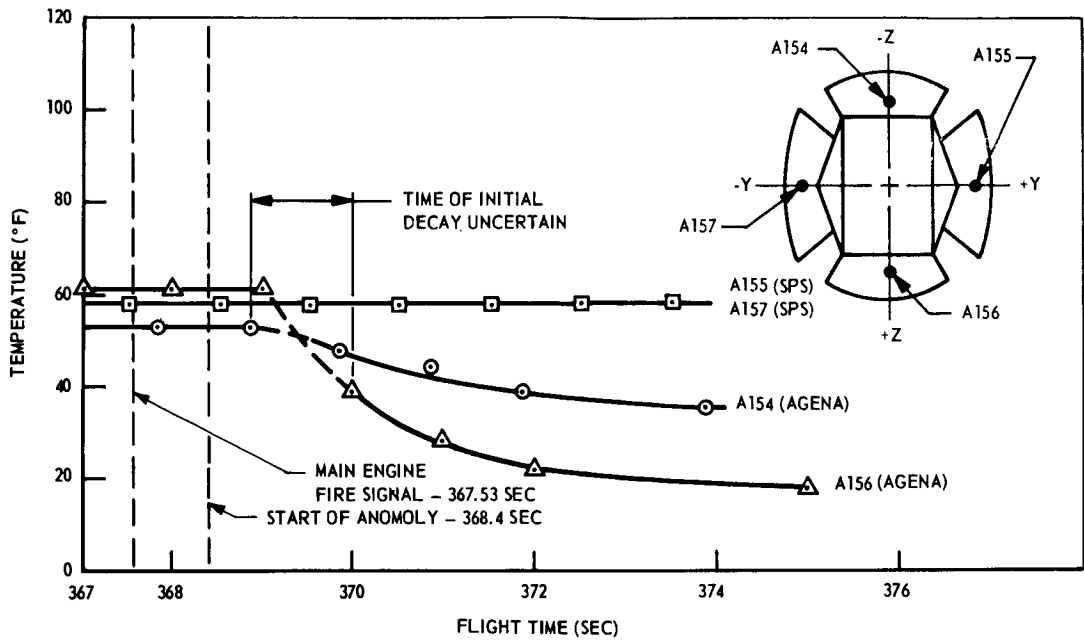
Fig. 3-13 Aft Bulkhead (A154 Through A157) Temperatures

The results of the initial flight data failure analysis are as follows (these results were used as a basis for further investigation and theoretical analysis):

Vehicle Loss. Vehicle loss was due to overpressurization and eventual rupture of the main propellant tanks. This is an expected occurrence if excessively premature engine shutdown occurs.

The fuel-pump-inlet pressure increase to 98.5 psi indicates that the fuel tank approached its ultimate limit; the abrupt loss of all telemetry signals is indicative of destruction of the vehicle.

CONFIDENTIAL

LOCKHEED MISSILES & SPACE COMPANY

<u>Failure of PPS to Achieve Steady State Operation</u>. No evidence has been found of any abnormal PPS condition prior to PPS fire signal. PPS data indicated normal start transient operation from fire signal until approximately the time of engine-thrust-chamber ignition. No evidence has been found of a major explosion in the aft rack area during the time inverval between PPS fire signal and loss of telemetry signals. Such an explosion would be expected to cause damage to the SPS, the attitude control system, or to the other equipment installed in the aft rack area; this damage would be reflected in the data for this equipment and in vehicle attitude and accelerations. No such indications were found.

PPS data indicate that the engine shut down shortly after the time of thrust chamber ignition. This conclusion is supported by cessation of thrust, and dropoff of turbine manifold pressure and turbine speed. Closure of the main oxidizer valve was established by the following: the oxidizer tank pressure indication showed that only an amount of oxidizer approximately equivalent to normal post-flow was withdrawn from the tank after the time of engine shutdown. Closure of the main fuel valve was established by the fact that fuel tank pressure rose when tank pressurization occurred. Closure of the gas generator valves was established by turbine manifold pressure dropoff and lockup of the venturi inlet pressures. Turbine overspeed did not cause shutdown. Pitch and yaw pneumatics were not re-enabled as they normally would be in the case of an overspeed shutdown.

<u>Leakage</u>. Leakage of one or both propellants occurred in the aft rack area. It apparently began at some time after the PPS fire signal — most probably after thrust chamber ignition. This conclusion is based on the following facts: (1) that most aft-rack temperature measurements that were not significantly shielded from the engine showed a marked decrease beginning at about the time of thrust chamber ignition and (2) aft rack pressure showed an increase from zero to approximately .12 psi at about the same time. No unusual pressure decreases were observed in such other aft rack systems as the SPS, the attitude control system, or the engine start tank assemblies. Therefore, the leak occurred in one or both of the propellant feed systems or in the engine itself (other than the start tank assemblies).

LOCKHEED MISSILES & SPACE COMPANY

In an attempt to corroborate the existence of a propellant leak following engine shutdown, a pressurization system analysis was conducted. The expected pressure-time behavior of the two GATV propellant tanks in the absence of leaks was calculated by employing telemetered pressure data from a previous standard Agena flight vehicle that was pressurized to rupture. By comparing the predicted pressures with those that actually occurred, and assuming that the GATV tanks had similar stretch properties to the previous vehicle, it was concluded that the GATV fuel tank could have experienced a liquid leakage rate of approximately 0.6 lb/sec. By the same reasoning, possible oxidizer leakage could not be determined due to the uncertainities of oxidizer tank stretching.

Pressure Surge in Oxidizer System. A pressure surge apparently occurred in the oxidizer side of the engine and feed systems. Oxidizer pump inlet pressure went off scale (and remained there), and oxidizer venturi inlet pressure went through a high-low pressure cycle shortly after thrust chamber ignition. A high pressure surge may also have caused a propellant leakage in the oxidizer feed system.

Fire in Aft Area. Nozzle extension temperature (B185) increased during the 4 sec prior to telemetry loss. The probability that a fire actually occurred is considered to be relatively low.

Fuel-Valve-Actuation-Pressure Anomaly. Fuel-valve-actuation pressure went off scale at approximately the time of thrust chamber ignition and remained there until loss of telemetry. The most probable cause of this failure is that the transducer was damaged by structural shock generated by thrust chamber ignition.

Engine Switch Group Anomalies. The engine switch group data after 368.40 sec cannot presently be correlated with any single electrical malfunction mode that would explain the characteristics obtained after 368.4 sec.

LOCKHEED MISSILES & SPACE COMPANY

Thrust Chamber Measurement Anomalies. At this time, no explanation for the inconsistency in chamber pressure (B6) has been found. It should be noted that this pressure measurement did not detect large overpressures or ignition spikes in the thrust chamber; however, B6 system response could have missed measuring such an occurrence.

Sequencing. The order of initiation of the following events cannot be established at this time:

    a.   Thrust-chamber-measurement anomalies

    b.   Fuel-valve-actuation-pressure anomaly

    c.   Oxidizer-system-pressure-surge initiation

    d.   Propellant leak initiation

    e.   Engine-switch-group anomalies

The intermittent data sampling technique does not allow establishment of exact data shift times.

3.3.2.2.5 Investigations and Evaluations. The following areas, which are discussed below, have been investigated and evaluated since the completion of the initial flight data failure analysis:

    a.   Model 8247 engine testing at LMSC

    b.   Electrical power loss

    c.   Erroneous plumbing hookups and propellant analysis

    d.   Effects of SPS and turbine exhaust products

    e.   Propellant leakage considerations

    f.   Trapped pressurization gas in oxidizer feed system

    g.   Oxidizer sump failure

    h.   AEDC* data evaluation

    k.   Thrust-chamber-fuel lead/combustion considerations

---

*Arnold Engineering Development Center.

Propulsion Test Vehicle Assembly (PTVA). The Model 8247 engine was hot-fired at LMSC during the Gemini Propulsion Test Vehicle Assembly (PTVA) test program. A review of the test results verified that engine operation and performance were normal and within specification limits with the following exceptions:

    a. The main fuel valve exhibited "slow opening" characteristic during the first start of test 001G. The anomaly was attributed to air in an unbled, excessively long main-fuel-valve-actuation-pressure transducer line. This condition was corrected and normal main-fuel-valve opening was observed during the remainder of the program.

    b. The oxidizer-gas-generator valve exhibited a relatively slow closing characteristic at BAC (0.130 sec vs a nominal of 0.100 sec) during all tests. This characteristic (which was very repeatable) was not considered to be detrimental to PPS operation.

At the completion of the problem, all engine components were shown to be compatible with the GATV PPS and no engine hardware changes were recommended. (See Appendix B.)

Vehicle 5001 Hot Firing. The Model 8247 engine was also hot-fired during the vehicle 5001 acceptance test. PPS operation and performance were satisfactory. At the completion of the program, the PPS was shown to be compatible with the vehicle and no PPS hardware or procedure changes were recommended.

Electrical Power Loss. The Model 8247 engine has never been subjected to a test program or a complete theoretical analysis wherein the effect of removal of electrical power during the start transient has been evaluated. Therefore, the effect of closing the main fuel valve during the start transient on thrust chamber ignition and combustion characteristics has not been fully defined.

Erroneous Plumbing Hookups and Propellant Analysis. An investigation was conducted to determine effects of possible plumbing hookup errors and to verify that propellants loaded in the vehicle met specification requirements. Only one plumbing hookup error is possible, and this possibility was eliminated by correlation with observed

flight data. Verification was obtained that propellant samples were analyzed and that they did meet specification requirements. Therefore, these items were eliminated as possible contributors to the observed flight anomalies.

Effects of SPS and Turbine Exhaust Products. A theoretical analysis indicated that the SPS and/or turbine exhaust products could not collect in any significant amount in the Model 8247 engine thrust chamber or coolant jackets prior to ignition. An analysis of the effect of SPS hot-exhaust-gas impingement on the PPS fuel lead after it begins to leave the combustion chamber indicates that there is no significant effect.

Propellant Leakage Considerations. An analysis of the oxidizer side of the engine and feed systems indicates that if a structural failure occurred because of a pressure surge, the failure probably would be a crack in the sump or in the propellant isolation valve case.

Trapped Pressurization Gas in the Oxidizer Feed System. The evaluation showed that, since normal loading procedures were followed, gas was not trapped in the sumps. It also showed that, even if gas had been trapped in the sumps prior to liftoff, the dynamic loads during boost were more than adequate to force it out. Therefore, this condition was eliminated as a possible cause of failure.

Oxidizer Sump Failure. This evaluation was concerned with breakup of internal sump parts and subsequent ingestion into the engine. The standard Agena sump system has been extensively tested on the ground and has also been flown on several other programs. The only observed failure occurred during ground handling when the turning vane in the outlet of the oxidizer sump was broken off. This vane has since been strengthened. If the vane became detached and moved to the oxidizer pump inlet, it would have probably damaged oxidizer-pump-inlet temperature (which recorded normally during PPS operation). The probability of vane failure having occurred during this flight is believed to be very low.

AEDC Data Evaluation. The Model 8247 rocket engine has been tested at an altitude of approximately 110,000 ft in the facility at Arnold Engineering Development Center (AEDC). However, high-response dynamic instrumentation of the type used to measure ignition shocks was not employed, and the engine tested was of an earlier configuration that the one flown in Vehicle 5002. A review of the data indicated that, within the limitations of the instrumentation used, there was no indication of any "hard" starts.

Main-Propellant-Valve-Configuration Changes Since AEDC. The main-oxidizer-valve configuration was not changed. The following changes were made to the main fuel valve and its actuation circuit to obtain more repeatable opening characteristics:

    a.   Decreased spring preload for reduced cracking pressure

    b.   Movement of the actuation-pressure takeoff port closer to the pump case to obtain higher actuation pressures.

These changes resulted in an increase in normal thrust chamber fuel lead of 2.0 ±1.0 lb.

Thrust-Chamber-Fuel Lead/Combustion Considerations. A theoretical evaluation was made of possible thrust-chamber, hard-start causes and variations with respect to: (1) hard vacuum vs soft (AEDC) vacuum, (2) zero vs 1 g, (3) oxidizer preflows vs fuel preflows, and (4) small fuel leads vs larger fuel leads. The evaluation was made in an attempt to determine if the AEDC test environment was significantly different from that encountered in flight. The following hard start mechanisms were examined:

    a.   Ignition delay

    b.   Monopropellant reaction of fuel preflow

    c.   Backflow of liquid fuel into oxidizer manifold cavities and subsequent combustion in these cavities.

Firm conclusions were not reached regarding effects of the first two mechanisms (a and b, above). It was preliminarily concluded that the item c mechanism offerred a possibility and that both a hard vacuum and a large fuel preflow would tend to increase the amount of liquid fuel in the oxidizer manifold (vapor mass is relatively unimportant because of its low energy content). This theory requires test demonstration to prove its validity.

3.4 STRUCTURES

This section includes discussions of structural dynamics, analyses of separation events, and evaluations of acceleration, pressure, and temperature flight data. The summary, presented below (par. 3.4.1), lists conclusions; this is followed by a detailed discussion of the flight data. Recommendations and conclusions are summarized in Section 4.

3.4.1 Summary

- Winds aloft were less severe than customary and created mild loading conditions that approached neither structural nor control limits.
- Pressure time histories were normal, within the accuracy of the sampling system, with shock-induced pressure indications representing VECO separation and pyro-actuated helium valve actuation on the forward pressure transducer.
- Atlas-Agena separation was nominal although the primary separation monitor failed to provide a normal indication.
- Accelerometers mounted near the engine mounting ring were rendered inoperative at Atlas-Agena separation, probably as a result of pyrotechnic shock to the amplifiers.
- Lateral accelerometer data appeared nominal.
- Axial accelerometer data were obtained and anomalies were recorded; though primarily for vibration analysis, these data may be used to analyze hypothetical power buildup and decay models.

    (1) Elastic response to very sudden thrust buildup could be largely due to excitation of the second longitudinal mode. Explosive buildup to a normal thrust level with gradual tailoff could account for the highest acceleration sample measured.

    (2) A normal thrust buildup would not account for the highest peak measured during the anomaly unless the thrust level reached about 28,000 lb.

3-41

LOCKHEED MISSILES & SPACE COMPANY

(3) Lack of elastic overshoot in negative g's following the anomaly would indicate that thrust removal was no more rapid than normal thrust buildup.

● Maximum skin temperatures were considerably lower than the design temperatures, and were normal.

● Secondary propulsion system temperatures indicate normal operation.

● Structural and equipment temperature histories indicate propellant leakage in the aft-rack engine compartment. It is not possible to determine whether the leakage was fuel or oxidizer from temperature data alone or to determine the exact time that leakage began.

● Some type of high-energy reaction was indicated in the vicinity of the nozzle extension exit plane.

● Target docking adapter functions were normal.

3.4.2 Structural Loads and Dynamics

3.4.2.1 Winds Aloft. The wind environment was monitored during the Gemini pre-launch period starting with a forecast for the time of launch made 2 days prior to the launch and continuing at intervals until the final sounding balloon was released at 1550 GMT on the day of launch. Figures 3-14 and 3-15 present three wind velocity profiles and the corresponding wind azimuths as a function of altitude; these profiles were measured by balloons released at approximately 8 hr, 5 hr, and 15 min before launch. As can be seen from the relative shape of these profiles, the winds were relatively stable over this 8-hr period prior to launch.

To determine the effect of the wind environment on the structural and control capabilities of the total vehicle, each profile was used as an input to a 6 degree-of-freedom simulation of the ascent flight of the GATV. This digital computer simulation then defined the total vehicle response to the wind perturbations and provided a measure of the structural and control capability utilized. The winds measured by the balloon released just prior to liftoff are the most significant to the postflight analysis. The computer analysis of this profile indicated that the winds aloft would not create a loading or control critical situation. The actual percentages of structural and control capability required in response to this wind were 27 and 12 percent, respectively.

3-42
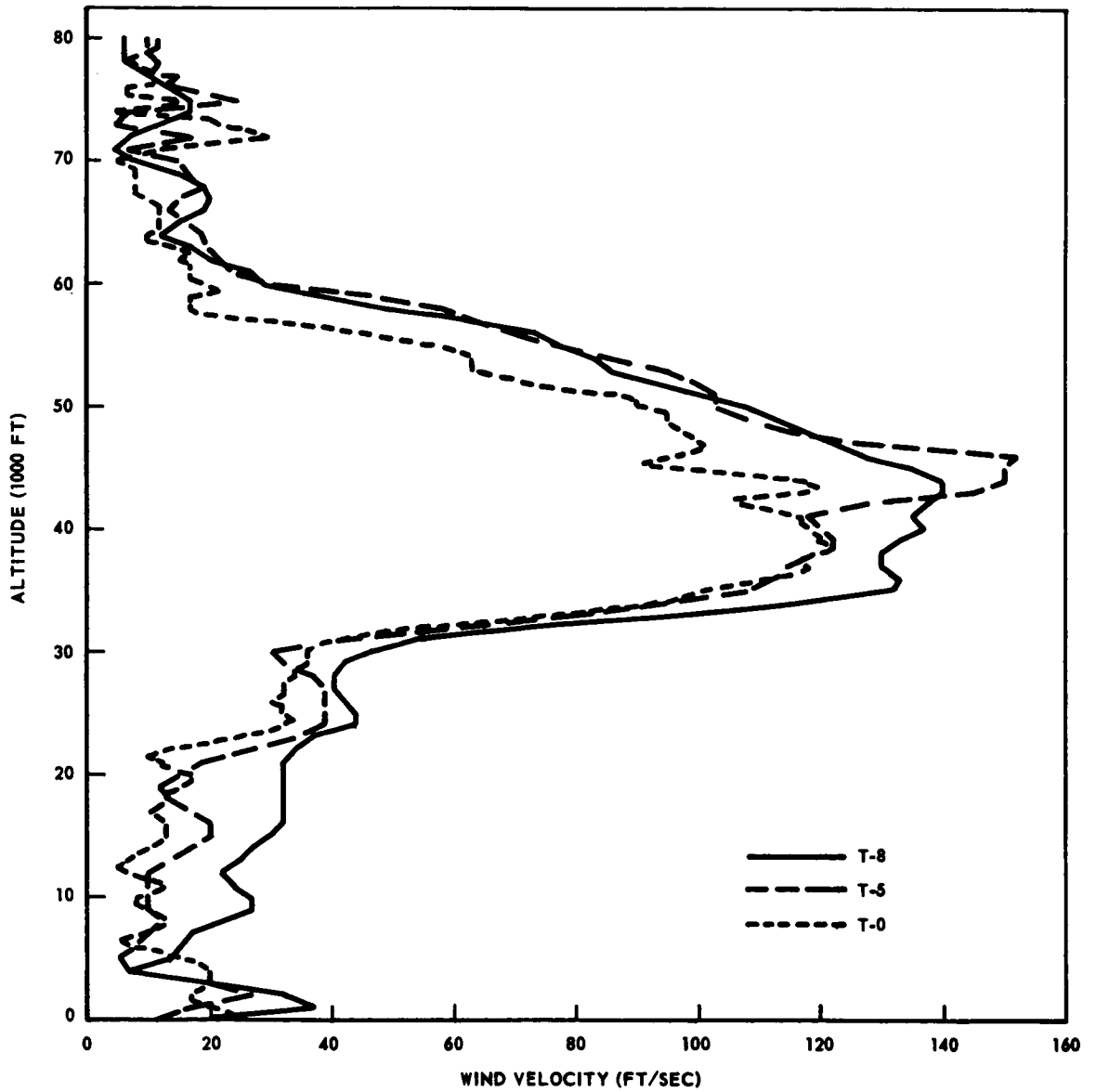
Fig. 3-14 Wind Velocity Profiles

3-43
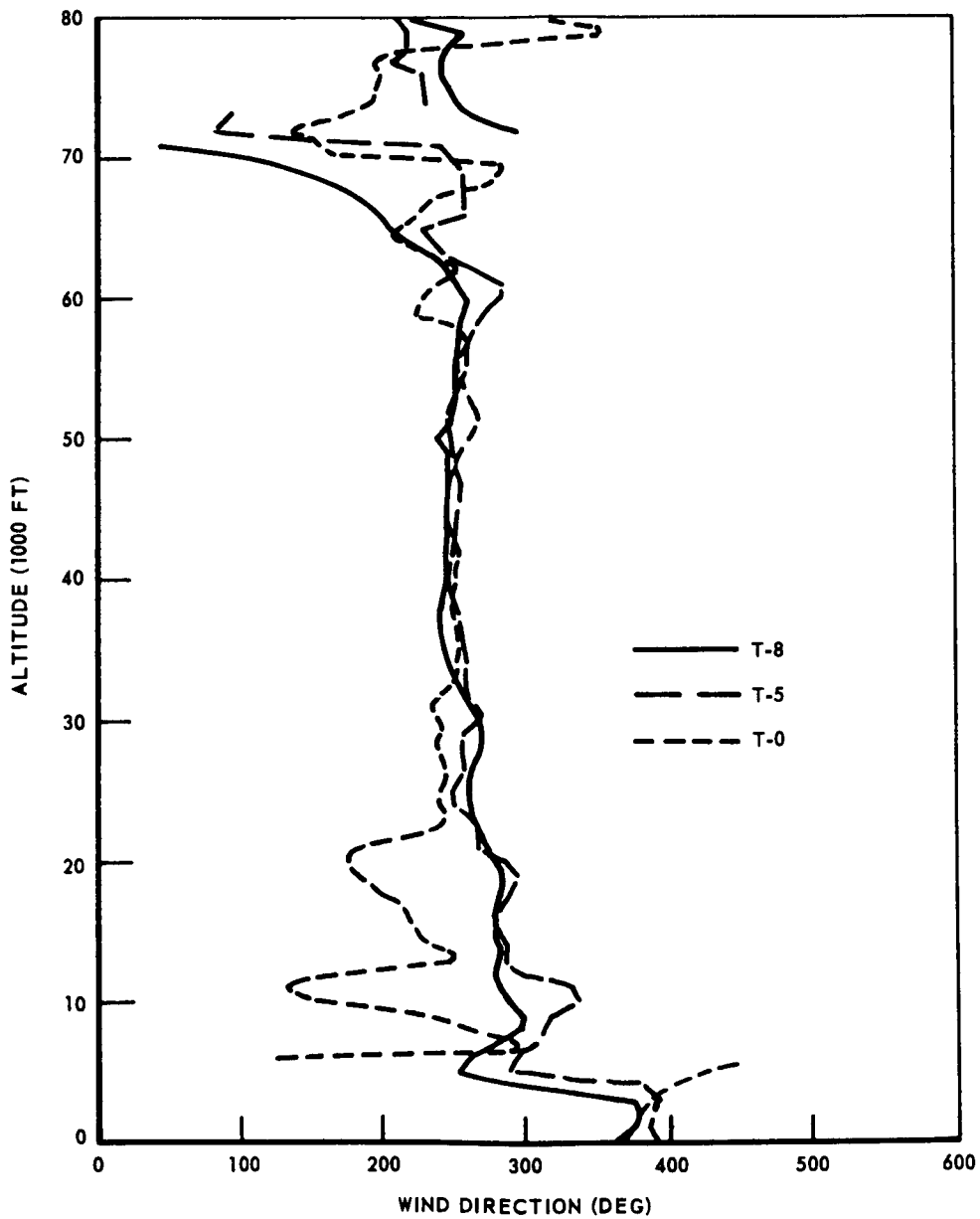
Fig. 3-15 Wind Direction Profiles

3-44

LOCKHEED MISSILES & SPACE COMPANY

It can be concluded from the computer simulation of the ascent flight and the examination of additional flight test data that the wind environment was not severe and did not create a loading condition beyond the structural or control capability of the vehicle.

3.4.2.2 Compartment Pressure. GATV 5002 carried absolute pressure transducers in the forward and aft racks to measure the internal pressure environment of these areas during ascent. Figure 3-16 shows the pressure history of the forward and aft racks, as measured by the pressure transducers, in comparison to the ambient pressure that existed at the time of launch. As can be seen, the internal pressure followed the ambient pressure normally throughout the booster phase of flight. The activity indicated on the forward compartment pressure measurement (Figs. 3-16 and 3-17), which occurs at 303.72 sec and 305.98 sec, corresponds identically to the times of VECO and Atlas-Agena separation and represents a probable pyrotechnic shock response.

As the ambient pressure in the vicinity of separation (724,500 ft) is basically zero, the pressure rise at 303.72 and 305.98 sec could be attributed to a shock occurring at these times, with the forward pressure transducer reacting with an indicated pressure rise. Another possibility would be that these indications represent the pressure rise created by the firing of a pyrotechnic device; but this does not occur at VECO. Atlas-Agena separation is accomplished by the firing of the separation joint followed by ignition of the Atlas retrorockets, which would tend to increase pressures locally, but more in the region of the aft section than the forward section. As the aft pressure transducer does not react at this time, the possibility of a shock reaction on the forward transducer is again indicated. An examination of the accelerometer data in the TDA to verify the presence of shock indicated that these data were incapable of reflecting the higher frequencies required to define the shock level. The existence of a significant shock is further indicated by the fact that accelerometers A5 and A522, located on the engine cone (Figs. 3-18 and 3-19), dropped out at Atlas-Agena separation, probably because of pyrotechnic shock.
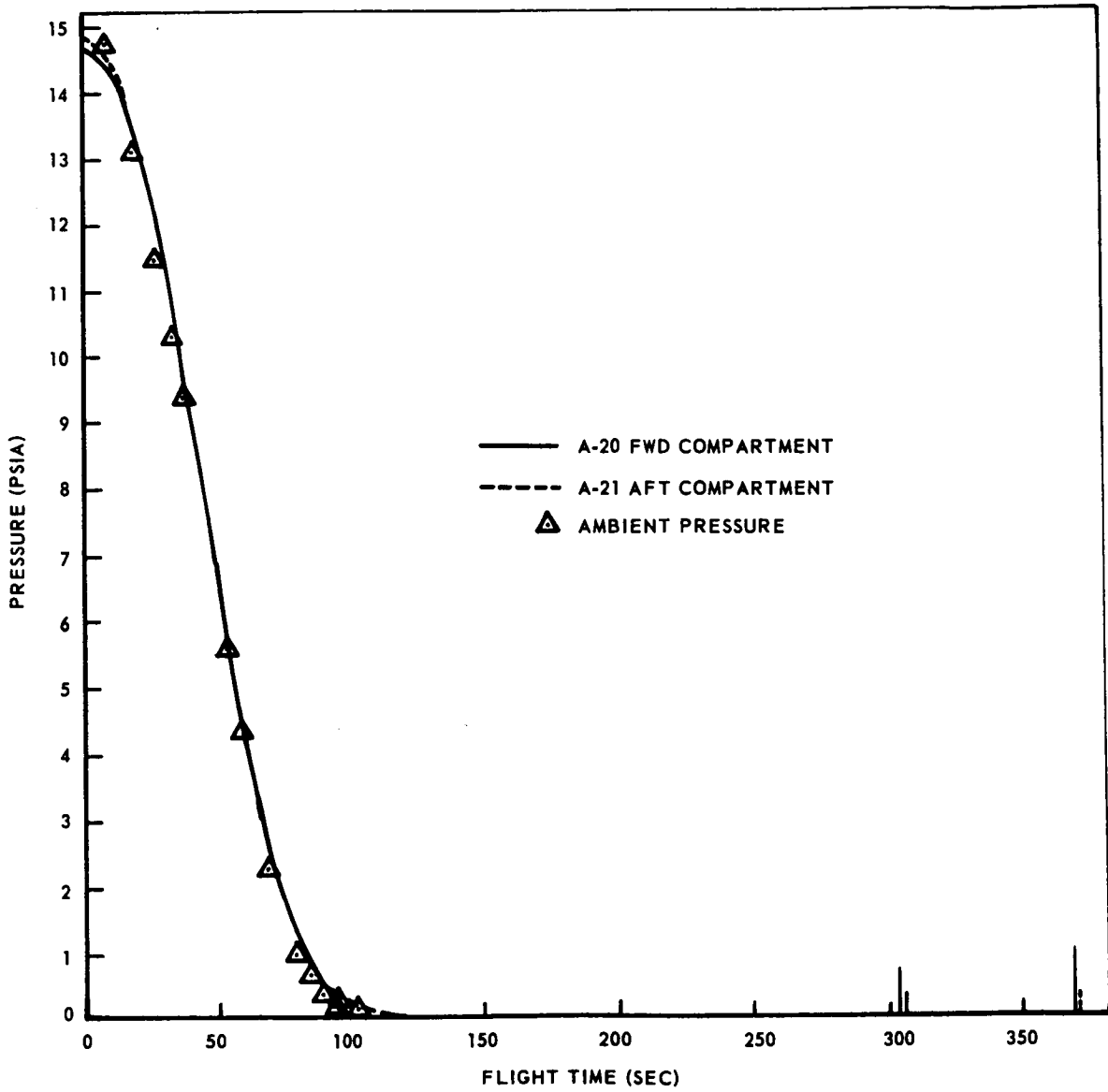
Fig. 3-16 Pressure Time History From Liftoff to 114 Sec

3-46
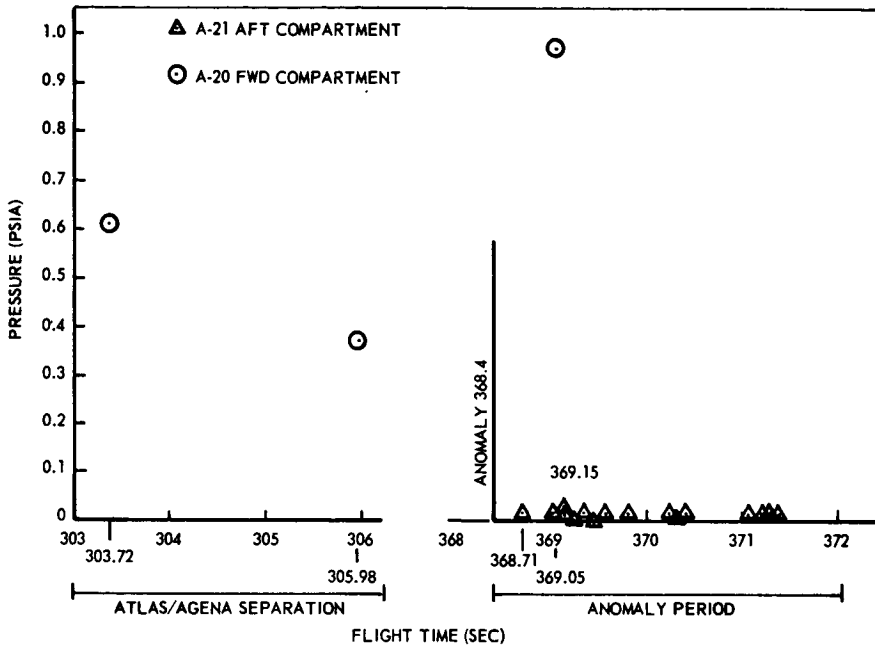
Fig. 3-17 Pressure Time Histories During Atlas-Agena Separation and During Anomaly
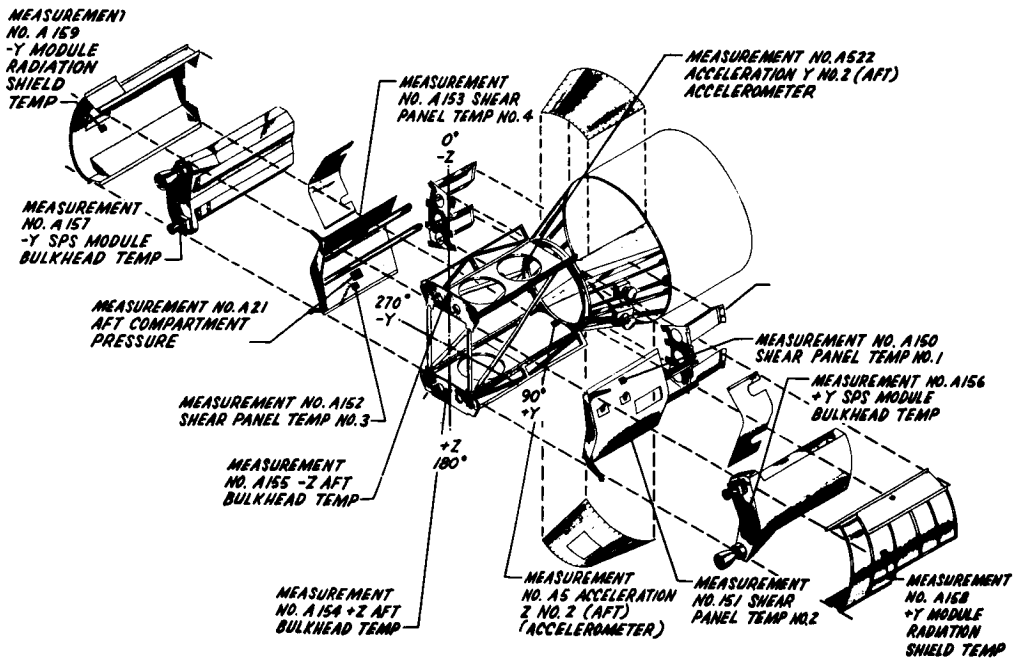
Fig. 3-18 GATV Aft Section Showing Location of Temperature, Pressure, and Acceleration Measurements
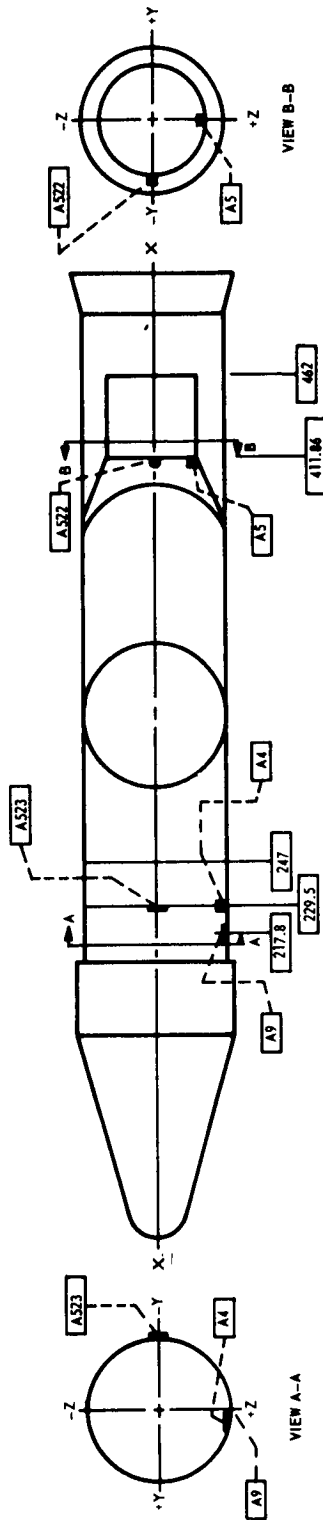
MEASUREMENT NUMBER	MEASUREMENT DESCRIPTION	AGENA BODY STATION	FREQUENCY RESPONSE (CPS)	RANGE (g)	TRANSDUCER ORIENTATION	SAMPLE RATE (PER SEC)
A9	ORBITAL AXIAL ACCELERATION	217.85	0 – 200	±3.0	+ X	64
A4	ORBITAL TANGENTIAL ACCELERATION	226.35	0 – 150	±1.5	Y – Y	32
AS23	ORBITAL TANGENTIAL ACCELERATION	228.25	0 – 150	±1.5	Z – Z	32
A5	ORBITAL LATERAL ACCELERATION	411.86	0 – 150	±1.5	– Z	32
AS22	ORBITAL LATERAL ACCELERATION	411.86	0 – 150	±1.5	– Y	32

Fig. 3-19 Structural Dynamic Flight Instrumentation

3-48

Indicated pressure rise at these times could also be explained as a signal dropout or loss of synchronization occurring at these times, although this is not verified by other telemetry records.

The forward-rack pressure transducer shows a further sharp pressure rise at 369.05 sec, which coincides (considering PCM sampling rate accuracy) with the firing of the pyrotechnic-operated helium valve located in the forward rack. The coincidence of this pressure response with the activation of the pyrotechnic device should explain the rise in pressure indicated on this transducer as either a response to a shock or the local increase in pressure due to the detonation.

The fact that the aft-rack pressure transducer apparently did not respond to the helium valve activation can be readily explained by the relative location of the transducer with respect to the helium valve, which was located in the forward rack. The Mariner flight test data indicated that only those instruments in the immediate vicinity of this pyrotechnic device recorded a shock of significant level. The aft-compartment pressure transducer responded with an erratic pressure history (Fig. 3-17) starting at 368.71 sec and continued until the loss of signal. This aft-rack pressure transducer behavior is anomalous and does not match any of the events that occur during this period. The 0.12 psia data indication is only the accuracy of the least significant bit (0.12 psia) and is believed to represent noise.

3.4.2.3 Dynamic Flight Data Analysis. Five accelerometers were carried on the Agena. Three of these were mounted on the TDA and oriented along the X (longitudinal), Y (lateral), and Z (vertical) axes; and the remaining two, which were mounted at the interface between the engine cone and the aft rack (Sta 411.86), were oriented along the Y and Z axes. (See Fig. 3-19.) Data from all five instruments were telemetered at sampling rates of either 32 or 64 per second.

The low sampling rate of the accelerometer data prevents the construction of a true time history of the signals generated by each accelerometer. However, the amount of activity, or perturbation, that took place in the signal generated at any given discrete time during flight may be determined by noting the maxima and minima of the data in some small time range on each side of this discrete time.

Figure 3-20 shows the results of this data analysis in the form of envelopes of the maximum and minimum signals from each of the five accelerometers versus flight time. This "broad-brush" treatment of the dynamic activity occurring throughout flight indicates the expected high activity at liftoff and during the transonic phase. The low sensitivity of the longitudinal instrument caused it to become saturated at about 50 sec after liftoff when the steady state acceleration approached +3 g. Details of the SECO, VECO, and separation events do not appear in Fig. 3-20 because of the large time scale. However, examination of the high-speed records of these events indicated no abnormalities. High-speed records of the PPS startup for the three forward accelerometers, which will now be discussed, are shown in Figs. 3-21 and 3-22. (The rear-mounted accelerometers became inoperative at Agena-Atlas separation.)

All the acceleration values obtained at discrete times on each side of the time of commencement of the flight anomaly (368.4 sec after liftoff) have been joined by straight lines, and the resulting plots are shown in Fig. 3-21 for the two operational lateral instruments, and in Fig. 3-22 for the longitudinal instrument. These plots, represent, at best, a mean line through the oscillations, and quite large deviations from this line could have occurred between sampling points and gone undetected. Figures 3-21 and 3-22 will be discussed in more detail in the paragraphs that follow.

As illustrated in Fig. 3-20, three accelerometers exhibited partial or complete failures during various stages of flight. The TDA Z-axis accelerometer (A523) was intermittent but operation otherwise appeared normal. The two accelerometers (A5 and A522) mounted in the engine cone were lost completely during the pyrotechnic separation event. The loss of A5 and A522 appears to be a clearcut case of pyrotechnic shock at separation.

ACCELEROMETER
A–9
X-AXIS
TDA
(G) 0

SENSITIVITY
± 3.0 g

NOTE: CROSSHATCHED AREAS SHOW
EXCURSION OF SAMPLED DATA

3.0
2.0
1.0
-1.0
-2.0
-3.0

ACCELEROMETER
A–4
Y-AXIS
TDA
(G) 0

SENSITIVITY
± 1.5 g

ACCELEROMETER
A–523
Z-AXIS
TDA
(G) 0

SENSITIVITY
± 1.5 g

LOST
CHANNEL

ACCELEROMETER
A–522
Y-AXIS
ENG. CONE
(G) 0

SENSITIVITY
± 1.5 g

ACCELEROMETER
A–5
Z-AXIS
ENG. CONE
(G) 0

SENSITIVITY
± 1.5 g

0   50

LOST CHANNEL

STAGING

BECO

FLIGHT TIME (SEC)

100   150   200

3-524

Fig. 3- 20 Accelerometer Status Time History

3-52-2

TDA ADAPTER ACCELEROMETER A 523
Z-Z DIRECTION
SAMPLE RATE: 32/SEC

ACCELERATION G'S

TDA ADAPTER ACCELEROMETER A-4
Y-Y DIRECTION
SAMPLE RATE: 32/SEC

FLIGHT TIME (SEC)
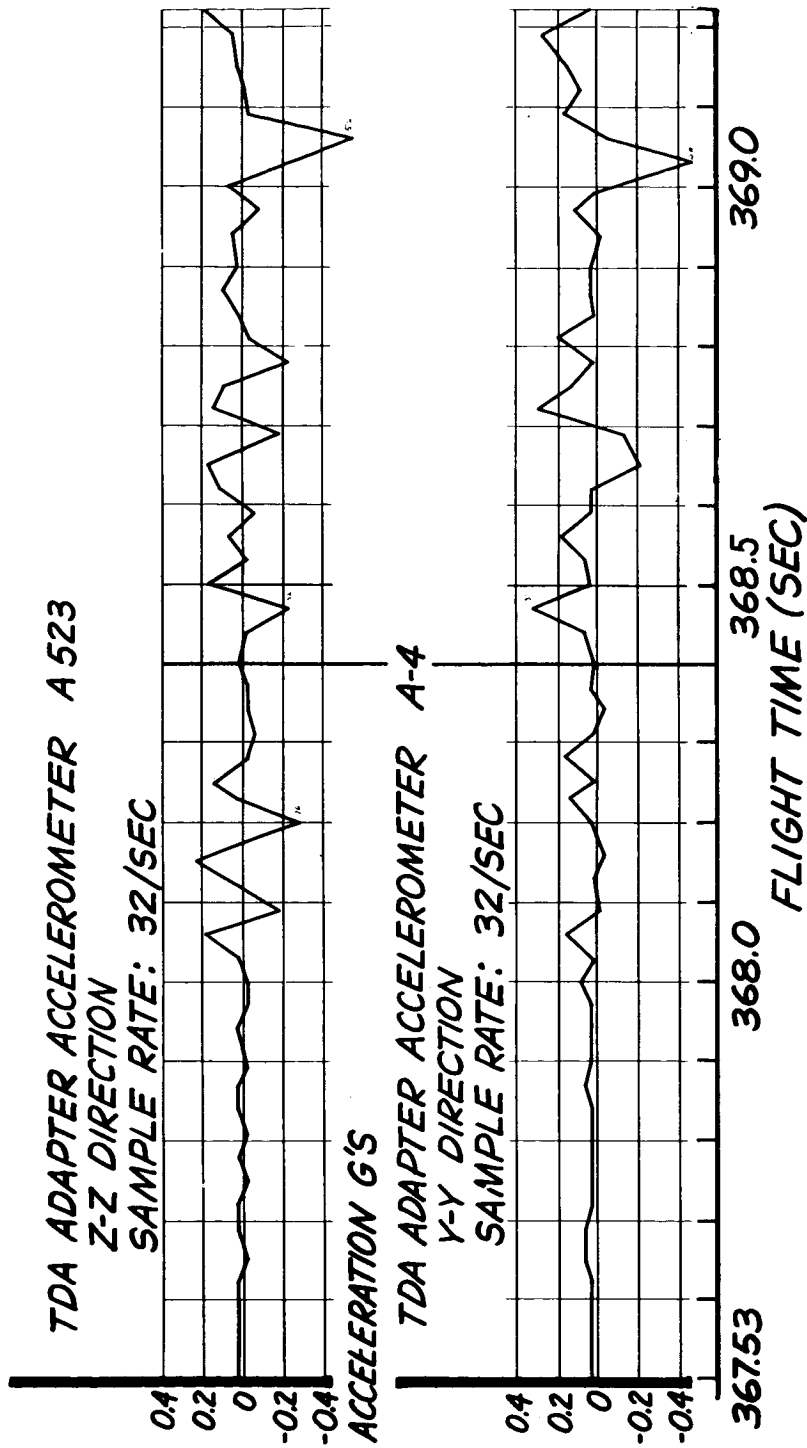
Fig. 3-21   Target Docking Adapter Accelerometers A523 and A4 (Z and Y Axes) During Anomaly Phase

LOCKHEED MISSILES & SPACE COMPANY
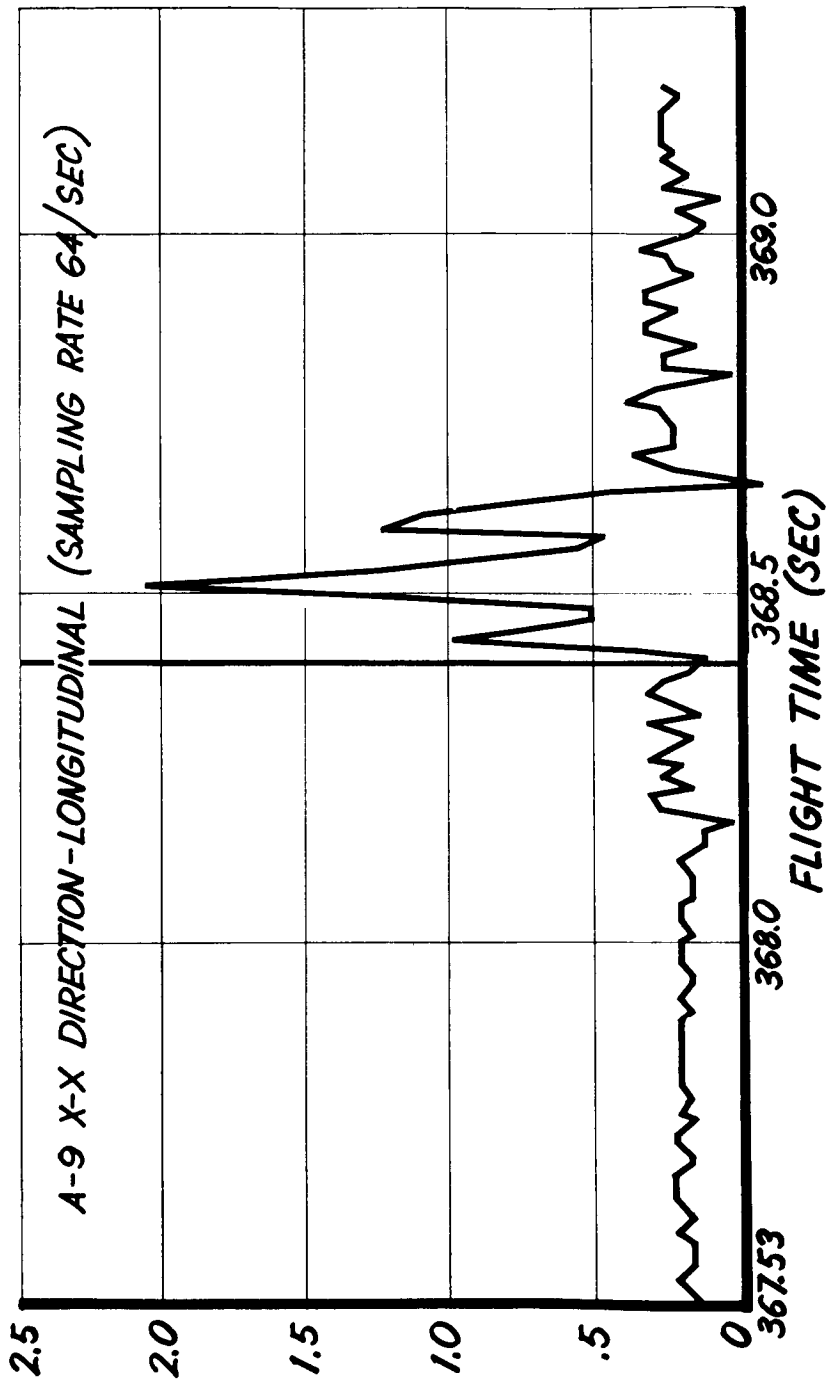
Fig. 3-22 Target Docking Adapter Accelerometer A9 (X Axis) During Anomaly Phase

LOCKHEED MISSILES & SPACE COMPANY

SAFE-ARM
J-BOX

AMPLIFIER A5

FREQUENCY
SENSITIVE
RELAY

STATION 411.86

+Z

VIEW LOOKING AFT

STATION 348

+Y

POWER
DISTRIBUTION
J-BOX

AMPLIFIER
A522

SIGNAL
CONDITIONER
BOX
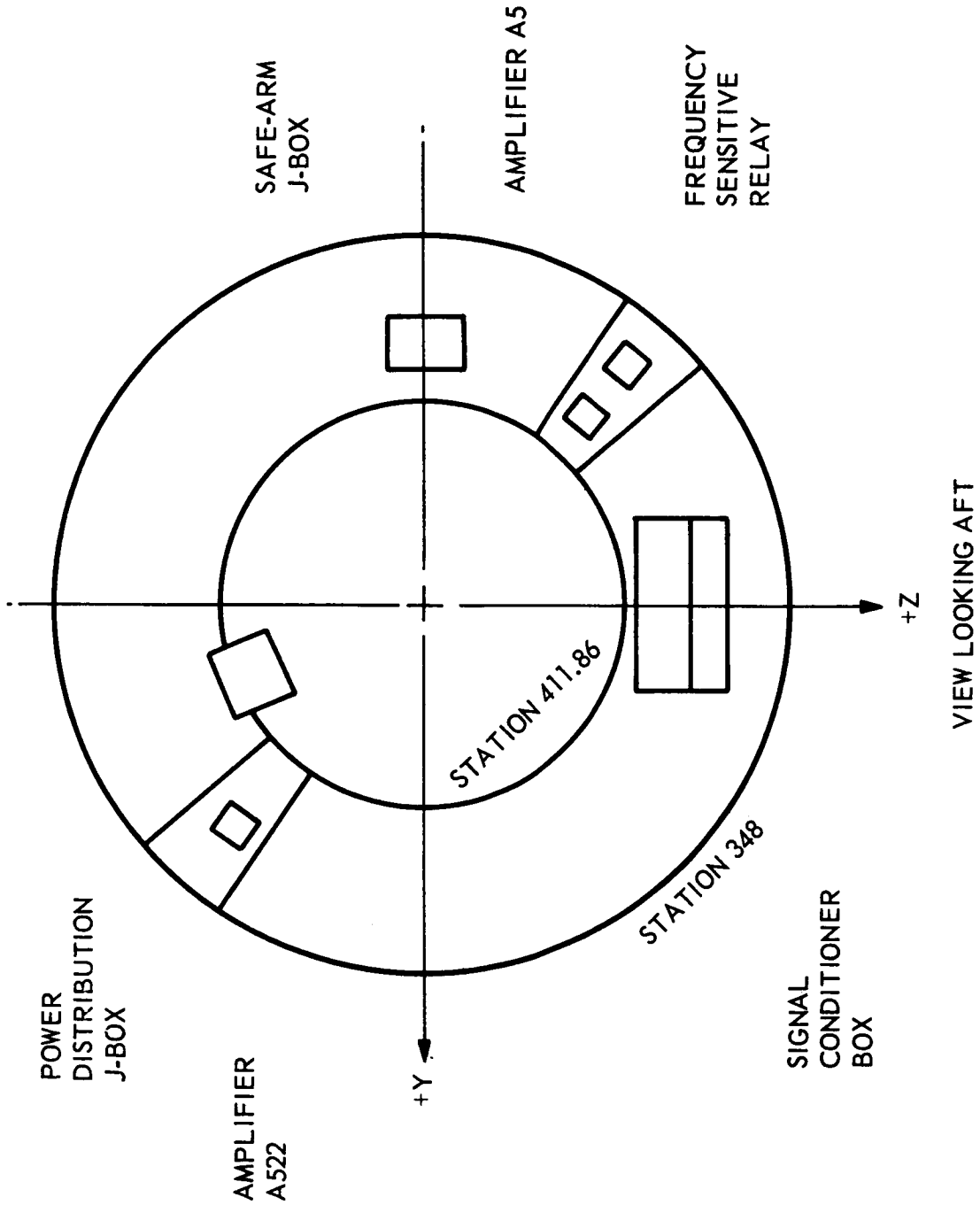
Fig. 3-23   Locations of Aft Area Equipment and Instrumentation of Interest for the Pyrotechnic Shock Event

3-55

Primacord separation, as used on the 5002 vehicle, produces a severe shock environ-ment in the engine cone area. The effect becomes rapidly less severe with rearward movement along the aft rack. Agena vehicles 1171 and 1172 flew accelerometers mounted just aft of Sta 412, with their associated amplifiers also mounted to the aft rack. Although these vehicles were also subjected to primacord separation, loss of the measurements did not occur – most likely because the amplifiers were placed in a shock environment several orders of magnitude less severe than the amplifiers on the engine cone of GATV 5002. (See Figs. 3-18 and 3-23.)

Pyrotechnic shock events, because they had a considerable influence on Vehicle 5002 flight data, are discussed more fully below.

The pyrotechnic booster separation generates high amplitude shocks in the booster adapter skin. Although the precise nature and formation mechanism of these shocks are not fully understood, it is thought that the impingement of the charge on the skin induces both compression and bending waves that are transmitted along the adapter skin. These shock waves continue to travel into the engine cone, engine, and aft-rack structures. Two LMSC documents* show that the resulting environment has been determined in ground test and partially verified by flight tests. These references also show by shock spectrum analysis that the pyrotechnic shock causes excitation of a broad frequency spectrum; i.e., the excitation exists at all frequencies up to 10 kc that the measurement system can detect. It is suspected that the excitation exists at frequencies well beyond the measurement capability. Of considerable interest is the observation from the shock spectrum analysis that the high level excitation appears to occur at frequencies above 800 cps. Although still somewhat conjectural, this type of excitation seems to have a detrimental effect on the performance of relays and other electronic components; it is therefore advisable to test the effect of the shock on electronic equipment.

---

*LMSC-A391566, "1163 Vehicle Separation Tests Conducted at SCTB," A.D. Houston, 17 October 1963.
LMSC-A704799, "Discussion of Pyrotechnic Shock Environment Existing in the Agena Vehicle in Light of Recent Flight and Ground Test Requirements," A. D. Houston, 25 June 1964.

3-56

Equipment components are normally exposed to a half-sinewave pulse-shock test during flight qualification (Environmental Test Specification, LMSC-6117B). Ascent shock spectrum analyses of this type of shock have shown that this test is inadequate as a simulation of the pyrotechnic shock environment. Figure 3-24 shows a comparison between the spectra generated by a typical half-sine pulse shock and by the pyrotechnic shock. This illustration also shows the estimated shock environment for equipment mounted on isolators of the type shown in Fig. 3-25.

Relocation of equipment away from the source of the pyrotechnic shock is an effective means of reducing the environment. Data indicate that a 50 percent reduction in shock amplitude is obtained for every 20 in. from the shock source, but that the frequency content remains essentially unchanged. Other techniques for reducing the shock environment are to reduce the explosive loading or the thickness of the separation plate cut by the primacord.

It is difficult to deduce the nature of the force input to the GATV structural system that caused the accelerometer activity during the anomaly period. Without a continuous response record it is impossible to determine the frequency content of the structural response or the peak values present in it. Certainly no basic conclusions can be drawn from the accelerometer data alone, and it can have only limited use in backing up or disproving hypotheses based on other flight data. However, an attempt has been made to analyze the response of the X-axis accelerometer during the anomaly period based on known structural characteristics. The attempt involves the following observations, assumptions, and hypotheses*:

  a. Basic Observations. Figure 3-22, the X-axis accelerometer sampled data plot, shows the following:

    (1) A bias error in acceleration of about 0.2 g

    (2) No evidence of accelerations occurring in the negative g region

---

*Two hypotheses have been tested separately to see how closely the available flight data points fit the results. In each case, the hypothesis was chosen to reflect some aspect of normal thrust buildup.
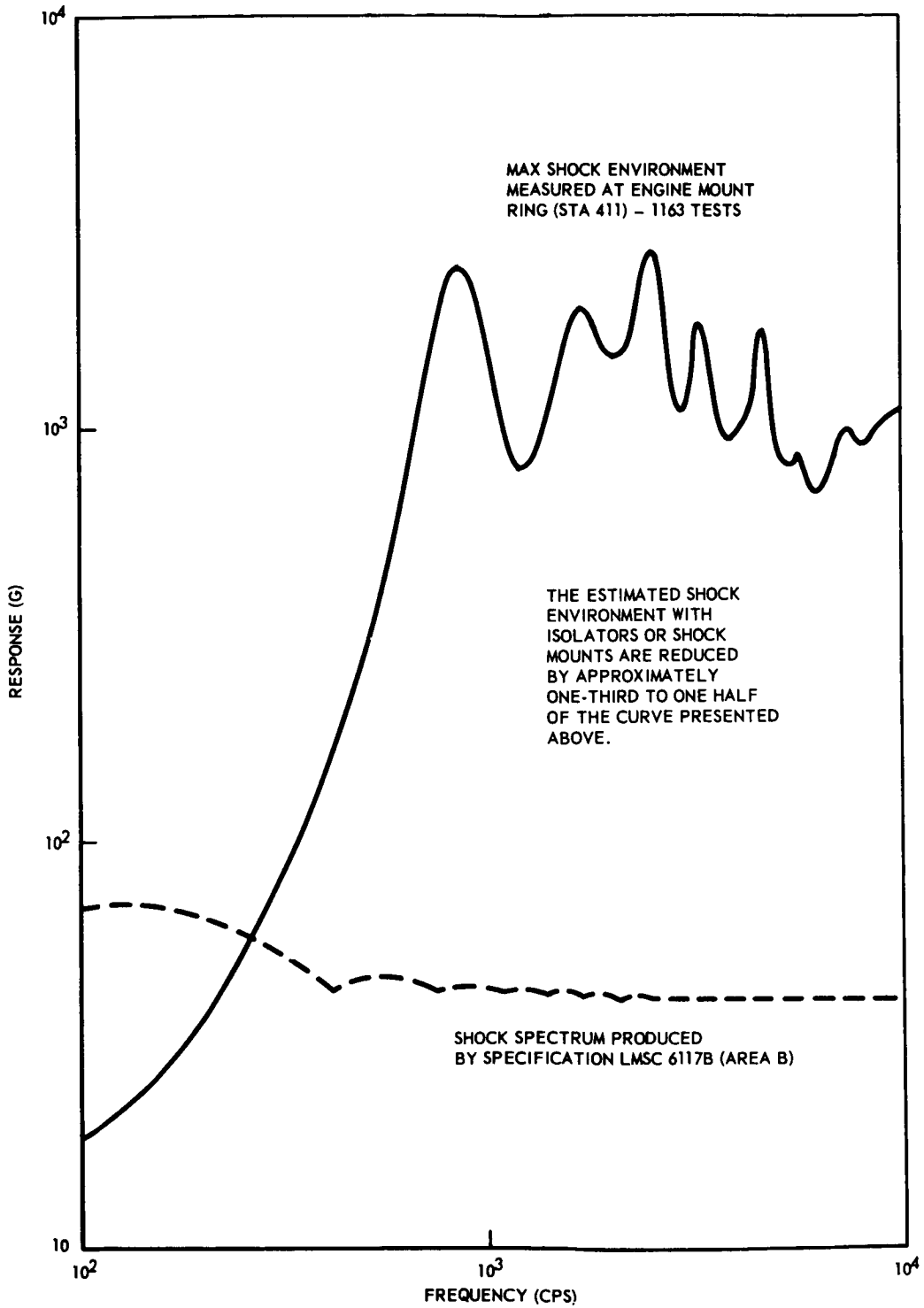
Fig. 3-24 Shock Spectra Comparison

LOCKHEED MISSILES & SPACE COMPANY
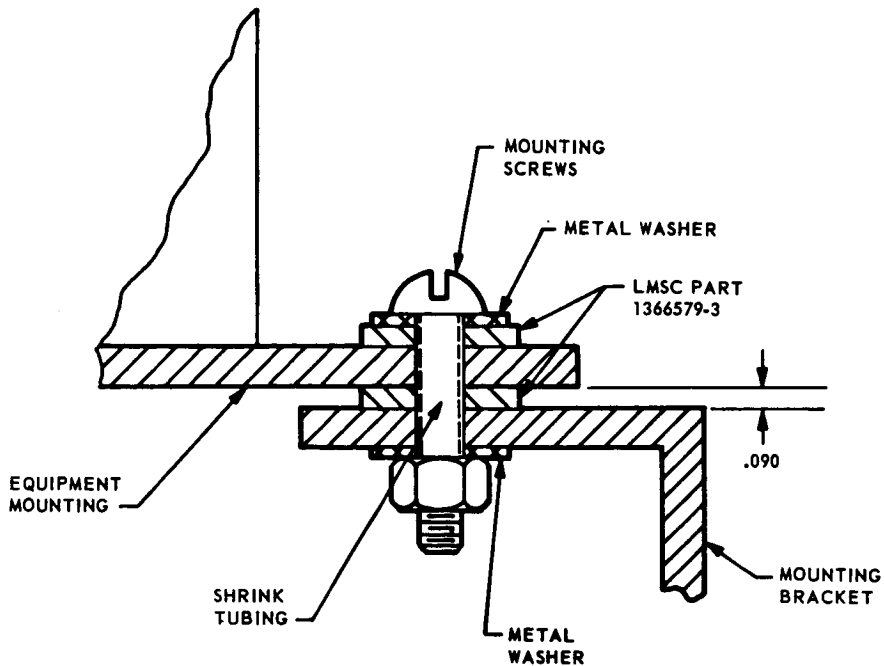
Fig. 3-25 Shock Isolation Installation

b. Basic Assumptions

    (1) The prepondenace of positive -g data points is taken to indicate that the thrust did indeed build up to some level

    (2) Elastic body response has been considered in the first and second longitudinal elastic modes (34 and 68 cps natural frequencies, respectively)

c. Hypothesis A. Thrust builds up to its normal maximum level, 19,200 lb, but does it instantaneously. It then falls off linearly to zero within the noted accelerometer activity time, which is about 0.26 sec.

d. Hypothesis B. The thrust buildup rate is normal but attains the maximum level necessary to produce the combined elastic/rigid body response of 1.85 g sampled during the anomaly.

Using hypothesis A, it was found that at the Agena station of the X-axis accelerometer (Fig. 3-19) the maximum structural dynamic response is about 0.37 g maximum for the first elastic mode, and about 1.0 g maximum for the second elastic mode. The time response envelope exceeded the 1.85-g level measured in flight by about 0.1 g at the corresponding time.

Using hypothesis B, it was found that a thrust level of about 27,700 lb would have to be realized with the normal buildup rate to produce the 1.85-g level sampled during flight. The elastic response obtained from the first and second longitudinal modes contributes less than 0.1 g, each. The absence of data overshoot (structural elastic) into the negative g region is indicative of a gradual rather than a sudden tailoff rate.

A detailed analysis of the Y and Z-axis accelerometers in the TDA was not attempted. The uncertainties involved in interpreting the commutated data points are certainly no less prevalent than in the X-axis case. The general character of the lateral responses during the anomaly phase seems reasonable enough when reviewing Fig. 3-21. The disturbance in the traces just prior to the anomaly is ordinarily seen on other flights and is known to be caused by the propellant-pump turbine spin-up. The peak samples found on both accelerometers following the main anomaly activity are directly attributed (in time) to the firing of the pyro-actuated helium valve. The levels shown are higher, however, than are normally seen with continuously monitored signals for this event. This may be due to the fact that the commutated system is used to sample and transmit the higher-g, higher-frequency components of structural response. The commutated system is unfiltered at the source, while the continuous FM-FM system has inherent low-pass filter characteristics.

3.4.3 Atlas-Agena Separation and Nose Cone Separation

The Atlas-Agena flight separation data were reviewed, and it was concluded that a nominal separation did occur.

The step switches appeared to have voltage level problems; the voltage exceeded the telemetry limits of 5v as the second switch was contacted. (See Fig. 3-26.) No usable data were obtained from the step switches thereafter.
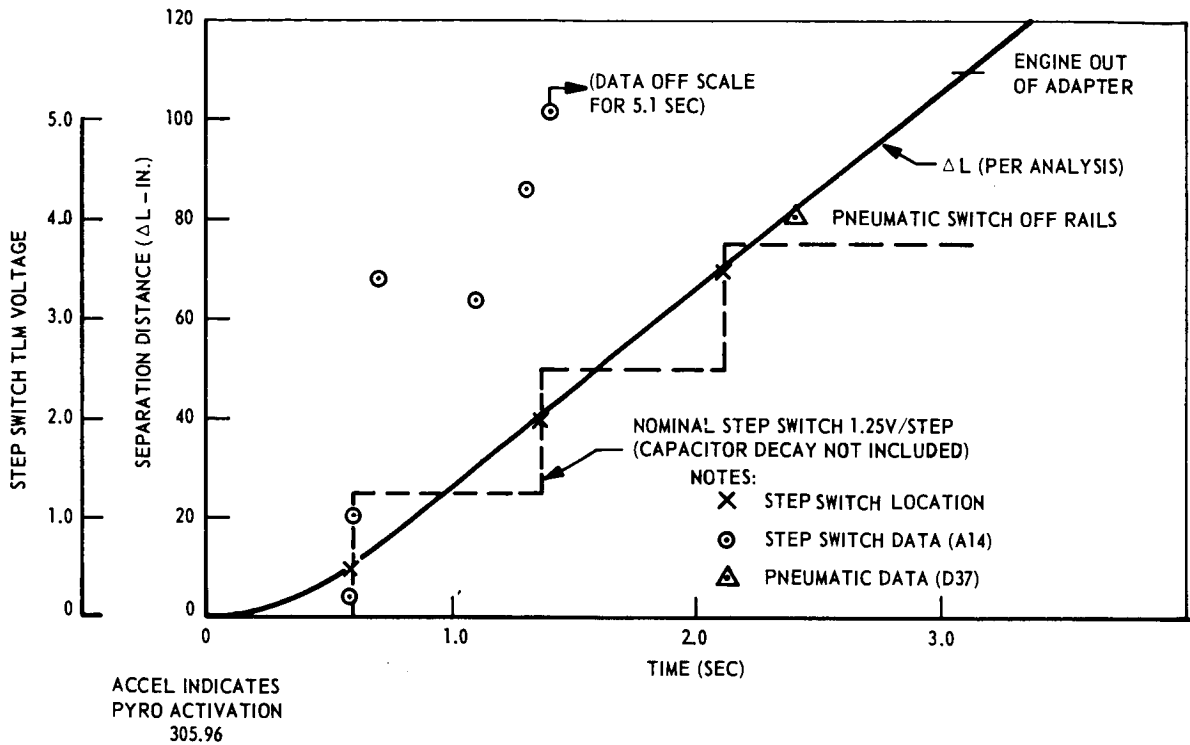
Fig. 3-26 Relative Separation Velocity

The pneumatic actuation switch indication functioned approximately 2.4 sec after the first pyrotechnic shock was noted on the accelerometers. To verify the expected separation time, an analysis was performed. It was assumed that the separated mass consisted of the Atlas wet mass and 100 percent effective residual fuel mass; the retrorockets were assumed to provide a nominal impulse output as prescribed by Rocket Power, Incorporated; a recent analysis concerning effective retrorocket angles was also incorporated. The results showed that the expected time for actuation of the pneumatic switch was 2.36 sec, which was considered in excellent agreement with the 2.4 sec observed (Fig. 3-26). The relative separation velocity was approximately 40 in./sec.

3-61

The shroud separation monitor showed a voltage change at liftoff + 369.5 sec; however, this was after the main engine anomaly and is thought to be an effect of other problems. This premise is based on the data from the TDA accelerometers, which show no indication of the shroud pyrotechnics being activated.

3.4.4 Thermal Evaluation

The location, type, and range of the skin temperature instrumentation employed on Vehicle 5002 are presented in Table 3-4. One resistance thermometer was located on the inner surface of the Agena horizon sensor fairing. Seven thermistors were mounted on the skin of the docking adapter to provide indications of the heating effects of flow separation aft of the shroud/docking adapter interface. Six resistance thermometers were mounted on the inner surface of the fiberglass shroud.

The temperature data obtained from flight are presented in Figs. 3-27 through 3-31 as temperature-history curves faired through the data available from the data reduction and processing equipment (DRAPE). Each illustration also presents the corresponding design temperature. For all measurements, the liftoff temperatures were consistent with the liftoff temperature of other vehicle components. As in the case with Atlas-boosted vehicles at approximately 60 sec after liftoff, skin temperatures increased because of aerodynamic heating. Although the DRAPE did not present temperatures at 60 sec after liftoff, the curves through the available data were drawn to reflect this behavior.

The temperature response of measurement A210 on the Agena horizon-sensor fairing in Quadrant 2 is presented in Fig. 3-27. The response was similar to that obtained from measurements in this area on other vehicles. There was loss of signal at approximately 303.7 sec after liftoff, corresponding to the normal occurrence at jettisoning of the fairing. The maximum temperature of 504°F indicated by the data is lower than the standard Agena design temperature of 850°F for the fairing.

Table 3-4

LOCATION, TYPE, AND RANGE OF SKIN TEMPERATURE INSTRUMENTATION

Measurement Numbers	Area	Type	Temperature Range (°F)	Station Number	Quadrant	Angular Position
A210	Horizon Sensor Fairing	R.T.*	+ 32 to +600	260	2	43° to +Y
A388	Docking Adapter	S.C.**	-100 to +500	210	3	13° to -Y
A389	Docking Adapter	S.C.	-100 to +500	215	3	13° to -Y
A390	Docking Adapter	S.C.	-100 to +500	220	3	13° to -Y
A391	Docking Adapter	S.C.	-100 to +500	225	3	13° to -Y
A392	Docking Adapter	S.C.	-100 to +500	210	2	17° to +Z
A393	Docking Adapter	S.C.	-100 to +500	210	1	13° to +Y
A394	Docking Adapter	S.C.	-100 to +500	210	4	17° to -Z
AD40	Shroud Cylinder	R.T.	0 to +450	198.6	2	20° to +Z
AD41	Shroud Cylinder	R.T.	0 to +450	198.6	4	20° to -Z
AD42	Shroud Cone	R.T.	0 to +300	138.6	2	10° to +Z
AD43	Shroud Cone	R.T.	0 to +300	138.6	4	10° to -Z
AD44	Shroud Cone	R.T.	0 to +400	113.7	2	10° to +Z
AD45	Shroud Cone	R.T.	0 to +400	116.2	4	10° to -Z

 * Resistance thermometer.
** Semiconductor.
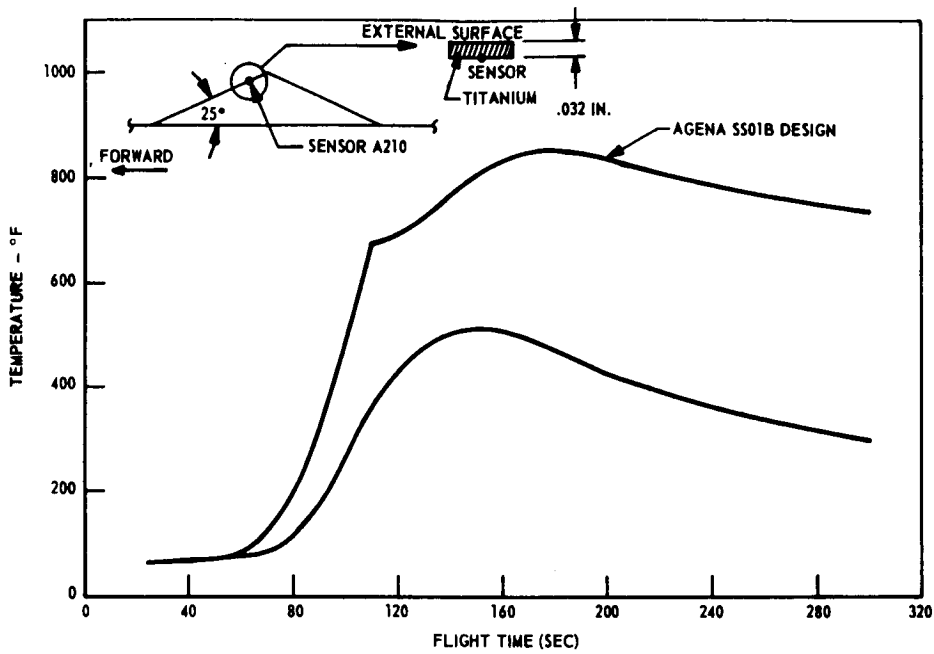
Fig. 3-27 Horizon–Sensor Fairing (A210) Ascent Temperature Histories
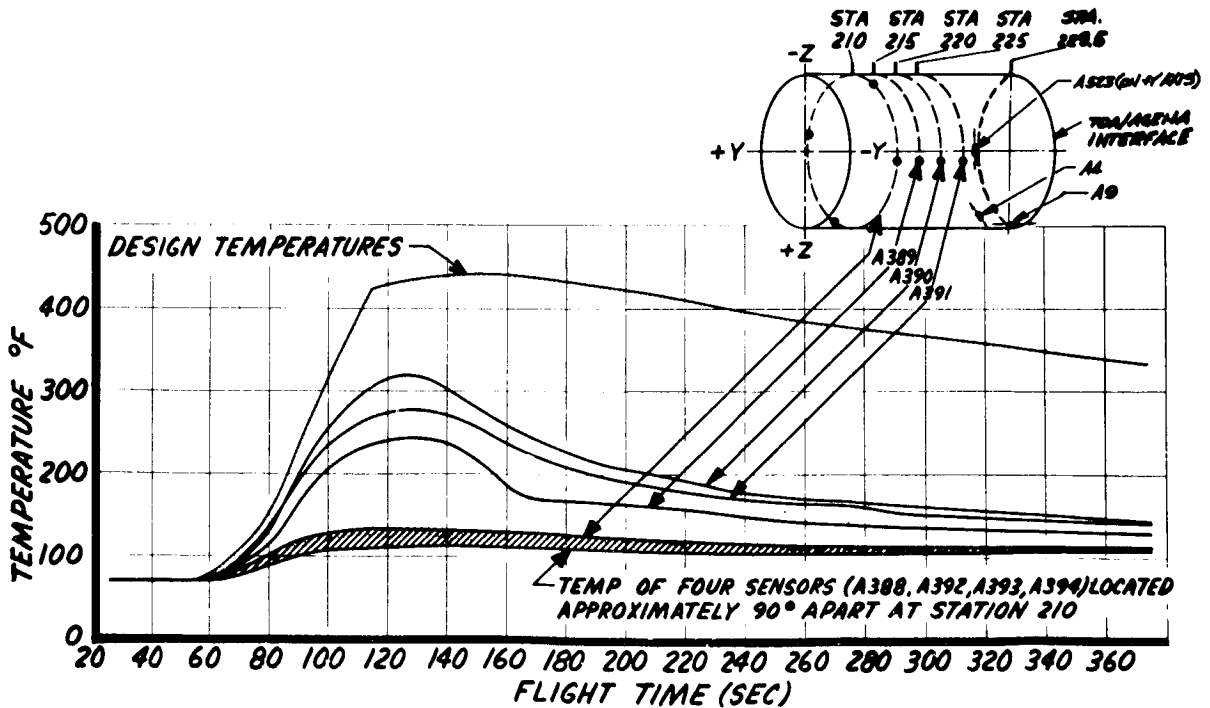
Fig. 3-28 Docking Adapter External Surface (A388 Through A394) Ascent Temperature Histories

LOCKHEED MISSILES & SPACE COMPANY
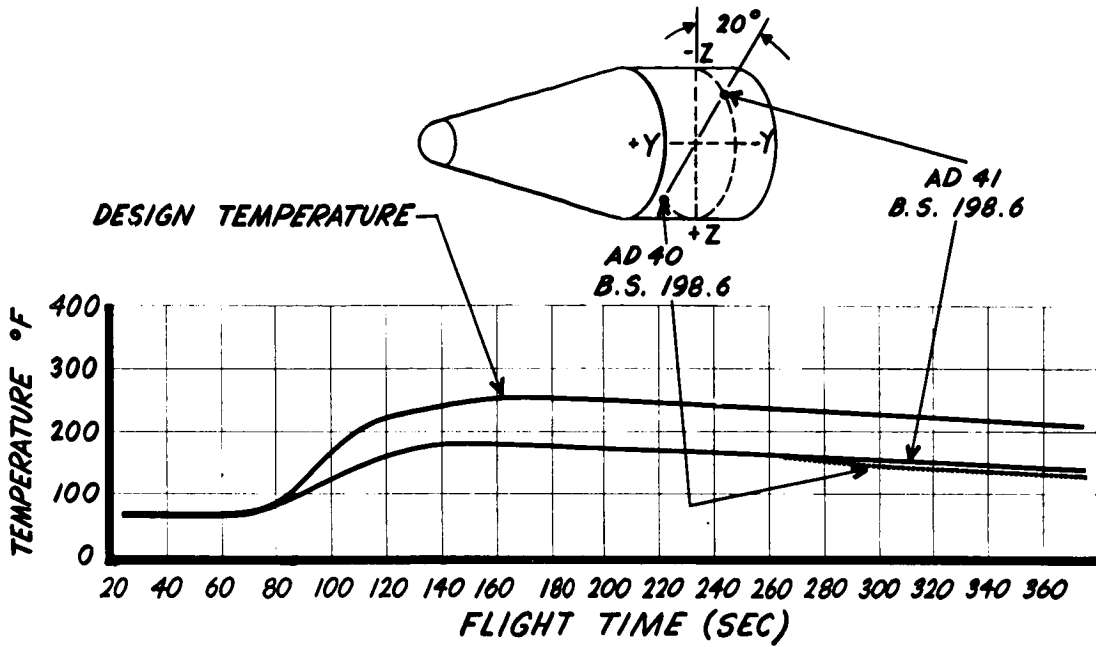
Fig. 3-29 Payload Shroud Internal Surface (AD40 and AD41) Ascent Temperature Histories
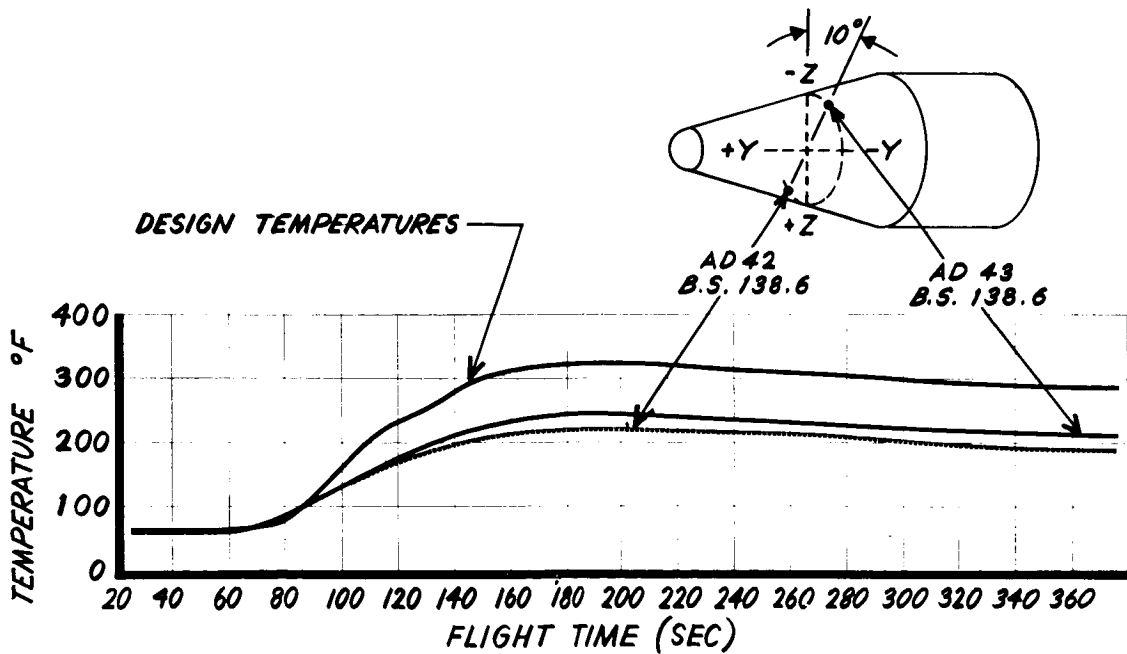
Fig. 3-30 Payload Shroud Internal Surface (AD42 and AD43) Ascent Temperature Histories

LOCKHEED MISSILES & SPACE COMPANY
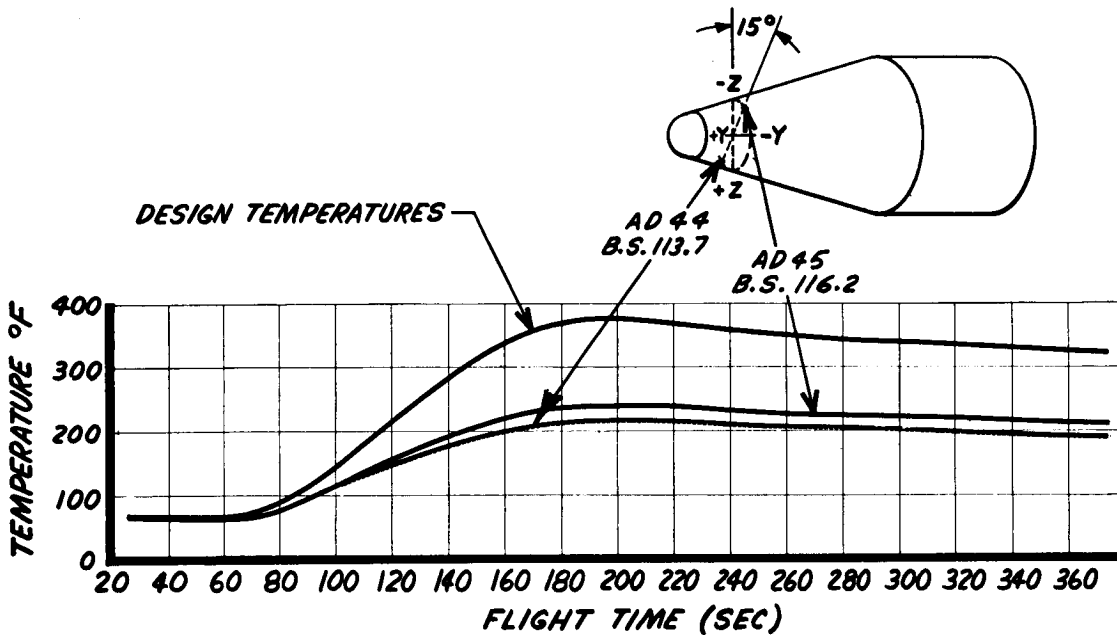
Fig. 3-31 Payload Shroud Internal Surface (AD44 and AD45) Ascent Temperature Histories

The temperature history presented in Fig. 3-28 for measurements A388, A392, A393, and A394 is a band faired through the data available from the print plots. Due to boundary-layer separation at the shroud/docking adapter interface, the heating of the vehicle in the area of these four sensors is less than at points downstream where the flow was reattached. The maximum temperature of 130°F indicated by the data is well below the design temperature of 440°F, based on the assumption of attached flow.

The temperature histories for measurements A389, A390, and A391 are also presented in Fig. 3-28. These three measurements are located in a line aft of the shroud/docking adapter interface. The data indicate the heating effects of flow separation and reattachment. The maximum temperature of 238°F, 305°F, and 269°F for A389, A390, and A391, respectively, are below the design temperature of 440°F in the area.

The temperature response of measurements AD40 through AD45 on the fiberglass shroud are presented in Figs. 3-29, 3-30, and 3-31. These illustrations also show the inner surface design temperatures at the corresponding three locations. The maximum temperatures indicated by the data are in all cases lower than the design temperatures. The temperature gradient around the circumference of the shroud indicated by the data is due to vehicle angle-of-attack effects. The information obtained indicates valid data were received from the six sensors up to 374.50 sec after liftoff.

Temperature data were received from 70 instrumented components and structural elements during the approximate 376 sec of telemetered ascent. Figure C-1 shows the temperature instrumentation locations on the Gemini Agena Target Vehicle. Most of the individual temperature measurements were sampled once every second. Exceptions were the hydraulic oil return line temperature (D5) and the control gas supply temperature (D70), which were sampled 16 times per second.

3.4.4.1 Prelaunch. All GATV equipment was temperature-controlled by supplying air at the rate of 100 lb/min at a temperature of 50°F. A summary of equipment liftoff temperatures is given in Table 3-1. All equipment, structural, and propellant temperatures were normal at liftoff. However, one battery temperature (C13) measured 119°F (normal is 60°F) and remained constant until loss of signal (LOS). It is reported that a technician who checked the battery with a hand-held pyrometer prior to liftoff verified that its temperature was essentially the same as the ground cooling air. This high-temperature indication can be attributed to a data calibration shift. The data indicated a constant 119° temperature subsequent to liftoff.

Liftoff temperatures of the main engine, SPS, and aft rack components in direct view of the Atlas LOX tank were somewhat lower than the ground cooling air supplied to the GATV. These low temperatures were likely the result of radiation heat transfer from the GATV components to the Atlas LOX tank and associated structure and have been seen on previous Atlas-boosted flights.

3.4.4.2 Ascent (Booster). All equipment and structural temperatures monitored were normal from liftoff to booster separation, with the exception of the erroneous battery temperature mentioned above. Normal temperature changes were experienced due to internal power dissipation in equipment and ascent heating effects on the structure. Figures 3-32 through 3-34 present the temperature time histories during the entire flight of the instrumented components in the forward rack and auxiliary forward rack.

The battery temperatures remained constant during the flight, and most equipment experienced only moderate temperature increases due to normal internal power dissipations. The L-band transponder face plate, which increased 23°F during the flight, is in close contact with the TDA external skin and is therefore temperature-sensitive to the ascent heating pulse.
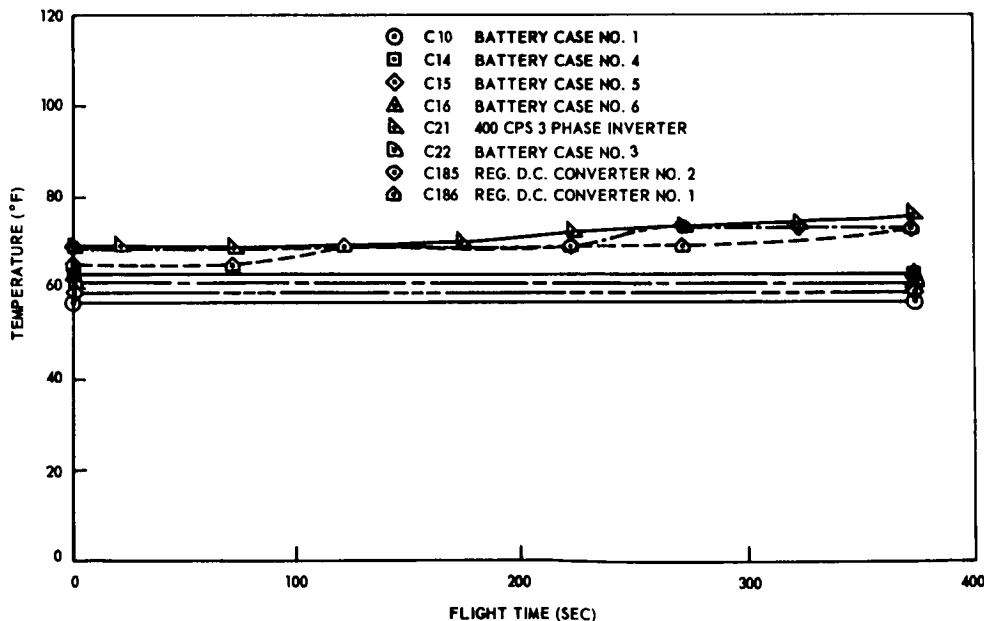
Fig. 3-32 Temperature Histories of Subsystem C Components in Forward Rack
(C13, C14, C15, C16, C21, C22, C185, and C186)

3-68
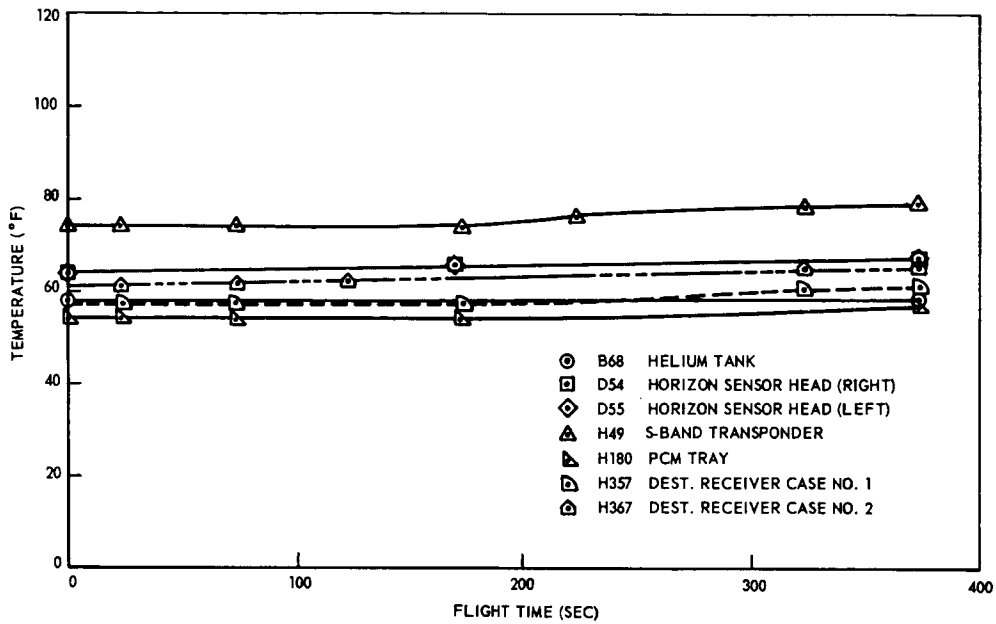
Fig. 3-33 Outputs (Temperature Histories) of B68, D54, D55, H49, H180, H357, and H367 in Forward Rack
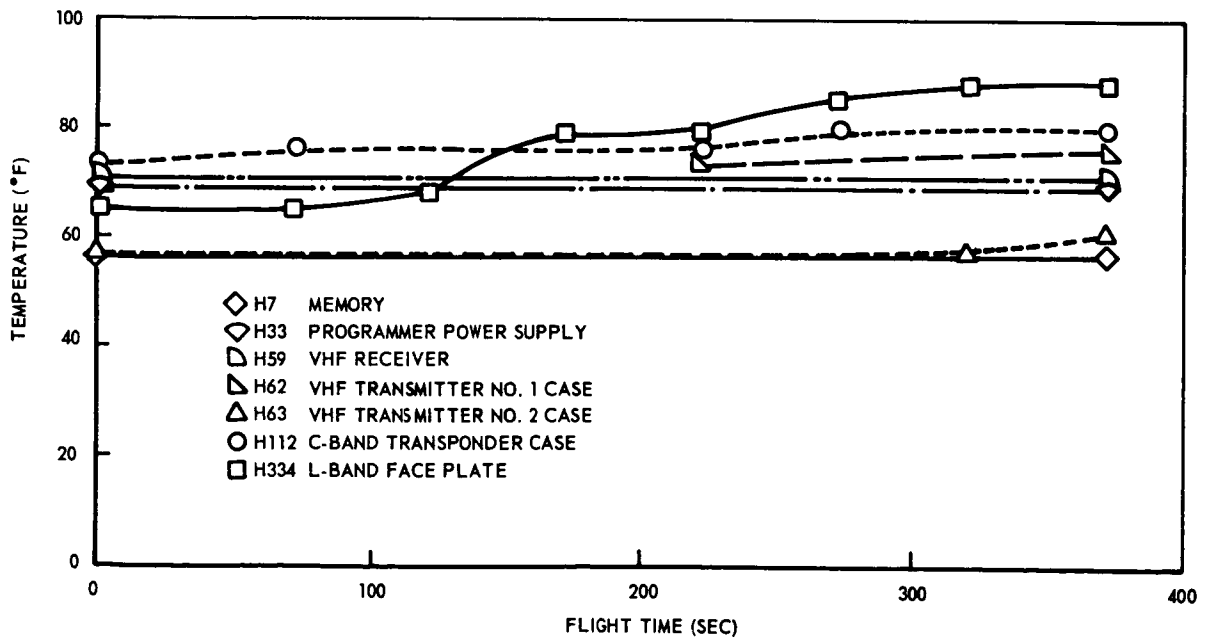
Fig. 3-34 Temperature Histories of C&C Components in Forward Rack (H7, H33, H59, H62, H63, H172, and H334)

The PPS propellant tank temperatures remained constant during the flight as was expected, since the mass of the propellants acts as a heat sink (Fig. 3-35). The aft rack components and structural temperatures were also normal during Atlas boost as can be seen in Figs. 3-36, 3-37, 3-38, 3-39, 3-40, and 3-41.

3.4.4.3 Booster Separation. All temperatures measured were normal from booster separation through SPS Unit I thruster ignition. Subsequent to booster separation, some aft rack structural temperatures decreased and some increased, indicating removal of the adapter and exposure of the aft rack to the space environment. Temperature increases of from 4°F to 8°F were experienced on the SPS heat shield (A158 along the +Y axis) (Fig. 3-36), and on the hydraulic return oil line (D5 along the -Z axis) (Fig. 3-37). These component temperatures increased because of exposure to the sun. The attitude control gas supply temperature (D70) and the valve cluster temperatures (D46 and D47) decreased from 4°F to 12°F during the same interval. The cold gas attitude control system is activated at booster separation, and the normal cooldown of the supply and valve clusters verifies expected control gas flow (Fig. 3-38).

3.4.4.4 SPS Ignition. Temperature histories of both Unit I SPS thrusters indicated ignition and normal operation (Fig. 3-39). These two thrusters remained at a constant 40°F temperature from liftoff to initiation of Unit I firing at approximately 350.4 sec at which time the temperature began to increase normally. The output of B246 (the measurement for one of the two Unit I thrusters) indicated a maximum temperature of 1590°F at approximately 370 sec. At the same time, the measurement for the other thruster (B247) reached a maximum of 1910°F, then cooled to 1670°F at loss of signal while measurement B246 cooled to 1510°F (Fig. 3-39). The 320°F difference in maximum temperature reached by the two thrusters was attributed to a difference in thermocouple locations on the respective thrust chambers. Measurement B246 was broken off at the launch base and rewelded to a slightly different location.
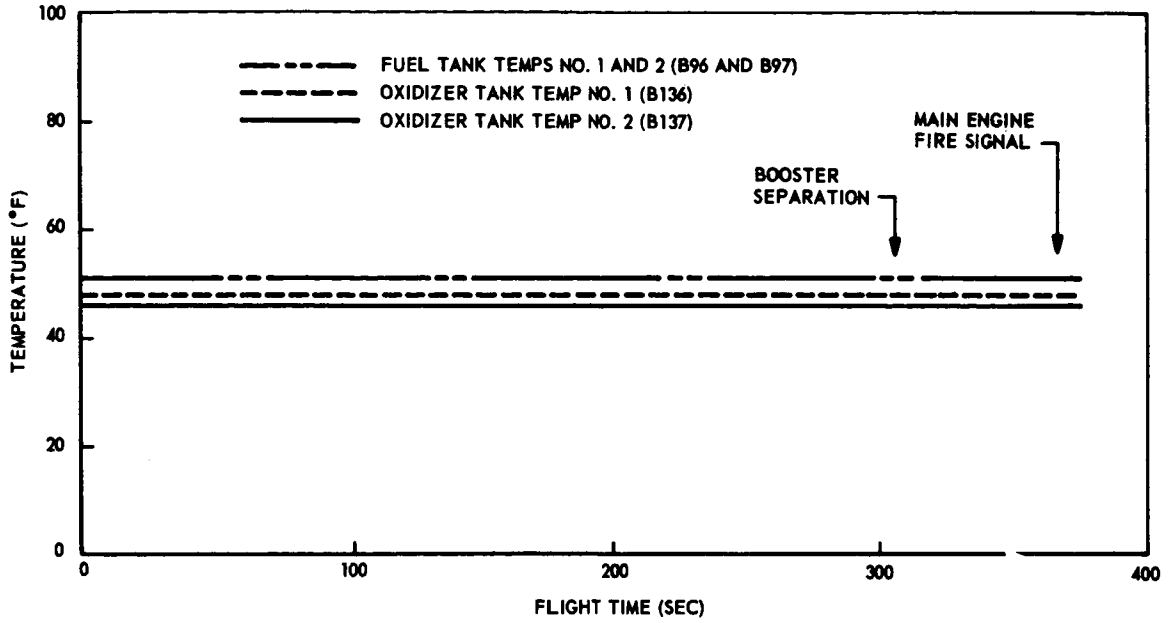
Fig. 3-35 Propellant Tank Temperatures (B96, B97, B136, and B137)
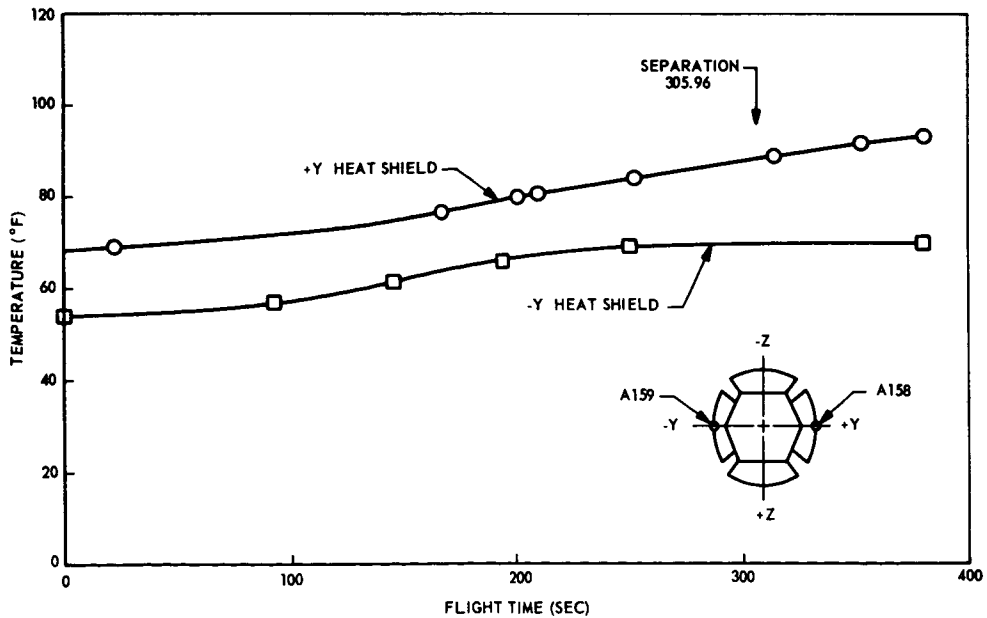
Fig. 3-36 SPS Heat Shield (A158 and A159) Temperatures

LOCKHEED MISSILES & SPACE COMPANY
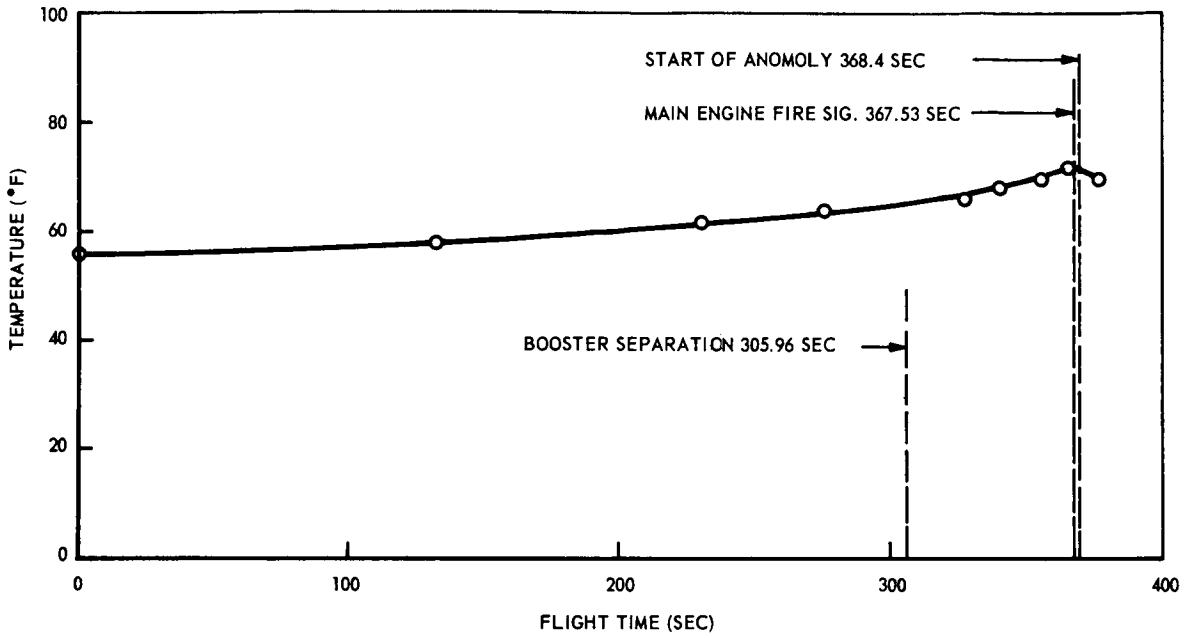
Fig. 3-37 Hydraulic Return Oil Line Temperatures
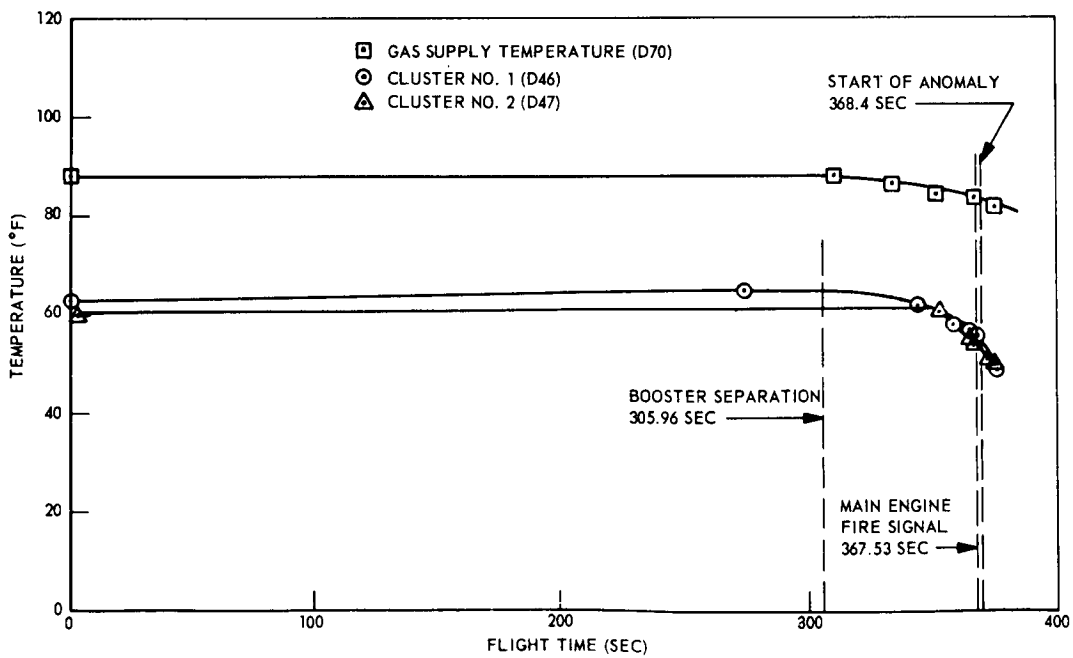
Fig. 3-38 Gas Supply and Valve Cluster (D70, D46, and D47) Temperatures

LOCKHEED MISSILES & SPACE COMPANY
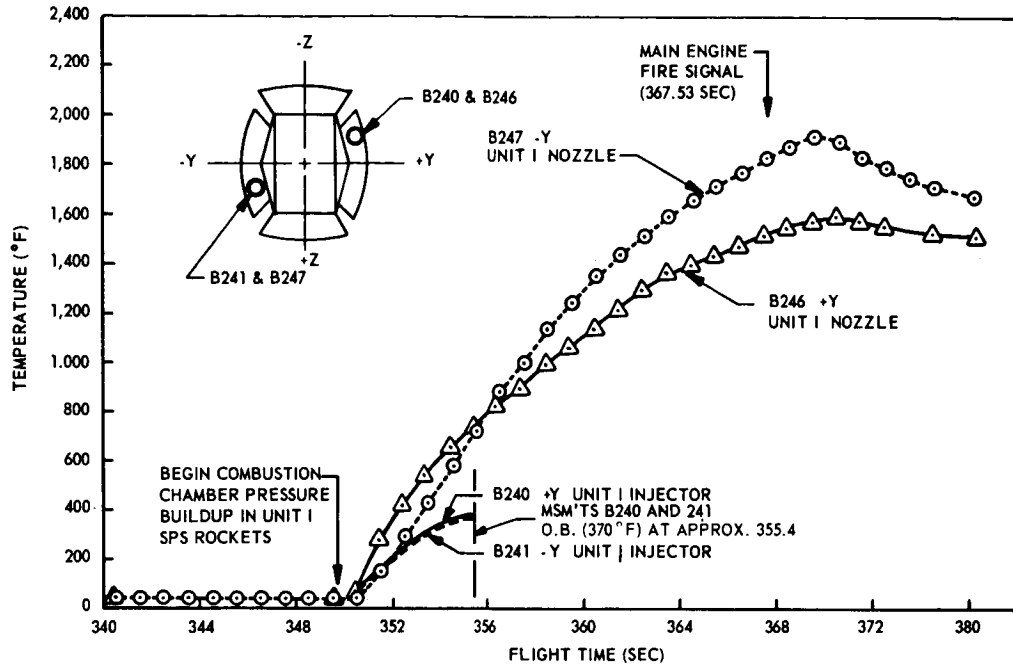
Fig. 3-39   Unit I SPS Nozzle and Injector (B240, B241, B246, and B247 Temperature Data)

The two Unit I injector temperatures (B240 and B241) began to increase simultaneously with the thruster skins at approximately 350.4 sec.   These temperatures are also shown in Fig. 3-39 .   Both of the injector temperatures went out of band at approximately 355.4 sec and remained above the maximum calibrated temperature (379°F at a telemetry voltage of 5.0v) until telemetry loss of signal.   The out-of-band voltage did not indicate an abnormal SPS thruster operation.

The temperature sensors were selected to indicate values down to -100°F, and consequently, the ranges do not include the maximum expected temperatures (900°F).

The effect of the SPS burn was observed on the nozzle extension (B184), where the temperature increased from 70°F to 103°F because of radiation from the SPS nozzle and from exhaust plume impingement (Fig. 3- 40).   Sensor B184 is approximately 2 ft aft of the Unit I nozzle exit plane and at approximately the same angle as the nozzle from the vehicle vertical (Z) axis.

LOCKHEED MISSILES & SPACE COMPANY
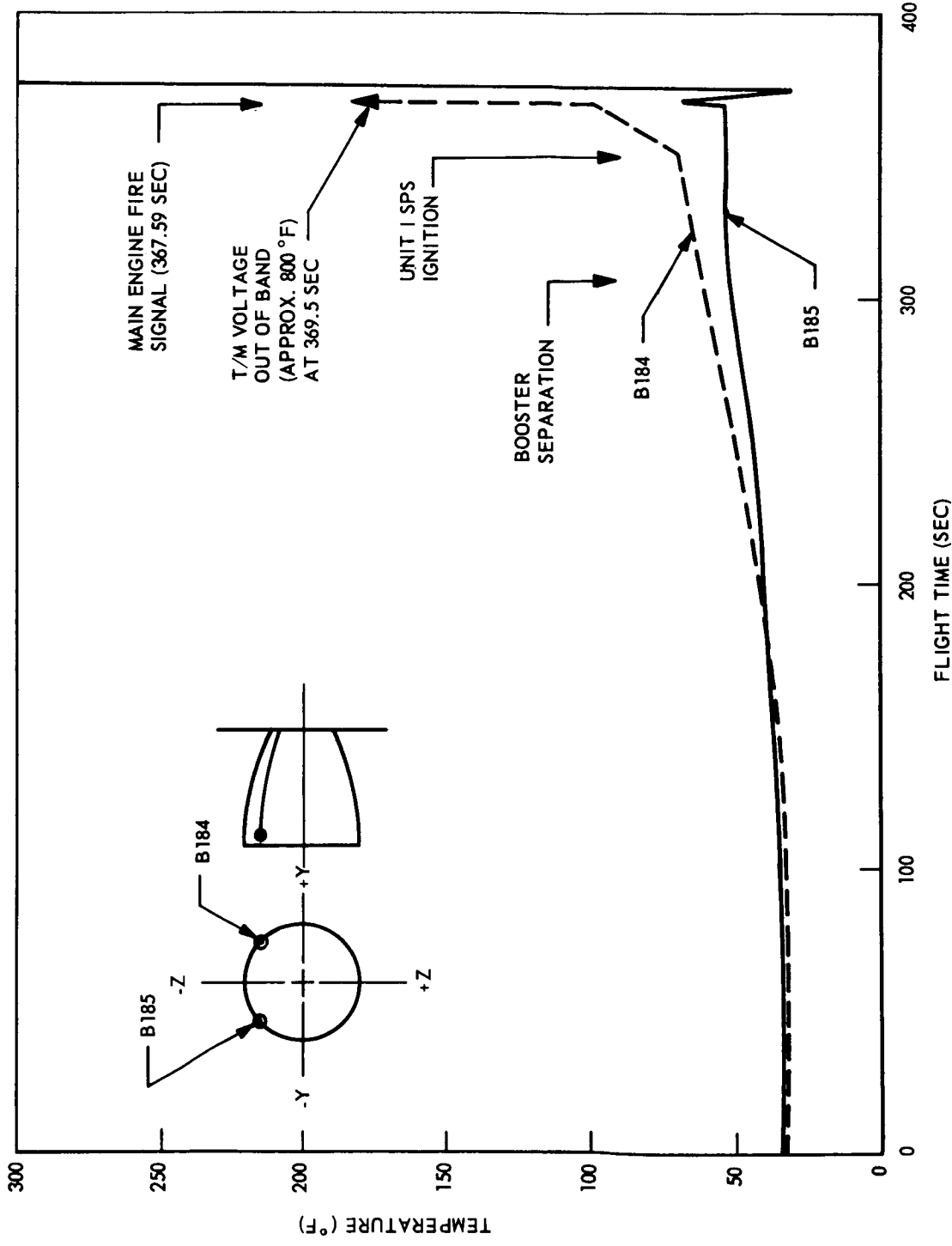
Fig. 3-40 Nozzle Extension (B184 and B185) Temperatures

LOCKHEED MISSILES & SPACE COMPANY

The temperatures of SPS components that were located within the module shields remained nearly constant during the flight (Fig. 3-41). The two Unit II thruster temperatures also remained constant (Fig. 3-42).

3.4.4.5 Primary Propulsion System. At 367.53 sec, the normal PPS start sequence was initiated. Shortly thereafter, an anomalous sequence-of-events occurred that resulted in abnormal PPS behavior. PPS and aft-rack structural temperature data indicate the thermal characteristics of events subsequent to initiation of PPS ignition. Up to the time of the anomalous events, temperature data indicated normal and expected conditions and gave no indications of the impending anomaly.

The temperatures of the aft rack shear panels, to which the SPS modules are mounted, were between 50°F and 60°F (nearly equal to the ground cooling air temperature) with very small changes during the Atlas boost phase of flight and up to PPS ignition, as was expected. However, shortly after PPS ignition, three of the four shear panel temperatures started falling sharply. Two of the shear panels eventually dropped about 70°F in approximately 7 sec to a temperature of -10°F (Figs. 3-10, 3-11, and 3-12). At about the same time, the two PPS start tanks located forward of the PPS combustion chamber showed similar temperature decreases (Fig. 3-9). The two Agena aft bulkheads on the vehicle Z-Z axis also experienced temperature decreases at the same time, although somewhat less severe than the shear panel measurements (Fig. 3-13).

It was postulated that such rapid temperature drops could only result from the high-heat transfer coefficients commonly associated with boiling or flashing liquids, where the change in phase from liquid to vapor involves considerable energy exchange. Leaking propellants were immediately suspected, and investigation of the thermodynamic properties of the propellants was undertaken. It was determined that the thermodynamic properties were indeed in the proper ranges to produce the indicated phenomenon.

LOCKHEED MISSILES & SPACE COMPANY
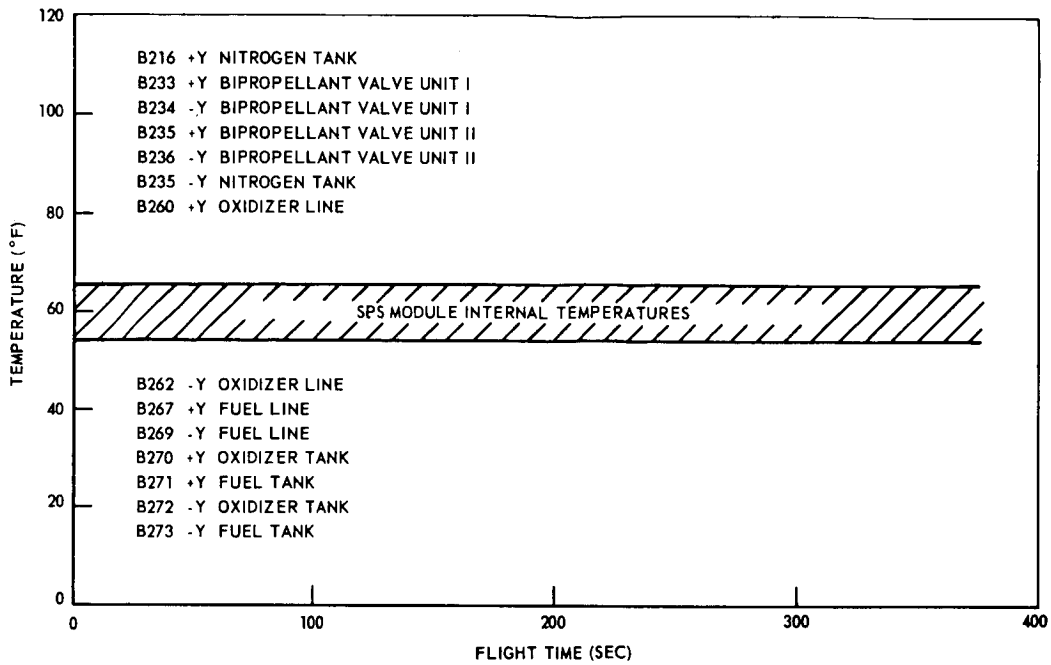
Fig. 3-41 SPS Module Component Internal Temperatures (B216, B233, B234, B235, B236, B253, B260, B262, B267, B269, B270, B271, B272, and B273)
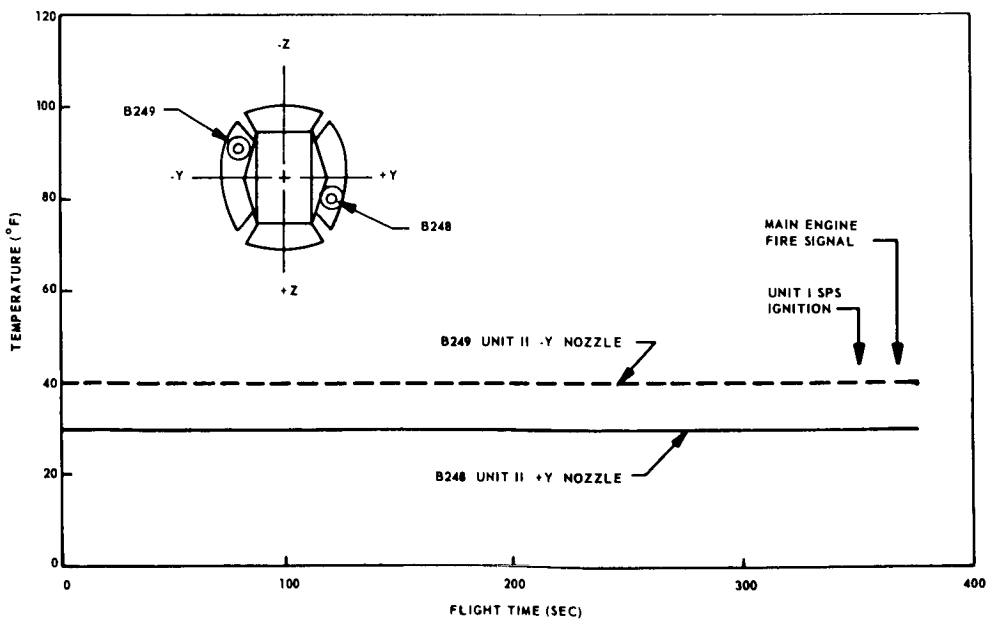
Fig. 3-42 Unit II SPS (B248 and B249) Temperature Data

LOCKHEED MISSILES & SPACE COMPANY

It is estimated that heat-transfer coefficients in the order of 100 to 200 BTU/hr °F ft^2 are required to produce the observed temperature drops. Heat-transfer coefficients resulting from simple gas expansion at sonic velocities are not considered sufficiently large to produce these indicated temperature changes since heat-transfer coefficients of only 5 to 10 BTU/hr °F ft^2 are produced under such conditions.

Analyses were then performed to try to estimate the amounts of leakage that would be required to simulate the temperature drop. On the basis of the 70°F cooldown of those surfaces that dropped in temperature, it was estimated that 0.5 to 1.0 lb/sec leakage would be required. The oxidizer and fuel have similar heats of vaporization, so either could have been leaking.

Another method used to estimate the quantity of leakage was to assume the 0.12-psia compartment pressure indicated by the data and sonic (choked) flow out through the annular space between the combustion chamber and the aft rack structure. Based on these assumptions it was determined that a leakage rate of 2.5 lb/sec would be required to produce the 0.12-psia compartment pressure. For compartment pressures of .05 and .01 psia, flows of 1.25 and .25 lb/sec would be required.

Furthermore, flow from a tube 1 ft long and .25 in. in diameter, with a pressure differential of 100 psi, was calculated to be 1.6 lb/sec. Such leakage could be hypothesized from a transducer feedline or a small control line.

These three methods of determining the propellant leakage are not particularly accurate, but do give some indication as to the magnitude of the leakage. It can be concluded at this time that the leakage was probably in the order of 1.0 lb/sec.

Since the temperatures are sampled only once per second, the exact time of the initial temperature decay due to the suspected impinging propellants is uncertain within about one second. The area of time uncertainty is indicated on Figs. 3-9 through 3-13. However, the actual time that the temperature decay was initiated is less significant

to the PPS failure analysis than determination of the exact time that the suspected propellant leakage occurred. The structural temperatures could start falling only after the leakage occurs. A finite time is required for the propellants to travel to the affected area and flash or boil, causing heat to be removed from the shear panel and finally from the sensor.

At this time it is not possible to determine whether the suspected propellant leakage occurred just prior to, coincident with, or after the start of the anomaly.

The PPS propellant pump inlet temperatures remained constant throughout the flight until shortly after PPS ignition. Approximately one second after the PPS engine fire signal, the oxidizer-pump inlet temperature started to drop, indicating that relatively cool propellant started to flow into the pump inlet. This temperature drop was consistent with normal PPS engine start transient temperatures noted on many previous flights. The oxidizer-pump inlet temperature sensor did not change significantly for the last few seconds of flight. This sensor does not normally give indications of engine shutdown until 5 to 9 sec after shutdown.

The fuel-pump inlet temperature sensor, however, did not indicate a drop in sensed temperature, implying lack of fuel flow after the fire signal. Instead, the data indicate a constant temperature sensed at the fuel pump inlet until 2 to 3 sec after the fire signal, at which time the temperature data indicate a rise from 50°F to approximately 55°F. The dashed line in Fig. 3-8 indicates a possible curve shape if the fuel temperature had not dropped. However, it is probable that this temperature actually did start to drop after the fire signal, but that the decrease was not monitored by the telemetry system because of the one-per-second sample rate. It should have dropped, since other engine parameters indicate some fuel flow. Assuming it did start to drop, the shape of the temperature curve is probably more similar to that indicated by the dash-dot line in Fig. 3-8. Based on these assumptions, the temperature rise started earlier than the dashed line indicates and the PCM telemetry sampled the temperature as it was rising through the 50°F level. This temperature rise at the

3-78

fuel-pump inlet appears similar to, but is not identical with, temperature rises seen
for a normal PPS shutdown. The shape of the temperature-time curve is almost the
same, but normally the fuel-pump inlet temperature rises 10°F after shutdown because
the pump impeller churns the fuel after flow is stopped by closure of the fuel valve.
The temperature rise for this instance is only about 4 to 5°F. It is postulated that the
reason for the smaller temperature rise here is due either to slower pump (and turbine)
speed at the time of shutdown or to a small amount of continuing fuel flow. Fuel flow
through the pump could result from a line failure downstream of the pump or a partially
opened fuel valve that allowed the propellant to enter the combustion chamber.

The PPS combustion-chamber throat skin temperature data (B83) during these anoma-
lous events is subject to question. The indicated temperature was normal until shortly
after the main-engine fire signal, when it went out of band at 5v (indicating approxi-
mately 171°F). (See Fig. 3-7). The B83 sensor was calibrated to measure its
nominal temperature range (-50° to +150°F), primarily because it was intended to
indicate the on-orbit stabilized temperature rather than the history resulting from a
PPS firing (during which the temperature normally rises to about 375°F). Past flight
data indicate temperature rises of up to 205°F within one second after PPS ignition.
Consequently, the fact that this sensor indicates an out-of-band reading (171°F) after
PPS ignition may be the result of a normal temperature rise (up to 375°F) associated
with combustion in the chamber.

The out-of-band reading could also be the result of instrumentation failure. It can
only be speculated as to what the temperature history of the combustion chamber
should have been for the short indicated firing, and therefore there is no way at this
time to determine whether or not this reading was valid.

The combustion-chamber throat skin temperature history as indicated by the data
may be considered in relation to the temperature histories of the two sensors located
on the PPS titanium nozzle extension (B184 and B185). Figure 3-7 shows these
sensors along with the combustion-chamber throat temperature. The nozzle extension

temperatures are normal from liftoff through the time of the main engine fire signal. After PPS ignition, the indication from the sensor B184 rose to an out-of-band reading (5v, corresponding to over 800° F). No physical phenomemon can be postulated to account for an 800° F rise in this sensor; it is presently concluded that this sensor failed because of an open circuit, which resulted either from sensor failure or nozzle extension failure. The nozzle extension temperature indicated by sensor B185 appears to be valid. After the main engine fire signal, this sensor indicates one second later a temperature rise of 25° F to 70° F, then a temperature decrease in the next 3 sec to 27° F, followed by a sharp rise during the last 4 sec of data to 320° F.

The initial temperature rise to 70°F probably is the result of the initiation of combustion in the PPS chamber. The reason for the cooldown to 27°F in the following 3 sec is not entirely clear at this time. Other aft-rack structure and equipment experienced sharp temperature drops at approximately this same time, which has been postulated as resulting from the cooling effect of leaking propellants. It is possible that these propellants, suspected of leaking, also impinged on the nozzle extension; the extension would be directly in the path of the expansion of propellant liquid and vapor (probably at sonic velocities) out of the aft-rack engine compartment. It is also possible that the temperature drop is indicative of a true PPS engine shutdown where oxidizer post-flow tends to cool all parts of the thrust chamber. The combustion chamber throat skin temperature did not give any indication of such a cooldown, but it is not certain that this sensor was indicating valid temperatures.

The rapid temperature increase after the short cooldown, beginning at approximately 371.5 sec, is more difficult to explain. The indicated temperature rise of 300°F in the last 4 sec of telemetered data appears to be valid since there are four successive data points showing a smooth temperature rise. This temperature rise was very similar to nozzle extension temperature increases associated with the normal start transients noted on past flights. However, other PPS parameters indicate that engine shutdown had progressed to the point where no more combustion should be taking place.

Although there are indications of PPS engine shutdown, it is difficult to postulate an alternate reaction that would result in the 300°F nozzle extension temperature rise. The magnitude and rate of the rise requires a high-energy release normally associated with a combustion reaction. The aft-rack bulkhead temperatures (A154 and A155) and the SPS-module bulkhead temperatures (A156 and A157) do not indicate a reaction external of the nozzle extension of the magnitude necessary to raise the nozzle extension temperature 300°F in 4 sec (Fig. 3-13). Had a combustion type reaction (and the associated thermal energy release) occurred in the vicinity of the aft rack and external to the engine, other component and structural temperatures should also have indicated a detectable temperature increase. The only place where combustion could have occurred and not be in conflict with combustion-chamber pressure data, X-axis accelerometer readings, and aft-rack temperature data would be aft of the nozzle throat and contained primarily in the volume enclosed by the nozzle extension. Such a reaction might have been possible if fuel was the leaking propellant in the aft rack and the fuel was expanding out of the aft rack compartment and combining with the oxidizer post-flow in the vicinity of the nozzle extension ~~exit~~ plane.

3.4.5 Target Docking Adapter (TDA) Measurements

The following sensors were installed to transmit C&C data from the TDA:

   a. H347, "L-Band Antenna Extended" Measurement. A McDonnell installed switch, normally open, closed when the antenna boom has been extended

   b. H379, "Docking Cone Unrigidized" Measurement. A McDonnell installed switch, normally open, closed when the docking cone is moved from the rigidized position to the unrigidized position

   c. H380, "Docking Cone Rigidized" Measurement. A McDonnell installed switch, normally closed, indicates that the docking cone is in a rigidized position

   d. H381, "Docking Cone Unlatched" Measurement. A McDonnell installed switch, normally open, closed when the docking cone is unlatched

~~CONFIDENTIAL~~

LOCKHEED MISSILES & SPACE COMPANY

3.5 ELECTRICAL

3.5.1 Summary

No anomalies of the electrical system were observed from preliftoff through loss of telemetry signals. Special emphasis was placed upon data analysis at liftoff, separation, and engine ignition. All values remained nominal and within acceptable tolerance ranges.

It should be noted that the timewise sampling of the electrical data in several critical areas makes close-response correlation almost impossible. This is especially notable with the interrelation of the following values:

a. Unregulated Bus Voltage (16 samples/sec)
b. Unregulated Bus Current (1 sample/sec)
c. Structure Current (1 sample/sec)
d. Pyro Bus Voltage (1 sample/sec

All electrical voltages and currents were stable to the end of data transmission. This is significant since this indicates that no shorts, overloads, or open circuits in excess of 60 milliseconds could have occurred. This fact has a decided bearing upon any analysis or hypothesis concerning the engine switch group and vehicle failure.

3.5.2 Bus Potentials

3.5.2.1 Main Bus Voltage. The main-bus-voltage range was between 28.5v and 29.0v. It was above the nominal battery 25.0v during this period because the batteries had not depleted the initial electrochemical high–voltage potential.

The main-bus-voltage trace does not appear to respond in a synchronous timewise mode with the engine-switch-group signal and the battery current response. This is indicative of the following:

a. There could not possibly be a mirror trace of these data because the engine switch group is sampled 32 times/sec, the main bus voltage is sampled 16 times/sec, and the unregulated bus current is sampled 1 time/sec. The sampling rate of the latter value makes it impossible to deduce any timewise out-of-step evaluation because of overlapping data points.

b. The main bus voltage will lag the engine-switch-group trace, and the corresponding solenoid loads, because the batteries present a massive low-impedance load sink, and the resultant increase in internal voltage drop will not be instantaneous.

c. The engine switch group, besides being resistive, is capacitive-reactance biased under a switch-on or chatter mode. In a capacitive-reactive circuit, the voltage will lag the current.

d. The PPS fuel, oxidizer, and pilot-operated-solenoid valves, which are connected to the same input circuit, are inductive-reactance biased under a switch-on or chatter mode. In an inductive-reactive circuit, the current will lag the voltage.

From the above, it is seen that no abnormality can be attributable to the comparative response of these data.

3.5.2.2 <u>Pyro Bus Voltage.</u> The pyro bus voltage range was between 29.4v and 29.7v. Isolation of the pyro battery from the main bus batteries was evident by the voltage differential between the two buses. The pyro bus voltage was above the nominal battery 25.0v during this period; this was because the battery was virtually without load, and the initial electrochemical high-voltage potential had no appreciable depletion. The recorded voltage is above the specified, system upper limit of 29.25v; however, the system would experience absolutely no detrimental effects at the indicated level. With the battery maximum potential specified as 29.8v, the system voltage was greater as a result of the following:

a. The battery initial activation potential retained an upper voltage charge.

b. The distribution system dc resistance was lower than expected resulting in a low internal voltage drop.

c. The telemetry monitor inherent tolerances favored the high side of the accuracy range.

3.5.2.3 <u>Inverter Bus Voltage.</u> The 400-cps inverter phase AB and phase BC voltage buses held constant at 114.9v rms. This compares favorably with the specified nominal voltage of 115.0v rms and a tolerance range of 112.7 to 117.3v rms.

3.5.2.4 <u>Regulator No. 1 Bus Voltages.</u> The positive bus for regulator No. 1 ranged between 28.1 and 28.2v, and the negative bus held constant at -28.0v. These voltages compare closely with the specified nominal voltage of 28.3v (absolute value) and a tolerance range of 27.7 to 28.9v (absolute value).

3.5.2.5 <u>Regulator No. 2 Bus Voltages.</u> The 60 w bus for regulator No. 2 held at around 28.6v and the 20 w bus held around 28.7v. These voltages compare reasonably with the specified nominal voltage of 28.3v and a tolerance range of 27.7 to 28.9v.

3.5.3 Loads

3.5.3.1 <u>Unregulated Bus Current.</u> The unregulated bus current values were normal; the highest demand was 23.0 amp, the lowest demand was 12.3 amp, and the average load was 15.4 amp. This is a lower average demand than for the full pre-orbital phase, since the most stringent loading period had not been sustained.

The unregulated bus current does not correspond exactly with the switch group actuation nor with the reflection of the main bus voltage because the timewise sampling base is seriously restricted. This is explained in sufficient detail under par. 3.5.2.1.

The unregulated bus current showed an increase from 15.6 to 23.0 amp at PPS initiate. This 7.4-amp increase is considered nominal (7.48 amp was predicted). The next sample point indicated a level of 17.2 amp, a 5.8-amp decrease. The engine solenoid loads had, of course, dropped off prior to the 17.2-amp data point, but another load had to have been picked up <u>between</u> the two data points to account for the net gain of 1.6 amp. Roll gas valves Nos. 3 and 6, sampled at a rate of 48 times/sec, had a minimum of 28 actuations in a span of 1.13 sec during this period. Thus, 1 amp of load (0.5 amp per valve) was picked up between the two data points. Also, it is highly

probable that a roll heater cycle, lasting normally about 900 ms, had occurred; this would require approximately 1 amp. In either case, had one or both of these loads been sliced by the 1-sec sample period of the unregulated bus current monitor, the additional load would be accounted for well within the resolution of the telemetry where the least significant bit corresponds to 800 ma. This analysis is further substantiated by the next data point reading of 12.3 amp, a drop of 4.9 amp from the previous 17.2 amp reading. At this time the SPS load of 3.0 amp (1.5 amp per unit) had dropped off, and the two single ampere loads had terminated; thus the net loss of 5.0 amp agrees most favorably with the indicated telemetry drop of 4.9 amp, disregarding the telemetry resolution of ± 800 ma.

3.5.3.2 <u>Structure Current.</u> The structure current values were nominal; 1.30 amp was the highest indication, and 880 ma the lowest reading. The average reading was 900 ma.

The large current reading prior to liftoff corresponds to the turn-on of the GD/C inverter. This was as anticipated.

Electrical actuation of the SPS units definitely increases the structure current. During flight, the structure current reading was constant at 880 ma. At approximately 334 sec, coinciding with "Open SPS Pressurization Start Valve," the structure current went up 400 ma to 1.3 amp, which is the telemetry resolution for this monitor. The structure current then switched back and forth between the resolution until 349 sec, which coincides with "Open SPS 16 lb Bipropellant Valves," when it stayed constant at 1.3 amp until 368 sec. At this time, "Close SPS 16 lb Bipropellant Valves" and "Close SPS Pressurization Start Valve" was initiated, and the structure current returned to 880 ma; it remained steady until the end of data acquisition. No direct reason for this influence is evident from the schematics that show the wiring and shielding design. The SPS modules, and the exact solenoid wiring, will be further analyzed.

LOCKHEED MISSILES & SPACE COMPANY

3.5.4 Temperatures

3.5.4.1 Power-Supply Temperatures. The inverter temperature and the two converter temperatures were nominal. A temperature increase of approximately 7°F for these units occurred — from the upper midsixties to the near midseventies. (See Fig. 3-32.) This temperature rise resulted from equipment operation in a near vacuum environment — after exposure to atmospheric convective airconditioning.

3.5.4.2 Battery Temperatures. All six battery temperatures were nominal; the indicated reading of battery temperature No. 2 was faulty. The temperature sensor for battery No. 2 was found, prior to liftoff, to be indicating about twice that of normal. A poor or damaged solder joint, with its corresponding increase in resistance, is the most probable cause. All battery temperatures held practically constant at around 60°F because of the relatively large heat-sink mass of the batteries (Fig. 3-32).

3.5.5 Capacity

3.5.5.1 Ampere-Hours. Internal power was switched on at -401 sec, and data acquisition ended at 376 sec. Thus, the total time on internal battery power was 777 sec, or 0.216 hr. At an average load of 15.4 amp (par. 3.5.3.1), the electrical capacity consumed was 3.33 amp-hr.

3.5.5.2 Ampere-Hour Meter. No response was received from the ampere-hour meter. Since the ampere-hour meter advances in 10 amp-hr step increments, no response shrould have been evident in accordance with par. 3.5.5.1.

3.5.6 Range Safety

3.5.6.1 Premature Destruct. No signal was evident from the premature destruct system.

The separation monitor out-of-band indication was probably caused by a faulty component. (See the instrumentation summary, par. 3.2.2.1, f for a detailed discussion.)

3.5.6.2 Command Destruct. No engine inhibit command destruct signal was evident. The signal strengths and temperatures of the receivers were satisfactory.

3.5.7 Electrical Analysis of Flight Anomaly

3.5.7.1 Engine Switch Group. The operation of the engine switch group was closely analyzed from an electrical performance viewpoint; no one evaluation can be considered conclusive since the monitored data do not appear to support a definitive solution. Figure 3-43 presents the most important electrical system flight performance data.
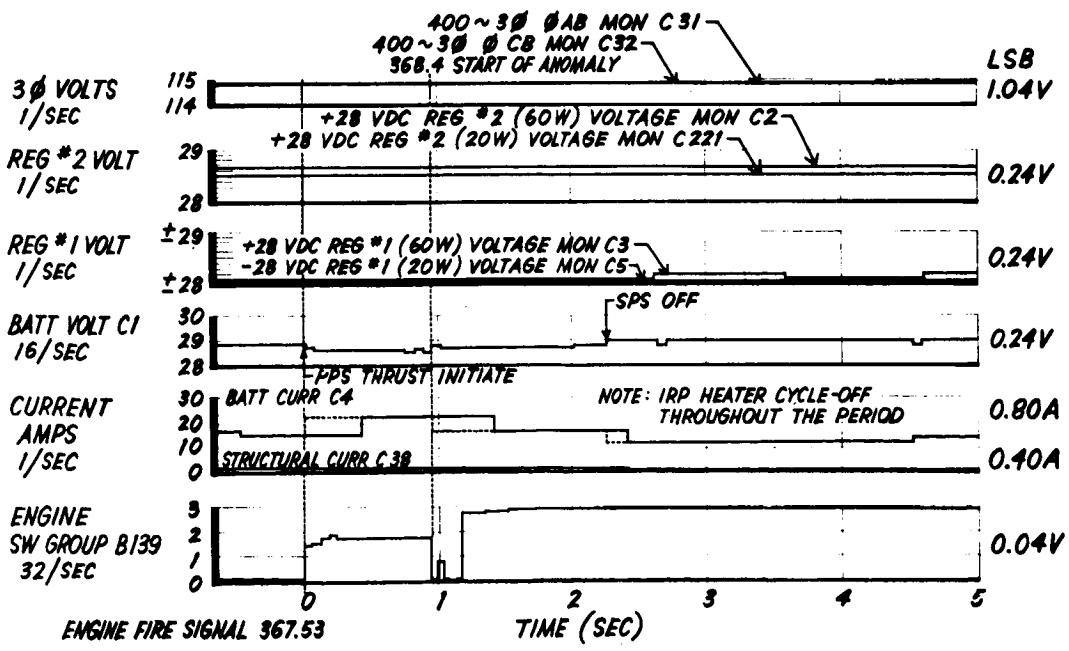
Fig. 3-43 Electrical System Performance

LOCKHEED MISSILES & SPACE COMPANY

The most probable explanations are presented below (they are listed in the order and amount of detail of the most likely evaluation):

a. The shock and white noise of the PPS hard start was severely transmitted to the BAC electronic gate J-box. Latching relays K1 and K2, the only components within the J-box that contain movable assemblies, went into a contact transition chatter mode. Power to the engine solenoids was simultaneously interrupted. Approximately 50 ms later, the contacts in the two relays simultaneously transferred to the normal latch-up position, as indicated by the 0.8v telemetry data. This position lasted only approximately 55 ms, as the contacts continued the transition chatter until after the peak shock period; then, by pure probability of chance, relay K2 ended in its initial position and relay K1 ended in a transfer position. This position is supported by the reading of 2.84v at telemetry point B139. The total time from the start of relay transfer and chatter to the two final positions took approximately 255 ms. During this period, because of one or more of the following reasons, continuity to P6011 pin W was impaired or broken by the same shock:

   (1) Cracked relay header

   (2) Relay debris (i.e., chips, etc.)

   (3) Snapped-off upper movable transfer contact of relay

   (4) Damaged (increased impedance) or severed (open circuit) terminal connections

It should be noted that an impedance of approximately 200 ohms or greater would reduce the voltage across relay coil K7 in the aft safe-arm J-box to below its pull-in voltage. Also, the relay mounting structure and axis alignment are very critical insofar as triggering the above conditions.

b. Two conductors connecting the BAC electronic gate J-box to the aft safe-arm J-box follow a different routing (these two conductors do not have to pass through the 502 safe-arm plug). One conductor would not be energized during this period; the other connects with the critical relay K7 coil. Thus, the engine hard start could have damaged these two conductors because of different exposure areas and connector egress tension. Again, an impedance of 200 ohms or greater would reduce the voltage across relay coil K7 to below its pull-in voltage.

c. Wires to pins E and F of connector P6011 in the BAC electronic gate J-box were severed, intermittent contact was made, and a resistance to pin D developed. Commensurate with the telemetry indication, this resistance would have to be 45.9 K ohms. If the wire to pin D was entirely disconnected, this resistance would have to be 24.6 megohms. Since this impedance is the result of parallel paths (pin E to pin D and pin F to pin D), the individual conductor resistance could be approximately 50 megohms. This does not appear to be an unreasonable magnitude for a damaged cable in the presence of oxidizer. It should be noted that if cable damage were the result of PPS reaction, pins D, E, and F would be the ones most vulnerable, since these pins are aligned inboard towards the gas generator. However, it remains difficult to explain the apparent steady-state output of the above configuration.

d. Wires to pins E and F of connector P6011 in the BAC electronic gate J-box were severed; subsequently, contact was made again, and a relatively high resistance in the return lines of pins X and Y appeared. If the engine solenoids had become disconnected, and 28v present at pin E and/or F, a resistance of 922 ohms would allow the circuit to agree with the telemetry indication. If the solenoids had remained connected, the resistance would have to be 290 milliohms. This analysis would not only require a complicated cable failure mode, but it would again require a steady-state inadvertent impedance.

3.5.7.2 Transducer Failures. A review of harness routing was made to determine if there was a correlation between instrumentation failed transducers and a common interface. On this theory, if a common area (harness, connector, terminal, etc.) was discovered, it could be virtually concluded that a vehicle malfunction or failure had occurred. No common point existed in the electrical system.

3.6 GUIDANCE AND CONTROL

3.6.1 Summary

The guidance and control system performed nominally and within specification tolerances. Measurement D37, "Booster Command Monitor," and

the thrust valve monitors gave no indication of pitch and yaw pneumatics becoming enabled after engine shutdown. This establishes the conclusion that the engine was not shut down by one of the normal first-burn shutdown signals, velocity meter cutoff, turbine overspeed, or ascent timer backup.

The fact that the yaw actuator did not turn the vehicle back toward null during the short thrust period indicates that the yaw correction force was enough to stop acceleration, but not enough to change velocity direction caused by a disturbance initiated at turbine spin-up. The force due to this disturbance ceased during thrust because the vehicle had a constant yaw rate after engine shutdown. This disturbance was also noted in the last Mariner flight (Agena Vehicle 6932); however, in that flight the PPS thrust was normal and the vehicle position was corrected as it should have been.

3.6.2 Performance From Separation to PPS Thrust Initiate Signal*

3.6.2.1 Pitch Axis Control. Gyros were uncaged at VECO (303.7 sec). The pitch separation rate appeared normal, approximately 0.27 deg/sec. The pneumatics were properly activated by separation switch control (308.5 sec). The pitch pneumatic system polarity was correct; and the magnitude of the static gain, dynamic gain, and deadband were nominal. The pitch-horizon-sensor error was greater than +5 deg (telemetry saturation) at separation. The pitch-horizon-sensor error indicated -5 deg at VECO because of the heating of the horizon sensor fairings. The output recovered to greater than +5 deg after the fairings were blown. (See Fig. 3-44.)

The pitchdown maneuver was initiated at 334.8 sec. The gyro and vehicle response to the torquing input was nominal. The maximum gyro offset due to the torquing input was +2 deg. The pitchdown rate was measured at 1.485 deg/sec (1.5 ±.09 deg/ sec is the specification tolerance) from horizon sensor and gyro position telemetry. Vehicle position at separation was approximately +19.5 deg. An accurate measurement

---

*All times are mission time ±0.1 sec.

LOCKHEED MISSILES & SPACE COMPANY
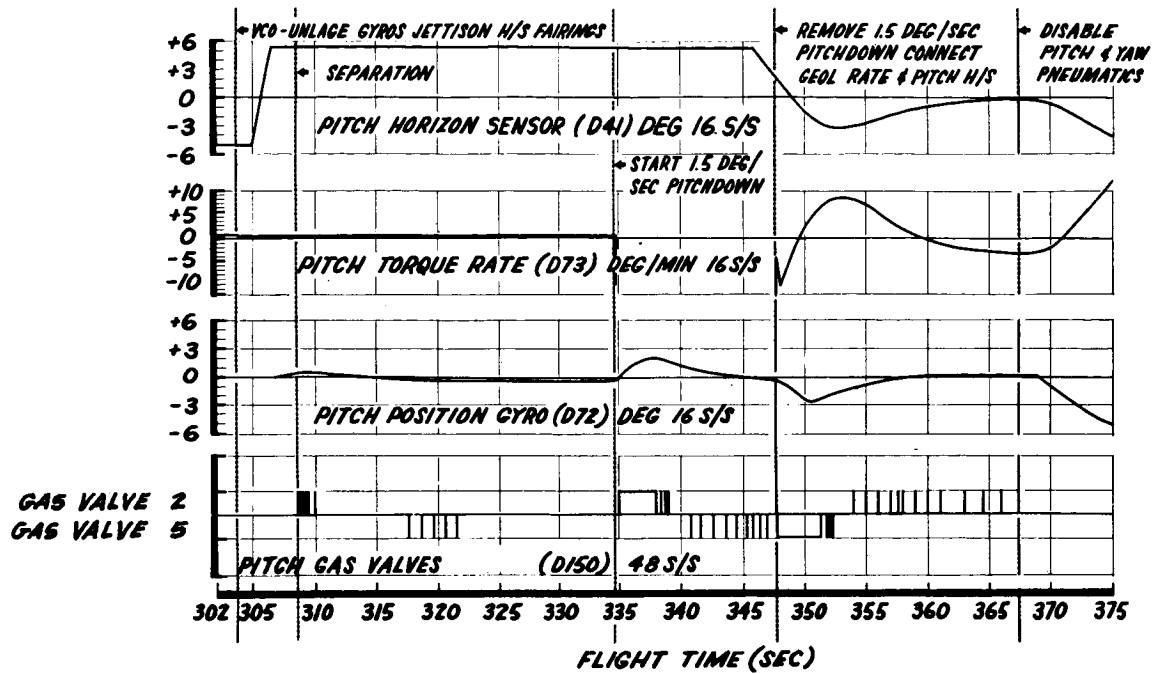
Fig. 3-44 Pitch Axis Control Performance
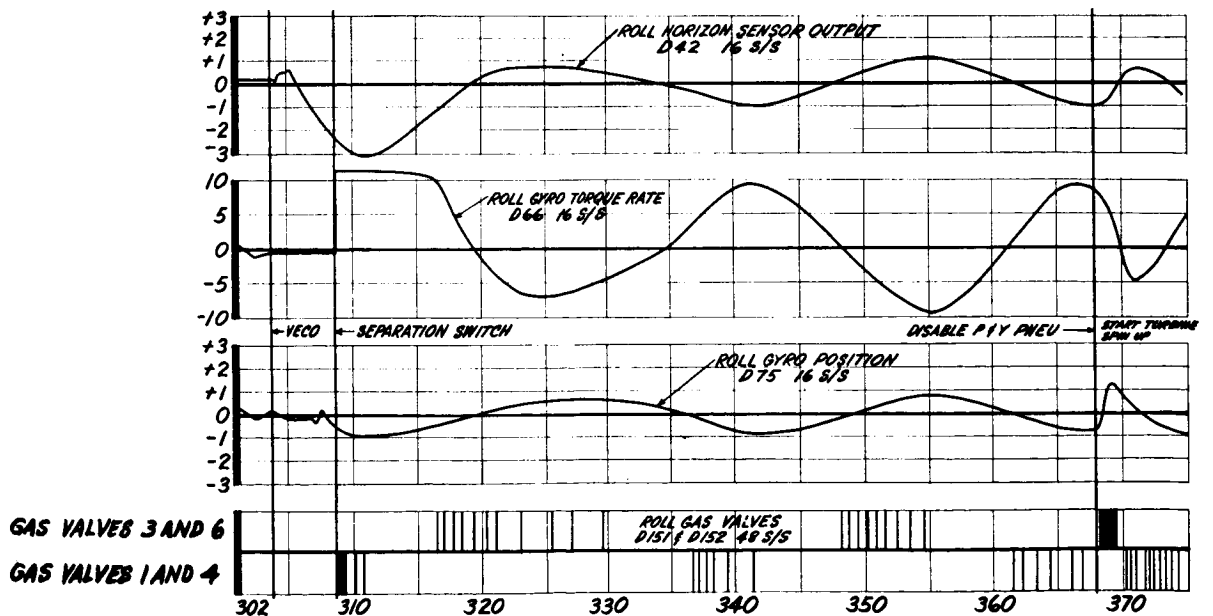
Fig. 3-45 Roll Axis Control Performance

LOCKHEED MISSILES & SPACE COMPANY

of initial position and pitchdown rate is impeded because of telemetry saturation of gyro torquer and horizon-sensor outputs. The pitchdown torquing voltage was removed at 347.65 sec; geocentric-rate and horizon-sensor-torquing voltage were applied this time. The geocentric rate was measured at -4.0 deg/min (3.99 ±.24 deg/min is allowed value), and the horizon sensor to gyro gain was measured at 3.26 deg/min/deg (3.0 ±0.6 deg/min/deg is allowed). At the time of PPS thrust initiate signal, the pitch horizon sensor indicated -0.34 deg, and the gyro indicated +0.25 deg.

3.6.2.2 Roll Axis Control. The roll-axis-separation rate appeared normal at approximately 0.6 deg/sec. The roll error at the time of pneumatic activation by separation switch was -3 deg on horizon sensor telemetry. The roll-horizon-sensor signal was connected to the roll gyro at separation switch activation. The gain was measured at 9.1 deg/min/deg (9.0 ±1.8 deg/min/deg allowed). The polarity, static gain, dynamic gain, and deadband of the roll pneumatic system were nominal. Roll-limit-cycle magnitude was ±1 deg with a 50-sec period. Roll attitude at the PPS thrust initiate signal was -1 deg on horizon sensor telemetry and -0.8 deg on gyro position telemetry. (See Fig. 3-45.)

3.6.2.3 Yaw Axis Control. The yaw-axis-separation rate looked normal at approximately 0.1 deg/sec. The polarity, static gain, dynamic gain, and deadband of the yaw pneumatic system were nominal. The yaw limit-cycle magnitude was ±0.15 deg with a 70-sec period. The yaw gyro indicated a position of +0.05 deg at the PPS thrust initiate signal. (See Fig. 3-46.)

3.6.3 Performance From PPS Thrust Initiate Signal to LOS

Hydraulic pressure buildup was coincident with turbine spin-up and looked nominal. (See Fig. 3-47.) Buildup started at 367.8 sec, reached 2600 psi by 368.25 sec, varied from 2600 to 2720 psi at 368.7 sec, and then decreased rapidly to 240 psi at 369.12 sec; this indicated loss of UDMH pressure to the hydraulic power package.
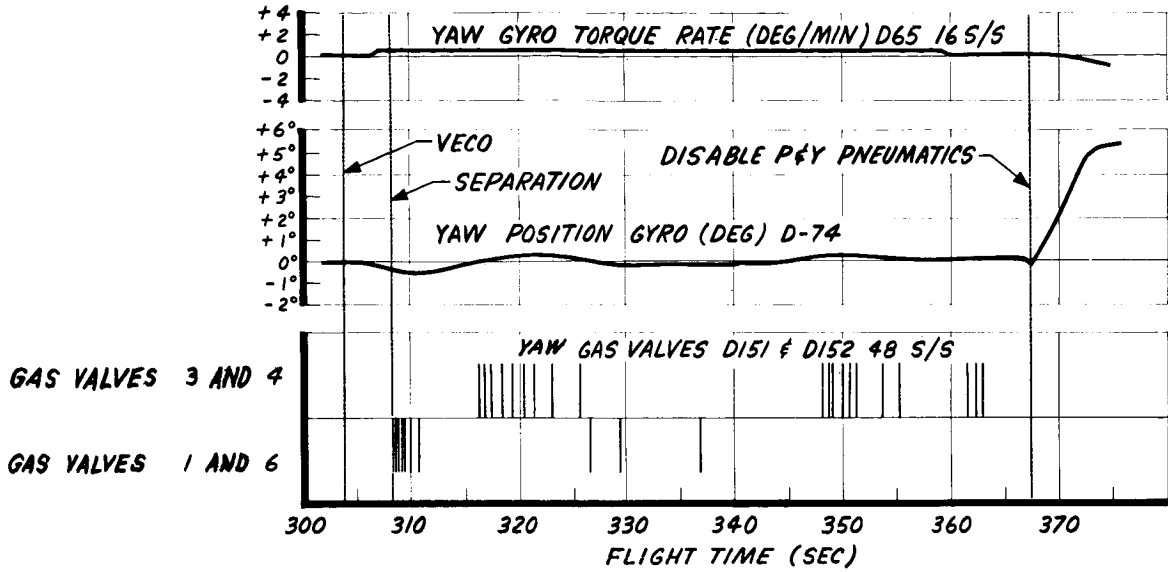
Fig. 3-46   Yaw Axis Control Performance
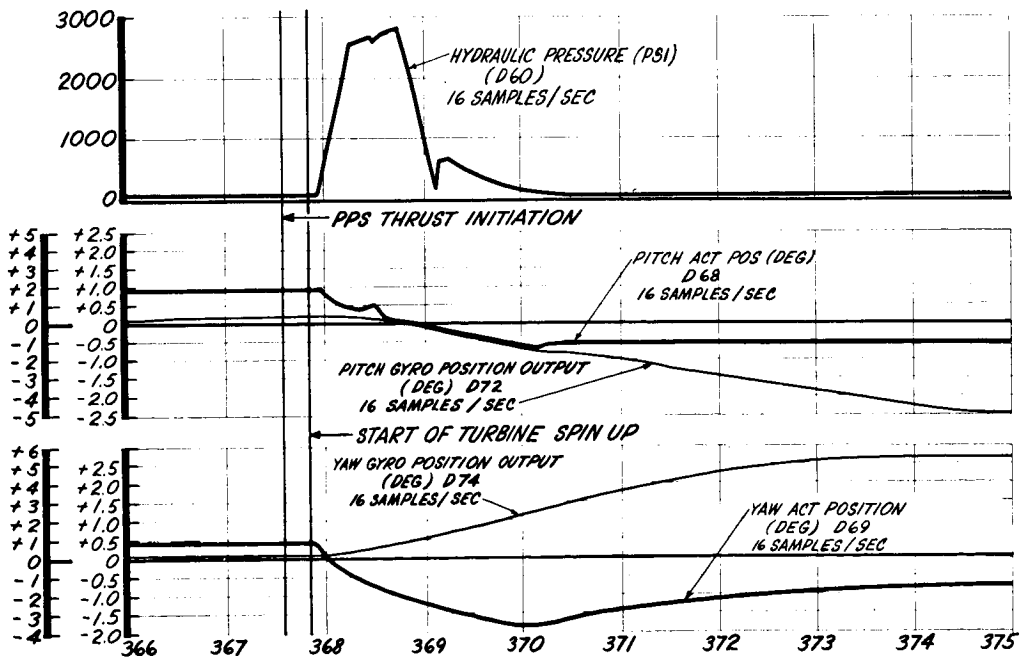
Fig. 3-47   Yaw and Pitch Actuator Positions Between 366 and 375 Sec

LOCKHEED MISSILES & SPACE COMPANY

Pitch channel performance was nominal. There was no pitch-gas valve activity after PPS thrust-initiate signal. The initial actuator offset was +0.94 deg. The actuator dynamic response was nominal, with correct polarity. Assuming a 20 percent overshoot, the pitch hydraulic static gain was calculated to be approximately 2.04 deg engine/deg vehicle (2.1 ± 0.21 allowed). An accurate calculation was not possible because of the short duration of hydraulic pressure. At 368.4 sec, the pitch actuator applied initial correction to the vehicle just prior to loss of hydraulic pressure. The initial motion in pitch is detected at 368.25 sec. After loss of pressure, the vehicle moved nose down at approximately 0.8 deg/sec. (See Fig. 3-48.)

Yaw channel performance (Fig. 3-47) was nominal. There was no gas valve activity after the PPS thrust initiate signal. The initial actuator offset was +0.46 deg. Coincident with turbine spin-up (at 367.8 sec), the yaw gyro indicated an acceleration from 0 deg/sec to approximately 1.2 deg/sec by 368.75 sec. This yaw motion is initiated prior to any evidence of engine thrust. The gyro position indicates no slope reversal due to engine gimbal position, leading to the conclusion that the correction force during the short thrust period was approximately equal to the transient disturbance force. (See Figs. 3-47 and 3-49.) The hydraulic channel polarity was correct, the dynamic response nominal, and the static gain approximately correct; but no accurate gain calculation was possible due to gyro motion.

Roll channel performance (Fig. 3-50) was nominal. There was normal gas valve activity throughout this period. At turbine spin-up, Fig. 3-47 the vehicle rolled from -1 deg to +0.6 deg, and the roll pneumatic channel applied the proper correction force.

3.6.4 Other Guidance and Control Performance

All other parameters operated normally. (See Fig. 3-51 and Table 3-5.) The decrease in thrust valve cluster temperature was caused by flow of ACS control gas through the nozzles; it cannot be associated with the extreme cooling indicated by the aft rack temperature transducers.
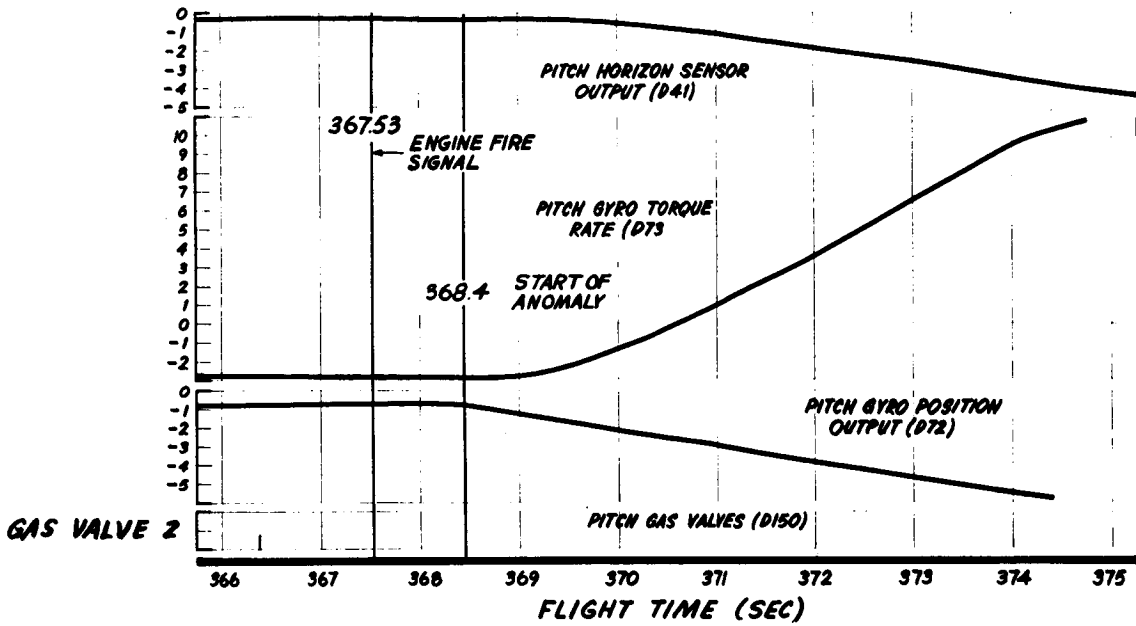
Fig. 3-48 Pitch Channel Output Between 366 and 375 Sec
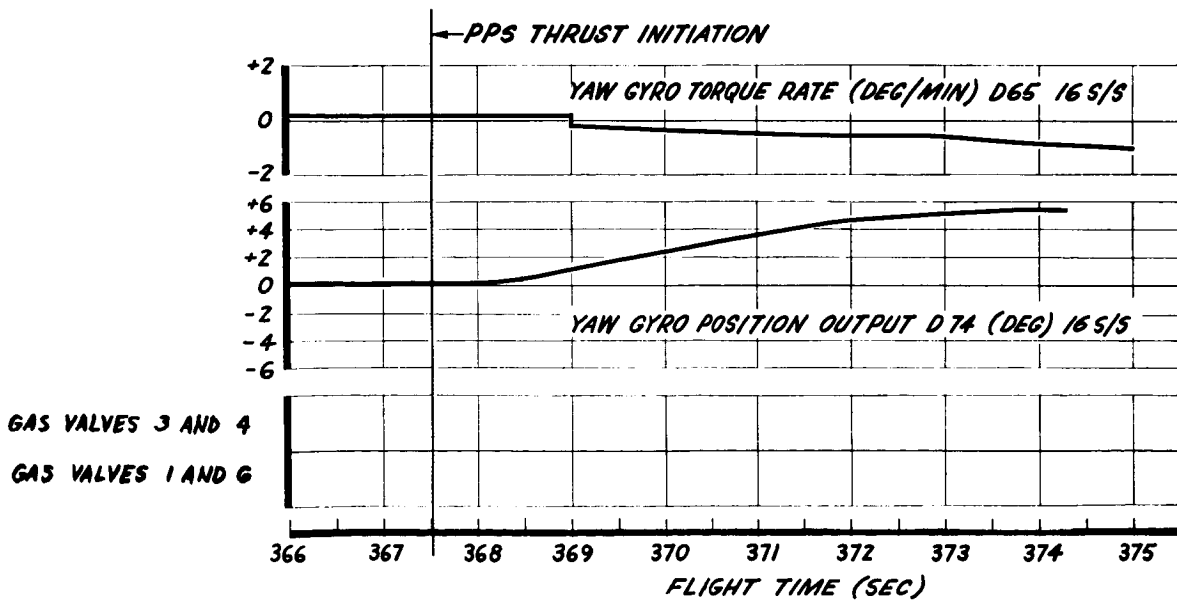
Fig. 3-49 Yaw Channel Output Between 366 and 375 Sec

LOCKHEED MISSILES & SPACE COMPANY
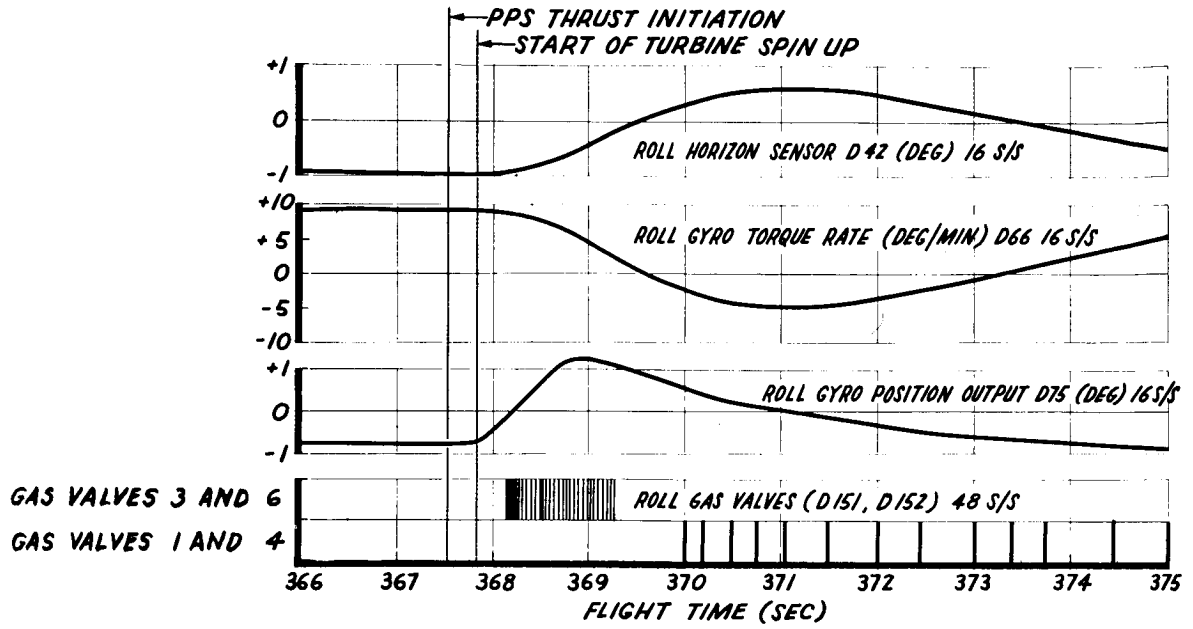
Fig. 3-50 Roll Channel Output Between 366 and 375 Sec
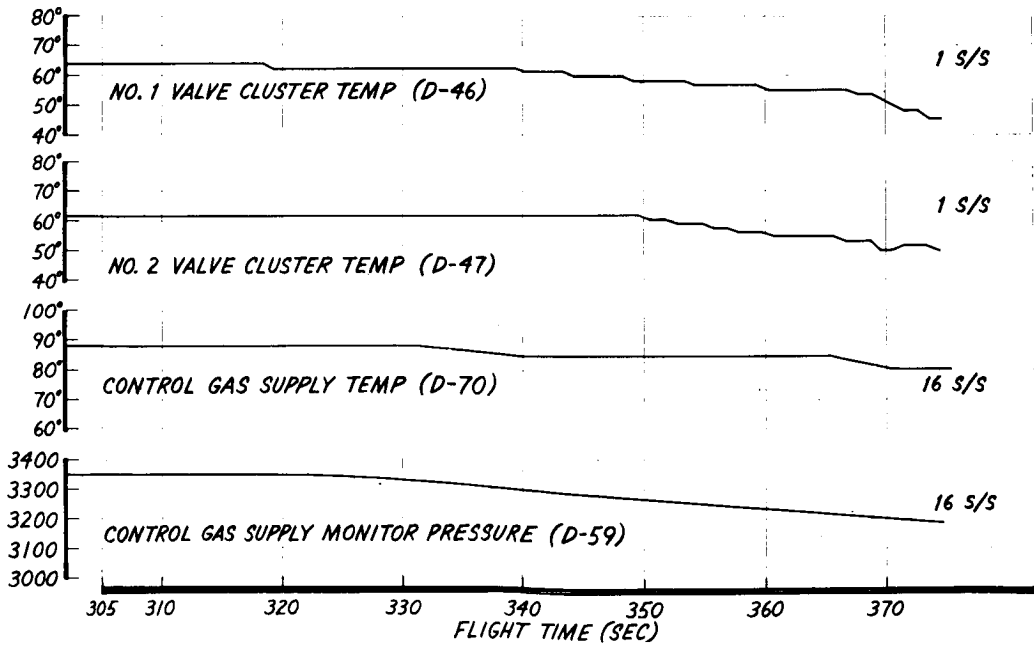
Fig. 3-51 Thrust Valve Cluster Temperature and Control Gas Supply Pressure

Table 3-5

ADDITIONAL GUIDANCE PARAMETER MEASUREMENTS

No.	Name	Recorded Value Liftoff	Recorded Value Variation	Remarks
D54	Horizon Sensor Right Head Temp	65.1° F	Steady increase to 67.8° F at LOS	Normal
D55	Horizon Sensor Left Head Temp	63.8° F	Steady increase to 66.5° F at LOS	Normal
D5	Hydraulic Oil Return Line Temp	55.8° F	Max Temp 71.5° F	Normal
D32	Hydraulic Oil Low Pressure	54.5 psig	Max 72.3 psig at 368.3 sec	Normal
D58	Control Gas Reg. Press No. 1	129.1 psig	Min 106.7 psig; Max 129.1 psig	Normal
D57	Control Gas Reg. Press No. 2	20.7 psig (Telemetry Saturation)		0 to 20 psig range for low pressure in orbit mode
D129	IRP Internal Case Temp	143.4° F	Constant to LOS	Normal
D183	SMRRD Monitor	1.61v dc	1.54v dc at LOS	Normal Correct = (2 ± 0.8) v dc Incorrect = (4.7 ± 0.5) v dc
D88	Velocity Meter Stored Word	15,856 Counts	None	Normal
D85	Velocity Meter Elec Oven Temp	4.65v dc	Min = 4.41v dc Max = 4.45v dc	Normal
D87	Velocity Meter Oven Temp	4.65v dc	4.61v dc at LOS	Normal
D86	Velocity Meter Cutoff	0.00v dc	0.00 at LOSS	Normal

3-97

LOCKHEED MISSILES & SPACE COMPANY

3.6.5 Control Gas Consumption

The following listing shows control gas consumption from 308.5 to loss of signal (LOS).

Time (sec)	Gas Supply (lb)
308.5 (Activate pneumatics)	139
334.0 (Prior to pitch down)	139
353.0 (After pitch down braking pulse)	137
376.0 (Prior to PPS initiate signal)	137
LOS	136.9

3.7 INTERPRETATION OF ANOMALY

This paragraph lists the significant data anomalies, relates them to the apparent malfunction, and presents a possible sequence-of-events. The limitations of the telemetry system in defining the exact mode and sequence of failure is also described.

It is apparent that the flight up to PPS fire signal (367.53 sec) was perfectly normal. The only significant anomaly noted was the loss, at Atlas-Agena separation, of the two accelerometers mounted on the engine thrust cone. These accelerometers are located in a region of severe pyrotechnic shock environment, which accounts for their loss. No other damage in the aft rack area from this shock is evident from the data. The initial phase of the engine start sequence appears normal until approximately 368.4 sec, which is arbitrarily defined as the apparent start of the malfunction. The following paragraphs define the events that occurred in the period immediately following and attempt to interrelate them in a logical manner.

3.7.1 List of Anomalies

Data from the following measurements constitute the observed anomalies:

- **Engine Switch Group (B139).** Dropped from normal 1.75v at 368.404 sec to zero volts in sampling period prior to 368.435 sec; then rises to 2.9v and remained steady. However, pitch and yaw pneumatics were not activated.
- **Oxidizer Pump Inlet Pressure (B2).** Went from normal reading to off-scale at 368.68 sec.
- **Oxidizer Venturi Inlet Pressure (B11).** Increased from 830 psi to 1080 psi, then decreased to 0 psi, and then recovered to 840 psi.
- **Oxidizer Injector Pressure (B148).** Large oscillation from 368.42 to 368.56 sec.
- **Fuel Valve Actuating Pressure (B82).** Increased to full scale at start of anomaly.
- **Shear Panel Temperatures (A151 to A153).** Showed a decrease from 70° F to -10° F near start of anomaly.

- Aft Bulkhead Temperatures (A154 to A157). Showed a decrease at time. of anomaly.
- PPS Start Tank Temperatures (B141 and B142). Showed a decrease at time of anomaly.
- Message Acceptance Pulse (H38). Spurious message acceptance pulse (MAP) occurred at 368.6 sec.

These anomalies indicate: (1) a pressure surge throughout the oxidizer system and also in a fuel transducer mounted on the engine, (2) a leak of one or both propellants, and (3) a failure in the engine electrical circuitry. To determine the cause of the malfunction, it is necessary to establish which occurred first – the electrical or the mechanical anomaly. The following discussion presents an attempt to do this.

3.7.2 Discussion of Major Anomaly

A rigorous analysis of the malfunction is limited by the inherent restrictions of the PCM telemetry system as previously described. All events appear normal up to 368.404 sec, as shown in Fig. 3-52. At this moment, the engine has received the fire signal, the gas generator solenoids are open, the pilot-operated solenoid valve (POSV) closes, and the turbine is coming up to speed.

Between 368.404 and 368.435 sec, an event occurs that results in removal of power from the gas generator valves and POSV. This is shown by the decrease of voltage on the engine switch group from its normal 1.8v to zero volts. Due to the sampling rate (32 per second), this voltage change could have occurred at any time within this interval, and it is necessary to examine other events that fall within the interval to determine the time relationship of the anomalous events.

Thrust-chamber pressure appears to rise normally after 368.404 sec but starts to decrease well before 368.435 sec, indicating that the entire thrust-chamber pressure pulse has occurred within this interval. The peak of the pulse occurred either prior to or after the Channel 115 indication of 428 psi.

368.404- 368.414- 368.423⁺ 368.433⁺ 368.443⁺

ENGINE SWITCH GROUP B139
FUEL VALVE ACTUATION PRESS. B82
OX. INJECTOR PRESS. B148
THRUST CHAMBER PRESS B6

22.9 MS

180 V   180 V   TIME UNCERTAINTY   0.04 V
316 PSI   316 PSI   1500 PSI
0 PSI   344 PSI
428 PSI
0 PSI   144 PSI   173 PSI   0 PSI

128   20   40   60   80   100   120   12   32   52   72
TELEMETER CHANNEL NUMBER   488 μ SEC BETWEEN CHANNELS
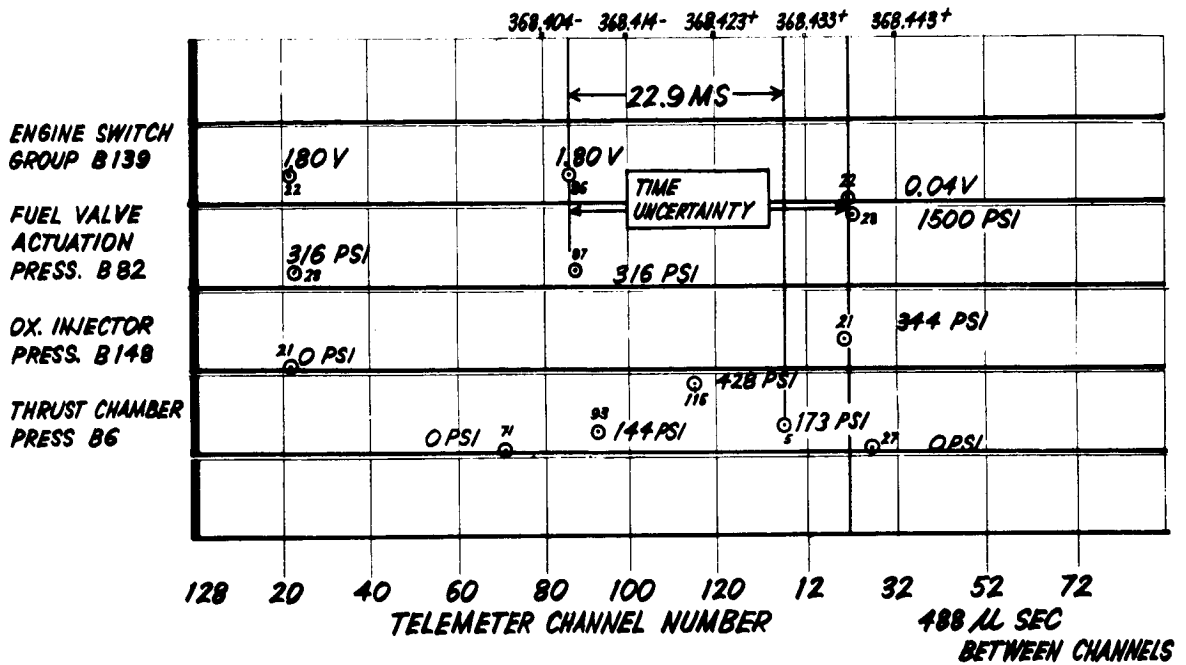
Fig. 3-52 Possible Sequence of Events

To establish the supposition that the mechanical failure (which was indicated as a pressure pulse) occurred prior to the electrical failure, it will be assumed that the reverse is true; i.e., the engine shutdown was caused by a power failure in the engine circuitry. This premise would assume that the switch group voltage went to zero immediately following 368.404 sec, and the thrust-chamber peak pressure was reached immediately prior to Channel 5, which occurred at 368.427 sec. This allows 22.9 ms for the main fuel valve to close after the POSV is de-energized. In actual tests, the minimum time for this event to occur was observed as 22 ms. Since this hypothesis places both events at their extreme times and allows no time for the peak pressure (which was at least 428 psi) to fall to 173 psi (Channel 5), the remaining 0.9 ms time increment is insufficient to support this hypothesis. In addition, this assumed failure mode (electrical leading mechanical malfunction) does not

explain the large pressure pulse noted in both the fuel and oxidizer systems (such a pressure pulse is not conventionally seen); removing power from the three solenoid valves is the conventional method for shutting down the engine.

It must therefore be concluded that the initiating event was an excessive pressure pulse in the engine (hard start); this, in turn, caused mechanical failure in the propellant system and resulted in a leak and a mechanical failure of the engine control circuitry.

3.7.3 Sequence-of-Events at Failure

At the time designated as the start of the anomaly, 368.404 sec, the engine was well into its starting sequence. The turbopump had supplied the propellants at a high enough pressure to the point where they were capable of overcoming the spring forces of their main valves. Approximately 1.9 lb of fuel had preceded the oxidizer into the thrust chamber. At this point, a high pressure detonation appears to have occurred either in the oxidizer cooling passages, because of hypergolic mixing of the propellants, or in the thrust chamber itself, because of a critical amount of propellants reacting. Detonation in the thrust chamber could also have been caused by combustion instability due to ignition delays. The limitations of the instrumentation and the PCM telemetry system sampling rate do not permit a more definitive evaluation.

The pressure pulse appeared to travel through the oxidizer system. The oxidizer venturi inlet pressure fell from its normal 1080 psi to 0 psi as the surge caused the oxidizer tank to act as an accumulator and momentarily permit the reverse flow of oxidizer. The pulse was of sufficient magnitude to cause physical damage to the oxidizer-pump inlet pressure transducer. The fuel valve actuating pressure transducer, located on the engine, was also disabled, but the pressure pulse did not appear in any of the upstream fuel system instrumentation. The pressure pulse also caused a failure in the oxidizer feed system − perhaps at the PIVs or oxidizer sump, which are the weakest points in the system. This resulted in a leak of approximately 0.5 to 1.0 lb/sec as calculated from the thermo data. This leak sprayed the interior

CONFIDENTIAL

LOCKHEED MISSILES & SPACE COMPANY

portion of the aft rack as noted by the drop in temperature on the shear panels, the
aft bulk-head, and the start tanks. (See Figs. 3-9, 3-12, and 3-13.)

The pressure pulse transmitted structurally, or the resulting mechanical failure also
caused a failure of the engine electrical circuitry either in the electronic gate or the
harness in close proximity to it. This is evidenced by the engine switch group voltage,
which dropped from the normal start signal to zero without command shutdown,
velocity meter shutdown, turbine overspeed, or activation of pitch and yaw pneumatics.
The voltage drop was caused either by relay chattering and failure in the box or by
severing of wires to pins E and F of connector P6011. The harness wire connected to
J6011 on the electronic gate developed a resistance to pin D that resulted in an off-
nominal voltage reading. (This latter failure mode has been verified by testing;
i.e., a telemetry reading of 2.8v was obtained by disconnecting P6011 and inserting
a high resistance between pins E and D of the cable connector.) The electrical
transients, in turn, caused a spurious MAP to be generated.

When power was removed from all engine solenoids, the engine shut down. The main
tanks continued to pressurize, and rupture occurred at or near the predicted value
(95 psi), which resulted in loss of telemetry.

LOCKHEED MISSILES & SPACE COMPANY

Section 4
CONCLUSIONS AND RECOMMENDATIONS

Section 4
CONCLUSIONS AND RECOMMENDATIONS

GATV 5002 was launched on schedule following a near-perfect countdown. Throughout the ascent phase, until shortly after PPS ignition, all subsystems of the GATV functioned within design parameters, and the data received by the ground stations indicated all events occurred at near nominal times. It has been established by evaluation of the flight data that a catastrophic disturbance started at 368.404 sec after liftoff and that a complete loss of signal occurred at 375.98 sec.

4.1 CONCLUSIONS

1. Tracking data indicated that incremental velocity of 6 ft/sec was imparted to the GATV by the primary propulsion system. The pulse shape and interval of the impulse could not be determined from tracking data.

2. The PCM system was found to provide large quantities of data, but because of its "commutation" characteristic, continuous information was not available, and exact timing of the onset of certain events was lost. The PCM system operated well, however, and provided approximately 97 percent of the instrumentation points scheduled.

3. Instrumentation operated satisfactorily in general. Pressure transducers indicated a significantly high overload with a failure mode indicating that a pressure pulse was received by certain of the mechanical diaphragm or bourdon-tube sensing devices. Aft accelerometers were found to have been mounted in an excessively severe pyrotechnic shock environment. Changes in measuring frequency appear desirable, particularly in the unregulated bus-current monitor and ampere-hour meter measurements.

4. The vehicle electrical system functioned normally up to the time of the anomaly.

4-1

LOCKHEED MISSILES & SPACE COMPANY

5. Communications and control equipment indicated receipt of a spurious message acceptance pulse (MAP) signal. This is attributed to an inductive pickup of a pulse associated with the electrical fire signal dropout to the engine.

6. The secondary propulsion system operated satisfactorily throughout the mission. Certain minor anomalies that were identified from flight data did not appear to impair the useful operation of the SPS. These anomalies require further analysis.

7. The primary propulsion system appeared to start up normally. After approximately one second in the startup transient, an anomaly occurred that caused shutdown of the engine. Investigation into the cause of the anomaly has centered on relative timing of electrical versus mechanical malfunctions and probability of occurrence of a multiple failure mode. From all data available, it would appear that a rough, explosion-like start in the combustion chamber or oxidizer manifold caused a pressure pulse to travel throughout the PPS oxidizer system. Shortly thereafter the fire signal to the engine was lost. The resulting engine shutdown caused propellants to cease flowing; the helium-blowdown-pressurization system continued to pressurize the propellant tanks until they burst. In addition, at the time of the pressure pulse through the PPS, leakage of propellant was observed. This resulted in rapid decrease of temperatures in the vicinity of the aft rack. Of the many failure modes that can be hypothesized to account for the engine fire signal loss, the single mode failure that could be the specific failure mode is a break in the harness leading to the turbine-overspeed-shutdown-electronics assembly.

To make sure that the shutdown of the engine could not have been caused by the vehicle electrical system, all aft instrumentation harnesses were examined. The result of this examination, shown in Fig. C-1, indicates that loss of the engine fire signal is not correlated with a disconnected plug.

8. Accelerometer indications appear to represent real impulsive acceleration rather than vibration. The accelerometers are relatively insensitive to high frequency, being 20 db down at 1500 cps. Correlation of elastic and rigid body response to a ramp impulse indicates that a near instantaneous increase in thrust to normal levels,

followed by a normal thrust decay, would provide the longitudinal accelerations reported and would provide the incremental velocities derived from tracking data. Temperatures on the aft rack of Vehicle 5002 decreased dramatically during the period of time following the PPS anomaly. These temperature changes were attributed to impingement of escaping propellants in the amount of approximately 1 lb/sec. The heat-transfer coefficients are relatively unknown for these propellants, and further analysis appears unwarranted.

9. The guidance and control system operated normally. No evidence of pitch and yaw control actuation after PPS startup was noted. This verifies that a normal engine shutdown command was not given to the engine.

4.2 RECOMMENDATIONS

1. Change the sampling rates of specific instrumentation measurements as indicated in Table 4-1.

Table 4-1

RECOMMENDED CHANGES TO SAMPLING RATES OF
INSTRUMENTATION MEASUREMENTS

Measurement		Sampling Rate (Samples/Sec)	
No.	Name	Present	Recommended
C4	28v dc unregulated current	1	16*
C38	Structure current monitor	1	16
C141	Pyro bus voltage monitor	1	16
C130,131,132	Ampere-hour meters	16	1
B1	Fuel pump inlet pressure	16	32
B2	Oxidizer pump inlet pressure	16	32
B3	Turbine manifold pressure No. 1	16	32
B7	Helium supply pressure	16	1
B11	Oxidizer venturi inlet pressure	16	32
B12	Fuel venturi inlet pressure	16	32

*Increase still more if spare channels are available.

Table 4-1 (Continued)

Measurement		Sampling Rate (Samples/Sec)	
No.	Name	Present	Recommended
B139	8247 engine switch group	32	96
B132	Turbine manifold pressure No. 2	32	None (delete)
D5	Hydraulic oil return line temperature	16	1
D70	Control gas supply temperature	16	1

2. Relocate accelerometers A5 and A522 from forward face of the aft bulkhead section of the -Y axis shear panel to the transverse bulkhead approximately 7.5 in. forward of Sta 462.5 on the -Z-axis side. Shock-mount the amplifiers to minimize the effects of pyrotechnic shock. Modify checkout and test requirements at the launch base to include functional verification of temperature transducers in the "as installed" condition.

3. Shock-mount the following equipment in the aft rack area:

    a. Aft safe-arm J-box

    b. Aft signal conditioner J-box

    c. Power distribution J-box

    d. Turbine overspeed detector relay

    e. Aft accelerometer amplifiers

These components should be shock-mounted against adverse affects from pyrotechnic shock, since they are mounted on the engine cone area close to the separation joint. The pyrotechnic testing device available at the Santa Cruz Test Base should be used to proof-test the mounting. To simulate the pyrotechnic shock environment, the above shock-mounted components should be tested while they are operationally stimulated in critical circuit areas.

4. Revise the application of electrical power to the PPS so as to bypass the turbine electronic gate for first burn only. In the event of turbine overspeed, use the relays in this electronic gate only to de-actuate relays providing power to the engine.

LOCKHEED MISSILES & SPACE COMPANY

Shock-mount the turbine overspeed shutdown gate, and proof-test it in a pyrotechnic shock environment as discussed in item 3.

5. Change the main fuel valve and oxidizer valve to the 8096 type. Install an oxidizer manifold-pressure switch and an oxidizer feed-pressure switch coupled so as to prohibit fuel lead into the combustion chamber. This circuitry should be designed in such a manner that loss of either the oxidizer manifold-pressure switch (OMPS) or the oxidizer feed-pressure switch (OFPS) will not cause shutdown of the engine. Verify all engine modifications through an altitude test (250,000 ft equivalent) so that the influence of hard vacuum will be observed, particularly in the engine-ignition phase. Parallel this activity with comprehensive sea-level testing of the modified engine.

As a result of exhaustive analysis of all flight data, LMSC is satisfied that the implementation of the preceding recommendations will minimize the possibility of a recurrence of the hard-start condition. The flight data indicated that all subsystems (structures, guidance and control, communications and command, SPS, and the PPS) met all design parameters up to the start of the anomaly. The flight data also indicate that GATV specifications, manufacturing procedures, test procedures, checkout procedures, and AGE are adequate and satisfactory for completion of the program.

Appendix A
DESCRIPTION OF MODEL 8247 ROCKET ENGINE

Appendix A

DESCRIPTION OF MODEL 8247 ROCKET ENGINE

A.1 COMPARISON OF MODEL 8247 AND MODEL 8096 ROCKET ENGINES

Major hardware and performance differences between the Model 8247 and Model 8096 rocket engines are as follows:

a. Gas-Generator Starting System. The 8096 solid-propellant starting system was replaced by an automatically recharged liquid propellant system consisting of fuel and oxidizer start tanks and check valves (Fig. 3-5) to provide multiple-start capability. The hydraulically actuated bipropellant yoke valve assembly was replaced with independent electrically actuated fuel and oxidizer gas-generator valves. The gas-generator starting system is initially loaded and pressurized on the ground prior to launch.

b. Main Oxidizer Valve. Cracking and reseat pressures were increased by use of a heavier spring and a larger preload to improve shutdown impulse characteristics, provide a lower minimum total impulse capability, and reduce oxidizer post flow.

c. Main Fuel Valve. Cracking and reseat pressures were increased by use of a heavier spring and a larger preload. Slipper seals were added to two of the three poppet O-rings, and the actuation line takeoff port was moved closer to the pump case to increase available actuation pressure. These changes were made to improve engine-shutdown impulse characteristics and to make the fuel valve compatible (start transient) with changes made to the main oxidizer valve.

d. Electrical System. The electrical system was simplified by the elimination of the oxidizer manifold pressure switch (OMPS), the thrust chamber pressure switch (TCPS), and their associated relay box. A turbine overspeed protection system (electronic gate) was added to prevent catastrophic

A-1

failure of the turbine wheel in the event that stored start-system energy (propellants) was released into the gas generator under conditions that caused one or both of the pumps to be unloaded. In addition, EMI suppression and nonsusceptibility components were added to provide protection against interference with, or by, other vehicle circuits.

e. Steady State. No change was made to steady-state performance (i.e., thrust, flow rates, mixture ratio, or specific impulse).

f. Transient. The Model 8247 engine incorporates the following changes to the transient-state performance of the Model 8096 engine:

   (1) Total Start Capability. The total starts per mission capability was increased from 2 to 15.

   (2) Preflow (Lead). Preflow was changed from approximately 5 lb of oxidizer to approximately 3 lb of fuel.

   (3) Shutdown Impulse. Impulse produced after application of a shutdown signal, when the engine has been operating under steady-state conditions within the temperature range of the +40° F to +60° F, was reduced from 3220 ±440 lb/sec to 2440 ±405 lb/sec.

   (4) Minimum Total Impulse. The Model 8247 engine was designed for a minimum total impulse* capability of 17,500 lb/sec when operating within the temperature range of +10° F to +140° F. A subsequent analysis has shown that it also has the capability of 13,750 lb/sec when operating within the temperature range of +6° F to +83° F.

   (5) Oxidizer Post Flow. Oxidizer post flow was reduced from approximately 35 lb to approximately 20 lb.

---

*Minimum total impulse is defined as the total impulse produced when the engine is operated just long enough to recharge the start system to a level sufficient to ensure operation within specification limits, during the remainder of its rated operating cycle.

A.2 ENGINE START SEQUENCE (FLIGHT)

At the predetermined time during the ullage orientation period, the engine start sequence begins with the application of a 28v dc signal to pins A and D of connector J6000, along with a simultaneous grounding of pins B and E. (Refer to the propellant flow schematic, Fig. A-1, and to the wiring diagram, Fig. A-2.) The start signal passes through the electronic gate circuitry, which acts as a junction box for dispersing the signal to the engine solenoid valves. Pins H and Z of P6011 furnish power to the gas generator fuel solenoid valve (GGFSV); pins J and $\underline{a}$ furnish power to the gas generator oxidizer solenoid valve (GGOSV); and pins K and $\underline{b}$ supply power to the pilot-operated solenoid valve (POSV). The three solenoid valves actuate simultaneously upon receiving the start signal.

Prior to launch, the start tank is pressurized and loaded with the proper volume of propellants. Opening of gas generator solenoid valves initiates start tank blowdown. With the opening of the solenoid valves, propellants flow into the gas generator due to the force of the gas pressure on the bellows. The propellants ignite hypergolically in the gas generator, which provides pressure buildup, resulting in turbine acceleration. Since the pumps are coupled to the turbine wheel, the pump-outlet pressures rise consistent with turbine speed increase. The process of start-tank-pressure decay and pump-outlet-pressure increase continues until the two pressures equalize, at which time propellant expulsion from the start tanks stops.

A-3

OX. FILL AND DRAIN Q.D.

FUEL FILL AND DRAIN Q.D.

B-2 OXID. INLET PR 0-100 PSIG

HYDRAULICS POWER PACKAGE

OXIDIZER FILTER 250 MICRON

B-136 OXID. TANK TEMP. (+Z) -15° TO +170°F

5.5 FLEX

ΔP SWITCH 3 ±2 PSID

B-8 OXID. TANK PRESSURE 0-60 PSIG

PROPELLANT ISOLATION VALVE (OXIDIZER) B 130

B-97 FUEL TANK TEMP. NO. 2 -15 TO +170°F

B-9 FUEL TANK PRESS. 0-60 PSIG

HELIUM FILL Q.D.

FUEL VENT Q.D.

OXIDIZER PUMP

ULLAGE CONTROL TUBE

FUEL 75.3 FT³ VOLUME

PROPELLANT TANK

STANDPIPE

OXIDIZER 98.4 FT³ VOLUME

FUEL PUMP

ORIFICE

SQUIBS 1 & 2   SQUIBS 3 & 4

ORIFICE

B-96 FUEL TANK TEMP. NO. 1 -15 TO +170°F

ULLAGE CONTROL TUBE

B-137 OXID. TANK TEMP. (-Z) -15° TO +170°F

PROPELLANT ISOLATION VALVE (FUEL) B 130

FUEL FILTER

PYRO-OPERATED HELIUM CONTROL VALVE
▬ PYRO ACTUATED
═ HELIUM PRESSURE ACTUATED

P/S   P/S

FUEL TANK PRESSURE SWITCH 15 ±2 PSIA

OX TANK PRESSURE SWITCH 15 ±2 PSIA

B-31 FUEL PUMP INLET TEMP. 0° 100°F

B-1 FUEL PUMP INLET PRESS 0-100 PSIG

OVERBOARD DRAIN

OXID. VENT Q.D.

HELIUM SPHERE 3653 IN³ 2500 PSI (OPERATING) 3000 PSI (PROOF)

P B-7 HELIUM SUPPLY PRESSURE 0-4000 PSIA

T B-68 HELIUM SPHERE TEMP. 0 TO 120°F

DUAL CHECK VALVE (OXIDIZER)

B-11 OX. VENTURI INLET PRESS. 0-1500 PSIG

GAS GENER OXID. SOLE VALVE

N₂ FILL VALVE OXIDIZER

OXIDIZER BLEED VALVE

B-141 OXID. START TANK TEMP. -10° TO 150°F

OXIDIZER START TANK

OXIDIZER VENTURI

OXIDIZER FILL AND DRAIN VALVE

A-4

Fig. A-1 Primary Propulsion System
Fluid Flow Schematic
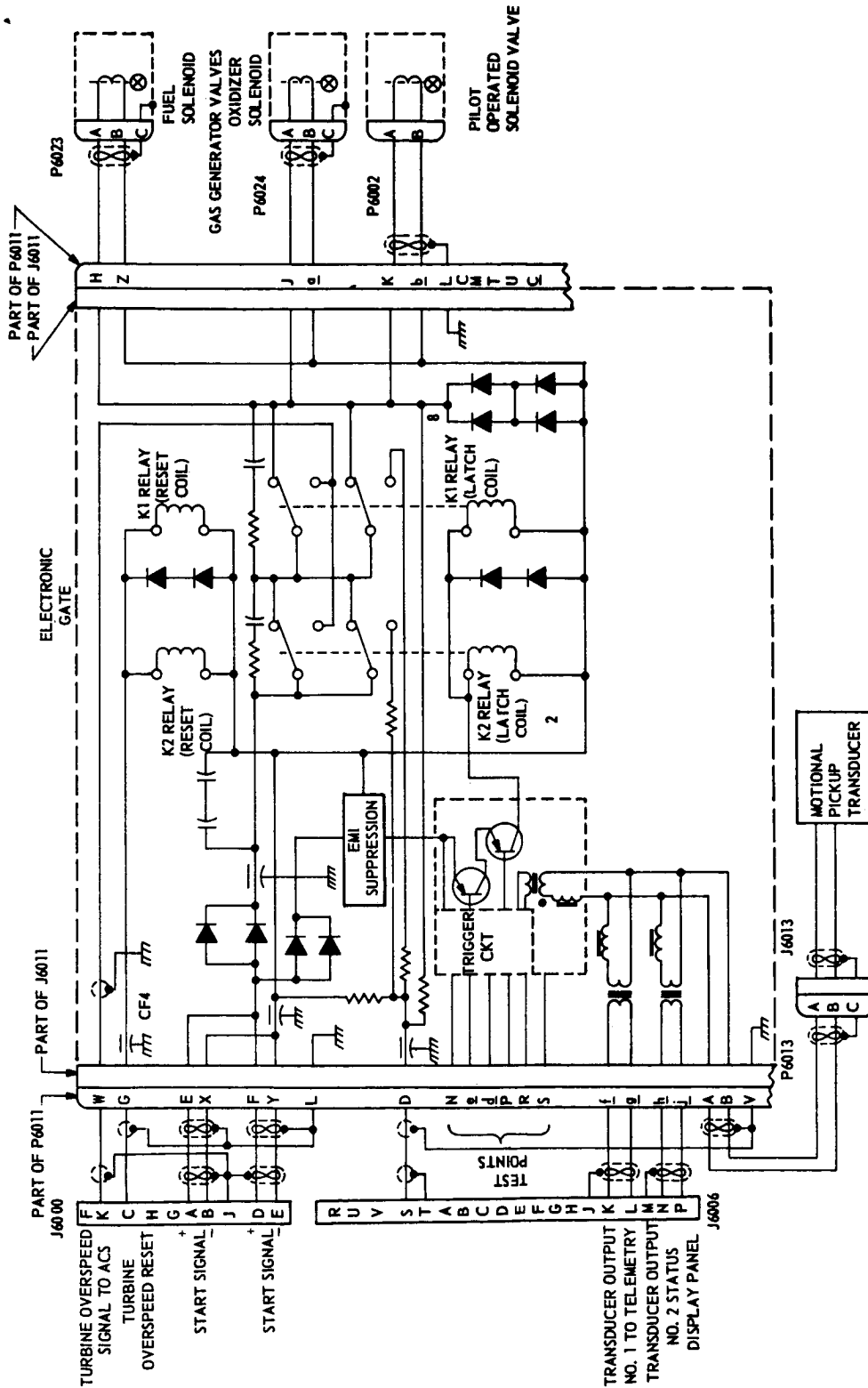
Fig. A-2 Rocket Engine Electrical Schematic Diagram

At this time, the gas generator is fed with the propellants from the pumps, and the bootstrap operation has been initiated. The fuel and oxidizer pump outlet pressures reach their stabilized values. After ignition, steady-state operation is achieved, and the start tank propellant supply is replenished and maintained by steady pump-discharge pressure. The dual check valves prevent backflow, thus containing the quantity of propellants within the start tanks and assuring subsequent starts.

At the same time that the GG solenoid valves open, the pilot-operated solenoid valve closes for initiating the sequence that allows actuation pressure to buildup. When the actuation pressure reaches 365 psig, the fuel valve main-poppet opens. On initial or phase "A" start, fuel flow to the thrust chamber, does not take place until the main-discharge pressure reaches 525 psig and ruptures the frangible disc. During subsequent starts, fuel flows into the thrust chamber immediately upon opening of the fuel valve.

Simultaneously with the rise in fuel-pump-discharge pressure, the oxidizer-pump-discharge pressure increases; at 225 to 300 psig, the main oxidizer valve is opened. As soon as this valve opens, the frangible disc ruptures. Oxidizer flows through the thrust-chamber cooling passages to the oxidizer injector manifold. Initial and subsequent start operations are identical, because the frangible disc ruptures almost immediately upon opening of the poppet. The frangible disc is used only to prevent leakage of propellant during the booster phase of flight.

Under normal operation conditions, fuel enters the thrust chamber first. Then oxidizer enters through the injector with two jets of fuel impinging on each oxidizer jet. These propellants ignite hypergolically to initiate thrust-chamber operation. The time from application of start signal to the time when 70 percent P_c (thrust chamber pressure) is reached, considered the start transient, is nominally 1 sec. Steady-state thrust is defined as the time from 70 percent P_c start to engine shutdown.

The engine continues to operate nominally as long as the start signal is applied and maintained.

is reached is considered the start transient, and is nominally 1 sec. Steady-state thrust is defined as the time from 70 percent P_c start to P_c decay on engine shutdown. If operating temperatures are below normal, the fuel may enter the thrust chamber before the oxidizer without appreciable change in the engine start transients.

Once steady-state thrust is achieved, the engine continues to operate nominally as long as the start signal is applied.

LOCKHEED MISSILES & SPACE COMPANY

Appendix B

AGENA TARGET VEHICLE PRIMARY PROPULSION SYSTEM HISTORY

Appendix B
AGENA TARGET VEHICLE PRIMARY PROPULSION
SYSTEM HISTORY

B. 1 ENGINE DEVELOPMENT

The initiation of development for the eventual procurement of the BAC Model 8247
(XLR81-BA-13) rocket engine occurred in June 1962. This development effort was
to culminate in the production of nine multiple restart rocket engines to be utilized
on the Gemini Agena Target Vehicle Program. The allocation of these production
engines was to be as follows:

S/N 801	—	PFRT at Bell Aerosystems Corp.
S/N 802	—	PTVA at Lockheed Missiles & Space Company
S/N 803	—	Vehicle 5001 flight backup
S/N 804 through S/N 809	—	Flight Vehicles 5002-5007

The aim of the program was to utilize the basic design of the flight-proven Model 8096
rocket engine to the maximum possible extent. Modification was to be made only to
include the design necessary to meet the constraints of the GATV mission and to gain
a "hardware-ready" time advantage while the already proven high reliability inherent
in the Model 8096 engine system design was to be maintained.

The Gemini mission dictated the requirements to remain on-orbit for a minimum 5-day
useful life span and be capable of performing four burns in addition to the burn required
to inject the vehicle into orbit. Simplification and improvement of the design of the
Model 8096 rocket engine was also required. The result of this redesign was termed
BAC Model 8247 rocket engine (XLR81-BA-13).

B-1

To conform to mission requirements, the following design studies and changes were made:

a. The "two-start" solid propellant charges were removed and replaced with metal bellows-type start tanks capable of multi-restart.

b. Elimination of the oxidizer manifold pressure switch to improve reliability resulted in a thrust-chamber fuel lead. A study and subsequent test effort proved the validity of this change. *

c. Both oxidizer and fuel dual-check valves were designed to implement the multiple restart requirement.

d. Individual solenoid valves were developed to control the gas generator start system; this eliminated the single-malfunction possibility of the Model 8096 gas-generator bipropellant valve causing an undesired engine start.

e. The main oxidizer valve was modified to use a heavier closing spring to effect a faster shutdown. This conserved oxidizer post-flow and obviated the need of the Model 8096 oxidizer fast-shutdown system.

f. The main fuel valve was modified to use a heavier closing spring and an improved Teflon slipper seal. This modification, by effecting faster shutdown, resulted in savings on fuel post-flow and improvement in valve reliability.

g. Minor changes were made to engine lines and mounts to accommodate the Model 8247 rocket engine.

h. An electronic gate was designed to take the place of the electrical relay box previously used to control the Model 8096 engine. The new device was required to perform the following functions, unique to the GATV:

   (1) Shutdown the rocket engine by means of a designed-in capability, in case of turbine overspeed.

   (2) Provide instrumentation tap-offs for monitoring turbine speed.

   (3) Provide EMI suppression for engine solenoids.

---

*The thrust-chamber titanium exhaust extension required verification testing for the five-start capability.

The following major items remained essentially unchanged from the Model 8096 original design:

- Turbopump assembly
- Gas generator assembly
- Thrust chamber assembly
- Basic main propellant valve design

B.2 DEVELOPMENT TESTS

Development testing was initiated once initial design concepts were established. The development testing was accomplished through testing on the component level, turbo-pump level, and engine level at BAC in Buffalo, N.Y., and altitude verification tests performed at Arnold Engineering Development Center (AEDC) in Tullahoma, Tenn.

B.2.1 Development Testing at BAC – Component Level

Testing on the component level included shock testing, vibration testing, acceleration testing, high- and low-temperature testing, component endurance testing, and (in the case of start system hardware) 38-day storage testing.

B.2.2 Development Testing at BAC – Turbopump Level

Testing on the turbopump level was accomplished in accordance with Table B-1. Exploratory testing was limited to preliminary investigations into the totally new start-system components to determine possible design philosophy changes or restrictions inherent in the then-proposed design. This testing encompassed transient analysis, start system blowdown characteristics, temperature-spectrum testing, and minimum recharge times. The tests proved the feasibility of the proposed start system.

Boilerplate tests followed, involving fabrication of heavy duty start tanks and further testing of transient effect, minimum recharge times, gas entrainment in the start tanks, and malfunction testing.

Table B-1

DEVELOPMENT TESTING ON TURBOPUMP LEVEL

Type of Test	Total Runs	Total Starts	Time (sec)
Exploratory	59	106	1,210
Boilerplate Hardware	25	49	1,876
Prototype	200	453	15,422
Totals	284	608	18,508

Prototype hardware was then fabricated and subjected to all previously mentioned tests on a more extensive basis.

B.2.3 Development Testing at BAC — Engine Level

Engine-level testing was accomplished to integrate all recently redesigned components into an engine system; it also included performing 150 hot-fire tests at BAC.

B.2.4 Development Testing at AEDC — Engine Level

Seventy engine firings at a simulated altitude of 110,000 ft were conducted at AEDC to establish confidence that the titanium thrust-chamber exhaust extension could sustain the proposed mission requirements for five-start transients. Tests that logged 15 starts on one extension proved hardware capability beyond defined requirements.

B.3 DEVELOPMENT PROBLEMS

Table B-2 presents all major design problems encountered during the development phase.

Table B-2
DEVELOPMENT PHASE DESIGN PROBLEMS

Component	Problem	Disposition
Gas generator bipropellant latching valve	Valve failed to relatch during AEDC hot-fire test	As a result of this failure, and a history of problems resulting from use of this valve, the gas generator control system design was redirected. This initiated design of dual solenoid valves to control flow of oxidizer and fuel to the gas generator.
Oxidizer start tank	Metal bellows sticking or hanging up in shell	This problem was solved by maintaining better surface finishes, introduction of permanent lubrication of bellows, and a configuration change to a flat movable head.
	Leakage in bellows and end members	This leakage was attributed to stress corrosion and intergranular corrosion. End members were then fabricated from closed-die forging with oriented grain billets. Tighter material control and changed heat treatments together with using thicker bellows attachment areas to enlarge the leak path solved the problem.
	Warping of bellows core	The problem, discovered by the vendor was solved as follows: a. Bellows blanks were to be heat treated to SCT 1025 condition. b. Forming, sizing, and welding were to be done in above condition. c. After fabrication effort was completed, the core was to be heat treated to an SCT 850 condition.

LOCKHEED MISSILES & SPACE COMPANY

Table B-2 (Cont.)

Component	Problem	Disposition
Fuel start tank	Same as for oxidizer start tank, above	Same as for oxidizer start tank, above.
Gas generator oxidizer solenoid valve	Mounting lugs cracked during vibration tests	Changed mount design and added pads to preclude vibration transmissibility.
	Static Leakage at valve	Changed from a "K" seal design to the "Omega" seal. Design change stopped leakage. However, during 38-day storage tests, Omega seal leakage forced a design change to an all-welded body flange.
	Plastic poppet seat distortion during high temperature testing	Poppet seat diameter was increased.
Gas generator fuel solenoid valve	Mounting pad cracked during vibration tests	Changed mount design and added pad to preclude vibration transmissibility.
	Valve opening and closing times excessive	Added a kick spring, increased amp-turns on armature, and increased armature spring preload.
	Excessive pressure drop across valve	Improved pressure drop by removing filter element previously incorporated in design. Valve filter was redundant with filter located on turbopump bootstrap supply line.
	Excessive seat leakage at high temperature and pressure	Redesigned seat employing a metal confined Teflon seat
Oxidizer dual check valve	Excessive seat leakage due to spring extrusion	Corrected problem by adding a poppet spring retainer sleeve.
	Poppet galling and sticking	Problem was eliminated by electrolizing poppet outer diameter.
	Poppet seating erratic	A heavier poppet spring and a smoother seat finish was incorporated into valve to promote positive poppet seating.

Table B-2 (Cont.)

Component	Problem	Disposition
Fuel dual check valve	Poppet galling and sticking	Problem was eliminated by "hardcote" application to poppet outer diameter.
	Excessive seat leakage	Corrected by better finish at poppet seat.
	Poppet spring guide cocked	Used improved spring guide retainer.

B.4 FLIGHT RATING AND VERIFICATION HISTORY

To prove that development of the PPS was sufficient to meet all requirements of the GATV mission, preliminary flight rating tests (PFRT) were conducted at BAC. During the performance of PFRT, several problems developed that necessitated component evaluation and redesign. Rather than terminate the PFRT program until redesigned components became available, testing continued to demonstrate the adequacy of other component design and system compatibility of components. The unsatisfactory components were redesigned and later checked out at component test level by satisfactory completion of a flight verification test program.

The flight rating and verification history may therefore be divided into testing and test problems associated with PFRT and the follow-on program of flight verification tests.

B.4.1 Preliminary Flight Rating Tests

The PFRT program of the Model 8247 rocket engine lasted from February 1964 until August 1964. Only one rocket engine used in the PFRT logged 37 starts and accumulated 577 sec of burn time. The PFRT consisted of the following:

  a. Weight and drainage tests
  b. Vibration and shock tests

B-7

  c. Fixed thrust calibration tests (hot-fire)

  d. High and low temperature tests (hot-fire)

  e. Humidity tests (hot-fire)

  f. Malfunction tests (hot-fire)

  g. Engine disassembly and inspection

B.4.2 PFRT Problems

The problems shown in Table B-3 were evidenced during the PFRT.

B.4.3 Flight Verification Testing

The following components were exposed to additional testing after redesign and modification following the PFRT program:

  a. Oxidizer dual-check valve

  b. Fuel dual-check valve

  c. Oxidizer gas-generator solenoid valve

  d. Fuel start tank

  e. Oxidizer start tank

The only component out of the above list that evidenced further problems was the oxidizer gas-generator solenoid valve, which had poppet and valve-liner difficulties. A redesigned poppet was incorporated; also an improved manufacturing and fabrication technique of the valve liner was adopted, and the valve then passed all component tests including hold-capability demonstration of 38 days duration. By September 1965, all components had completed testing at BAC and were considered flight ready.

B.5 DEVELOPMENT CONFIRMATION TEST HISTORY

To gain added confidence that the Model 8247 rocket engine was in a flight-ready configuration, and to establish compatibility between the engine and the vehicle flight environment, tests were run on a one-vehicle-only basis. These development confirmation tests were divided into an-engine-and-aft rack only test (PTVA) and a full-flight-ready-vehicle-hot-fire test. All testing was accomplished in a static test stand at the Lockheed Santa Cruz Test Base facility.

Table B-3

PROBLEMS DETECTED DURING PRELIMINARY FLIGHT RATING TESTS

Item No.	Component	Type of Failure	Test When Failure Took Place	Disposition
1	Fuel start-tank assembly	Bellows leakage 0.187 sccm (none allowed)	Functional tests – static leakage	Failed due to intergranular corrosion. **Action Taken** (1) Heat treatment sequence changed (2) No pickeling of bellows to take place after core pieces have been welded (3) Changed material to AM355 steel vacuum melt (4) Specific grain orientation required (5) Extra inspections to control manufacturing process, grain orientation, and material chemistry
2	Fuel valve	Excessive N_2 leakage past slipper seal	Functional tests – static leakage	Leakage due to metal contaminants scratching slipper seal upon valve assembly **Action Taken** Production valves to be assembled in "super clean" environment

LOCKHEED MISSILES & SPACE COMPANY

Table B-3 (Cont.)

Item No.	Component	Type of Failure	Test When Failure Took Place	Disposition
3	Fuel start-tank assembly	Tank shell leakage	Humidity test	Failure due to intergranular corrosion Action Taken Same as Item 1 above
4	Oxidizer start-tank assembly	Tank shell leakage	Prior to second humidity test	Failure due to intergranular corrosion. Action Taken Same as Item 1 above
5	Fuel dual-check valve	Inlet seat leakage	After first humidity test	Failure due to seat deformation Action Taken Seat design changed using a confined seat configuration
6	Turbine exhaust duct	Crack in duct	After first humidity test	Failure, which occurred after 23 starts, resulted from fatigue due to thermal stress. Action Taken A limited life of one mission cycle has been imposed

Table B-3 (Cont.)

Item No.	Component	Type of Failure	Test When Failure Took Place	Disposition
7	Gas-generator oxidizer solenoid valve	Acid attacked the liner in the copper braze area	During rework	Failure due to material sensitivity to acid etch Action Taken (1) Braze changed from copper to gold-nickel alloy (2) Braze depth controlled (3) Closer control of valve liner thickness (4) Liner material changed to 304L to preclude sensitivity to etching
8	Oxidizer primary seal mating ring	Excessive leakage	After first humidity test	Failure resulted because etched surface condition allowed excessive leakage. Action Taken Material changed to AISI 304L, which is insensitive to etching
9	Pilot-operated solenoid valve flange	Excessive leakage	Prior to second humidity test	Failure due to scratch on flange Action Taken Flange finish changed to "Hardkote"
10	Gas-generator fuel solenoid valve	Excessive leakage	Final functional test	Failure due to lack of lubricant on O-ring Action Taken Addition made to prints to call out proper lubricant to be used

B. 5. 1 Propulsion Test Vehicle Assembly (PTVA) Test

The PTVA was conducted on an 8247 rocket engine mounted in a prototype aft rack and supplied with propellants and gases from "battleship" or facility sources. The program was successful in all aspects and fully accomplished the following objectives:

    a.   Demonstrated the adequacy of the ATV pressurization system

    b.   Demonstrated the influence of prototype propellant-tank sumps on propellant residuals

    c.   Demonstrated no problem with thermal or acoustical interaction between PPS and SPS

    d.   Demonstrated the ATV-peculiar aft-rack structural adequacy

    e.   Demonstrated proper operation of the PPS in a simulated ATV flight profile

    f.   Developed and demonstrated the adequacy of test and checkout procedures (The initial procedures were utilized later to formulate AFETR procedures.)

    g.   Demonstrated the adequacy of the newly developed aerospace ground equipment (AGE) for PPS checkout and servicing

    h.   Demonstrated the capability of the PPS to maintain control of the rocket engine system during malfunction shutdown modes

B. 5. 2 Vehicle 5001 Hot-Fire

The hot-fire test was conducted to verify operation of various vehicle components while exposed to the propulsion environment to be encountered during flight. Although the test was not performed to verify propulsion operation, several additional data points were attained. Similar to the PTVA, the test was conducted at the Santa Cruz Test Base facility in January 1965. The propulsion system performed nominally throughout the test. Accomplishments demonstrated by the hot-fire test were as follows:

    a.   The adequacy and compatibility with the PPS of flight instrumentation systems

    b.   No thermal or acoustical interaction problem between the PPS and SPS (similar to the PTVA)

    c.   The adequacy of the flight pressurization system to support the GATV mission profile

    d.   A GATV flight profile (5 PPS burns)

    e.   Compatibility between the Agena Status Display Panel (Astronauts Panel) and the PPS

B.6 SUMMATION AND CONCLUSIONS

Design problems during development phases are to be expected in the evolution of the best possible system consistent with the present "state-of-the-art." These problems did occur, and some areas of concern developed during the PFRT; however, all were subsequently resolved by redesign effort and procedural change. A total design that best suited the GATV mission requirements resulted; this design maintained the original philosophy of close correlation with the existing Model 8096 engine system.

Appendix C

INSTRUMENTATION CHARACTERISTICS AND FAILURE MODE ANALYSIS

Appendix C
INSTRUMENTATION CHARACTERISTICS AND FAILURE MODE ANALYSIS

The instrumentation measurements carried aboard the GATV 5002 can be categorized as follows: 81 temperature, 33 pressure, 5 acceleration, 8 events, 1 turbine speed, 19 voltage and current, 2 vehicle destruct, and 33 miscellaneous measurements (such as position, rate, torque, attitude, signal level, PRF, etc.). The measurements of primary interest to this report are the failures, near failures, events occurring after T + 367.5 sec, and the measurements associated with the pressure anomaly. Figure C-1 presents a performance summary of these instrumentation measurements.

C.1 PRESSURE MEASUREMENTS

All pressure measurements on the GATV are made using transducers in which a mechanical displacement is transformed into an electric signal with a variable reluctance displacement-to-voltage converter. The carrier frequency is demodulated and suppressed, and a signal voltage is produced that is proportional to the applied pressure input. DC isolation between input and output circuits is obtained by transformer excitation and coupling. The output circuits have low impedance and fast recovery times. Use of junction resistors results in low noise and zero short-circuit instability — that is the input and output impedances will always be positive regardless of the circuit configuration.

Figure C-2 shows the pressure rise sequence on four selected transducers at, and immediately following, the activation of the engine firing sequence. This sequence is started by an electrical signal to the engine switch group (measurement B139).

Measurement B132, "Turbine Manifold Pressure No. 2," showed an increase to 120 psia, which is fullscale and normal, inasmuch as this transducer was especially selected to study start transients and could be safely overpressured. However, after approximately 1 sec, the output fell sharply and then gradually decreased until flight

C-1

MEASUREMENT	OPERATIONAL HISTORY
A152 SHEAR PANEL TEMP. NO. 3	1. Reading of +60°F until 367 sec. Cool to -8.3°F by 374 sec.
A153 SHEAR PANEL TEMP. NO. 4	2. Reading of approximately +60°F throughout flight.
A155 -Z AFT BULKHEAD TEMP.	3. Reading increases from +57°F to +64.8°F by 368 sec. Cools to +25°G by 373 sec.
A154 +Z AFT BULKHEAD TEMP.	4. Reading of +54°F until 368 sec. Cools to +37°F by 374 sec.
A522 ACCEL. "Y" NO. 2 (AFT) — LOCATED AT STA. 411.86 AT 270° (-Y SIDE OF VEHICLE)	5. Reading is normal until 306 sec; then reading goes to 0.00. Failure is attributed to excessive shock environment affecting the accelerometer or its amplifier located on aft rack near primacord.
B132 TURBINE MAN. PRESS. NO. 2	6. Transducer operates satisfactorily throughout flight.
A151 SHEAR PANEL TEMP. NO. 2	7. Reading of +60°F until 367 sec. Cools to +16°F by 374 sec.
A150 SHEAR PANEL TEMP. NO. 1	8. Reading of +60°F until 367 sec. Cools to -6.7°F by 374 sec.
B82 FUEL VALVE ACTUATION PRESS.	9. Measurement indicates normal operation until 368 sec; at this time the reading goes to full scale and remains there. Failure is attributed to excessive surge of pressure on element.
B6 COMB.	10. Measurement reads zero until time of engine burn. At this time a 30 ms pressure spike

C-2

Fig. C-1 Operational Performance Summary

Labels and boxes (left to right):

M71, M27, M93, M81, M21, M85 — C53P7, C53P6, C53P5

A50, A11, A13 — C53P16, C53P17, C53P22

M100, M36, M10, M125, M22, M86 — C53P5, C53P6, C53P7, C53P6

A73, A89 — C53P16, C53P17

C53P11, P450, C54P13

C53P20, P453, C54P10, C54P11

C53P11, P450, C54P13, C54P4

C4P1, C4P4, C4P2

T/C PWR SUP. — H63P2, H63P1

PRESS. NO. 1

B3 TURBINE MANIFOLD PRESS. NO. 1

B148 OX. INJECTOR PRESS.

B71 OX. PUMP LIP SEAL PRESS.

B141 OX. START TANK TEMP.

B142 FUEL START TANK TEMP.

A5 ACCEL. Z NO. 2 (AFT) — LOCATED AT STA. 411.86 AT 180° (+Z SIDE OF VEHICLE) AFT INST. J.BOX

B2 OX. PUMP INLET PRESS.

B1 FUEL PUMP INLET PRESS.

B139 ENGINE SWITCH GROUP — P6006

B184 NOZZLE EXT TEMP NO. 1

B185 NOZZLE EXT TEMP NO. 2

occurs. Transducer then becomes intermittent. Failure is attributed to excessive pressure surge on element.

11. Measurement read zero until +150 sec then drifts to 42 psig by 187 sec. Does not change at engine firing – should follow measurement B132. Reading indicates a failure in the electronics package of the transducer.

12. Measurement reads zero until 367 sec. Increases to 900 psi by 367.85 sec, then comes back to 100 psi at 368.8 sec. This probably indicates a zero offset of the pressure element caused by excessive pressure surge.

13. Measurement operates satisfactory throughout the flight.

14. Reading of +56°F until 367 sec. Cools to +23.4°F by 374 sec.

15. Reading of +56°F until 367 sec. Cools to +12.2°F by 374 sec.

16. Measurement operates normally until 306 sec, then goes to zero. Failure same as A522 (above).

17. MEASUREMENT INDICATES NORMAL OPERATION UNTIL 368 SEC. TRANSDUCER GOES TO FULL SCALE READING IN ONE SECOND AND REMAINS THERE. FAILURE IS INDICATED DUE TO PRESSURE SURGE OR STARTING SHOCK.

18. Measurement indicates normal operation throughout flight. Transducer goes slowly to full scale by 375 sec, but that was expected result of anomaly.

19. SEE q ON PAGE 3-23.

20. Measurement indicates normal operation. Reading increases during SPS firing, which is normal. Reading goes to full scale at 368 sec. Failure mode indicates an open thermocouple.

21. Measurement is normal throughout flight.

C-3

C-4 - BLANK PAGE
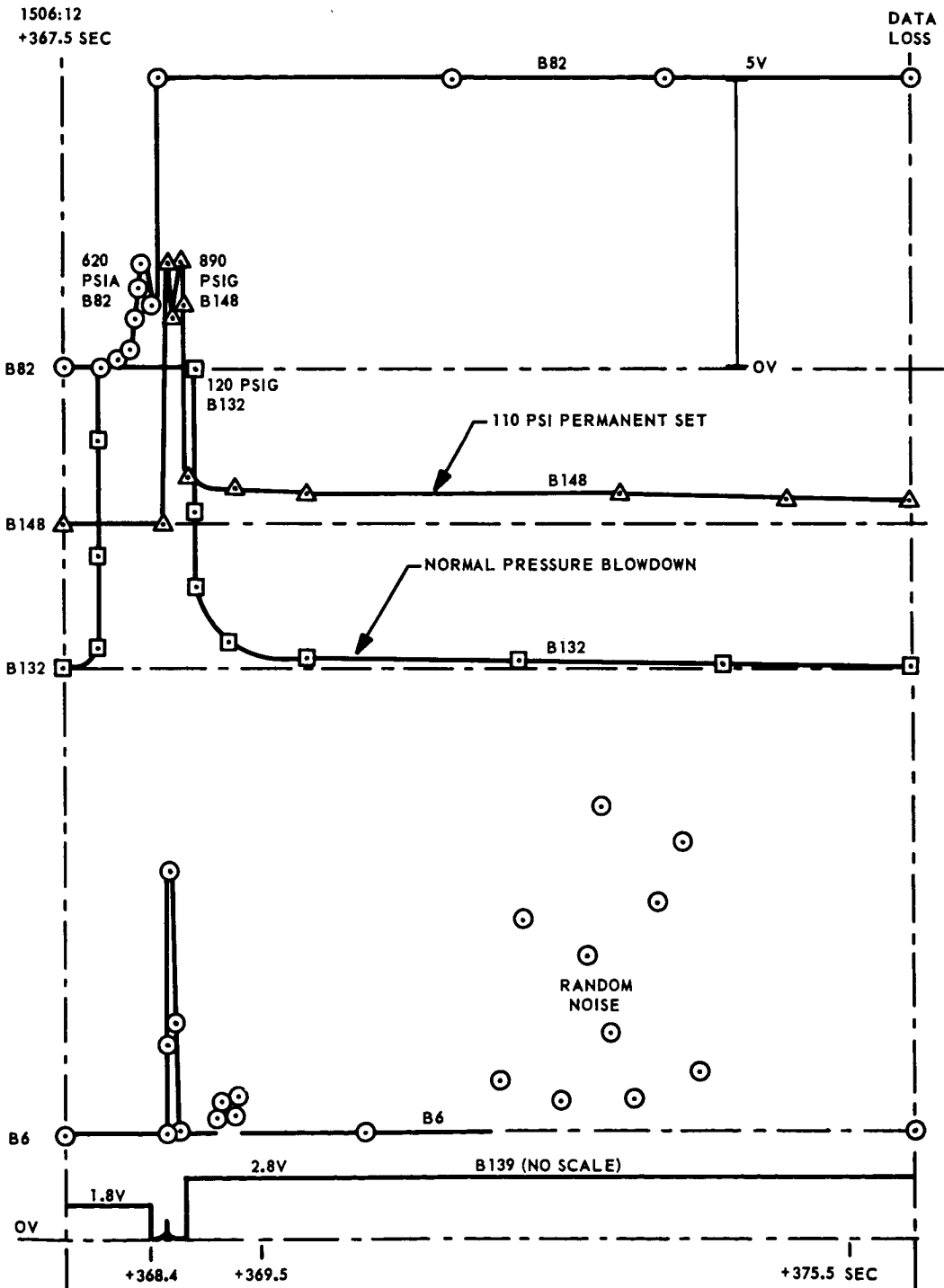
Fig. C-2 Gemini Pressures from Switch Group Actuation to Data Loss

termination. As a result of these data, it can be concluded that this transducer operated normally until flight termination.

Measurement B82, "Fuel Valve Actuation Pressure," indicated a rise to full scale in a few milliseconds and remained at full scale until flight termination. This failure mode, representing a level shift, indicates a distorted diaphragm.

Measurement B148, "Oxidizer Injector Pressure," rose to an indicated 890 psig pressure, fluctuated, and then fell off to a nonvarying value of about 100 psig, indicating that the transducer has undergone a level shift caused by bourdon tube damage.

Measurement B6, "Combustion Chamber Pressure No. 1," showed a steep rise and dropoff in the time vicinity of the anomaly and then exhibited a completely random output for a 2-sec period before flight termination, which could have resulted from a separation of the reluctance arm from the diaphragm or from a failure induced by a high-pressure pulse.

C.1.1 Operational Characteristics

On the average, 20 pressure transducers have been installed per Agena flight. During 168 flights, 78 pressure-transducer anomalies have occurred, or one per 43 transducers flown. Since the introduction of the standard Agena vehicle in 1962, there have been 24 malfunctions recorded during 87 flights, or one failure per 72.5 transducers flown.

In the present case, there were five anomalies in the 33 pressure transducers or one failure per 6.6 transducers flown, an unexpectedly high number.

A number of possible pressure-transducer failure modes are listed in Table C-1, and the mechanical arrangement of the Wiancko and Solid State Instruments pressure transducers are shown on Figs. C-3, C-4, and C-5. Some of the pertinent specifications are also shown on these sketches.

Table C-1

PRESSURE TRANSDUCER FAILURE MODES

Event	Relative Probability	Probable Indication	
		Wiancko	Solid State Instruments
Jammed Motion Transducer	Low	Steady Output	Steady Output
Blown Diaphragm or Tube	Low	Zero Output	Zero Output
Trapped Pressure	Low	Steady Output	Steady Output
Open Transducer Bridge Arm	Low	Steady > Full Scale Output	Steady > Full Scale Output
100-kc Oscillator Failure	High	Zero Output	Zero Output
DC Input Power Failure	High	Zero Output	Zero Output
Shorted Input Signal Path	High	Zero Output	Zero Output
Open Input Signal Path	High	Zero Output	Zero Output
Open Output Current Path	High	Zero Output	Zero Output
Shorted Output Current Path	High	Zero Output	Zero Output
Shorted Input/Output Current Path	Medium	Varying Output	Varying Output
Open Output Diode(s)	High	Exp. Decreasing Output	Exp. Decreasing Output
Shorted Output Diode(s)	High	Low Level AC Output	Low Level AC Output
Distorted Bourdon Tube/Diaphragm	High	Level Shift	Level Shift
Open AC Amp Feedback Loop	High	Not Applicable	High Output, Unstable
Component Value Change	Medium	None (Calibration Off)	None (Calibration Off)

Pertinent Transducer Specifications

Pressure Integrity*: 5000 psi Max Case Integrity; 1000% or 12,000 psi Diaphragm

Pressure Overload: 150% of Full-Scale Range

Acceptance and Qualification Test: LMSC Specification 1414678

*Psia only.

SECOND "E" CORE AND COIL SET
NOT USED ON GEMINI

ARMATURE

40G VIBRATION
WITHOUT DAMAGE
50G ACCELERATION

MAX. DIFF PRESSURE
WITHOUT DAMAGE
150% OF RANGE

ELECTRICAL COIL

MAX. CASE PRESSURE
WITH PORT CLOSED
3000 PSI (B148)

MAGNETIC "E" CORE

PRESSURE ELEMENT

PRESSURE INLET

NO SCALE

CROSSED WIRE FLEXURES

RESPONSE:

db	cps
0	40
-1	80
-2	100
-3	130
-6	160

RIGID JOINT

RANGE: ALL PRESSURE MEASUREMENTS
OTHER THAN B6 & B82

WIRE FLEXURE INSTALLATION

NOTE: ELECTRONIC PACKAGE NOT SHOWN

Fig. C-3 Pressure Sensor Assembly P2-3090 (Wiancko Engineering)

C-8

VARIABLE RELUCTANCE
OUTPUT TO ELECTRONICS

DUROCK HERMETIC SEALS

TYPE 347 SS
DIAPHRAGM
1,000% FS
OVERLOAD
OR 12,000 PSI

TYPE 347 SS
MIN BURST 5000 PSI

HELIARC WELD (TYP)

TYPE 347 SS

TYPE 347 SS
VACUUM SEAL-OFF

SCALE APPROX. 4:1

REMOVABLE PRESSURE PLUG
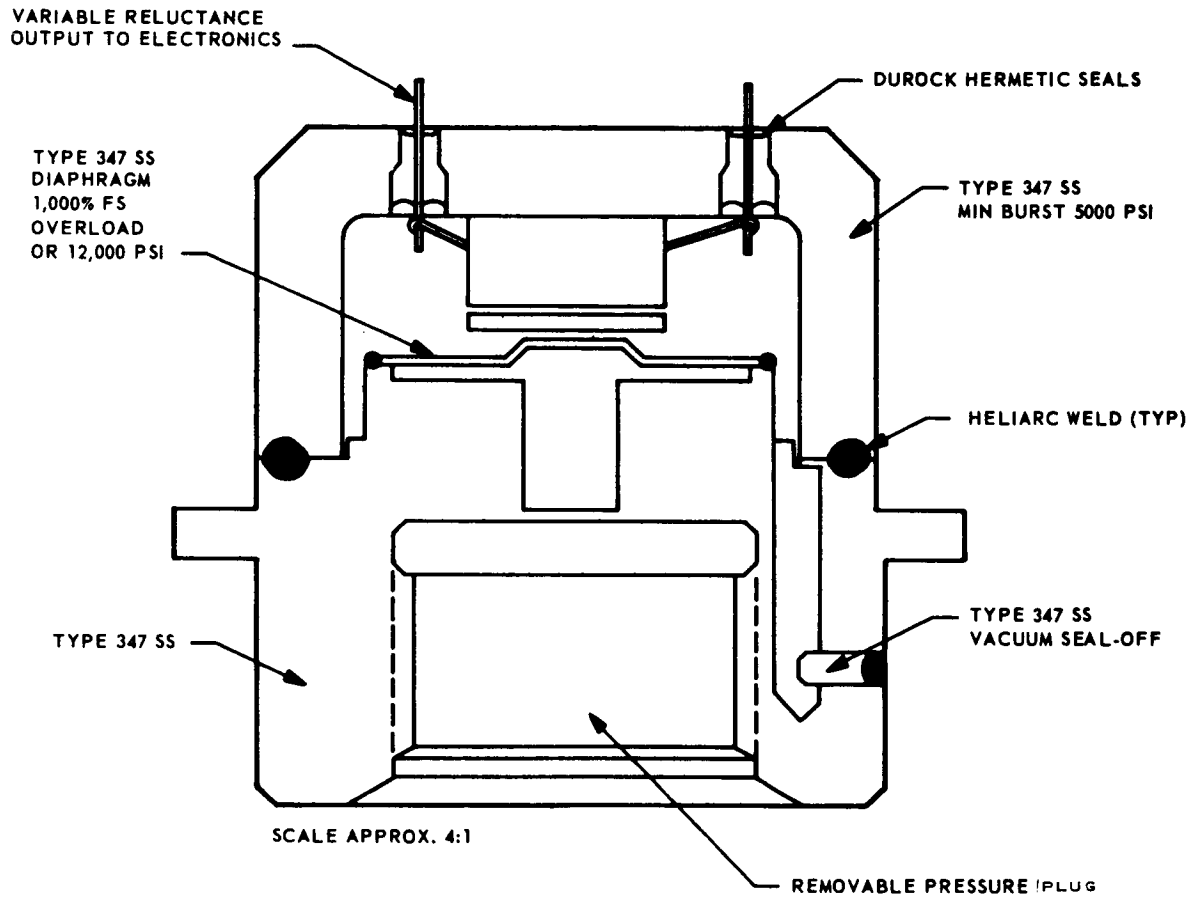
RESPONSE: RISE TIME, 1 MS 10% TO 90%
OVERSHOOT, 10% MAX
ROLLOFF, 40 DB/DECADE (-3 DB AT 350 CPS)

RANGE: B6 (COMBUSTION CHAMBER PRESSURE) 0 – 700 PSIA
B82 (FUEL VALVE ACTUATION PRESSURE) 0 – 1500 PSIA

NOTE: ELECTRONIC PACKAGE (POTTED) NOT SHOWN

Fig. C-4 Pressure Sensor Assembly P-102C (Solid State Instruments)

C-9

1366073-501 TUBE ASSY

1616164-7 TRANSDUCER
B148 OX. INJECTOR PRESSURE
WIANCKO ENGINEERING CO.

COMBUSTION CHAMBER

INJECTOR HEAD

GAS GENERATOR

FUEL VALVE

1616567-357 TRANSDUCER
B6 COMB. CHAMBER
PRESSURE NO. 1 SOLID
STATE INSTRUMENTS, INC.

1616567-25 TRANSDUCER
B82 FUEL VALVE ACTUATION PRESS.
SOLID STATE INSTRUMENTS, INC.

1366073-505 TRANSDUCER
B91 COMB. CHAMBER PRESSURE
NO. 3 (LOCATION REF ONLY
TRANSDUCER DID NOT FAIL)

Fig. C-5 Location of Failed Transducers

C.1.2 Postflight Testing

Due to the nature of the data from measurement B82, "Fuel Valve Actuation
Pressure," it was suspected that the transducer might have failed mechanically,
releasing propellants into the aft engine rack area. A test on this transducer
was accordingly conducted.

The objective was to subject the B82 pressure transducer (P/N 1616567-41,
S/N 1130) to shock tests incrementally from 35 g to 100 g while pressurized
with hydraulic fluid to 1000 psig. The tests were performed to determine struc-
tural adequacy of the unit. All shocks were normal to the longitudinal axis of the
pressure transducer.

The duration of all shock pulses from 35 g to 100 g in 5 g increments was from
1.4 to 2 ms, and the pulse approximated a half-sinewave. Photographs were
taken of each shock. A permanent Sanborn record was made of the transducer

LOCKHEED MISSILES & SPACE COMPANY

output with hydraulic pressure applied to the transducer during the shock tests. There was no evidence of damage or malfunction of the test specimen as a result of the shock tests.

C.2 TEMPERATURE MEASUREMENTS

Temperature measurements on the GATV are made with four, well known, basic transducer types: thermocouples, resistance thermometers, thermistors, and semi-conductors. Associated with these transducers are standard excitation and output signal conditioning circuits. Pertinent specifications for these devices are listed in Table C-2, and possible failure modes in Table C-3.

Figures C-6 and C-7 present circuitry for signal conditioning and thermocouple circuitry. Figure C-8 is a curve relating temperature and time for measurement B184, "Nozzle Extension Skin Temperature No. 1."

Table C-2

THERMOMETER SPECIFICATIONS

Thermocouple

Specifications

Range:	$-200^{\circ}F$ to $+2800^{\circ}F$
Sensor:	Chromel-alumel, platinum +13% rh
Reference Temperature:	$-200^{\circ}F$, $-100^{\circ}F$, $32^{\circ}F$
Reference:	Modified bridge
Acceptance Test Specification:	LMSC-6117B

Manufacturer

Consolidated Ohmic Devices Inc., BAC-472100

LMSC-1618747

BAC-477110

LOCKHEED MISSILES & SPACE COMPANY

Table C-2 (Cont.)

Resistance Thermometer

Specifications

Range:	-50°F to +1000°F
Sensor:	Platinum wire
Calibration:	13 points over the range -200°F to +1000°F
Self-heating:	No accuracy degradation to 15 ma operating current. Normal operating current approximately 5 ma
Acceptance Test Specification:	LMSC-6117B

Manufacturer

Transonics, Inc., LMSC-1062939

Thermistor

Specifications

Range:	-15°F to +350°F
Sensor:	Fenwall GB32M92-D thermistor (probe) Fenwall G815, G828, K134, K135 (surface)
Base Resistance:	2000 ohms ±2% at 77°F
Acceptance Test Specification:	LMSC-6117B

Manufacturer

Fenwall, LMSC-1618702 (surface)

LMSC-1461855 (probe)

LMSC-1062960 (probe)

Semiconductor

Specifications

Range:	-100°F to +500°F
Sensor:	Microsystems 103003-0002

C-12

Table C-2 (Cont.)

Semiconductor

Specifications (Cont.)

Base Resistance: 2000 ohms ±2% at 78°F

Acceptance Test Specifications: LMSC-6117B

Manufacturer

Microsystems, Inc., LMSC-1616310

Table C-3

POSSIBLE FAILURE MODES (THERMOMETERS)

Event	Relative Probability	Probable Indication
Bridge Open Circuit	High	Zero to Full Scale
Bridge Short Circuit	Low	Zero
Power Supply Open/Short Circuit	Medium	Zero
Thermocouple Wire Open Circuit	Medium	Zero
Thermocouple Wire Loose	Medium	Random Output
Differential Amplifier Open Circuit	Low	Full Scale
Resistance Wire Open	High	Full Scale
Signal Conditioning Open/Short Circuit	Low	Zero to Full Scale

SIGNAL CONDITIONING CIRCUIT
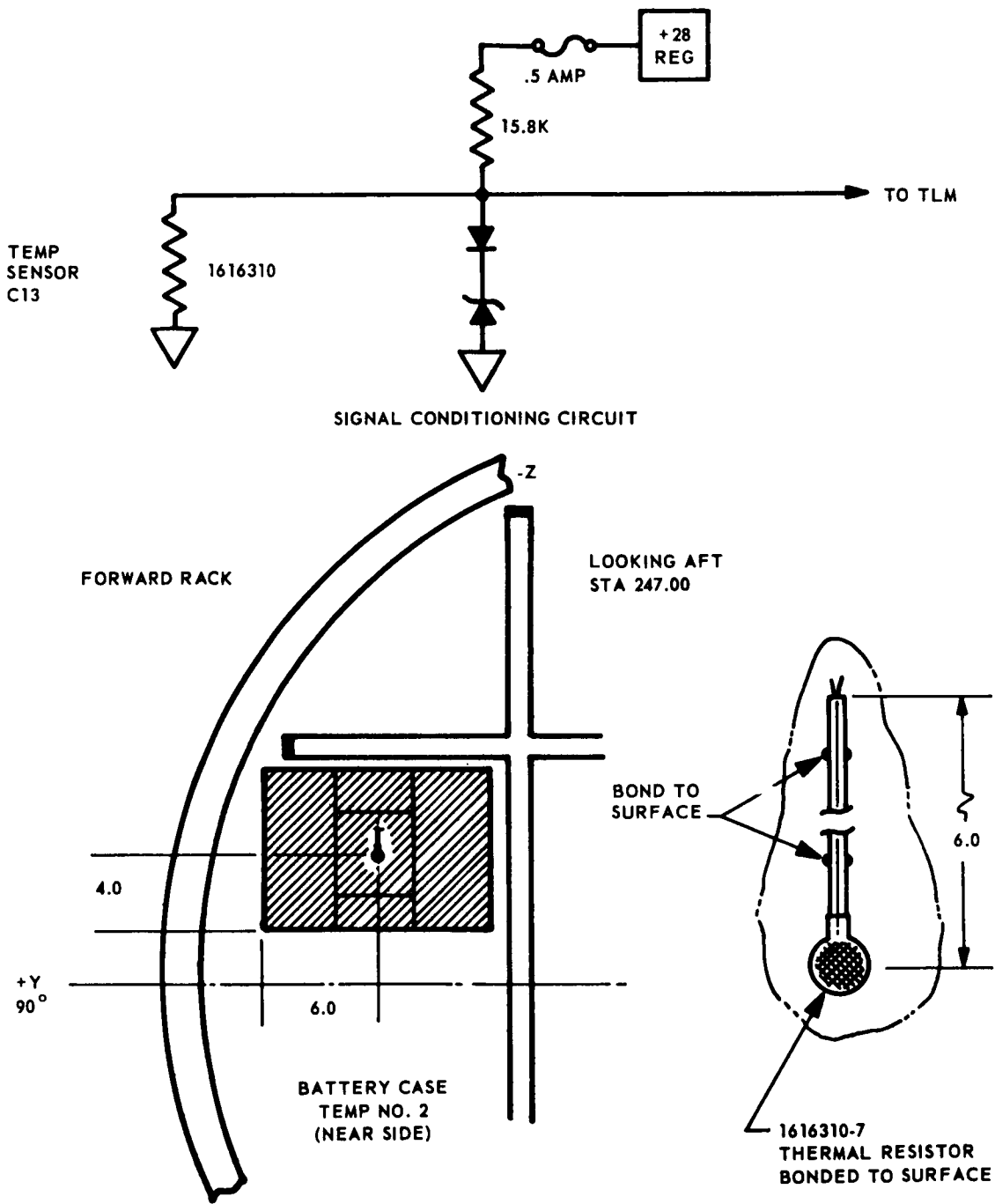
Fig. C-6 Signal Conditioning Circuit

C-14

TO TLM ← [DIFF AMPL] ── [POWER-SUPPLY] ┈ [ ] / [BRIDGE CIRCUIT] ──── ✕ THERMOCOUPLE JUNCTION

THERMOCOUPLE SYSTEM

TO BRIDGE CIRCUIT ←

TC JCT

MEAS. NO. B184 (FAR SIDE)

Ⓧ

STA 494.0
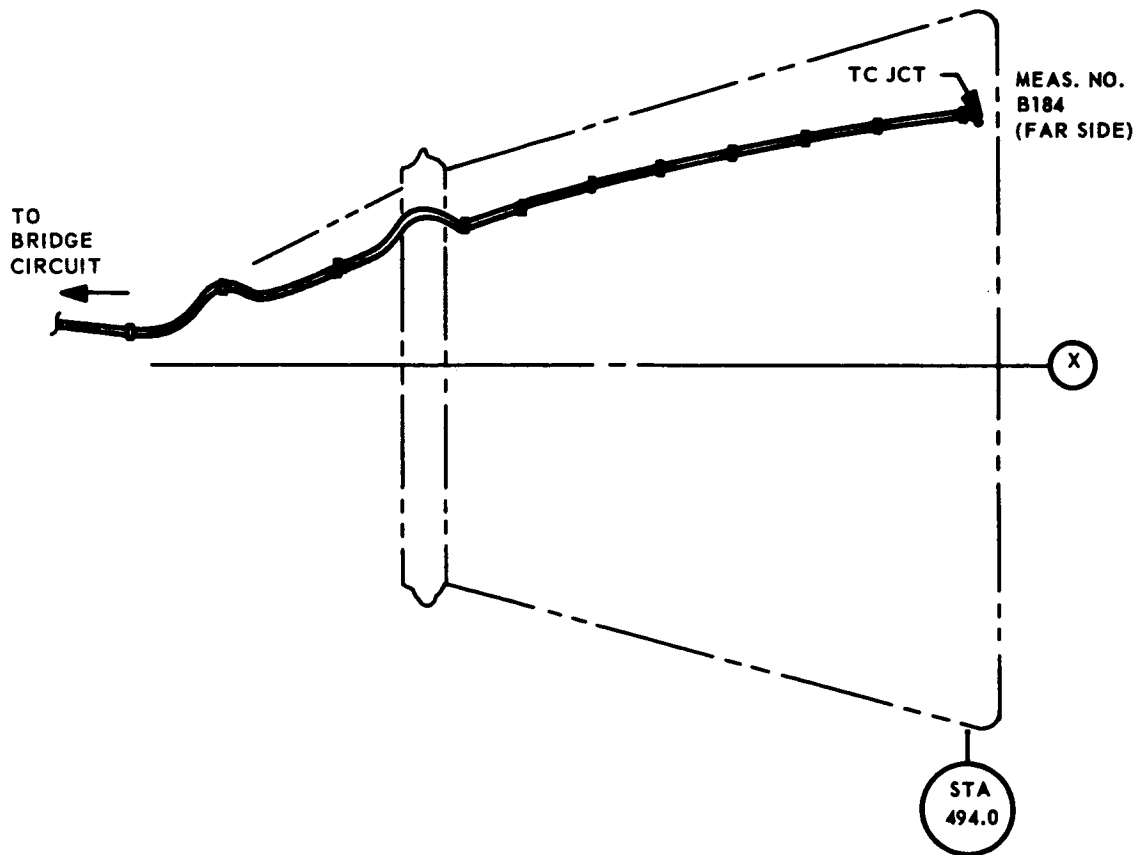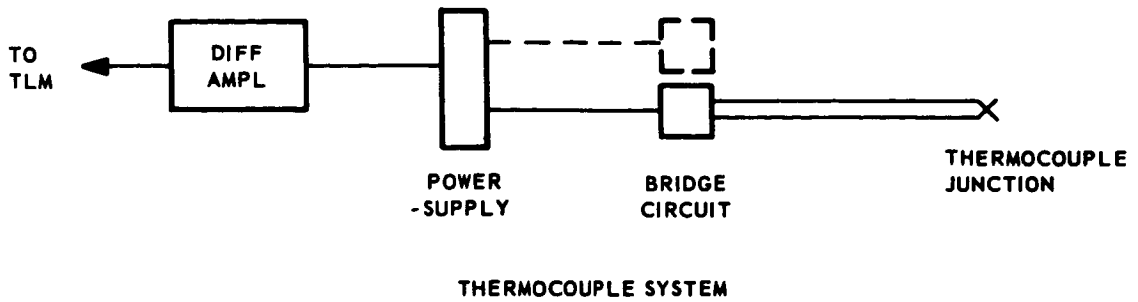
Fig. C-7 Thermocouple System

C-15
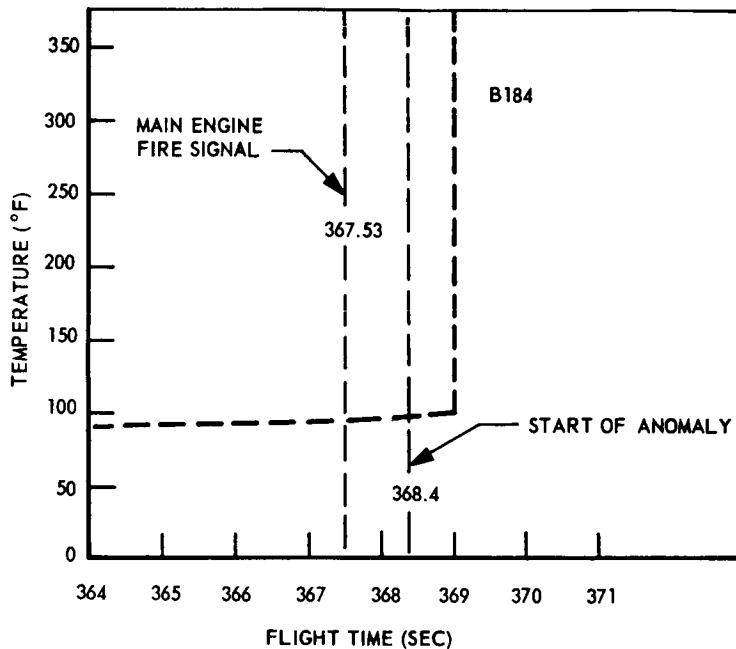
Fig. C-8 Nozzle Extension Temperature No. 1

Measurement C13, "Battery Case Temperature No. 2," indicated abnormal temperature prior to liftoff. The transducer may have been damaged when the battery was installed.

Measurement B184, "Nozzle Extension Skin Temperature No. 1," showed normal temperature up to +369.2 sec, and then the output rose to full scale in 1 sec and remained at full scale to flight termination. This abnormal behavior is attributed to a possible open thermocouple wire.

Temperature sensors have exhibited an extremely low failure rate during Agena flights. More than 4000 have been flown, with the few failures occurring being conclusively connected with poor installation practice or improper handling.

C.3 ACCELERATION MEASUREMENTS

All acceleration measurements on the GATV are made with standard unbonded strain gage accelerometers and amplifier systems. For convenience the measurement numbers, technical specifications and failure modes of five GATV acceleration measurements are listed in Table C-4. Physical locations of these transducers are shown in Fig. C-9 and C-10.

Table C-4

ACCELEROMETER CHARACTERISTICS

MEASUREMENT NUMBERS	
A522 Accel Y No. 2 (Aft)	±1.5 g
A4 Accel Y No. 1 (TDA)	±1.5 g
A5 Accel Z No. 2 (Aft)	±1.5 g
A523 Accel Z No. 1 (TDA)	±1.5 g
A9 Accel X No. 1 (TDA)	±3.0 g

TECHNICAL SPECIFICATION	
Vendor	Statham Instrument Company
Vendor Type Accel	A69TC Amp CA17
LMSC P/N 1354540	
Range	±1.5 g to ±3.0 g
Frequency Response	150 cps
Maximum Shock (System)	55 g at 9 ms/200 g at 1 ms
Temperature Limit	-40°F to $+200^{\circ}$F

FAILURE MODES		
Event	Relative Probability	Probable Indication
Amplifier Internal Open/Short	High/Medium	Zero to Full Scale
Connector Short		
+28v dc to Output	Low	Full Scale
Output to Ground	Low	Zero
+28v dc to Ground	Low	Zero
Transducer Bridge Open/Short	High/Low	Zero/Zero to Full Scale
Excitation Open	Medium	Random

C-17
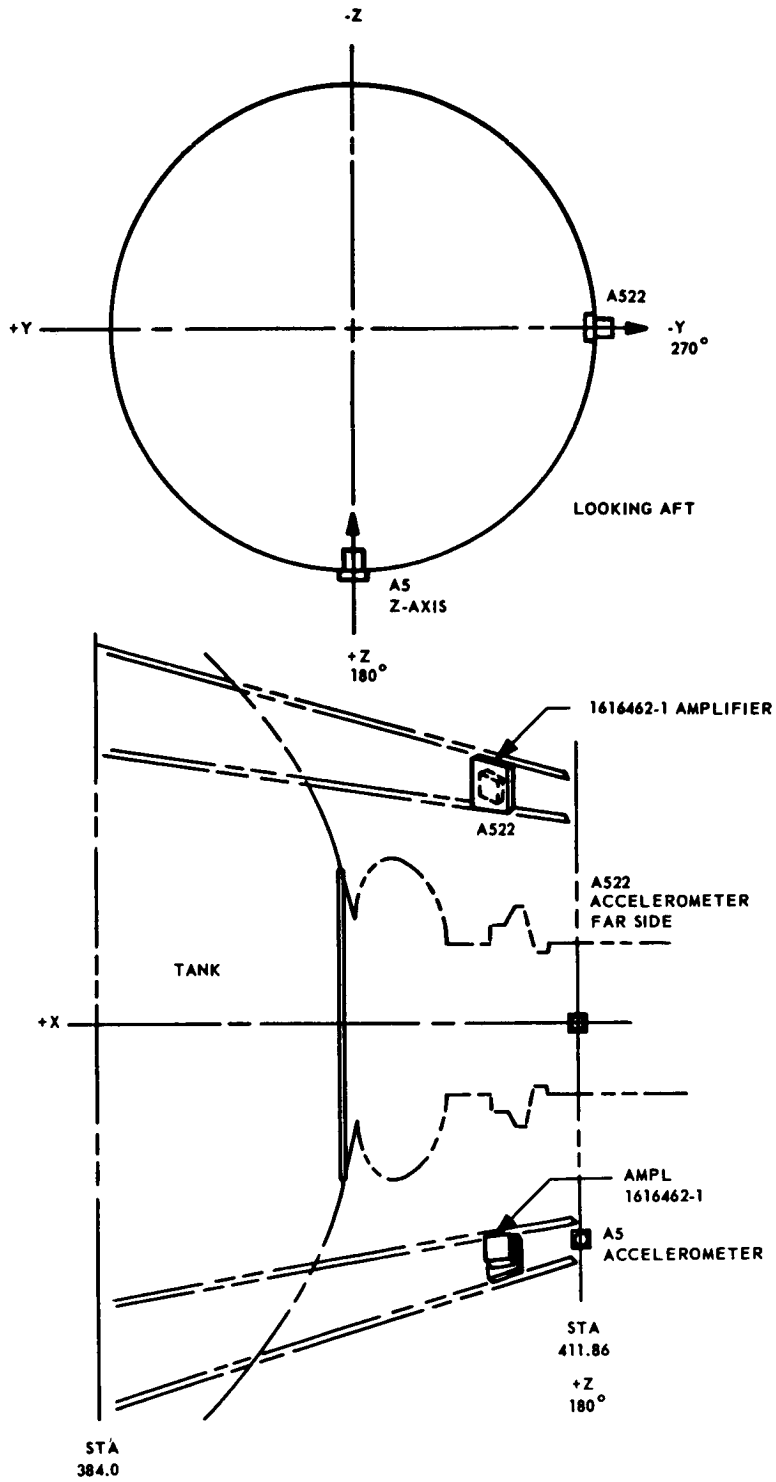
Fig. C-9 Accelerometers (Aft)
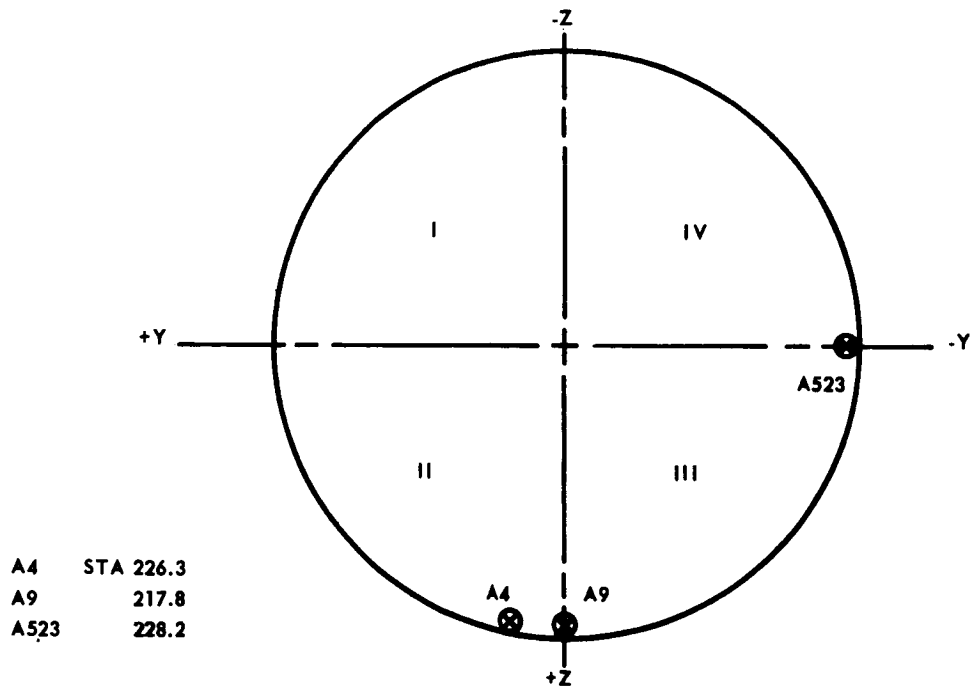
Fig. C-10 Accelerometers (TDA)

The unbonded-type strain gage acceleration transducer operates on the mass and spring principle. When the case is displaced, relative movement between the mass and case is produced; this is sensed by strain-sensitive wires supporting the mass. The strain-sensitive wires are a part of an electrical bridge circuit, and the resulting output is amplified. Typically, such a transducer will utilize a suspended mass on the order of 0.05 oz, which will move distances on the order of ±.0025 in. during a ±10 g displacement. The Statham A69TC accelerometer is oil-damped at approximately 0.7 of critical at 78°F. Output is approximately ±20 mv.

The Statham Type CA17 amplifier is a small (4.25 oz) transistorized strain-gage signal amplifier used to excite and amplify the output of the accelerometer. It contains an oscillator, amplifier, and demodulator. Output is 0 to 5v dc. A special 4-ft cable is provided to connect the amplifier to the accelerometer.

C-19

"Acceleration Z-Axis No. 2 (Aft)," measurement A5 (±1.5 g), functioned normally until T + 306.22 sec; then the output signal dropped to zero, indicating failure of the transducer. Separation primacord squibs were fired at this time, and it is believed the shock level created exceeded the maximum level of the transducer or amplifier.

"Acceleration Y-Axis No. 2 (Aft)," measurement A522 (±1.5 g), experienced the anomaly that occurred in conjunction with the primacord firing. It is analyzed the same as for measurement A5, above.

"Acceleration Z-Axis No. 1 (TDA)," measurement A523 (±1.5 g), provided an intermittent output during the following times: from T + 83 sec to T + 99.5 sec and from T + 261 sec to T + 306.22 sec. Operation at other than the intermittent periods was satisfactory. This anomaly is attributed to a loose or broken wire to the accelerometer or amplifier.

Accelerometers fall into the same category as pressure transducers in that the flight history establishes a confidence factor above the norm. Over 519 accelerometers have been flown (Polaris program not counted) with a total of 10 failures.

C.4 ATLAS/AGENA SEPARATION MONITOR MEASUREMENT

A14, the "Atlas/Agena Separation Monitor," measurement indicated excessive voltage increase, about 3.5v instead of the 1.25v normally expected, during the first closure of the microswitch. The second closure occurred about 0.75 sec after the first closure, giving a separation rate of 40 in./sec. The voltage increased beyond the 5v telemetry input limit during the second closure of the microswitch. The third closure of the microswitch was not observed on the telemeter because the voltage had increased above 5v during the second closure of the microswitch.

The Atlas/Agena separation monitor was tested during vehicle system testing and the data indicated normal operation; i.e., the voltage increased 0.81v, 1.79v, and 2.44v with first, second, and third closure of the microswitch respectively.
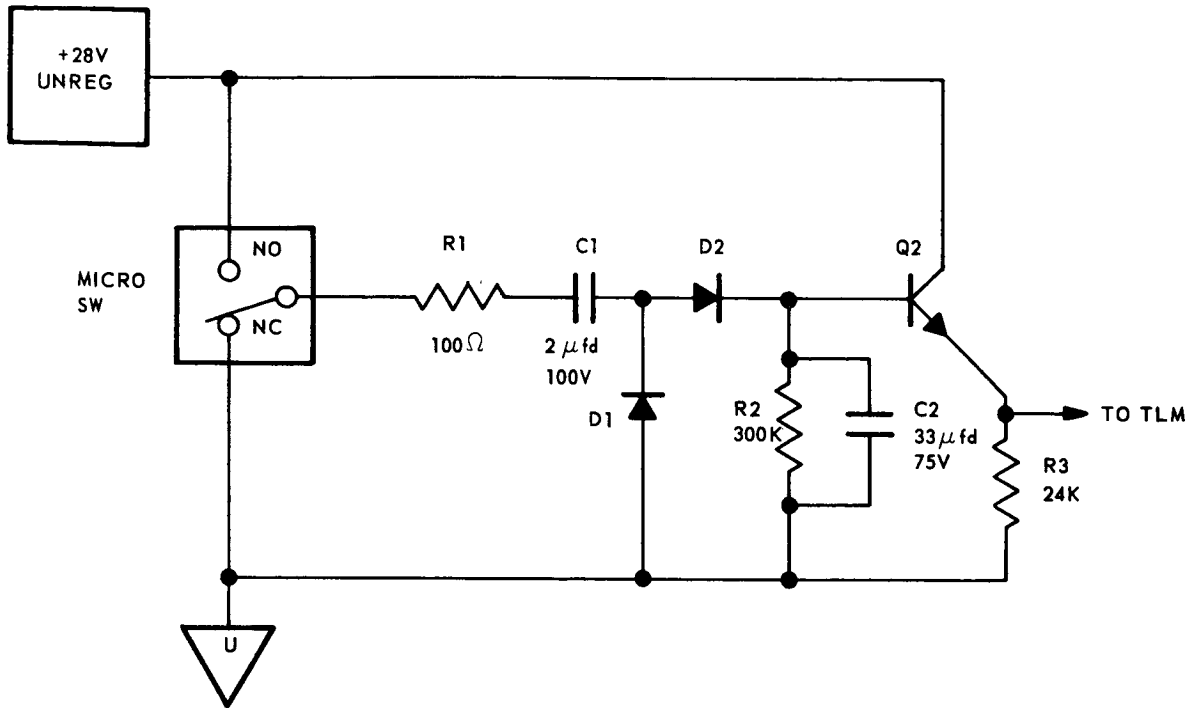
Fig. C-11 Schematic of Atlas/Agena Separation Monitor

Fig. C-11 shows the schematic diagram of the Atlas/Agena separation monitor. During normal operation, capacitor C_2 is charged to about 1.2v, 2.4v, and 3.6v during the first, second, and the third closure of the microswitch, respectively. The flight data for Vehicle 5002 show that capacitor C_2 charged to about 3.5v during the first closure and above 5v during the second and third closures of the microswitch. The cause of this excessive voltage is suspected to be leakage of capacitor C_1. If capacitor C_1 is leaking, capacitor C_2 will accumulate a larger charge, hence a larger voltage during the time the microswitch is closed. This hypothesized failure of capacitor C_1 is random in nature and could be caused by the following:

a. A manufacturing defect that, with aging, might have caused a failure.

b. Diode D_1 might have shorted out, causing voltage on the order of 2v to 3v to be applied to tantalum capacitor C_1 in the reverse direction. Repeated application of this reverse voltage during testing might have caused the capacitor failure. However, as stated before, the separation circuitry operated satisfactorily during vehicle system tests.

Appendix D

TELEMETRY INSTRUMENTATION SCHEDULE

Appendix D

TELEMETRY INSTRUMENTATION SCHEDULE

This appendix presents the Vehicle 5002 instrumentation schedule, as follows:

    a.   Multiplexer Main Frame, 128 Channels (Table D-1)

    b.   Multiplexer Subframe A, 128 Channels (Table D-2)

    c.   Multiplexer Subframe C, 16 Channels (Table D-3)

    d.   Command Function Status Monitor, Subframe C (Table D-4)

Only data required to interpret flight results are included: the channel number, the measurement name, the measurement number, the sampling rate, and the transducer range. Ground checkout and Atlas instrumentation and multiplexer matrices are not included.

The complete GATV 5002 instrumentation is presented in LMSC-1352266, Telemeter System Instrumentation Schedule, Model 37205, Vehicle 5002.

Table D-1

INSTRUMENTATION SCHEDULE, MULTIPLEXER MAIN FRAME

Channel No.	Measurement		Sampling Rate	Transducer Range
	Name	No.		
1	Sync	NA		
2	Sync	NA		
3	Sync	NA		
4	Message Acceptance Pulse	H38	48	0−5v
5	Combustion Chamber Pressure No. 1	B6	96	0−700 psia
6	Accelerometer Z No. 1 (TDA)	A523	32	±1.5 g
7	28v dc Unregulated Supply	C1	16	0−30v dc
8	Gas Jet No. 1 and No. 3 Monitor	D151	48	0−5v
9	Units I and II Pilot Solenoid -Y On Off	B225	16	0−5v
10	Oxidizer Pump Inlet Pressure	B2	16	0−100 psig
11	+Y and -Y Start Valve (SPS) On Off	B223	16	0−5v
12	Combustion Chamber Pressure No. 3	B91	16	475−550 psig
13	Accelerometer X No. 1 (TDA)	A9	64	±3.0 g
14	Fuel Tank Pressure	B9	16	0−60 psig
15	Gas Jet No. 2 and No. 5 Monitor	D150	48	0−5v
16	Subframe A	NA		
17	Subframe B	H32	−	Programmer
18	Subframe B	H32	−	Memory
19	Subframe B	H32	−	Readout
20	Accelerometer Y No. 1 (TDA)	A4	32	±1.5 g
21	Oxidizer Injector Pressure	B148	32	1000 psig
22	8247 Engine Switch Group	B139	32	0−5v
23	Fuel Valve Actuation Pressure	B82	32	0−1500 psia
24				
25	Oxidizer Venturi Inlet Pressure	B11	16	0−1500 psia
26	Pitch Hydraulic Actuator Position	D68	16	±2.5 deg
27	Repeat No. 5	B6	96	
28	Roll Horizon Sensor Output	D42	16	±5.0 deg

D-2

Table D-1 (Cont.)

Channel No.	Measurement		Sampling Rate	Transducer Range
	Name	No.		
29				
30	Gas Jet No. 4 and No. 6 Monitor	D152	48	0−5v
31	Hydraulic Oil High Pressure	D60	16	0−4000 psig
32	Subframe A	NA		
33	Control Gas Regulator Pressure No. 1	D58	16	0−125 psia
34	Accelerometer Y No. 2 (Aft)	A522	32	±1.5 g
35	Control Gas Supply Manifold Pressure	D59	16	0−4000 psia
36	Accelerometer Z No. 2 (Aft)	A5	32	±1.5 g
37	Unit I, +Y Chamber Pressure	B212	32	0−100 psig
38	Control Gas Supply Temperature	D70	16	−50°, +200° F
39	Unit II, +Y Chamber Pressure	B214	32	0−120 psig
40	Propellant Iso V On Off	B130	32	0−5v
41	Cal +	NA		4.9v
42	Yaw Hydraulic Actuator Position	D69	16	±2.5 deg
43	Pitch Horizon Sensor Output	D41	16	±5.0 deg
44	Oxidizer Tank Pressure	B8	16	0−60 psig
45	Repeat No. 13	A9	64	±3.0 g
46	Turbine Manifold Pressure No. 2	B132	32	0−120 psia
47	Repeat No. 4	H38	48	0−5v
48	Subframe A	NA		
49	Repeat No. 5	B6	96	
50	Repeat No. 8	D151	48	
51	+Y Oxidizer Feed Pressure	B204	16	0−300 psig
52	Units I and II Pilot Solenoid +Y On Off	B224	16	0−5v
53	Unit I, −Y Chamber Pressure	B213	32	0−100 psig
54	Velocity Meter Cutoff	D86	32	0−5v
55	Unit II, −Y Chamber Pressure	B215	32	0−120 psig
56	Nose Cone Separation Monitor	A52	16	0−5v
57	Repeat No. 15	D150	48	

Table D-1 (Cont.)

Channel No.	Measurement Name	No.	Sampling Rate	Transducer Range
58	Hydraulic Oil Low Pressure	D32	16	0 − 100 psig
59				
60	-Y Fuel Feed Pressure	B209	16	0 − 300 psig
61	Yaw Position Gyro	D74	16	.5v/deg
62	Fuel Venturi Inlet Pressure	B12	16	0 − 1500 psia
63				
64	Subframe A	NA		
65	He Supply Pressure	B7	16	0 − 4000 psia
66	Amp Hour Meter 10-30	C130	16	0 − 5v
67	+Y Fuel Feed Pressure	B208	16	0 − 300 psig
68	Amp Hour Meter 40-120	C131	16	0 − 5v
69	Control Gas Regulated Pressure No. 2	D57	16	0 − 20 psig
70	Repeat No. 6	A523	32	
71	Repeat No. 5	B6	96	
72	Repeat No. 30	D152	48	
73				
74	Aft Compartment Pressure	A21	16	0 − 15 psia
75				
76	Pitch Position Gyro	D72	16	.5v/deg
77	Repeat No. 13	A9	64	
78				
79	Hydraulic Oil Return Line Temperature	D5	16	0°, 250° F
80	Subframe A	NA		
81	Turbine Manifold Pressure No. 1	B3	16	0 − 750 psig
82	Amp Hour Meter 160-480	C132	16	0 − 5v
83	-Y Oxidizer Feed Pressure	B205	16	0 − 300 psig
84	Repeat No. 20	A4	32	
85	Repeat No. 21	B148	32	
86	Repeat No. 22	B139	32	
87	Repeat No. 23	B82	32	

Table D-1 (Cont.)

Channel No.	Measurement Name	No.	Sampling Rate	Transducer Range
88				
89	Tank Manifold Pressure +Y	B202	16	0−300 psig
90	Repeat No. 4	H38	48	0−5v
91	Yaw Gyro Torque Rate	D65	16	.23v/deg/min
92	Repeat No. 8	D151	48	
93	Repeat No. 5	B6	96	
94	Roll Gyro Torque Rate	D66	16	.25v/deg/min
95				
96	Subframe A	NA		
97	+Y SPS Gas Sphere Pressure	B200	16	0−4500 psia
98	Repeat No. 34	A522	32	
99	Repeat No. 15	D150	48	
100	Repeat No. 36	A5	32	
101	Repeat No. 37	B212	32	
102	Pitch Gyro Torque Rate	D73	16	.23v/deg/min
103	Repeat No. 39	B214	32	
104	Repeat No. 40	B130	32	
105	Tank Manifold Pressure −Y	B203	16	0−300 psig
106				
107	Booster Command Monitor	D37	16	0−5v
108	Cal Z	NA		0.00v
109	Repeat No. 13	A9	64	
110	Repeat No. 46	B132	32	
111				
112	Subframe A	NA		
113	−Y SPS Gas Sphere Pressure	B201	16	0−4500 psia
114	Repeat No. 30	D152	48	
115	Repeat No. 5	B6	96	
116	Roll Position Gyro	D75	16	

Table D-1 (Cont.)

Channel No.	Measurement Name	No.	Sampling Rate	Transducer Range
117	Repeat No. 53	B213	32	
118	Repeat No. 54	D86	32	
119	Repeat No. 55	B215	32	
120	A/A Separation Monitor	A14	16	0−5v
121	Forward Computer Pressure	A20	16	0−15 psia
122				
123				
124	Subframe C	NA		
125	Fuel Pump Inlet Pressure	B1	16	0−100 psig
126				
127				
128	Subframe A	NA		

Table D-2

INSTRUMENTATION SCHEDULE, MULTIPLEXER SUBFRAME A

Channel No.	Measurement		Sampling Rate	Transducer Range
	Name	No.		
1	Horizon Sensor Fairing Temperature	A210	1	32°, 600° F
2	+Y Fuel Tank Temperature	B271	1	-50°, +150° F
3	+Z Aft Bulkhead Temperature	A154	1	-30°, +250° F
4	28v dc Unregulated Current	C4	1	0 − 100 A
5	Shear Panel Temperature No. 1	A150	1	-10°, ±120° F
6				
7	+Y SPS Module Bulkhead Temperature	A156	1	-20°, +300° F
8	Fuel Feed Line Temperature Unit II +Y	B267	1	-50°, +150° F
9	Docking Adapter Temperature No. 1	A388	1	-100°, +500° F
10				
11	Oxidizer Start Tank Temperature	B141	1	-10°, +150° F
12	Pyro Buss Volt Monitor	C141	1	0 − 30v dc
13	Fuel Start Tank Temperature	B142	1	-10°, +150° F
14	SMRDD Monitor	D183	1	Correct = 2 ± .8v Incorrect = 4.7 ± .5v
15	Structure Current Monitor	C38	1	0 − 50 A
16	S-Band Input PRF Monitor	H47	1	0°, 1600 pps
17	-Y Fuel Tank Temperature	B273	1	-50°, +150° F
18	-Z Aft Bulkhead Temperature	A155	1	30°, +250° F
19	+28v dc Regulated Power Supply No. 1	C3	1	0 − 30v dc
20	Docking Adapter Temperature No. 5	A392	1	-100°, +500° F
21	Shear Panel Temperature No. 2	A151	1	-10°, +120° F
22				
23	-Y SPS Module Bulkhead Temperature	A157	1	-20°, +300° F
24				
25	-28v dc Regulated Power Supply No. 1	C5	1	0 − 30v dc

Table D-2 (Cont.)

Channel No.	Measurement		Sampling Rate	Transducer Range
	Name	No.		
26	Docking Adapter Temperature No. 2	A389	1	-100°, +500° F
27	He Sphere Temperature	B68	1	0°, +120° F
28	400 cps 3ϕ Inverter (PH CB)	C32	1	0, 130v ac
29	Thrust Chamber Skin Temperature	B83	1	-50°, +150° F
30	Horizon Sensor Temperature (R H)	D54	1	-50°, +200° F
31	Oxidizer Feed Line Temperature Unit I +Y	B260	1	-50°, +150° F
32	S-band Output PRF Monitor	H48	1	0°, 1600 pps
33	Shroud Temperature No. 1 (MT-401)	AD40	1	0°, +450° F
34	400 cps 3ϕ Inverter (PH AB)	C31	1	0 − 130v ac
35	Oxidizer Pump Inlet Temperature	B32	1	0°, +100° F
36	IRP Internal Case Temperature	D129	1	-50°, +155° F
37	Shear Panel Temperature No. 3	A152	1	-10°, +120° F
38	Docking Adapter Temperature No. 6	A393	1	-100°, +500° F
39	+Y Module Radiation Shield Temperature	A158	1	-100°, +200° F
40				
41	Docking Adapter Skin Temperature No. 3	A390	1	-100°, +500° F
42	Velocity Meter Accelerometer Oven Temperature	D87	1	0°, +185° F
43	+Y N_2 Sphere Temperature	B216	1	-50°, +150° F
44	UHF Phase Lock Monitor	H171	1	0 − 5v
45	-Y N_2 Sphere Temperature	B253	1	-50°, +150° F
46	Horizon Sensor Temperature (LH)	D55	1	-50°, +200° F
47	+Y Oxidizer Tank Temperature	B270	1	-50°, +150° F
48	S-Band Transponder Temperature	H49	1	-40°, +167° F
49	Shroud Temperature No. 2 (MT-402)	AD41	1	0°, +450° F
50	Oxidizer Lipseal Pressure	B71	1	0 − 30 psia
51	Fuel Pump Inlet Temperature	B31	1	-0°, +100° F
52	Docking Adapter Temperature No. 7	A394	1	-100°, +500° F
53	Shear Panel Temperature No. 4	A153	1	-10°, +120° F
54	No. 1 Valve Cluster Temperature	D46	1	-50°, +150° F

Table D-2 (Cont.)

Channel No.	Measurement		Sampling Rate	Transducer Range
	Name	No.		
55	-Y Module Radiation Shield Temperature	A159	1	-100°, +200° F
56				
57	Docking Adapter Skin Temperature No. 4	A391	1	-100°, +500° F
58				
59	Unit I +Y Bipropellant Valve Temperature	B233	1	-50°, +250° F
60	Unit I Module +Y Injection Temperature	B240	1	-100°, +500° F
61	C-Band Transponder Case Temperature	H172	1	-50°, +200° F
62	C-Band Output PRF Monitor	H174	1	0 − 1600 pps
63	Oxidizer Feed Line Temperature Unit I -Y	B262	1	-50°, +150° F
64	Programmer B+ No. 1 (+5.7)	H29	1	0 − 5v
65	Shroud Temperature No. 3 (MT-403)	AD42	1	0°, +300° F
66	+28v dc Regulated Supply No. 2 (60w)	C2	1	0 − 30v dc
67	Skin Temperature Unit No. 1 +Y (Thrust Chamber)	B246	1	32°, +2800° F
68	+28v dc Regulated Supply No. 2 (20w)	C121	1	0 − 30v dc
69	Oxidizer Tank Temperature (+Z)	B136	1	-15°, +170° F
70	Programmer B+ No. 2 (+40)	H28	1	0 − 5v
71	Fuel Tank Temperature No. 1	B96	1	-15°, +170° F
72				
73	Nozzle Exterior Skin Temperature No. 1	B184	1	-200°, +800° F
74	Programmer B+ No. 3 (+60)	H27	1	0 − 5v
75	Unit I -Y Bipropellant Valve Temperature	B234	1	-50°, +250° F
76	Clock Temperature	H6	1	-50°, +220° F
77	Unit I Module -Y Injection Temperature	B241	1	-100°, +500° F
78	Programmer B+ No. 4 (-5.7)	H30	1	0 − 5v
79	-Y Oxidizer Tank Temperature	B272	1	-50°, +150° F
80	Docking Cone Unrigidized	H379	1	0 − 5v
81	Shroud Temperature No. 4 (MT-404)	AD43	1	0°, 300° F
82	Command Controller Power (+6)	H35	1	0 − 5v

Table D-2 (Cont.)

Channel No.	Measurement		Sampling Rate	Transducer Range
	Name	No.		
83	Skin Temperature Unit No. 1 -Y (Thrust Chamber)	B247	1	32°, +2800° F
84	Memory Temperature	H7	1	-50°, +200° F
85	Oxidizer Tank Temperature -Z	B137	1	-15°, +170° F
86	UHF Receiver Signal Level	H60	1	-133, -103 dbw
87	Fuel Tank Temperature No. 2	B97	1	-15°, +170° F
88	Destruct Receiver No. 1 Case Temp Temperature	H357	1	-50°, +200° F
89	Nozzle Exterior Skin Temperature No. 2	B185	1	-200°, +800° F
90	Destruct Receiver No. 2 Signal Level	H364	1	0−5v
91	Unit II +Y Bipropellant Valve Temperature	B235	1	-50°, +250° F
92	Safe-Arm-Fire (Destruct No. 1)	H101	1	0−5v
93	No. 2 Regulated d-c Converter Temperature	C185	1	0°, +200° F
94	L-Band Boom Antenna Extent	H347	1	0−5v
95	400 cps 3ϕ Inverter Temperature	C21	1	0°, +200° F
96	Cal +	NA		4.9v
97	Shroud Temp No. 5 (MT-405)	AD44	1	0°, +400° F
98	Destruct Receiver No. 1 Signal Level	H354	1	0−5v
99	Skin Temperature Unit No. II +Y (Thrust Chamber)	B248	1	32°, +2300° F
100	Prog Power Supply Temperature	H33	1	-50°, +200° F
101	Battery Case Temperature No. 1	C10	1	0°, +200° F
102	UHF Receiver B+	H57	1	0−5v
103	Battery Case Temperature No. 2	C13	1	0°, +200° F
104	UHF Receiver Temperature	H59	1	-30°, +165° F
105	No. 1 Regulated d-c Converter Temperature	C186	1	0°, +200° F
106	Destruct Receiver No. 2 Case Temperature	H367	1	-50°, +200° F
107	Unit II -Y Bipropellant Valve Temperature	B236	1	-50°, +200° F

Table D-2 (Cont.)

Channel No.	Measurement		Sampling Rate	Transducer Range
	Name	No.		
108	Safe-Arm-Fire (Destruct No. 2)	H103	1	0 − 5v
109	Docking Cone Rigidized	H380	1	0 − 5v
110	Fuel Feed Line Temperature Unit II -Y	B269	1	−50°, +150° F
111				
112				
113	Shroud Temperature No. 6 (MT-406)	AD45	1	0°, +400° F
114	PCM Tray Temperature	H180	1	−50°, +200° F
115	Skin Temperature Unit No. II -Y (Thrust Chamber)	B249	1	+32°, +2300° F
116	VHF Transmitter No. 1 Case Temperature	H62	1	−50°, +200° F
117	Docking Cone Unlatched	H381	1	0 − 5v
118	Cal Z	NA		0.00v
119	No. 2 Valve Cluster Temperature	D47	1	−50°, +150° F
120	VHF Transmitter No. 2 Case Temperature	H63	1	−50°, +200° F
121	Battery Case Temperature No. 3	C22	1	0°, +200° F
122	Coder Lock-On Monitor	H52	1	0 − 5v
123	Velocity Meter Oven Temperature	D85	1	0°, +185° F
124	Sync-A1			
125	L-Band Face Plate Temperature	H334	1	−103°, +176° F
126				
127	L-Band RF Power Level	H331	1	1.5v/amp
128	Sync-A2			

Table D-3

INSTRUMENTATION SCHEDULE, MULTIPLEXER SUBFRAME C

Channel No.	Measurement		Sampling Rate	Transducer Range
	Name	No.		
1	Command Function Status	H34	DD[a]	Bits -1 -8
2	Command Function Status	H34	DD	Bits 9 -16
3	Vehicle Time Word	H165	DD	LSB[b]
4	Vehicle Time Word	H165	DD	
5	Command Function Status	H34	DD	Bits 17 -24
6	Command Function Status	H34	DD	Bits 25 -32
7	Turbine Speed	B35	DD	LSB
8	Turbine Speed	B35	DD	MSB[c]
9	Command Function Status	H34	DD	Bits 33 -40
10	Command Function Status	H34	DD	Bits 41 -48
11	Velocity Meter Stored Word	D88	DD	LSB
12	Velocity Meter Stored Word	D88	DD	MSB
13	Command Function Status	H34	DD	Bits 49 to 56
14	Command Function Status	H34	DD	Bits 57 to 64
15	Turbine Speed	B35	DD	LSB
16	Turbine Speed	B35	DD	MSB

(a) Direct digital
(b) Least significant bit
(c) Most significant bit

Table D-4

COMMAND FUNCTION STATUS MONITOR, SUBFRAME C

Channel No.	Bit	Measurement	Binary "1"	Binary "0"	Pickup Points
1	1	C-Band Beacon	ON	OFF	Incl in equip
	2	S-Band Beacon	ON	OFF	Incl in equip
	3				
	4	Engine Start Sequence A	OFF	ON	Command Control
	5	ACS Gain Hi/Low	HI	LOW	F/C J-Box
	6	Pitch/Yaw	Plus	·Minus	FCLP
	7	V/M Mode IV	ON	OFF	FCLP
	8				
2	9	L-Band Antenna Select	Dipole	Spiral	
	10	Eng Start Seq B	OFF	ON	Command Control
	11				
	12	Horizon Sensor	ON	OFF	FCLP
	13	Stored Time Readin	ON	OFF	Incl in Equip
	14	Pitch/Yaw Rate	HI	LOW	FCLP
	15				
	16	Pitch/Roll/HS Gain Hi	ON	OFF	FCLP
5	17	MSB − Vehicle Time Word	$>2^{16}$ sec	$<2^{16}$ sec	Programmer
	18	Pitch H/S to Yaw IRP	Pitch	Roll	FCLP
	19	ACS	ON	OFF	F/C J-Box
	20				
	21	Engine Start Sequence C	OFF	ON	Command Control
	22	Stored Time Readout On	ON	OFF	Incl in equip
	23				
	24				
6	25	Overspeed Relay Reset	ON	OFF	FCLP
	26				
	27	V/M	Enabled	Disabled	FCLP
	28	Boom Antenna	Extend	Reset	FCLP
	29	Engine Stop Sequence	OFF	ON	Command Control
	30	Recorder Tape Direction	RCD-CW PLY-CCW	RCD-CCW PLY-CW	Incl in equip

D-13

Table D-4 (Cont.)

Channel No.	Bit	Measurement	Binary "1"	Binary "0"	Pickup Points
	31	Stored Program Command Disable	ON	OFF	Command Control
	32				
9	33	L-Band Beacon	ON	OFF	Fwd Dist Pwr Box
	34				
	35	Reset Timer	Running	Timed Out	Command Control
	36				
	37	Adapter	Rigidized	Unrigidized	FCLP
	38	Reset Timer 1-min Ind[a]	ON	OFF	Command Control
	39				
	40				
10	41	VHF Antenna Switch	Ascent	Orbit	Fwd Dist Pwr Box
	42	H′S to Yaw	In Phase	Out of Phase	Guid J-Box
	43	Hydraulics Gain	Docked	Undocked	F′C J-Box
	44				
	45	Geocentric Rate	ON	OFF	FCLP
	46	Recorder Status	OFF	ON	Incl in equip
	47	ACS Deadband	Narrow	Wide	FCLP
	48	ACS Pressure	Hi	Low	FCLP
13	49	Agena Status Display	ON	OFF	FCLP
	50	Agena Status Display	Bright	Dim	Fwd Dist Pwr Box
	51	Pwr Relay Reset	Reset	Off	FCLP
	52	Pitch Rate Cmd	ON	OFF	FCLP
	53	Geocentric Rate	Normal	Reverse	FCLP
	54				
	55				
	56	Overspeed Shutdown	Shutdown	Normal	Freq Sensitive Relay

(a) Two pulses-per-minute square wave

Table D-4 (Cont.)

Channel No.	Bit	Measurement	Binary "1"	Binary "0"	Pickup Points
14	57	Acq Light	ON	OFF	FCLP
	58	ACS Gain Hi-Undocked/ Docked	Undocked	Docked	FCLP
	59	Gyrocompassing	ON	OFF	FCLP
	60				
	61	Yaw Rate Cmd	ON	OFF	FCLP
	62	UHF Command Receiver	Enable	Disable	FCLP
	63	Approach Lights	ON	OFF	FCLP
	64				